University of Bath

PHD

Novel aspects of the activity and function of xanthine oxidase

Millar, T. M.

Award date:
1999

Awarding institution:
University of Bath

Link to publication

General rights
Copyright and moral rights for the publications made accessible in the public portal are retained by the authors and/or other copyright owners and it is a condition of accessing publications that users recognise and abide by the legal requirements associated with these rights.

- Users may download and print one copy of any publication from the public portal for the purpose of private study or research.
- You may not further distribute the material or use it for any profit-making activity or commercial gain
- You may freely distribute the URL identifying the publication in the public portal ?

Take down policy
If you believe that this document breaches copyright please contact us providing details, and we will remove access to the work immediately and investigate your claim.

Download date: 22. May. 2019

Novel aspects of the activity and function of xanthine oxidase

Submitted by Timothy Marc Millar

For the degree of PhD

Of the University of Bath

1999

COPYRIGHT

Attention is drawn to the fact that copyright of this thesis rests with its author. This copy of the thesis has been supplied on condition that anyone who consults it is understood to recognise that its copyright rests with its author and that no quotation from this thesis and no information derived from it may be published without the prior written consent of the author.

This thesis may be made available for consultation within the University Library and may be photocopied or lent to other libraries for the purposes of consultation.

Signed 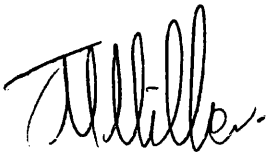

UMI Number: U601649

All rights reserved

INFORMATION TO ALL USERS
The quality of this reproduction is dependent upon the quality of the copy submitted.

In the unlikely event that the author did not send a complete manuscript
and there are missing pages, these will be noted. Also, if material had to be removed,
a note will indicate the deletion.

UMI U601649
Published by ProQuest LLC 2013. Copyright in the Dissertation held by the Author.
Microform Edition © ProQuest LLC.
All rights reserved. This work is protected against
unauthorized copying under Title 17, United States Code.

ProQuest LLC
789 East Eisenhower Parkway
P.O. Box 1346
Ann Arbor, MI 48106-1346

UNIVERSITY OF BATH
LIBRARY
80 10 MAY 2000

Acknowledgements

In the preparation of this thesis I would like to thank those people who have given of their time and effort

Dr Cliff Stevens for taking me on in the first instance and for the encouragement to develop ideas, guidance and support throughout my time in his research labs.
Dr Tulin Bodamyali for her broad minded and philosophical approach to pontification, science and problem solving from which we can all learn.
Mr (Dr) Janos Kanczler for excellent technical chats and for having to go through the same process at the same time. An invaluable source of help.
Dr Stewart Abbot for excellent discussions and technical advice on all things especially endothelial.
To all the clinicians and nurses that have provided help with sample collection and blood letting.
To the technical staff of the department of Pharmacy and Pharmacology, University of Bath for the supply of bacterial strains.
To all the staff and students of the Bone and Joint group in both its guises in London and Bath for making life have never a dull moment.
To Prof. David Blake for continued support and inspiration

Dedication

To mum, dad and Angela

Abstract

Xanthine oxidase (EC 1.1.3.22) is a 300KDa molybdenum, flavin, iron-sulphur protein known for its hydroxylation reactions of purines with the final generation of uric acid. It has long been known that the redox reactions of purine turnover generate the one electron addition product superoxide radical and two electron addition product hydrogen peroxide in the presence of oxygen as an electron acceptor. Much work has focussed on this activity in terms of pathological implications following the hypoxia reperfusion hypothesis suggested by McCord in 1985.

Owing to the similarity between xanthine oxidase and other molybdenum containing enzymes particularly nitrate reductase, the nitrate reductase activity of xanthine oxidase was assessed. This was found to occur under reduced oxygen concentrations and is thought to be due to oxidation of the enzyme via the loss of electrons to nitrate at the molybdenum site. It was then possible to generate nitric oxide from nitrite utilising an apparent nitrite reductase activity with a variety of substrates which was also molybdenum site dependent. The possibility of peroxynitrite generation at intermediate oxygen concentrations re-opened the discussion as to the function of xanthine oxidase.

The antibacterial action of peroxynitrite and a range of oxidants was assessed. The appearance of xanthine oxidase in high concentrations in human and bovine milk suggests this enzyme as a possible natural antibiotic.

The appearance of a circulating form of radical activity has also been suggested to be xanthine oxidase. In the light of the nitric oxide generating capacity of the enzyme, the binding of xanthine oxidase to live endothelial cells was assessed. In

this thesis endothelial cells were shown to express, bind and upregulate xanthine oxidase activity *in vitro*.

Abbreviations

%sat	Percentage saturation
1,2-GDN	Glyceryl dinitrate
7-ER	7-ethoxyresorufin
AIDS	Acquired immune deficiency syndrome
ALU	Arbitrary light unit
AMPS	Ammonium persulphate
AO	Aldehyde oxidase
ATP	Adenosine-tri-phosphate
C	Carboniferous
CA	Cambrian
cAMP	Cyclic adenosine mono phosphate
CFU	Colony forming units
cGMP	Cyclic guanosine mono phosphate
cGMP	Cyclic guanosine mono phosphate
CL	Chemiluminescence
CO_2	Carbon dioxide
cyt c oxidase	Cytochrome c oxidase
cyt P450	Cytochrome P450
cyt P450	NADPH-cytochrome P450 reductase
D	Devonian
DIDS	4,4'-diisothiocyanatostilbene-2,2'-disulphonic acid
DMSO	Dimethyl sulphoxide
DNA	Deoxyribose nucleic acid
dONOO-	Decomposed peroxynitrite
DPI	Diphenyleneiodonium
DTPA	Diethylenetriaminepentaacetic acid
EDRF	Endothelium derived relaxing factor
EPEC	Enteropathogenic E. coli
EPO	Erythropoetin
EPR	Electron paramagnetic resonance spectroscopy
FACs	Fluorescence activated cell sorting
FAD	Flavin adenine dinucleotide

FCM	Flow cytometry
Fe-S	Iron-sulphur cluster
FITC	Fluoresceine iso-thio-cyanate
FL1-H	Fluorescence parameter-1 height
FMN	Flavin mono nucleotide
FNiR	Formate nitrite reductase
FSC-H	Forward light scatter height
Gag	Glycosaminoglycan
GPO	Glycerophosphate oxidase.
GST	Glutatione S-transferase
GTN	Glyceryl-tri-nitrate
H_2O	Water
HCl	Hydrochloric acid
HIF-1	Hypoxia inducible factor-1
HM	HUVEC media
HUVEC	Human umbilical vein endothelial cells
IgG	Immunoglobulin G
IL-1	Interleukin 1
IL-2	Interleukin 2
IL-6	Interleukin 6
ISDN	Isosorbide dinitrate
ISMN	Isosorbide mononitrate
J	Jurassic
K	Cretacious
KDa	KiloDalton
KHS	Krebs-Henseleit solution
K_m	Michaelis constant
LB	Lab Lemco broth
LEC	Lucigenin enhanced chemiluminescence
L-NMMA	L-NG-monomethyl-L-arginine
LRF	Liver residue factor
LuEC	Luminol enhanced chemiluminescence
m	Metre
M	Molar

MAFF	Ministry of Agriculture Fisheries and Foods
MFCH	Mean fluorescence channel height
ml	Millilitre
Mo	Molybdenum
MPO	Myeloperoxidase
MPT	Marvel/PBS/Tween
NAD+	Nicotinamide adenine dinucleotide
NADH	Nicotinamide adenine dinucleotide reduced form
NADP+	Nicotinamide adenine dinucleotide phosphate
NADPH	Nicotinamide adenine dinucleotide phosphate reduced form
NED	N-1(-naphthyl)ethylenediamine dihydrochloride
NH_4^+	Ammonium
NiR	Nitrite reductase
NO	Nitric oxide (Nitrogen monoxide)
NO+	Nitrosonium ion
NO_2-	Nitrite
NO_2	Nitrous oxide
NO_3-	Nitrate
NOS	Nitric oxide synthase
NR	Nitrate reductase
O	Ordivician
O_2	Oxygen
OEC	Ozone enhanced chemiluminescence
OH	Hydroxyl radical
ONOO-	Peroxynitrite (Oxo-peroxo nitrate)
ONOOH	Peroxynitrous acid
P	Permian
PARS	Poly(ADP-ribose) synthetase
PBS	Phosphate buffered saline
PMT	Photomultiplier tube
ppb	Parts per billion
ppm	Parts per million
PT	PBS/Tween-20

RE	Responsive element
RT	Room temperature
S	Silurian
SAVR	Surface area to volume ratio
sec	Second
SF	Synovial fibroblasts
SMA	Superior mesenteric artery
SMEC	Synovial microvascular endothelial cells
SOD	Superoxide dismutase
SSC-H	Side light scatter height
T	Tertiary
TEMED	N,N,N',N'-Tetramethylethylene diamine
TR	Triassic,
U.K.	United Kingdom
U.S.A.	United States of America
UTIs	Urinary tract infections
VEGF	Vascular endothelial growth factor
vWF	von Willibrand Factor
XDH	Xanthine dehydrogenase
XO	Xanthine oxidase
XOR	Xanthine oxidoreductase
β-NADPH reduced form	β-Nicotinamide adenine dinucleotide phosphate

Table of contents

Table of contents

Table of contents

Table of contents

Table of figures

Chapter 1

Chapter 2

Chapter 3

Table of figures

Chapter 4

Chapter 1

General Introduction

Chapter 1

1.1 Introduction

1.1.1 Importance of the environment

The human body contains mechanisms to deal with the everyday and not so every day aspects of living function. The seven basic modes of life: respiration, reproduction, nutrition, locomotion, excretion, growth (division) and irritability (response to stimulus), represent characteristics which are shared by most species on earth (exceptions include some of the most basic forms of "existence" known some of which carry out only a selection of these seven functions). To survive in a hostile environment, the ability to adapt has helped the present species on earth to exist at a point in time where others cannot. Taking the estimates for the age of our universe as 15 thousand million years and our own planets existence as around four and a half thousand million years, life apparently began some thousand million years following the formation of the planet. The particular environment found at that time is thought to have encouraged the conglomeration of organic molecules to form the very basis of the first forms of life (Pirie, 1985). Life in terms of the first chemical processes involving organic molecules which could somehow reproduce themselves by purely chemical processes. Experiments to replicate the early earth atmosphere using simple molecules such as ammonia, methane, hydrogen and water vapour reacted under a low oxygen conditions reveal the building blocks of life. Isomers of sugars were formed following discharges of electricity such as lightning; a phenomenon that we still see today on our own planet and on others in the solar system (Mason, 1989). These early life forms were never captured in fossil form, the fossil record that does exist, however, shows slow progress over the

following two thousand million years. Before the Cambrian period (~ 500 million years ago) single celled organisms were joined by more complex multicellular organisms in what is referred to as the Cambrian explosion. A change in the environment has been suggested as the causation for this sudden change. According to recent research by Andrews in 1998, the suggestion is that a continental shift occurred, turning the continents through ninety degrees and causing a climate change. More precisely, it is believed that a movement of the Earth's lithosphere - the solid uppermost layer of the planet's crust - caused a climate change that propelled the evolution of new life forms. Analysis of rocks collected by the researchers suggest that all the major continents "experienced a burst of motion" at about the same time as the Cambrian explosion occurred in the geologic record. However, whether or not this phenomenon, known as "true polar wander", was enough to cause new life forms to emerge is an issue of great speculation (Andrews 1998).

Although the mechanism may still be under debate, it is clear that over the expanse of time, there have been great upheavals in the environment on earth that have had and are still having effects on life. Of particular interest is the change in the concentration of oxygen within the atmosphere. Oxygen, a gas first purified by Priestly in the 18th century, is essential to human life and to most other organisms. However, organisms exist to which oxygen is a poison, in that they cannot survive in an oxygen-enriched atmosphere. Presently the oxygen concentration in the Earth's atmosphere is ~ 21%. This is kept fairly constant by the buffering effect of the oceans, the generation of oxygen from green algae, plants and other photosynthesising organisms. However, oxygen is used up by other species and chemical processes which generate carbon dioxide as a by-product of energy utilisation and respiration.

Chapter 1

The earliest known fossils are found to date to around 3,500 million years ago, during the Archaen period. These microbacteria are thought to have lived under a reducing atmosphere. During this time the oxygen concentration in the atmosphere was very low, ~1% of today's values. About 2,200 million years ago iron oxides began to appear in paleosols (fossil soil) with the appearance of "red beds" containing metal oxides. Information collected from cosmic spherules – micrometeorites-submilimeter-sized particles derived from comets and asteroids – has been used to estimate oxygen concentration in the pre-Cambrian atmosphere. These cosmic spherules contain nickel-rich spinels that were crystallised and oxidised during atmospheric entry. This gives an estimate of the level of oxygen in the atmosphere at the time of arrival (Deutsch *et al*, 1998). This suggested a relatively rapid increase in oxygen concentration in the atmosphere at this time (Graham *et al*, 1995). The appearance of cyanobacteria 3,500 million years ago ties in with the rise in atmospheric oxygen and a change from a reducing atmosphere to one that was primarily oxidising. These photosynthetic organisms produced oxygen as a by-product of their metabolism and they became common and widespread in the Proterozoic era, 2,500 – 540 million years ago. This effect was so prolific as to raise the atmospheric oxygen content from 0 to 15% (Berner and Canfield, 1989, Holland, 1994 and Shields *et al*, 1997). It is possible that these cyanobacteria were the priming force for the explosion of species which occurred because of the change to oxygen utilisation for certain biochemical processes. The effect of the cyanobacteria on the ecology of the Earth reaches through to today in that the oil deposits are attributed to the activity of these organisms. They are also important providers of nitrogen fertilisers in rice cultivation as well as being the probable source of photosynthetic pigments in the eukaryotic plants by an endosymbiotic relationship.

The increase in oxygen allowed for the formation of further plant species notably the vascular plants – those containing xylem and phloem – which caused another great rise in oxygen and a reduction in carbon dioxide. During the Carboniferous period, large amounts of carbon were fixed from the atmosphere as the fossil fuels were laid down. The resultant drop in carbon dioxide levels is shown in figure 1.1.

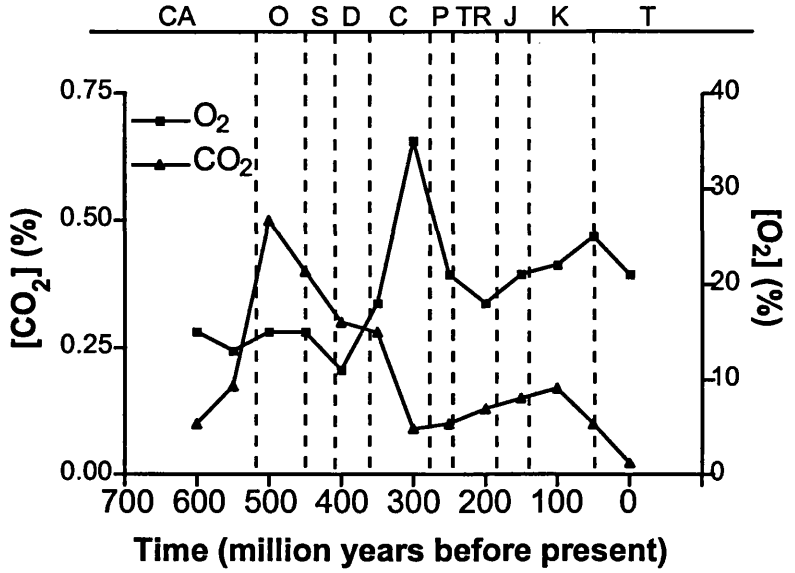

Figure 1.1. The change in atmospheric oxygen and carbon dioxide concentrations over the past 600 million years. CA Cambrian, O Ordivician, S Silurian, D Devonian, C Carboniferous, P Permian, TR Triassic, J Jurassic, K Cretacious, T Tertiary (After Dudley, 1998).

Following this time the oxygen concentration fell dramatically, coinciding with the mass extinction seen during the Permian. Not only did the change in oxygen have effects but also the carbon dioxide levels had effects on regulating temperature by greenhouse warming. The overall density of the atmosphere and atmospheric pressure was also affected enabling the first flying species to become prevalent (Dudley, 1998). The biochemistry of these organisms can only be guessed at, but it is possible that they evolved to utilise the available substrates or to lessen their

oxidative effects. This then shows the controlling effect of oxygen availability on life on earth.

1.1.2 Oxygen effects

On the switch from a reducing to an oxidising atmosphere, adaptations were required for survival. Oxygen itself had become a toxic entity, one that must be dealt with for the organisms to proliferate. The mechanisms by which this new oxidant was to be overcome must have evolved during the time of the rise in oxygen concentration, with those species able to adapt most quickly being the species to survive.

1.1.2.1 The mitochondrion and oxidative respiration

Oxygen plays a vital part in energy utilisation and metabolism. The mitochondrion is the organelle in eukaryotic organisms where energy is utilised. These organelles are thought to be the descendants of once free-living organisms that began a symbiotic relationship with other organisms as an energy provider (Margulis, 1970). Oxygen acts as the terminal electron acceptor in chains of enzyme-mediated reactions where electrons are taken from substrates during enzyme turnover. Glucose, a simple sugar, is broken down to pyruvate during glycolysis in the cell cytoplasm generating two molecules of energy-rich adenosine triphosphate (ATP) for each molecule of glucose under an oxygen-rich environment. The mitochondria house the pathways of energy generation from pyruvate. Pyruvate itself is fed into the Krebs cycle where a series of enzyme steps generates nicotinamide adenine dinucleotide reduced form (NADH) and carbon dioxide (CO_2) as by-products. The final stage of ATP generation occurs by electron transporting reactions known as the respiratory chain. Hydrogen atoms from NADH generated in the Krebs cycle

are converted to a proton and two electrons. These electrons are passed to the first of more than 15 different electron carriers in the respiratory chain. Each complex in the chain has a greater affinity for electrons than the previous complex and the electrons pass along this chain until they react with oxygen which has the greatest affinity of all for the electrons (Alberts *et al*, 1989). However, this system can be disrupted by the use of specific inhibitors of respiration such as cyanide or by the removal of oxygen. As oxygen is the terminal electron acceptor its levels in the cell will dictate the rate of ATP production. In fact, as oxygen concentrations are reduced the glycolytic pathway does not end with pyruvate but in the generation of lactate. Lactate acts as a storage product until the oxygen concentration is such that lactate can be converted to pyruvate and the cycle of ATP generation can restart. This system relies on oxygen availability for the smooth running of energy metabolism.

1.1.2.2 Adaptation to non-oxidative metabolism

Primitive organisms could generate ATP by the utilisation of organic molecules in a process probably similar to fermentation (Gest, 1980). The organic molecules are partly oxidised by the loss of a hydrogen molecule. In the reducing atmosphere of the time, hydrogen must have been transferred either by NADH or NADPH to a different organic molecule which thereby became more reduced. The products of fermentation are excreted into the media whereas others are retained in the cell for further biosynthesis.

The excreted products tend to be organic acids such as lactic, formic, acetic, butyric and succinic acids. The evolution of electron-storing transport chains allowed different substrates to be utilised such as non-fermentable organic compounds (Danson, 1988).

Certain parasites are found under reduced oxygen atmospheres and their biochemical adaptations reflect their ability to survive the changing environments. The protozoan Trypanosomes utilise a variety of adaptations and certain species are more "aerotolerant" than others because of their biochemical pathways. *T. brucie* generates pyruvate as its end product as they do not possess the enzymes involved in the Krebs cycle or an electron transport chain. Oxygen is utilised, when available, to directly oxidise NADH using the unique enzyme glycerophosphate oxidase (GPO). This system can be inhibited by the reduction of oxygen. However, this is not lethal as the organisms have two other energy metabolising activities one of which is anaerobic. This system, utilising an unknown oxidase, apparently accounts for 30-35% of the reducing power (Weimer *et al*, 1995).

The *T. congolense* group has pyruvate, acetate and succinate as end products of respiration. They do possess some Krebs cycle enzymes but function in the reverse direction. *T. cruzi* have a fully functional Krebs cycle and generate CO_2 and succinate but here again the system works in reverse (Perie *et al*, 1993).

However, other terminal electron acceptors are still used. Today, we still see adaptations to a reducing atmosphere. Free-living ciliates are generally regarded as aerobic and totally reliant on mitochondrial respiration for energy generation. However, several lineages have colonised anaerobic habitats where the role of the mitochondrion has been replaced by the hydrogenosome and obligate anaerobe ciliates now lack mitochondria (Brul and Stumm, 1994). These anaerobic ciliates are not phylogenetically related, implying that the process allowing their existence was not rare (difficult), and they have strong morphological ties to their aerobic relatives implying that the process was also recent (Frenchel, 1996).

The hydrogenosome is an organelle that produces hydrogen which can then go on to be used to replenish NADH levels following enzyme utilisation and ATP

production (Biagini *et al*, 1997 and Diaz and De Souza, 1997). In *Trichomonas sp,* oxygen can be used as the terminal electron acceptor. However as the levels of oxygen are reduced the ratio of end products changes. In aerobic conditions no hydrogen is produced and more acetate is formed than succinate. In anaerobic conditions the reverse is seen. The aerobic metabolism generates greater amounts of ATP but the anaerobic system can still generate significant amounts; seven molecules ATP to five molecules ATP per 1 molecule glucose respectively (Benchimol *et al*, 1996).

A further adaptation to the varying oxygen concentration is the utilisation of a cytoplasmic NADH oxidase. This acts as an oxygen scavenger that mops up the extra oxygen protecting the hydrogenosome. In comparison to the relatively aerotolerant *Tricomonas*, *Entamoeba sp.* have no mitochondria and their NADH oxidase activity is not compartmentalised. *T. foetus* can tolerate up to 20% oxygen for short periods whereas *E. histolitica* can only tolerate ~ 5% oxygen.

Clostridium perfringens is the microbe responsible for gas gangrene in open wounds, an infection usually contracted from contaminated soil although commensal organisms can also survive in the gut. The bacterium itself cannot survive in an oxygen rich atmosphere and so generates hydrogen gas contained within a biofilm within which it multiplies

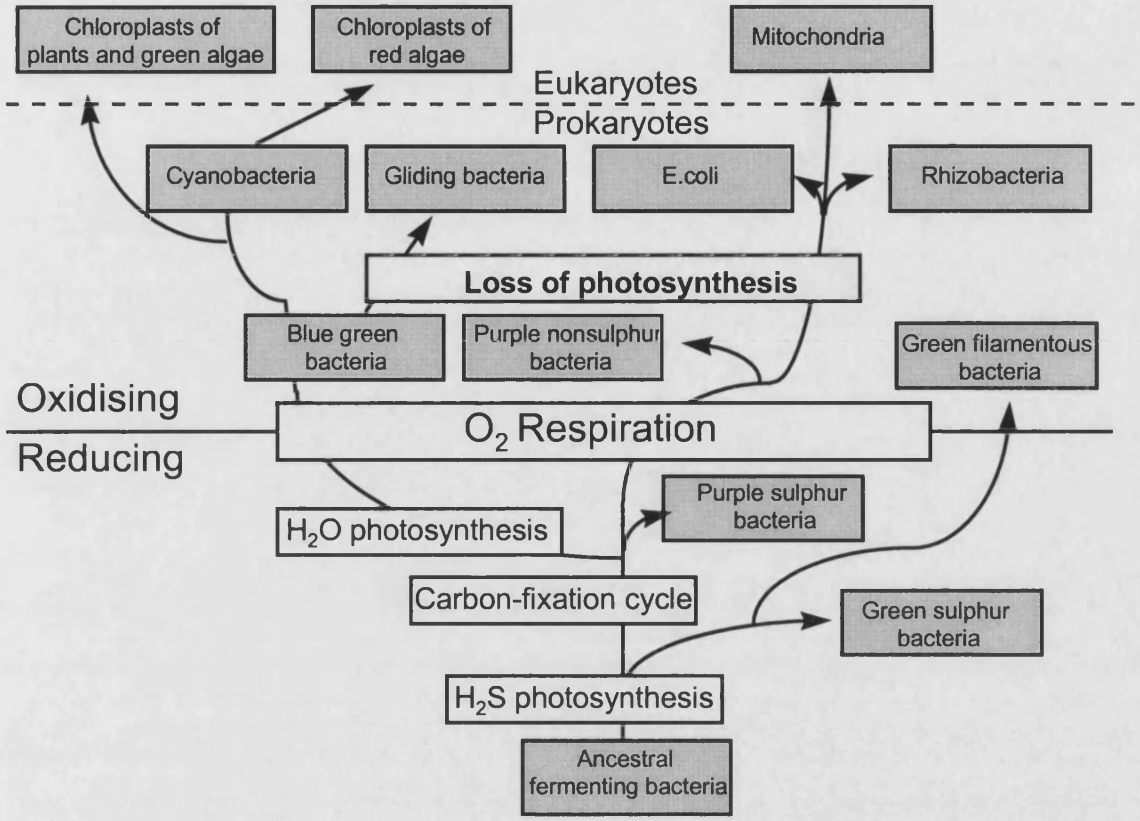

Figure 1.2. Summary of the evolution of the mitochondria and the change in atmosphere and alternative energy metabolism (After Alberts *et al*, 1989).

1.1.3 Oxygen and physiology

Using oxygen as the terminal electron acceptor in the generation of energy-rich compounds means that the availability of oxygen will determine many reactions and rates of metabolism. In a normal physiological situation at sea level the concentration of inspired oxygen is equivalent to the atmospheric concentration ~ 21% by saturation. Once inspired and bound to a transport protein, haemoglobin, myoglobin or haemolymph, which are iron based and copper based proteins respectively, the oxygen can then be transported to the tissues. Oxygen saturated transport proteins lose their oxygen in areas that are relatively low in oxygen for example respiring tissues. As the transport proteins move further away from their

site of oxygen saturation, such as the lungs, gills and skin, their level of oxygen saturation is reduced as oxygen is lost to the tissues and carbon dioxide is exchanged. It is therefore possible that, in the tissues furthest from the transport protein oxygen saturation point, there will be less oxygen available for respiration. These tissues may then be termed relatively hypoxic. However, using this term suggests that this tissue is under some respiratory stress compared to tissue with a greater oxygen supply when the oxygen supply to the "hypoxic" tissue is the normal or normoxic supply that it would receive.

The supply of sufficient oxygen to the tissues has controlled the evolution of transport protein and respiratory systems. From diffusion limitation over body surfaces to removal of oxygen from water by gaseous exchange over gills to breathing in air, each environment poses problems that have to be overcome. The atmospheric, and therefore aquatic, oxygen concentration also controlled the respiratory system of organisms and led to the development of gigantism in the late Palaeozoic (Dudley 1998). Among terrestrial vertebrates at that time, large amphibians reached body lengths of up to 2 meters but were probably limited to that size by cutaneous respiration which is known to restrict maximum body size in modern urodeles (Ultsch 1974). By increasing the concentration of available oxygen the diffusive flux into the tracheal system is increased. The limits of body size can then also increase as the supply and demand ratio changes in favour of supply (Graham *et al* 1995).

For aquatic organisms the variation in temperature affects the oxygen saturation of water: oxygen saturation decreasing with increasing temperature. To counteract this, adaptations to the environment have evolved. Changes in the saturated lipid content of cell membranes helps to control membrane fluidity which is temperature dependent (Coussins and Prosser 1978) and the evolution of temperature sensitive

and resistant enzymes allows function during dives where water temperature and therefore body temperature can change by over 20°C (Dunn *et al* 1983).

1.1.3.1 Hypobaric hypoxia

In humans, however, temperature is regulated to give a near constant core temperature of ~ 37°C. Oxygen availability however can become a problem at altitude. Although the percentage of oxygen in inspired air remains constant at varying altitudes, the fall in atmospheric pressure at higher altitudes decreases the partial pressure of inspired oxygen. This in turn decreases the driving pressure for gas exchange in the lungs. The atmospheric pressure and inspired oxygen pressure fall roughly linearly with altitude to be 50% of sea level value at 5,500m and 30% sea level value on the summit of Everest (~ 8,900m) (Peacock 1998).

To survive at these low oxygen partial pressures a range of physiological adaptations occur. At sea level, carbon dioxide is the main stimulus to ventilation. However, at altitude, the decrease in oxygen saturation of the blood is sensed by the carotid bodies, which stimulate an increase in ventilation to blow off carbon dioxide. By using a high-oxygen-sensitive potassium channel that is reversibly inhibited by low oxygen, the subsequent depolarisation stimulates calcium channels that mediate the signal in the nerves (Gonzalez *et al* 1992 and Schoene 1997).

The heart at altitude responds with an initial increase in output compared to physical work but acclimatises to sea level values soon after. At all times however there is an increased heart rate and decreased stroke volume for any given level of work and the maximum obtainable heart rate falls as higher altitudes are reached (Monge and Leon-Velarde 1991).

The oxygen saturation of the haemoglobin is reduced on moving to altitude thereby reducing the amount available to the tissues. During acclimatisation, the oxygen

saturation curve becomes left shifted. That is to say that the haemoglobin binds oxygen more avidly, increasing the blood oxygen saturation (Hsia 1997).

The blood volume also changes on a move to altitude with a two phase acute and acclimatisation response. The acute phase is caused by dehydration of blood plasma, which concentrates the haemoglobin and increases the amount of available protein able to carry oxygen per unit residence time in the lungs. The acclimatisation response is stimulated by the reduced oxygen concentration and the stimulation of the juxtaglomerula apparatus of the kidney and an increase in the production of erythropoietin (EPO) which in turn increases the haemoglobin concentration (Klausen *et al* 1996). The expression of vascular endothelial growth factor 1 (VEGF1) in the vasculature is linked with oxygen sensing and along with the expression of its receptor leads to angiogenesis especially in the heart and brain (Hochachka *et al* 1998).

1.1.3.2 Physiological hypoxia

During intense exercise the body can build up what is known as an oxygen debt. This occurs when the energy requirements outstrip their supply due to the loss of the terminal electron acceptor, oxygen. This reduces the electron cascades and the formation of high-energy metabolites. Glycolytic metabolism occurs in low oxygen to generate pyruvate which would normally go on to the Krebs cycle and be used for ATP generation. However, at times of oxygen debt, glycolysis switches to lactate production allowing turnover of the glycolytic enzymes. The lactate is stored until the oxygen concentration increases and Krebs cycle is initiated for the further, and more energetically efficient, generation of ATP. The measurement of the lactate-pyruvate ratio has been used by some as a marker of hypoxia or glycolytic metabolism in the absence of oxygen (Wasserman *et al* 1990).

1.1.3.3 Cellular response

The cellular response that leads to the macroscopic physiological response detailed above is mediated by environmental sensing systems. The carotid body initiates the hypoxic ventilatory response and pulmonary vascular oxygen sensors initiate the regulation of hypoxic pulmonary vasoconstrictor responses which matches lung and ventilation perfusion. Oxygen sensing in the vasculature causes VEGF1 expression with associated angiogenesis whilst oxygen sensors in the kidney and liver cause expression of EPO. Tissue specific oxygen sensing leads to metabolic reorganisation by altering the expression rates of hypoxia sensitive genes for metabolic enzymes and transporters (Hochachka *et al* 1998).

These adaptive responses to hypoxia feature the activation of genes for active proteins such as EPO, VEGF, endothelin, glucose transporters and glycolytic enzymes (Bunn and Poyton 1996). These genes share a common mechanism for oxygen-sensing and transcriptional activation. The key step in gene activation is the formation of the hypoxia-inducible factor-1 (HIF-1) protein complex and its binding to a DNA recognition sequence of the activatable gene (Wang and Semenza 1993). Semenza and Wang (1992) were able to show that a 50 nucleotide enhancer sequence from the human EPO gene could mediate a sevenfold transcriptional induction of EPO protein expression in response to hypoxia. This sequence was able to bind a specific nuclear transcription factor which was induced by hypoxia via *de novo* protein synthesis.

This led to the description of the oxygen sensitivity of HIF-1α expression and the constitutively expressed HIF-1β. During low oxygen the HIF-1α protein becomes stabilised as the ubiquitin-proteosome system is down regulated. HIF-1α is able to bind to HIF-1β to form a transcriptionally active complex (Salceda and Caro 1997)

and this complex can then bind to specific nucleotide sequences of particular genes to cause their transcription and expression of protein (Srinivas *et al* 1998).

One such hypoxia-regulated protein is the inducible nitric oxide synthase (Melillo *et al* 1995). The induction of a nitric oxide generating enzyme during hypoxic episodes would allow the generation of NO on reperfusion and may enhance the relaxation of constricted vessels thus ensuring greater blood perfusion to the tissues.

This acute hypoxic response has been linked to certain disease states where blood supply is reduced to cause a hypoxic or ischaemic episode. Ischaemia of the heart, brain and other organs is resolved on reperfusion when blood flow is initiated and oxygen concentrations in the tissues are increased. It has been suggested that this reperfusion phase is associated with the injury caused by these episodes. In particular the role of oxygen and nitrogen radical species has come under certain scrutiny with regard to their involvement in pathology.

1.1.3.4 Hypoxia reperfusion injury

The role of superoxide and derived radical species in reperfusion injury is dependent upon their generation on the reintroduction of oxygen to previously hypoxic tissue. Famously, McCord in 1985 suggested that oxygen-derived free radicals were involved in post-ischaemic tissue injury in a range of diseases including Intestinal and myocardial ischaemia and in circulatory shock. This came from data relating to the protective effect of the enzyme superoxide dismutase (SOD) treatment during hypoxia reperfusion cycles in cats. It had previously been suggested (Meerson *et al* 1982) that superoxide had a role in the ischaemic heart and that SOD could abrogate almost all of the reperfusion injury (Granger *et al* 1981).

The main protagonist in the generation of superoxide was suggested by McCord to be xanthine oxidase (XO). This enzyme was chosen because of its radical generating activity, its apparent wide tissue distribution and the availability of substrates that were thought to build up during the ischaemic episode. On reperfusion, oxygen would become available and with hypoxanthine present the generation of oxygen radicals could occur. The effects of allopurinol an inhibitor of XO was also shown to inhibit the effects of reperfusion on the permeability of cat intestine following local arterial hypotension and subsequent reperfusion (Granger *et al* 1981).

This hypothesis was taken up to explain many reperfusion injury pathologies.

However, more recently the value of xanthine oxidase as the mediator of reperfusion injury especially in myocardial ischaemia has become less favoured due to reports suggesting that the heart did not contain active enzyme (Schaper 1991). Further evidence was also suggested by using immunological detection methods that in humans did not show enzyme expression in the heart or brain (Linder *et al* 1999).

The recent discovery of a circulating form of xanthine oxidase however has led to the suggestion that injury to remote organs that did not contain measurable amount of active enzyme may be damaged due to the binding and generation of radical species of a circulating form released from the liver following an insult of some kind (Nielsen *et al* 1997). This debate remains unresolved so far and the evidence for the circulating form of the enzyme will be reviewed in a following section.

The role of xanthine oxidase as a generator of free radical species is therefore of importance particularly in its oxygen limited reactions.

1.2 Xanthine oxidase

1.2.1 Historical aspects

From the first measurements of enzyme activity in milk by Shardinger in 1902, the specific activity of XO has been under investigation. XO itself belongs to a group of proteins known as oxidoreductases. This reflects the redox activity of the enzyme and the fact that the enzyme can function with a range of substrates to yield a range of products over a range of environmental conditions.

Fridovich and Handler (1961) showed that bovine milk and calf liver xanthine oxidase along with rabbit liver aldehyde oxidase were able to cause the oxidation of sulphite in the presence of their substrates, xanthine and N-methyl nicotinamide respectively. This was not the case however among other similar flavoprotein-containing oxidase and dehydrogenase enzymes including succinic dehydrogenase, glucose oxidase and alcohol dehydrogenase.

Previously, Weber *et al* (1956) had studied the reduction of iron and cytochrome c by xanthine oxidase and suggested that hydrogen peroxide formation during the oxidation of hypoxanthine was responsible for this activity. However, they also noted that free hydrogen peroxide could not reduce cytochrome c and therefore the reduction mechanisms for iron and cytochrome c must differ.

These speculations were possible as Morgan, Stewart and Hopkins (1922) produced evidence of hypoxanthine oxidation in the presence of oxygen. This was followed by observations made by Thurlow in 1925 that oxygen was reduced to hydrogen peroxide and by Horecker and Heppel in 1949 showing that the reduction of cytochrome c was accelerated by oxygen (Morgan *et al* 1922 and Thurlow 1925 in Dixon, 1926).

It was also suggested that the activity reported by Totter *et al* (1960) of the hypoxanthine mediated oxidation of luminol or lucigenin followed by the emission of light was due to the same activity as that reported for the oxidation of sulphite. The reason for this apparent activity was the production of other oxygen derived radical species and in particular the one electron reduction of oxygen to yield superoxide radical.

This radical generating capacity led to the development of the idea for a role of XO in pathology.

1.2.2 Enzyme structure

1.2.2.1 Molybdenum and pterin cofactor

Further studies on the diet-dependent activity of rat liver xanthine oxidase enzyme identified a "liver residue factor" (LRF) which was not identified as a vitamin or other factor of known nutritional value at the time (Richert and Westerfeld 1951). The inclusion of the LFR increased the rat intestinal enzyme level 500-700 percent above the controls. By careful assay of intestinal and liver homogenates the LFR was suggested as being molybdenum and the inclusion of 0.1mg of molybdenum per kilogram of diet produced saturation levels of the enzyme in the intestine (Richert and Westerfeld 1953).

Further studies using EPR spectroscopy confirmed the requirement for molybdenum for enzyme activity in purified enzyme and began to suggest the possible reaction mechanism of xanthine turnover (Bray and Meriwether 1966).

Xanthine oxidase belongs to a group of mononuclear molybdenum enzymes that possess, at their active site, molybdopterin cofactor (Hille 1996). This has also been identified crystallographically in the similar enzymes, aldehyde oxidase and

DMSO reductase from various bacterial sources. The discovery of this cofactor came from work by Pateman *et al* (1964) on the xanthine dehydrogenase and nitrate reductase enzymes of *Aspergillus niger.* The generation of mutations in this fungus produced non-functional enzymes, inferring that a common pathway of cofactor synthesis had been lost. Further study saw the discovery of particular control genes for pterin cofactor synthesis, molybdenum uptake from the environment and insertion of molybdenum into the cofactor (Johnson *et al* 1991).

Hille (1996) proposed the reason for the possession of pterin cofactor to be the provision of a method by which electrons can be shuttled away from the molybdenum active site to allow a more rapid turnover and modulation of the molybdenum reduction potential.

The molybdenum cofactor may also be co-ordinated with molybdenum bound to oxygen or to sulphur, the oxo or sulphido ligands in the enzyme's oxidised form. Both of these liganded forms are inhibited by cyanide causing the release of the sulphur that is replaced by oxygen to give the inactive desulpho form of the enzyme. This form of the enzyme can be found naturally occurring and can be resulphurated by using sulphide under turnover conditions (Huber *et al* 1996). The enzyme can also be isolated in a demolybdo form or without an intact pterin cofactor, both of which are inactive as xanthine oxidases (Gardlick *et al* and Ventom *et al* 1988).

The molybdopterin cofactor has thus been specified as the site at which the purine substrates xanthine and hypoxanthine are oxidised to urate and xanthine respectively in the presence of oxygen as an electron acceptor.

1.2.2.2 Flavin

On further purification from the raw milk, it was found that the enzyme XO came as a brown solution. Visible spectrum analysis indicated the presence of a flavin moiety which was thought to be flavin adenine dinucleotide (FAD) (Ball, 1939 and Corran *et al*, 1939). The importance of the flavin has been shown in terms of enzyme turnover and the generation of superoxide. In the absence of oxygen and any other oxidising substrate the enzyme will gain electrons from hydroxylation of a purine substrate. This enzyme will now not be able to turnover as it is loaded with electrons and cannot return to the oxidised state without passing them on to an acceptor substrate. Oxygen has been shown to accept electrons from the electron rich enzyme with the formation of superoxide anion. This allows the turnover of the enzyme to carry out further hydroxylations of purine substrates.

Oxygen is supposed to bind and receive its electrons from the flavin thus allowing further turnover of the enzyme by utilising a second site removed from the molybdopterin.

The flavin is the apparent site at which NADH will donate electrons and cause the generation of NAD+. The electron-rich enzyme again in the presence of oxygen will give up its electrons to generate superoxide radical and allow further turnover of the enzyme. The flavin specific inhibitor Diphenyliodonium (DPI) has been shown to inhibit the oxidation of NADH to NAD+ by XO and also therefore to inhibit the production of superoxide radical by the same means of denying the enzyme electrons (Sanders *et al* 1997).

1.2.2.3 Iron sulphur

The requirement for iron in the activity of xanthine oxidation was described by Richert and Westerfeld (1954) using similar assays to those which showed the

requirement for molybdenum. Using EPR techniques a paramagnetic signal from resting XO enzyme that was not attributable to Mo or FAD was shown by Bray and colleagues (1961). This signal was suggested as iron and confirmed in 1964 by Palmer *et al* who also suggested that the iron was reduced from a ferrous to a ferric state during enzyme turnover. The EPR signal occurred following those attributable to Mo and FAD and therefore suggested an involvement in electron transport mechanisms that followed this order. Following these observations, Lowe *et al* (1972) attributed this iron signal to an iron sulphur moiety (Fe-S) that was similar to a signal generated from spinach ferredoxin which also contains an iron sulphur moiety.

1.2.2.4 Structurally related enzyme systems

XO belongs to a group of enzymes that share a common reaction mechanism and structure. Such examples include aldehyde oxidase, carbon monoxide dehydrogenase and formate dehydrogenase (Hille 1996). They possess a molybdopterin cofactor and under go similar hydroxylation reaction of their specific substrates. Other molybdenum-based enzymes also exist and can be grouped into the sulphite oxidase and DMSO reductase like families. Such sulphite oxidase type enzymes are the assimilatory nitrate reductases of plant and fungal origin. These enzymes are responsible for the first step in assimilation of nitrogen in the form of nitrate for these organisms. They are similar to XO in that they possess FAD and molybdopterin cofactors but differ in that they contain a cytochrome with haem iron as a further cofactor (Kay *et al* 1990).

These enzymes catalyse the reduction of nitrate to nitrite in an NADH- or NADPH-dependent manner. Their catalytic activity is apparently under tight control *in vitro* with a nitrate reductase specific kinase responsible for the short term down

regulation of nitrate reductase activity, which in plants follows the levels of photosynthesis generating the NADH and NADPH reducing equivalent. The control of nitrate reductase activity is also linked to light because of the generation of the nitrite, which can be toxic if not utilised by further enzyme systems (Ye *et al* 1994 and Douglas *et al* 1998).

The dissimilatory nitrate reductases are similar in their molybdenum cofactor to the DMSO reductases of *E. coli* and couple the reduction of nitrate to nitrite with menaquinol to generate a transmembrane proton gradient. This protein has membrane spanning regions with the catalytic subunit on the periplasmic side (Jones *et al* 1980). The dissimilatory pathway is used in the absence of oxygen for the generation of proton gradients to allow ATP formation. This utilises nitrate as the terminal electron acceptor and allows respiration to continue.

E. coli possess three distinct nitrate reductases: A, Z and an, as yet, undesignated form. It is the A form that is induced by anaerobic conditions. A fourth protein product from the regulatory operon is not incorporated into the active enzyme but is required for maturation and function possibly due to stabilisation of the message coding for the enzyme (Dubourdieu and DeMoss 1992).

The product of nitrate reduction in both the assimilatory and dissimilatory pathways is nitrite. This nitrite can itself be reduced further to ammonium ion (NH_4^+) or to NO by a series of nitrite reductases (Ye *et al* 1994 and Cole 1996). In *E. coli* two such nitrite reductases (NiR) are expressed in low oxygen concentration, are induced by nitrite and appear to duplicate each other in their function as they both form ammonium ions. However, they are the products of two independent genes one of which codes for an NADH nitrite reductase (NADH NiR) the other coding for a formate nitrite reductase (FNiR). The NADH NiR is located in the cytoplasm and has a detoxification function where as FNiR is located in the periplasm generating a

proton gradient, therefore having an energy conservation function. These two NiRs possess a different prosthetic group, NADH NiR having a sirohaem group to which the nitrite binds and the FNiR contains a cytochrome c haem moiety but both are based on iron.

Further types of NiRs exist such as the copper containing and the cytochrome cd1 nitrite reductases. The copper containing enzymes possess two copper molecules at the active site, one of which, the type II copper, binds the nitrite before it is reduced (Godden *et al* 1991). The cytochrome cd1 NiR has been shown in ~ 65% of all denitrifying organisms but in fewer genera than the copper containing organisms. These enzymes consist of two identical subunits of 60KDa each with one haem prosthetic group per subunit.

Along with the reduction of NO_2^- to NH_4^+ it has been suggested that nitrite could be reduced to nitrous oxide (N_2O) via NO by NiR and a NO reductase (Payne 1973). Following the proposal of several models, it was finally shown that nitrite reductases could generate NO from nitrite (Carr *et al* 1989) and that a specific NO reductase enzyme also existed to generate nitrous oxide (Carr and Ferguson 1990).

From the data presented above the nitrite reductase enzymes show similar electron transfer reactions including a NADH activity and the utilisation of iron for activity but seem not to involve the use of molybdenum as the active site for substrate reduction.

1.2.3 Enzyme reactions

Xanthine oxidase mediates a range of reactions and is known for its part in purine metabolism. Equations (1) and (2) below detail the oxidation of hypoxanthine to

xanthine and xanthine to uric acid by XO with the associated cofactors and products.

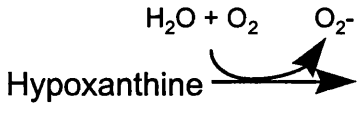

(1)

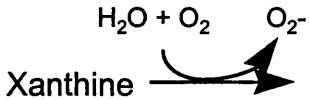

(2)

These reactions are inhibited by blocking the molybdenum centre of the enzyme with purine analogues such as allopurinol and oxypurinol. This reaction occurs in the presence of oxygen as the electron acceptor and is rate dependent on its concentration (Fridovitch and Handler 1962). The Michaelis constant (K_m) for xanthine and hypoxanthine are ~ 6μM under room air conditions and the K_m for oxygen reduction was 27μM and 800μM for the reduction of cytochrome c (Fridovich and Handler 1962).

The oxidation of NADH to NAD+ is shown in equation (3) with the electron again being given to oxygen to produce superoxide radical.

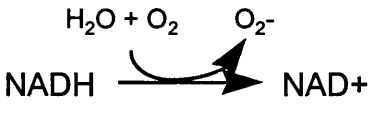

(3)

It has been reported that this reaction is not affected by the molybdenum site inhibitors allopurinol and oxypurinol in the presence of oxygen but is inhibited by NAD+ and also by the FAD specific inhibitor diphenyliodonium (DPI) (Sanders *et al* 1997). The K_m for the oxidation of NADH in both bovine-derived and human milk enzymes was calculated by Sanders *et al* (1997) to be 1.23 and 0.597μM respectively. This reaction was dependent on the availability of oxygen in the absence of any other electron acceptor. The K_m for oxygen utilisation in this

system was not been calculated but it was suggested, by Sanders *et al* (1997) that NADH oxidation was linearly increased over the physiological range in the absence of other electron acceptors.

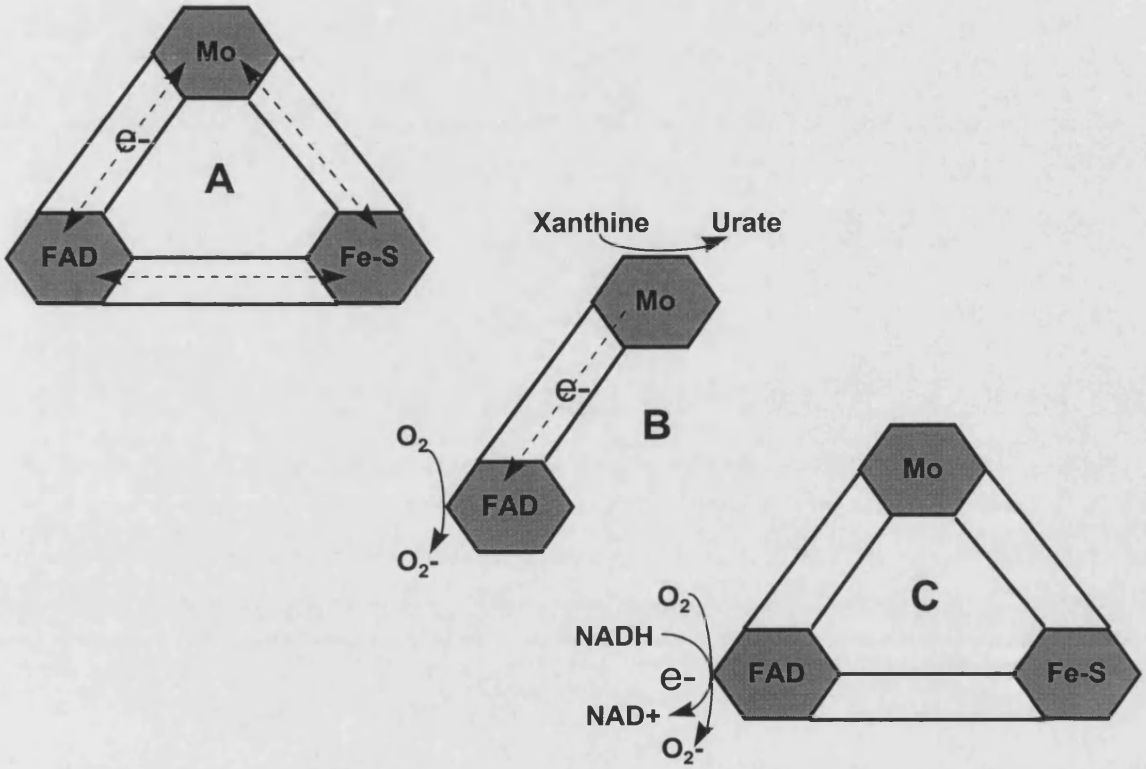

Figure 1.3. Diagrams to show the possible electron transfer through XO enzyme with the oxidation of xanthine or NADH with oxygen as the electron acceptor. **A** shows a generalised scheme of electron transport utilising the three redox centres of the enzyme Mo molybdopterin, FAD flavin centre and Fe-S the iron sulphur centres. **B** details the xanthine to urate reaction with the generation of superoxide anion. **C** shows the oxidation of NADH to NAD+ at the Flavin centre and the generation of superoxide radical.

More recently it has become clear that the XO enzyme isolated from a range of species and tissues show differences in the activities to certain substrates. The bovine milk enzyme is the most commonly studied and differs from certain sources

of the human enzyme in the rate at which it catalyses purines (Parks and Granger 1986 and DeJong *et al* 1990). These investigators showed that the human heart enzyme had reduced activity towards purines whereas the liver enzyme displayed similar activity to that of bovine milk.

It is clear, however, that a range of oxidation/reduction reactions can be mediated by this enzyme using a range of substrates, electron donors and acceptors.

1.2.4 Regulation

Xanthine oxidase is expressed in milk derived from both human and bovine sources. The protein is found associated with the milk-fat-globule membrane (Briley and Eisenthal 1975) during lactation and its expression and activity are regulated by a variety of mediators which is dependent on the cell type.

In the breast tissue during lactogenesis the process is characterised by a series of steps involving proliferation of the ductal buds and increased size and functional activity of the milk secreting alveolar myoepithelial cells. These phases are under the control of hormones and autocrine growth factors such as epidermal growth factor and prolactin. In the mouse the levels of XO mRNA and XO activity are relatively low until soon before the latter stages of pregnancy. This becomes elevated around the time of delivery and remains high until ~ ten days after the litter is removed from the mother after which it falls to pre-pregnant levels (Terao *et al* 1997).

In kidney epithelial cells XO mRNA was induced by cytokine stimulation along with phorbol esters which suggests a role in the signalling cascade for phospholipase C.

XO is the product of a single gene which has been located to chromosome 2 at band p22 where no other purine degrading or oxidase enzymes have yet been

shown (Xu *et al* 1994). The human gene itself is composed of 36 exons which spans at least 60kb and is apparently similar to the mouse gene (Hoidal *et al* 1997). Of particular interest are the responsive elements (RE) which are found upstream from the start codon. They lie inside the promoter region and allow binding of specific transcription factors. Sequences for IL-6 and AP-1 have been identified along with a sequence homologous to the hypoxia inducible factor initiation site at –61 bases from the start codon. This leads to a transcriptional regulation sequence in the promoter which can turn on the gene using a range of stimuli.

So far sequence analysis has not shown response elements for gamma interferon, tumour necrosis factor or IL-1 which are all known to modulate enzyme activity (Hassoun *et al* 1998 and Page *et al* 1998). With all stimuli the modulation in enzyme protein is thought to be at the level of gene expression with activity being modulated in a post-translational manner.

1.2.5 Evolution

The xanthine oxidase sequence homology between species is high (>90%) for bovine and human milk but the enzyme can be found in diverse organisms such as *Drosophila, Micrococcus* bacteria and western palearctic water frogs (Smith *et al* 1967, Hotz *et al* 1997 and Nishino *et al* 1997) where the sequence homology is reduced.

It is the similarity of XO to the enzyme aldehyde oxidase (AO) that suggests an ancient protein. This along with the single gene product and wide distribution in species expressing the protein has led to conservative estimates that the enzyme is older than 400 million years (Hotz *et al* 1997). It is also possible that the enzyme was primordial in that it was generated as the dehydrogenase form during the time before oxygen became abundant (Krenitsky 1978), the rise of AO being due to a

duplication in the XO gene which underwent some rearrangement. The enzymes have similar sizes and substrate specificity but differ in their tissue expression (Terao *et al* 1997).

The generality of the enzyme may therefore have allowed its conservation over evolutionary time where both reducing and oxidising environments were prevalent. It is for this reason that the xanthine oxidase enzyme may function with alternate substrates to generate reactive species of physiological and pathological importance.

1.3 Nitric oxide

Using the search criteria of "nitric oxide" the National library of Medicine Medline catalogue generated nearly 27000 hits (30/3/99). Voted as molecule of the year in 1992, this gaseous molecule has become an area of heightened interest and of a great deal of research (Koshland 1992).

1.3.1 The historical background of NO and physiology

The initial interest in nitric oxide as a physiological mediator came in the mid-1970s from investigations into the role of cyclic nucleotides guanosine and adenosine mono phosphates (cGMP and cAMP) in smooth muscle relaxation. The levels of cGMP were elevated by a potent vasodilator, glyceryl tri nitrate (GTN) in arterial and other tissues (Diamond and Holmes 1975 and Diamond and Blisard 1976). It was hypothesised by Ignarro and co-workers that agents that activate soluble guanylate cyclase should cause smooth muscle relaxation if cGMP was involved. It was also noted that sodium nitroprusside which was unstable in aqueous solution released nitric oxide and was a potent activator of guanylate cyclase. This therefore suggested that nitric oxide should also be a vasodilator.

Using nitric oxide gas and nitrosoguanidine compounds it was demonstrated that a marked relaxation occurred in preconstricted bovine coronary artery (Gruetter *et al* 1979 and Gruetter *et al* 1980). Other chemical agents were also shown to give similar effects including the use of inorganic sodium nitrite (Gruetter *et al* 1981a,b). Furchgott and Zawadski (1980) demonstrated the requirement of the endothelium for relaxation responses in vascular tissues and suggested a humoral factor, a lipoxygenase-derived or free radical species to be the endothelium derived relaxing factor (EDRF). Griffith and co-workers (1984) confirmed the humoral and endothelium-dependent nature of EDRF, but showed evidence against a lipoxygenase-derived species and against EDRF as a free radical in rabbit aortic preparations.

Further to these and other experiments in 1986 both Furchgott and Ignarro independently suggested nitric oxide or a closely related species was responsible for the effects of EDRF (Furchgott 1988 and Ignarro *et al* 1988). The effects of EDRF and NO were compared by Palmer *et al* (1987) on vascular smooth muscle and platelet aggregations and observed that their actions were identical.

1.3.2 Nitric oxide synthase

Following the discovery of the endogenous nitrodilator substance as NO, the mechanism of its formation became and important aspect of research. From experiments on the activated macrophage it was noted that these cells could generate nitrite and nitrate on the addition of L-arginine (Iyengar *et al* 1987). Further to this, the nitrogen atoms in the nitrate and nitrite were shown to come from the terminal guanidino nitrogen atoms of l-arginine by gas chromatography and mass spectroscopy of labelled precursor. Then in 1989 Palmer and Moncada gave evidence of an enzyme-generated source of NO from L-arginine that required

NADPH and calcium and generated L-citrulline as a by-product. The use of NG-monomethyl-L-arginine (L-NMMA) an analogue of L-arginine, caused a reduction in the stimulated release of NO from cultured endothelial cells (Palmer *et al* 1989) and caused an endothelial-dependent increase in vascular tone (Rees *et al* 1989). These data suggested that L-NMMA was an inhibitor of a nitric oxide synthase (NOS) and its effects on vascular tone were as a direct inhibition of NO generation.

1.3.2.1 NOS isotypes

NOS is a cytochrome P450 reductase-like haemoprotein and requires cofactors for the generation of NO. Flavin adenine dinucleotide (FAD), flavin mono nucleotide (FMN) tetrahydrobiopterin and calmodulin are all required and at least three distinct types that catalyse the production of NO have been described.

Type I NOS is a 168KDa protein found in the neurons which has been isolated and cloned (Bredt *et al* 1991). This enzyme is responsible for the calcium-dependent release of NO from neurones and non-adrenergic, non-colinergic nerves and also from skeletal muscle (Nakane *et al* 1993). The activity of type I and type III NOS enzymes is regulated by oestradiol which is a phenomenon observed during pregnancy (Weiner *et al* 1994).

Type II NOS has been shown to respond to bacterial endotoxin or inflammatory cytokines and is an inducible, calcium-independent, 130KDa protein. The rate of NO production is apparently raised over that of the previous two types mentioned and can be localised to macrophages (Lyons *et al* 1992). This isoform has associated with it a tightly bound calmodulin, which removes the requirement for calcium in stimulated NO formation. The induction of Type II NOS has been shown in vascular smooth muscle (Busse and Mulsch 1990) and cardiac myocytes (Schulz *et al* 1992).

Type III NOS is endothelial cell-derived and is a 135KDa protein which is activated by the increase in intracellular calcium concentration within the physiological range (Sessa *et al* 1992). This isoform is unique in that it can be localised to the cell membrane as it contains a N-myristolation site (Sessa *et al* 1993).

1.3.2.2 NOS enzyme reactions

The evidence for NOS has steadily grown and the reaction of L-arginine to L-citrulline has been followed in a variety of tissues. The reaction is given by equation (4).

(4)

The substrates for NOS are L-arginine, oxygen and NADPH (Marletta 1994). L-arginine is synthesised as a product of the urea cycle and circulates in the blood at ~ 100μM (Boger *et al* 1997). In endothelial cells, however, the apparent concentration has been estimated to be in the millimolar range (Arnal *et al* 1995). The apparent binding constant, the K_m for L-arginine and NOS has been calculated as ~ 5μM (Venema *et al* 1996) which suggests that the availability of this substrate is not limiting under normal physiological conditions.

However, Meyer *et al* (1991) and Heinzel *et al* (1992) have described the generation of hydrogen peroxide by purified porcine neuronal NOS at low concentrations of L-arginine. This was followed by the measurement of superoxide anion from purified rat neuronal NOS in a NADPH and calcium calmodulin dependent manner (Pou *et al* 1992). This leads to the possibility of peroxynitrite generation under certain conditions as discussed by Xia and colleagues (1996). Using a kidney cell line and transfecting with a stable rat neuronal NOS with spin-trapping techniques, this group were able to show that a reduction in L-arginine

resulted in the generation of superoxide anion. The simultaneous generation of NO and superoxide leading to the formation of peroxynitrite. It was also noted that under prolonged ischaemic conditions a lack of perfusion would lead to the depletion of L-arginine (Albina *et al* 1988) but the concentration of oxygen may control the rate of production for both products.

Recently the possible mechanism of superoxide generation by neuronal nitric oxide synthase has been suggested by Pou *et al* (1999). It was reported that superoxide could be measured in the presence of saturating levels of L-arginine. This leads to the relative competition for available electrons that can be donated to oxygen or to L-arginine.

The catalytic mechanism of NOS involves the flavin-mediated electron transport from NADPH to the terminal haem, where oxygen is bound and incorporated into NO and citrulline (Marletta *et al* 1988). The relative affinity of L-arginine (K_m ~5μM) compared to oxygen may give clues as to the activity of the enzyme under ischaemic and reduced L-arginine conditions.

1.3.2.3 The effect of oxygen concentration on conventional NOS activity

As can be seen from reaction (4), oxygen is an integral part of the generation of NO from L-arginine. Experiments have been carried out into the effect of oxygen concentration on the rate of enzyme reaction.

In the lung of normal individuals, NO is generated and can be measured in the expired air. Consequently, it has been suggested that NO plays a central role in oxygen-induced vasodilation (Dillon *et al* 1996). The lung contains all three NOS isotypes (Gaston *et al* 1994) and in animal studies NO was suggested as the oxygen sensitive vasodilator (Nelin *et al* 1996). Kantrow *et al* (1997) gave evidence to suggest that hypoxia inhibited NO synthesis in the isolated rabbit lung and

caused vasoconstriction which was reversed on the addition of oxygen to the perfusion system.

In human studies Dweik and colleagues (1998) measured the kinetics of purified NOS enzymes and from measurement of expired NO from subjects breathing a range of oxygen concentrations. They showed that the expired NO concentrations were dependent on the inspired oxygen concentration with a K_m of 190μM (~ 17%sat). From purified NOS II the K_mO_2 was 135μM (~ 10%sat) which, in the lung, covers the likely physiological range of oxygen concentrations. However, in tissues distant from the lung, the apparent oxygen concentration is reduced and this lung-derived NOS activity may therefore be limited.

The apparent activity of neuronal NOS was also studied in relation to oxygen concentration (Abu-Soud *et al* 1996). As discussed previously the NADPH-dependent reduction of bound oxygen will occur in the absence of L-arginine. The electrons donated from NADPH allow the NOS haem iron to bind oxygen which will then generate NO in the presence of L-arginine, or superoxide in its absence (Abu-Soud and Steur 1993). During NO generation, NOS apparently binds NO to the haem iron and generates an inactive ferrous-NO complex which decomposes in the presence of oxygen to ferric-NOS allowing the return of activity (Abou-Soud *et al* 1995). In the absence of oxygen, however, the ferrous NOS is stable and activity is reduced. In the absence of L-arginine NOS catalysed the simple reduction of oxygen and gave an apparent K_mO_2 of 40μM which saturated at 100μM. In the presence of NO the oxygen concentration dependence showed K_mO_2 values of 400μM which saturated at ~ 800μM. It was therefore suggested that the concentration of oxygen controlled the inactive ferrous-NOS, which in turn

controlled the rate of NO generation by altering the affinity of the haem iron binding to oxygen. This may also be a method of self-regulation for NOS-I.

Rengasamy and Johns (1996) used bovine brain, cultured aortic endothelial cells and rat macrophages to generate K_mO_2 values for NOS enzymes. They found a range of apparent values of ~ 25, 8 and 7μM respectively and suggested that pathophysiological conditions would decrease the NO production where oxygen concentrations were limiting.

The apparent difference between the results of Dweik *et al* (1996) and Rengasamy and Johns (1996) may reflect a tissue specific activity for NOS isoforms where adaptation to apparent oxygen concentration regulates the activity of the NOS enzymes.

1.3.3 NOS-independent NO generation

For many years the therapeutic application of nitrate drugs has given relief from angina pectoris by a mechanism which remains obscure. Formation of NO from glyceryl tri nitrate (GTN) has been demonstrated in intact bovine pulmonary and coronary artery and in cultured porcine aortic smooth muscle cells (Bennett *et al* 1994). Both enzymic and non-enzymic methods have been proposed with an unidentified microsomal protein of 160-210KDa from bovine coronary artery mediating NO formation from GTN (Chung *et al* 1992) and the interaction with cysteine at high concentrations of GTN (Feelisch and Noak 1987). The location of nitrate reduction was investigated by Feelisch *et al* (1995). They showed the generation of NO from cultured endothelial cells using oxyhaemoglobin oxidation, cGMP accumulation and the inhibition of platelet aggregation; a bioassay of NO generation. The results suggested that human endothelial cells were capable of

the bioactivation of organic nitrates and to some extent this was via an enzymic mechanism that had some requirement for thiols.

1.3.3.1 Organic nitrate reduction

The organic nitrate nitroglycerin or glyceryl tri nitrate (GTN) a polyol ester of nitric acid was first synthesised in 1846 by Sobrero as an explosive and reported as a therapeutic agent in 1879 by Murrell for the relief and prophylaxis of angina pectoris. This was preceded by the use of the organic nitrite, amylnitrite, in 1857 for the treatment of angina and was the first described use of a nitrovasodilator.

Their mechanism of action is proposed to be dependent on bioactivation once in the circulation, with consequent relaxation of the vessels to reduce the pressure on the heart during an attack of angina. Early work described the effect of nitrate drugs on dog and rabbit arteries (Bogaert and DeSchaepdryver 1968) and further evidence of a mechanism came with the description of the guanylate cyclase enzymes and the effects of azide and other NO donors by Kimura *et al* (1975).

In 1980 Ignarro and colleagues published a possible mechanism requiring the reduction of nitrates intracellularly by sulphydryl donors to form an S-nitrosothiol active intermediate that in turn directly, or by degrading to nitric oxide, activated guanylate cyclase. As discussed above, these and other experiments led to the description of the EDRF and NOS enzyme systems.

1.3.3.1.1 Glutathione S-transferase

Other methods of bioactivation have been suggested. Oberst and Snyder described the metabolism of GTN to inorganic nitrite by rabbit liver homogenates (1951). Using a pig liver enzyme Heppel and Hilmoe (1950) observed that GTN reacted with reduced glutathione to form oxidised glutathione and inorganic nitrite. This led to the suggestion by Needleman and Hunter (1965) that the major route for

GTN transformation appeared to be denitration in the presence or reduced glutathione.

Using liver homogenates Pasodas del Rio (1970) gave apparent K_m values for the reduction of GTN of $1.5x10^{-5}$ M but the reduction of the dinitrate and mononitrates occurred at much slower rates. The final end product of GTN denitration is glycerol but this was not measurable following incubation with readuced glutathione and liver homogenates (Needleman *et al* 1971). In terms of blood pressure depressants GTN was shown to be at least 10 times more potent than glyceryl di-nitrate, 40 times more potent than inorganic nitrite and inorganic nitrate had no measurable effect (Needleman *et al* 1969).

More recently Simon *et al* (1996) measured an inhibition of response of cGMP production from nitrates by the addition of the glutathione S-transferase inhibitor Basilen Blue (BB) by electroporation into porcine epithelial kidney cells. Using an alternative inhibitor of GST, ethacrynic acid, Kenkare and Benet (1993) on rabbit aortic strips were able to inhibit relaxation responses to GTN treatment and also to inhibit the increase in cGMP generation. Nigam *et al* (1993) using the GST inhibitors Basilen Blue, bromosulphophthalein, Rose Bengal, haematin, chlorotriphenyltin and (octyloxy)benzoylvinylglutathione were able to show no inhibition of rabbit aortic strip relaxation by GTN when the strips were pre-constricted by phenylephrine. In contrast, both Basilen Blue and bromosulfophthalein significantly inhibited GTN-induced relaxation of potassium-contracted aortic strips and Basilen Blue significantly inhibited GTN biotransformation in aortic strips pre-exposed to 25mM potassium. This was suggested to be due to a more favourable electrochemical gradient for entry of the inhibitors into membrane-depolarized tissues.

1.3.3.1.2 Cytochrome P450

Evidence for the role of NADPH-cytochrome P450 reductase (cyt P450) system in the biotransformation of organic nitrates has been obtained using hepatic microsomes (Servent *et al* 1989) to generate NO in the presence of NADPH and GTN. NADPH-dependent biotransformation of GTN in rat aortic microsomes was inhibited by SKF525A, carbon monoxide and oxygen (McDonald and Bennett 1993). Furthermore, GTN-induced relaxation is enhanced under low oxygen conditions and in aortae from animals treated with inducers of cytochrome P450 (Bennett *et al* 1992a). However, using inhibitors of cyt P450 in intact blood vessels, evidence has been shown to have both a positive and negative outcome. Treatment of blood vessels with the classical cyt P450 inhibitors SKF525A, metyrapone, cimetidine or carbon monoxide did not affect the GTN-induced relaxation or GTN biotransformation. This suggests that either cyt P450 is not involved in the mechanism of GTN biotransformation, or that isoforms not sensitive to the inhibitors used are present (Bennett *et al* 1992 and Liu *et al* 1993).

Using the cyt P450 substrate, 7-ethoxyresorufin (7-ER) and the flavoprotein inhibitor diphenyleneiodonium (DPI), it was reported that a substantial inhibition of GTN-induced relaxation occurred and these compounds also reduced cGMP accumulation and inhibited transformation of GTN to 1,2-GDN (Bennett *et al* 1992b and Oyekan *et al* 1991).

DPI, however, is not specific for any one flavoprotein, it is also known to inhibit neutrophil NADPH oxidase (Hancock and Jones 1987) and the NADH oxidase activity of xanthine oxidase (Sanders *et al* 1997). It has additionally been reported to affect potassium and calcium currents in isolated pulmonary smooth muscle cells (Weir *et al* 1994) and its use in organ based bioassays must be treated with caution.

1.3.3.2 Nitrate and nitrite reduction *in vivo*

Over recent years it has become apparent that other mechanisms of NO generation exist under normal physiological and pathological conditions or through the utilisation of reducible, naturally occurring substrates. Nitrite is such a substrate that may be reduced to NO in the body.

Zweier *et al* (1995) pointed out the non-enzymic reduction of nitrite to NO in the ischaemic heart. It was shown that the acidotic nature of the ischaemic heart led to a reducing atmosphere that caused the reduction of nitrite to NO. This NO generation was independent of NOS and NOS inhibitors had only minimal effects on the NO generated. Using labelled nitrite ions they were able to demonstrate that nitrite can be reduced to NO in this model and was negatively correlated with intracellular pH and the production of NO with a threshold for NO detection at pH6.

Human saliva contains both nitrate and nitrite. Dietary nitrates, which are derived from green leafy vegetables, are absorbed in the gastrointestinal tract (Tannenbaum *et al* 1976). Apparently nitrate is concentrated in the saliva up to 25% of circulating levels and is secreted during salivation (Spiegelhalder *et al* 1976). The reduction of salivary nitrate to nitrite by bacteria on the tongue has been described by Duncan and colleagues (1995) and this source of nitrite could be reduced to NO in the stomach following reduction in the acid conditions found in the adult (Lundberg *et al* 1994). Levels of nitrite in the stomach have been measured at 14ppm in the fasting subjects, which was increased to ~ 90ppm following the ingestion of nitrate (McKnight *et al* 1997). It was suggested then that the reduction of nitrate by commensal bacteria on the tongue generate nitrite which will then be reduced further to NO in the acidic environment of the stomach.

This generation of NO was also described on the skin surface. Weller *et al* (1996) were able to increase the NO generated from skin by the topical addition of nitrite or by acidification of the skin. This was not inhibitable by classical NOS inhibitors and was suggested to follow a similar mechanism to the generation of NO in the stomach from nitrite utilising commensal nitrate reducing bacteria.

1.3.4 Reactions of nitric oxide

The accumulation of nitrate and nitrite in the body may be through ingestion but also from the reaction products of NO itself. Nitric oxide will react with a range of compounds, dependent on the particular environment and available reactants.

1.3.4.1 NO reaction with oxygen

The best known gas-phase reaction of NO is its conversion to nitrogen dioxide (NO_2) given in reaction (5).

$$2NO + O_2 \longrightarrow 2NO_2 \quad (5)$$

This reaction occurs rapidly at apparently high concentrations and forms characteristic brown fumes (Butler *et al* 1995). However in the aqueous phase, the reaction of NO and molecular oxygen is slow with a half-life of several hours (Wink *et al* 1993). The suggested physiological half-life of NO, ~ 3 to 50 seconds (Moncada *et al* 1988) in solution, rules out its oxidation by molecular oxygen (Kharitonov *et al* 1994).

NO_2 reacts with water to give a mixture of nitrate and nitrite although it is suggested that nitrite is the major product obtained from this reaction (Wink *et al* 1993). The reaction of NO with NO_2 is supposed to occur quite readily to produce N_2O_3, an anhydride of nitrous acid (Equations (6) and (7)).

$$NO_2 + NO \longrightarrow N_2O_3 \quad (6)$$

$$N_2O_3 + H_2O \longrightarrow 2HNO_2 \quad (7)$$

The oxidation of NO_2^- to NO_3^- occurs readily especially in the presence of oxyhaemoglobin (Spagnuolo *et al* 1987).

1.3.4.2 With nitrosothiols

These compounds contain NO and have received attention in discussions concerning EDRF and the physiological role of NO (Feelisch *et al* 1994). Nitrosothiols can occur in human plasma as the nitrosothiol of human serum albumin (Stamler *et al* 1992) but no particular function was assigned to them in this study. The biosynthetic generation of these nitrosothiols has also come under some scrutiny. It was suggested by Ignarro and Gruetter (1980) that NO reacts with thiol at ~ pH7. However more recent evidence has suggested that the required species is the nitrosonium ion (NO+) but this also has its problems in that it is reported as a transient species in solution at pH7. Pryor *et al* (1982) were able to use NO_2 as the reactant with thiol to produce nitrosothiols. However, this is also an unlikely biosynthetic mechanism due to the slow rate of NO_2 formation from NO and molecular oxygen in solution (Lewis and Deen 1994).

More recently the possible interaction of peroxynitrite with excess NO may cause the production of the nitrosonium ion, as peroxynitrite can cause one electron oxidations, which may then go on to form nitrosothiols by a nitrosation reaction (Pryor *et al* 1994). Peroxynitrite itself is apparently not capable of this nitrosation reaction but in the presence of metal catalysts it can act as a nitrating agent (Beckman *et al* 1992).

1.3.4.3 With iron to form iron-nitrosyls

The reaction of NO with iron is possibly the most significant in terms of biological activity. It is the reaction of NO with iron in guanylate cyclase that allows its activation (Craven and DeRubertis 1978). The related reaction is the binding of NO to haemoglobin to form nitrosylhaem and this has been extensively studied due to the electron paramagnetic spectrum that is generated (DeRubertis *et al* 1978). As the switch for guanylate cyclase activation, NO binding to haem must be reversible and this is apparently the case (Henry *et al* 1991). This is important with respect to the active site of many haem-containing oxidase enzymes, including NOS.

The binding of NO to biological non-haem iron has also been reported. The inhibition of nitrogen fixation has been observed by the binding of NO with iron-sulphur (Fe-S) clusters of nitrogenase enzymes using electron paramagnetic resonance spectroscopy (EPR) (Meyer 1981 and Henry *et al* 1993). The binding of NO to Fe-S to form the Fe-S-NO adduct contrasts with NO-haem binding in that it usually causes the destruction of the Fe-S cluster. This method has been suggested as the cytotoxic mechanism for NO action on key enzymes, especially the inhibition of cytoplasmic aconitase (Gardner *et al* 1997).

1.3.4.4 With superoxide to form peroxynitrite

In recent years it has become apparent that the reaction of NO with superoxide radical is possibly the most likely reaction to occur *in vivo*. Peroxynitrite is a strong oxidant and the cytotoxicity previously ascribed to NO or superoxide alone may actually be due to their reaction and degradation products. The reactions are shown below

$$NO + O_2^- \longrightarrow ONOO^- \quad (8)$$

The reaction occurs at a rate constant near the diffusion-controlled limit (Huie and Padmaja 1993). The rate constant for peroxynitrite formation has been calculated by a variety of methods and the most recent figure was measured by Kissner *et al* (1997) using laser flash photolysis. By subjecting peroxynitrite to a burst of laser energy superoxide and nitric oxide is formed. By measuring the rate of recombination to form peroxynitrite the rate of reaction has been calculated as 1.9 $\pm 0.2 \times 10^{10}$ M^{-1} s^{-1}. This is important when assessing the reaction characteristics of nitric oxide and superoxide when other reactions may occur. The reaction of superoxide with superoxide dismutase would reduce the production of ONOO- but the rate constant for superoxide with SOD is given as $2x\ 10^{9}$ M^{-1} s^{-1} (Huie and Padmaja 1993). The rate of reaction of NO with haem compounds varies depending on the nature of the haem. For example myoglobin has a rate constant ranging from 10^{3} to 10^{7} M^{-1} s^{-1} depending on the source of the myoglobin. The rate constant also varies with the type of haem, ie ferrous or ferric in nature, with ferrous compounds having rate constants ~ $2x\ 10^{7}$ M^{-1} s^{-1}. The relative reactions are therefore dependent on the concentrations of NO, superoxide, SOD and haem compounds in the general milieu (Pryor and Squadrito 1995).

Peroxynitrite itself, apparently exists in equilibrium with its conjugate acid peroxynitrous acid (ONOOH) at pH 7.2. The decomposition of ONOO- is complicated (Pfeiffer *et al* 1997), as the anion is stable in alkaline conditions but decays rapidly to ONOOH at physiological pH with a pKa 6.8 (Radi *et al* 1991 and Koppenol *et al* 1992). Three pathways of ONOOH decomposition have been proposed. It was suggested by Beckman *et al* (1990) that ONOOH decomposes to form hydroxyl and NO_2 radicals based on the sensitivity of peroxynitrite induced reactions to hydroxyl radical scavengers. This was independently supported by EPR data suggesting evidence of free hydroxyl radicals on decomposition of

peroxynitrite (Pou *et al* 1995). However Koppenol *et al* (1992) concluded from molecular dynamic calculations that homolytic cleavage of ONOOH was improbable. This led to the hypothesis by Pryor *et al* (1996) of a caged radical form of ONOOH - ONOOH* which decomposes to radical species that rapidly react again due to the viscosity of the surrounding media and the diffusion limited reaction. They also suggested that ~ 99% of the caged radicals [HO' 'NO_2] would return to reform ONOOH and just ~ 1% would form nitrate, the isomer of ONOO-.

A third decomposition mechanism was suggested by Pfeiffer *et al* (1997) suggesting that the decomposition of authentic peroxynitrite prepared by two different methods produced nitrite and oxygen in a 2:1 stoichiometry at pH7.5. It was suggested that this mechanism was due to the reaction with ONOO- to form biologically active metabolites which may contribute to physiology and/or pathology of NO and superoxide.

The metabolic generation and fate of peroxynitrite remains an area of intense study with many complex reactions and interactions occurring. The physiological actions of nitric oxide and superoxide or peroxynitrite are leading to a reassessment of their individual and combined activities.

1.3.5 NO in physiology and pathology

The physiological role of NO has been studied since the mid-1970s due to its effects on guanylate cyclase and on smooth muscle relaxation. The pathological role of NO has been noted previously as a toxic gas and a constituent of smog formation from exhaust fumes and industrial pollution.

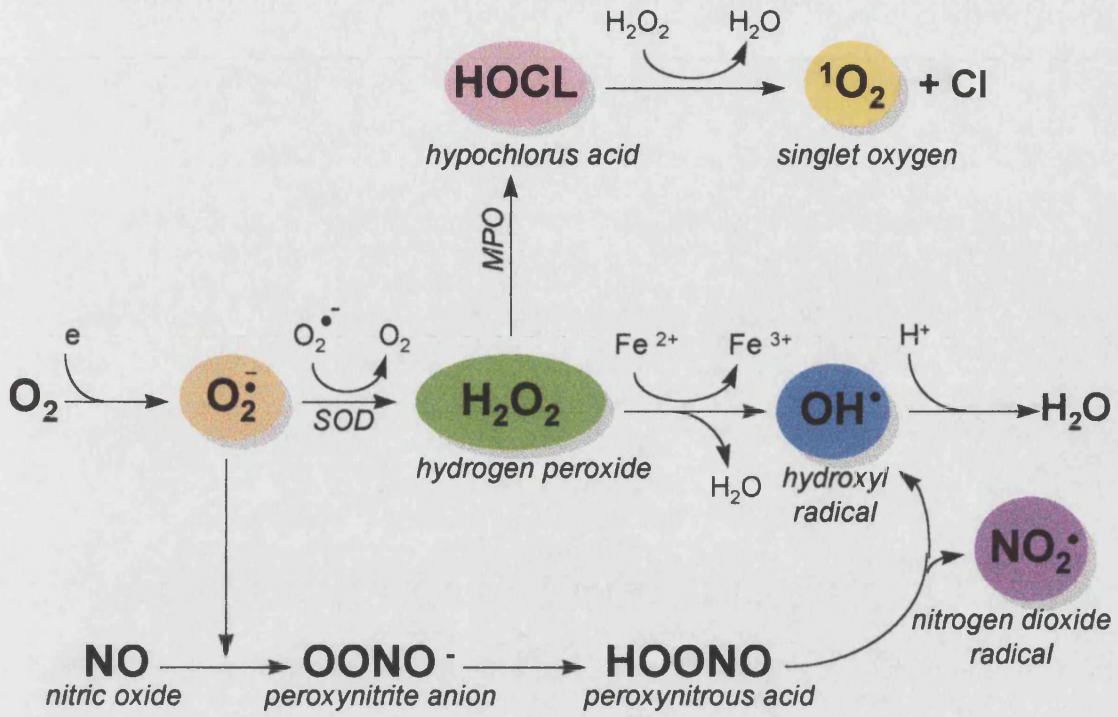

Figure 1.4. Summary of the possible reaction products of nitric oxide and superoxide with some of the breakdown products and metabolising enzymes.

Sir Humphry Davy in 1800 showed the toxicity of NO during experiments on the effectiveness of inhaled gases for relief of asthma in his work on nitrous oxide. The paradoxical actions of nitric oxide may come down to the particular concentration and duration of production and also on the availability of molecular targets and reactions with other available substrates (Laurent *et al* 1996).

The concentration of NO that causes a physiological or pathological effect *in vivo* has been difficult to elucidate. The apparent K_m for NO binding to guanylate cyclase enzyme is in the nanomolar range and the steady state concentration of NO of ~ 4-5μM can be reached in the immediate vicinity of a cell monolayer (Laurent *et al* 1996). The diffusion distance of NO secreted by a single cell has been calculated to be 150 – 300μm in 4 – 15 seconds but the concentration over the larger distances will be diluted (Lancaster 1994). The focal nature of cellular

toxicity was demonstrated by Steiner *et al* (1997) using activated macrophages or islet endothelial cells to cause the lysis of syngeneic islet cells within 15 hours with ~ 15 – 40μM NO over that time. It is therefore possible that the nature of NO actions is dependent on the relative concentrations of the NO produced, with higher concentrations responsible for pathological actions.

1.3.5.1 Regulatory role

The regulation of vascular tone has been dealt with previously in this chapter as it was the first description of NO generation in a physiological role. The generation of continuous amounts of NO from endothelial cells allows relaxation of the vessels and the control of both local and systemic blood pressure.

Penile erection is apparently regulated by the oxygen sensitivity of NOS enzyme in the corpus cavernosum. On stimulation the oxygen tension in the corpus cavernosum is increased from a near venous level to an arterial level of saturation (Azadzoi *et al* 1995). The trabecular smooth muscle of the corpus cavernosum is stimulated by NO and relaxation of smooth muscle occurs. Endogenous NO generation is regulated by the oxygen concentration ~ 25mmHg in the flaccid penis compared to the relaxation induced by the addition of endogenous nitric oxide which was oxygen concentration independent ~ 100mmHg (Kim *et al* 1993).

Previously in this chapter the use of organic nitrates was discussed in terms of their bioactivation to NO *in vivo*. These drugs are used in a clinical setting for the relief of angina pectoris. The major effect of the organic nitrates is in the modulation of blood pressure to reduce the load on the heart itself. Their action tends to be greatest in the venous circulation followed by the coronary arteries and at high concentrations they have effects in the arterial system (Ghio *et al* 1992). Their combined response is to cause a reduction in venous return and an augmentation

in coronary flow and these effects are most pronounced in the poststenotic collateral vessels (Abrams 1980 and Brown *et al* 1981). The net result of venodilation and coronary vasodilation is a decrease in ventricular filling pressure and in wall tension and an augmentation in coronary flow. The oxygen demand is reduced and improved oxygen delivery occurs particularly in ischaemic regions (Vatner *et al* 1972).

The organic nitrates also appear to have antithrombotic properties. Loscalzo (1992) was able to demonstrate the inhibition of platelet aggregation with GTN. GTN, or a metabolite of it, causes the activation of guanylate cyclase in the platelet and increases cyclic guanosine monophosphate (cGMP). This is accompanied by inhibition of agonist-mediated calcium flux and reduction of fibrinogen binding to the glycoprotein IIb/IIIa receptor. This system was also seen to reduce platelet adhesion to damaged intimal linings (Lam *et al* 1988) and can possibly dissolve platelet aggregates (Stamler *et al* 1989).

1.3.5.2 Protective role

The antioxidant role of NO comes from its reaction with oxygen, carbon and nitrogen centred radicals and can be seen to have a scavenger role under a range of conditions (Grisham *et al* 1999). This is because of the unpaired electrons of NO which react rapidly with alkoxyl and alkyl hydroperoxyl radicals at near diffusion reaction rates ($2x10^9$ $M^{-1}s^{-1}$ Padjama and Huie 1993). It is these reactions that have been suggested to have a modulatory role in enzyme- or metal-catalysed lipid peroxidation (Rubbo *et al* 1994).

Peroxidation of polyunsaturated lipids is thought to be an important pathological event involved in the development of tissue damage and dysfunction. In recent studies, Rubbo and colleagues (1994) demonstrated that NO inhibits lipid

peroxidation and therefore may be important in the modulation of the inflammatory response by inhibiting the formation of proinflammatory lipids.

The iron or haemoprotein catalysed oxidative reactions may mediate the responses associated with acute and chronic inflammation. In the post-ischaemic, reperfused heart the role of oxidant stress has been linked with increases in leucocyte adhesion and transendothelial cell migration from oxidant production within the microcirculation (Grisham *et al* 1998). This is probably caused by an increased expression in adhesion molecules or the fixation of transiently expressed adhesion molecules by the peroxidation of membrane lipids which reduces membrane fluidity (Beaudeux *et al* 1997 and Kurose *et al* 1997). This oxidant stress may also lead to apoptosis induction, DNA damage, inflammatory mediator synthesis and regulate gene expression (Granger and Kubes 1996, Grisham *et al* 1998 and Wink and Mitchell 1998).

NO was shown by Kanner *et al* (1991) to inhibit iron-catalysed oxidation reactions by binding to ferrous complexes. It was also shown (Miles *et al* 1996) that NO inhibited the superoxide driven Fenton reaction which, in the presence of iron, generates hydroxyl radical (OH) *in vitro*. By adding varying amounts of NO to a Fenton reaction process the hydroxylation of benzoic acid was reduced. This demonstrates that depending on the fluxes of the different reactive species, NO may have an antioxidant capability.

1.3.5.3 Deleterious role

In an almost reverse manner to those mentioned above, the reaction of NO with oxidants may lead to the generation of toxic compounds that may cause cellular damage. NO itself has been suggested as an enzyme inhibitor. This has been suggested as having a direct effect by binding to enzymes or by inhibition of

enzyme assembly processes. The pig neutrophil NADPH oxidase is one such system where the assembly process is inhibited by NO. Fujii and colleagues (1997) were able to demonstrate neutrophil NADPH oxidase inhibition which was not due to direct interaction of NO and enzyme nor to the reaction of peroxynitrite with the enzyme, but was greatly enhanced during the assembly process.

Direct reaction of NO with enzymes has been shown for cytochrome c oxidase (cyt c oxidase). The reaction of NO with the binuclear metal centre of cyt c oxidase apparently leads to the formation of nitrite at the active site (Torres *et al* 1998) the mechanism of which was described as the opposite of nitrite reduction to NO by non-haem nitrite reductases (Averill and Vincent 1993). The inhibition was caused by the binding of NO to the reduced copper centre of the enzyme rather than the expected reaction with Fe^{2+}.

Nitric oxide binding to the aconitases and specifically the four iron - four sulphur (4Fe-4S) domain of mammalian cytoplasmic and mitochondrial enzymes has been suggested to be part of pathology (Gardner *et al* 1997). These are inorganic prosthetic groups whose iron atoms are co-ordinated to inorganic sulphides and usually liganded to protein by cysteine thiolates (Drapier 1997). By co-culturing L10 hepatoma cells with NO producing mouse macrophages, Drapier and Hibbs (1986) were able to show that there was a hierarchy in sensitivity of the mitochondrial Fe-S-containing enzymes. Aconitase was most sensitive to NO, followed by complex I and complex II, with complex III unresponsive to NO treatment. This gradation in sensitivity to NO was suggested as being caused by access to the cluster, or by the interaction of NO with the ligands that anchor the cluster to the protein.

The reaction of NO with iron, Fe-S and haem proteins leads to the possibility that there may be regulation of certain protein activities due to the binding of NO. NO

generation itself relies on the binding of oxygen and nitrogen to the haem moiety of NOS enzymes. NOS activity has been linked to the binding of NO to haem iron of neuronal NOS in both the ferrous and ferric states under anaerobic conditions to generate a stable NOS haem iron-NO complex (Abu-Soud *et al* 1995). This binding caused an inhibition in NO generation from NOS and may therefore be a method of NO regulation. In fact, the same group (Abu-Soud et al 1996) has also suggested this in the case of oxygen availability as a regulator of NOS activity. In this case the rate of the ferrous NO complex breakdown in neuronal NOS was dependent on oxygen concentration. It is this complex breakdown that is vital for enzymic turnover with the ferrous NO complex remaining stable at low oxygen concentrations.

Over production of NO can lead to mutagenesis and cell death and has been shown to be mutagenic in a variety of systems (Burney *et al* 1999). These range from mutations in *E. coli* and human cell lines (Routledge *et al* 1993) to an *in vivo* mouse model (Gal and Wogan 1996). Using cell lines as an *in vitro* model of NO toxicity, a range of pathways have been identified from inhibition of DNA synthesis, mitochondrial damage, apoptosis, cell cycle distribution changes and DNA strand breaks (Burney *et al* 1997). An effect on ribonuclease reductase activity has also been shown, which seemed only to be temporary in nature and the activation of poly(adenosine 5'-di-phosphoribose) synthetase has also been attributed to both NO and ONOO- (Burney *et al* 1999).

The formation of the anhydride (N_2O_3) from equation (6) can lead to both direct and indirect DNA damage. Direct action results from nitrosation of primary amines on DNA bases which leads to deamination and at physiological pH, N_2O_3 has been demonstrated to be the most important species (Lewis *et al* 1995). Indirect actions are due to mutations that can arise from the deamination of bases where guanine

deaminates to xanthine, mispairing of which can cause a G:C to A:T transition which will ultimately lead to single strand breaks (Lindahl and Andersson 1972).

The action of ONOO- on DNA rather than deamination is oxidative and ONOO- addition leads to more damage than treatment with an equivalent amount of NO. The spectrum of ONOO- damage is also increased over NO, which is probably accounted for by their relative reactivity. The addition of ONOO- to naked plasmid DNA can cause strand breaks using as little as 2-5μM compared to no detectable strand breaks in NO treated plasmids at millimolar concentrations (Kennedy *et al* 1997 and Tamir *et al* 1996).

(The effect of ONOO- on DNA damage will be discussed further in chapter 3 and is refered to here to complete the possible deleterious effect of NO on DNA).

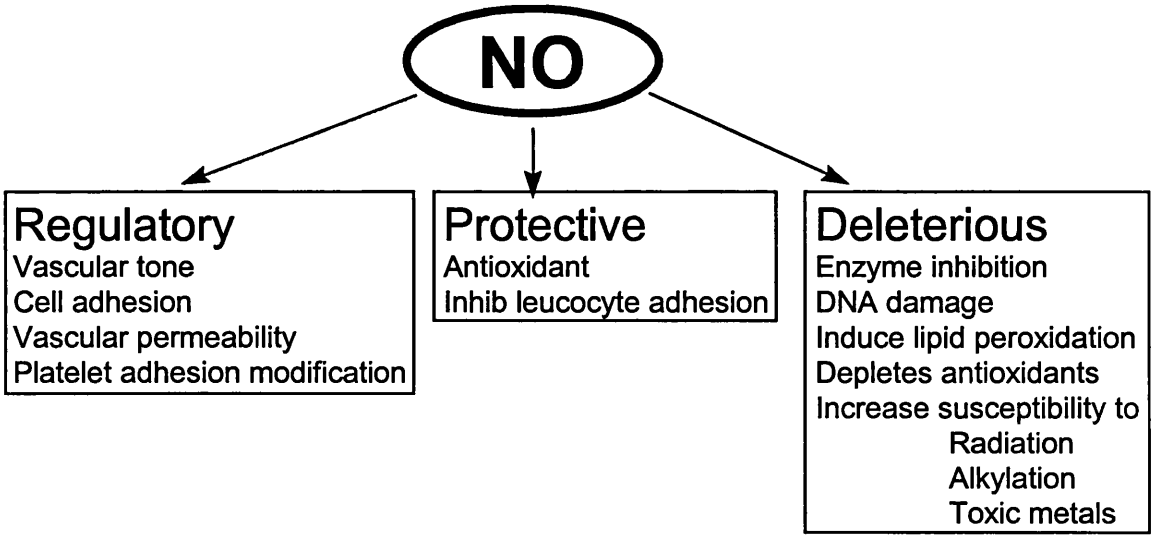

Figure 1.5. Summary of the possible physiological and pathological effects of NO generation. After Grisham *et al* 1999.

1.4 Bacterial infections, enteritis and scours

1.4.1 Bacterial infections and their diseases

1.4.1.1 Introduction

In 1990 it was estimated that 4,123 million of the greater than 5,000 million global population (~78%) lived in developing countries. Of the 40 million deaths in these countries ~ 9 million were estimated to be caused by infectious and parasitic disease; diarrhoeal infections being the fourth most common cause of death worldwide. Apparently, 98% of deaths in children occur in the developing countries and most of those as a result of some form of infection (Murray and Lopez 1997). Diarrhoeal disease is a major cause of mortality and morbidity in developing countries (Turnidge 1998). Rotavirus infections are an important cause of the disease in infants, whereas bacteria are the most common pathogens in older children and adults (Cunliffe *et al* 1998).

1.4.2 Disease-causing pathogenic bacteria

1.4.2.1 *E. coli*

E. coli are Gram-negative, rod-shaped bacteria belonging to the family Enterobacteriaceae. There are currently four classes of enterovirulent *E. coli* that cause gastroenteritis in humans. These are the enterotoxigenic, enteropathogenic, enterohaemorrhagic and the enteroinvasive *E.coli*. While all cause a similar type of disease on infection in humans it is the enteropathogenic (EPEC) strains which are most prevalent. These bacteria cause their infection using mechanisms separate to the generation of toxins as compared to the enterotoxigenic strains.

Infections are sporadic in nature and therefore the source of infection is often difficult to identify. Human, bovine and swine can be infected by this group of bacteria but all contain commensal strains in their gut flora that may prevent further infection by pathogenic organisms

The disease most often associated with this type of infection is infantile diarrhoea. EPEC cause either a watery or bloody diarrhoea, the former associated with the attachment to, and physical alteration of, the integrity of the intestine (Donnenberg and Kaper 1992, Donnenberg *et al* 1995). Bloody diarrhoea is associated with attachment of the bacteria and an acute tissue-destructive process, apparently caused by a toxin similar to that of *Shigella dysenteriae*, also called verotoxin. In most of these strains the shiga-like toxin is cell-associated rather than excreted (Frankel *et al* 1998).

The infective dose is presumed to be low in infants under 6 months old as the infectivity of these bacteria is high. The infectivity, however, is reduced as the host ages and adults are only infected with high doses following stomach acid neutralisation with bicarbonate (Levine *et al* 1978). Common causes of outbreaks include infected beef and chicken, although any food associated with faecal to oral contamination may harbour these strains. The passage of bacteria from infected infants can be through contaminated bed linen, toys and towels and was suggested to be present in dust and transmitted by aerosols (Rogers 1951). Infected but asymptomatic mothers and carers have been implicated in the continuation and spread of a particular outbreak in hospitals and nurseries from a single infected infant (Bower *et al* 1989, and Wu and Peng 1992). However, vehicles of contamination are often weaning foods and formulas.

In the developed countries, the frequency of EPEC infection has apparently dropped since the 1940s and 50s, where mortality rates of up to 50% were

common in explosive community acquired outbreaks (Robins-Browne 1987). However, in developing countries EPEC is still a major cause of infant diarrhoea and particularly in the 0-6 month age group. Up to 40% of infant diarrhoea has been attributed to EPEC infections in a variety of countries (Brazil, Mexico and South Africa) and settings (hospitals and rural environments) (Nataro and Kaper 1998).

It has also been noted that breast-feeding is protective against diarrhoea caused by EPEC (Rothbaum *et al* 1982 and Blake *et al* 1993). Both colostrum and milk strongly inhibit the adhesion of EPEC to an epithelial cell line HEp-2 in vitro with activity being found in both sIgA and oligosaccharide fractions (Cravioto *et al* 1991 and Camara *et al* 1994). Also a variety of antibiotics have been used to treat EPEC and have reduced the severity of infection, however, multi-antibiotic-resistant strains are becoming more common (Mietens 1997).

1.4.2.2 Salmonella species

Salmonella is a rod-shaped, motile bacterium – non-motile exceptions are *S. gallinarum* and *S. pullorum*, nonsporeforming, stains negative in Gram stain and of the genus bacteriaceae. There is a widespread occurrence in animals, especially in poultry and swine. Environmental sources of the organism include water, soil, insects, factory surfaces, kitchen surfaces, animal faeces, raw meats, raw poultry, and raw seafoods, to name only a few (Tauxe 1998).

The acute symptoms of infection include nausea, vomiting, abdominal cramps, diarrhoea, fever, and headache. Chronic consequences may show arthritic symptoms up to 3-4 weeks after the onset of acute symptoms. The onset time from ingestion is 6-48 hours and the infective dose can be as low as 15-20 cells; depending on the age and health of the host and strain differences among the

members of the genus. The duration of acute symptoms may be 1 to 2 days or may be prolonged, again depending on host factors, ingested dose, and strain characteristics. All age groups are susceptible, but symptoms are most severe in the elderly, infants and the infirm. AIDS patients suffer salmonellosis frequently (estimated 20-fold more than general population) and suffer from recurrent episodes (Mathews *et al* 1998).

The actual cause of these symptoms and disease are due to the penetration and passage of *Salmonella* organisms from the gut lumen into the epithelium of the small intestine where inflammation occurs. There is evidence that an enterotoxin may be produced, perhaps within the enterocyte (Hamzaoui and Pringault 1998 and Raupach *et al* 1999).

It is estimated that from 2 to 4 million cases of salmonellosis occur in the United States (U.S.) annually. The incidence of salmonellosis is apparently rising both in the U.S. and in other industrialised nations. *S. enteritidis* isolations from humans have shown a dramatic rise in the past decade, particularly in the northeast United States (6-fold or more) and the increase in human infections is apparently spreading south and west, with sporadic outbreaks in other regions (Djuretic 1997).

1.4.3 Resistance to treatment

Since the isolation of antibiotics in the 1930s and '40s, the first line of treatment for bacterial infections has been through their administration for a variety of infectious diseases. So much so that soon after their introduction the first signs of resistance began to emerge (Moellering 1995). Since that time, further antibiotics have been developed by modifications of the original penicillin and the generation of other molecules but resistance has also become a problem with these forms as well (Harrison and Svec 1998).

Resistance develops from an interplay of micro-organisms, infected people or livestock and the particular environment including antibiotic use and infection control procedures in which the two are found (Struelens 1998). Hospitals and particularly intensive care units are an important environment for the development and spread of resistant bacteria. The reason for this is the high doses of antibiotics in use in conjunction with a high concentration of people including attendant staff giving an enhanced potential for cross infection (Gold and Moellering 1996).

The molecular basis of resistance relies on four basic mechanisms: Antibiotic modification, blocking antibiotic entry or removal at a rate higher than uptake, alterations to the target rendering the antibiotic less efficient and by the production of an alternative target (Hawkey 1998). Resistance can be intrinsic or acquired. This may arise by spontaneous mutation of the genome in the presence or absence of antibiotic to leave a particular bacterium with an advantage over non-mutant types. DNA can also be acquired from resistant bacteria in the form of plasmids. These are pieces of DNA outside of the host genome that can confer resistance on the recipient that was once sensitive to a particular antibiotic. The overuse of antibiotics forces this bacterial evolution by selecting out those individuals that are resistant to the strategy in use.

1.4.4 Use in animals

The first use of antibiotics in the veterinary field was to treat mastitis (Foley *et al* 1946). In the United Kingdom (U.K.), antibiotics have been used in the livestock industry as veterinary medicinal products to treat or prevent animal disease or as zootechnical feed additives to aid feed conversion. Diseases most often requiring anti-microbial drugs are respiratory and enteric diseases in pigs and cattle and mastitis in dairy cattle (Johnston 1998). In the U.K. in 1997, there were a total of

1,900 drugs under licence for use in animals with a market value of £379 million. Anti-microbial agents, both for farm and pet animals, totalled some £80 million with growth promoters for foodstuffs valued at £12 million (Johnston 1998).

The prophylactic use of antibiotics had raised questions as to their efficacy, their concentration in the food chain and the possibility of the development of antibiotic resistance in the animal, in turn causing resistance in human borne diseases. The Swan report of 1969 was the first inquiry into these problems by the Joint Committee on the Use of Antibiotics in Animal Husbandry and Veterinary Medicine (MAFF 1998). This issue was raised again with the banning of several antibiotics, for use as growth promoters, by the European Community including Avoparcin in 1997.

Avoparcin was used as a growth promoter when added to feed to increase its utilisation in animals. In 1995, Denmark and then Germany in 1996 banned the use of avoparcin. This was due to concerns that avoparcin overuse was not only leading to an increase in resistance against itself as an anti-microbial but also to a similar antibiotic vancomycin which is still used in human medicine. As vancomycin is used as an antibiotic of "last resort" in humans for a number of pathogenic bacteria the loss of its efficacy due to resistance would be an important factor (Woodford 1998).

1.4.5 Measures to counteract resistance

To overcome resistant strains of bacteria, a range of strategies have been introduced. It has been suggested (Murray 1994) that a prime aim is to reduce the use of antibiotics by greater education on their effectiveness, regulatory measures on their availability, public health surveillance to reduce outbreaks and further research into alternatives.

The apparent fitness of bacterial strains may also be an area for exploitation by using a particular treatment that may combat resistance. It has been noted that in the absence of antibiotic, some resistant strains of bacteria are not as fit as the wild type, non-resistant strains (Levy 1994). By the removal of the antibiotic, the resistant strains will be out-competed by the non-resistant strains until the main infectious agents will consist of the antibiotic-sensitive bacteria. The antibiotic can then be reintroduced and the drug regains its efficacy. However, the above set of experimental observations apparently did not take into account the effect of multiple generations and "forced evolution" (Lenski 1997). Cells which are transfected with a resistance plasmid do not compare well with the wild-type in the absence of the antibiotic to which it now has resistance to. Over time however, the resistant strain begins to evolve a strategy to overcome this short fall and over ~ 500 generations will compete with the wild-type as effectively without the antibiotic present (Spratt 1996 and Schrag *et al 1997*).

The reduction in drug usage over time may still mediate an effect in a mixed population with reversions back to the resistant wild type but at a much slower rate than was previously thought. Work by Levin *et al* (1997) using mathematical models of population growth shows an increased likely hood of reversion only if the sensitive strains have some advantage. This may be in the form of reduced drug concentrations and helped by the relative proportions of sensitive and resistant strains in the population.

Therefore, along with the education and surveillance strategies suggested above, alternative treatments are required.

With the growing calls for a reduction in the use of antibiotics, other strategies need to be sought. Education and surveillance strategies will work in the medium to long

term, but it is what to do in the meantime to combat infection whilst the long-term measures begin to show their effects.

1.5 Effectiveness of human milk

As was described above, infantile diarrhoea is a major cause of illness in the 0-6 month age group. The prevalence of disease has been linked to the use of formula feeds made up with contaminated water (Hart and Cunliffe 1997).

Previously, up until the mid 20th century, human infants were routinely fed human milk with greater than 90% of children aged 0-6 months receiving at least partial breast-feeding (Grulee *et al* 1934). The benefits of breast-feeding were apparent at the time, with some estimates suggesting that mortality in non-breast-fed infants was greater than 50-fold higher than in those infants receiving human milk (Stevenson 1947). Epidemiological studies have been important in demonstrating that breast-feeding clearly protects infants against respiratory and gastointestinal infections, or at least decreases the severity of these infections (Welsh and May 1979, Martinez *et al* 1981, May 1988 and Beaudry *et al* 1995).

The primary protective factors in breast milk are thought to be the presence of specific antibody and anti-adhesion factors. However, a variety of antimicrobial factors have been detected in human milk over the years and most of these factors are not destroyed by pasteurisation (62.5°C for 30 minutes) (May 1994). At present, provision of the bioactive components contained within human milk to the infant, rather than just its value as a source of essential nutrients, is apparently one of the strongest indications for breast-feeding the human infant.

Initial experimentation to characterise human milk components focused on the antibody titre, cells and non-immunoglobulin factors with potential protective effects such as lactoferrin and lysozyme. *In vitro* experiments suggested that many of

these components had beneficial effects in mediating antimicrobial actions in the broad protection against infection given by human milk (Welsh and May 1979).

By the examination of epidemiological data, the protective attributes of immunoglobulins in milk achieve less prominence since infants were shown to develop infections despite "protective" levels of immunoglobulin in the milk they were fed (Ruiz-Palacios *et al* 1990). Indeed, in a study of Gambian mothers, where the levels of immunoglobulins were measured there was no change in secretion of immunoglobulins in infection and in particular during diarrhoeal infections (Prentice *et al* 1984). A non-immunoglobulin defence component lactoferrin was also studied. The *in vitro* effect of its anti-microbial actions were apparent but were not shown *in vivo* (Sanchez 1992).

Human colostrum contains large numbers of neutrophils (Pickering *et al* 1983), which are replaced by lower numbers of mononuclear phagocytes as milk production matures (Ho *et al* 1979). The ability of these cell types to mediate immunity by removing infectious material suggests that their presence in human milk is for that specific task. However, using mixed and separated populations of leucocyte, a range of results have been generated that conflict on one hand but support an alternative hypothesis for their inclusion as useful mediators. The leucocytes are inflammatory cells which when tested were shown to be hyporesponsive; have reduced adherence, aggregation and microbicidal activity compared to blood-derived cells (Prentice *et al* 1987 and Buescher and McIlhern 1993). It was suggested therefore that colostrum exposure suppressed the usual inflammatory responses of the milk-derived cells. The alternative hypothesis suggested milk as being anti-inflammatory, preventing maternal inflammation-related leucocytes from causing damage to the infant (Goldman *et al* 1986 and Buescher and McIlhern 1993).

Scouring calves are those that show either overeating or infective diarrhoea like disease. In the case of over eating scours, the effect on the fourth stomach, the abomasum, is such that the *Lactobacillus* bacteria cannot form curd from the ingested milk or formula feed by acidification which leads to low digestion and loss of non fermented feed by excretion. This can lead to further infective scours and dehydration as the calves can becomes weak and compromised.

Infective scours are similar to those seen in the human infant, with bacterial: *E. coli* and *Salmonella* species and viral: Rotavirus causing an inflammation and diarrhoea like disease.

As compared to the human infants, calves are removed from the mother's milk soon after birth. Calves are then given a "replacer" formula feed which is a mixture of nutrients that are similar to human infant formula feeds and contain dried milk powder. The incidence of scouring due to infection arising from bacteria is increased in calves fed on replacer compared to those fed cow's milk or colostrum (Nocek *et al* 19984).

In the light of our earlier findings and the fact that both human and bovine milk is rich in XO protein, it was hypothesised that active XO could be exploited to generate reactive nitrogen and oxygen species. In the presence of infective organisms, the formation of the strong oxidant peroxynitrite may cause a reduction in viability and reduce their numbers to such an extent as to reduce the severity of disease in both human and bovine enteritis.

1.6 Circulating Xanthine oxidase

The possibility effectiveness of XO as a generator of superoxide, nitric oxide and or peroxynitrite may be enhanced by the release of the enzyme from protein rich stores and its relocation to sites low in or devoid of enzymic activity. Pathological

conditions which exhibit enhanced plasma XO include hepatitis, acute viral infection, ischaemia reperfusion and hypercholesterolaemia (Radi *et al* 1997). Other pathological conditions show radical generating systems in plasma that are not seen in normal controls. Rheumatoid arthritis is one such disease that shows a circulating plasma radical generating activity which has been associated with flares in the disease. In the presence of NADH rheumatoid plasma shows superoxide generation as measured by lucigenin enhanced chemiluminescence (Blake *et al* 1997). The presence of elevated XO was also shown in patients with inflammatory and autoimmune rheumatic diseases (Miesel and Zuber 1993). This same study was also able to show that cortisone treatment of these patients caused a normalisation of the serum XO levels to that of the healthy controls.

A circulating enzyme can therefore have systemic effects which may out-weigh the localised effects in protein rich tissues.

The binding of XO to endothelial cells was described by Tan *et al* (1993) and was said to bind in a partially heparin-reversible manner. Further evidence suggested heparin as an inhibitor of cell damage by XO derived oxidants by a mechanism not related to the scavenging of oxidants (Lapenna *et al* 1992). Proteoglycan synthesis was also enhanced by low level radical generation from XO and inhibited at high levels of radical generation suggesting a link between proteoglycan synthesis and oxidant production (Panasyuk *et al* 1994).

Heparin is a polyanionic glycosaminoglycan and has been shown to dissociate proteins from cells by competition for protein binding to anionic cell surface proteoglycans (Kjellen and Lindahl 1992). XO itself is known to bind to heparin above heparan sulphate and chondroitin sulphate

A mechanism of binding at sites distant to the site of generation is therefore suggested and has been investigated in this thesis by *in vitro* methods with cultured endothelial cells.

The existence of a circulating anti-trypanosome activity in the Cape buffalo has also been described and shown to be xanthine oxidase (Muranjan *et al* 1997). It is therefore possible that a circulating enzyme may have effects on systemic infections or can be directed to points of infection via the circulation.

In the light of the above discussion, xanthine oxidase enzyme from a variety of sources was assessed for its ability to generate nitric oxide from nitrogen containing compounds under conditions of hypoxia and with increasing oxygen concentrations. The possible oxidants derived from this enzyme may suggest a role in the cytotoxicity of human and bovine milk on infective micro-organisms. The fact that the enzyme circulates in a range of disease states suggests that a NO and superoxide generating and circulating enzyme may mediate pathology and therefore the binding of XO enzyme to endothelial cells was assessed in relation to the effect of hypoxia on endothelial cell expression, activity and adhesive interactions.

Chapter 2

The nitrate and nitrite reductase activity of xanthine oxidase

Chapter 2

This chapter deals with the activity of xanthine oxidase in terms of its ability to generate nitric oxide from a range of substrates.

2.1 Introduction

2.1.1 Known xanthine oxidase reactions

The classically known activities of xanthine oxidase involve the oxidation of hypoxanthine to xanthine and the subsequent oxidation of xanthine to uric acid. During this process, in order for the hypoxanthine and xanthine to be oxidised, the enzyme itself must be reduced. Xanthine oxidase has long been associated with the mechanism of gaining and losing electrons in an apparent electron shuttling capacity. The specificity of the enzyme for substrates or electron donor substrates derives from its multi-centre structure. The limited substrate specificity was shown early on in the history of XO enzymic analysis by Dixon in 1926. In his report he described the need for a donor of electrons and an acceptor of electrons to be present for reactions to occur. He studied the specificity for electron donors compared to hypoxanthine using oxygen or methylene blue as the electron acceptor. Then in the reverse of this protocol, the specificity of the enzyme for electron acceptors in the presence of hypoxanthine as electron donor was shown. It was noted that xanthine and hypoxanthine were oxidised by purified milk enzyme in the presence of methylene blue which followed work by Morgan *et al* (1922). Also the oxidation of aldehydes was measured and led to the discussion of a possible separate aldehyde oxidase enzyme from the milk preparation (although Dixon pointed out that the oxidation of aldehydes was possible without a specific catalyst). Out of 35 electron donor substances used, including caffeine, uracil and

amino acids, only three, hypoxanthine, xanthine and aldehydes, were oxidised by the milk enzyme.

In the case of electron acceptors, the specificity was said to be "immaterial". Oxidising substances were used in the presence of enzyme and hypoxanthine. Oxygen, methylene blue, iodine and picric acid were all capable or oxidising the enzyme. Dixon also repeated the experiments of Dixon and Thurlow (1924) and showed that nitrate could oxidise hypoxanthine and xanthine in the presence of XO and itself becoming reduced to nitrite. This followed on from the work of Bach (1911) where aldehydes were able to reduce nitrates in milk preparations.

The reduction of nitrates by xanthine oxidase then became almost lost as its importance was not noted to any great extent.

Fridovich and Handler, in a series of papers on xanthine oxidase, refer to experiments using nitrate as an electron acceptor in the absence of oxygen. In 1962 they followed the reduction of nitrate by measuring the accumulation of nitrite under "rigorously anaerobic conditions". They noted that nitrate reduction was not observed in the presence of oxygen and confirmed this by recovery studies of the nitrate suggesting that the lack of nitrite accumulation was not due to the aerobic reduction of nitrite by xanthine oxidase.

The next references to the nitrate reductase activity of XO include German and Russian titles on the inhibition of nitrate reductase activity (Hackenthal and Hackenthal 1966), nitrate and nitrite reductase activity of XO (Alikulov *et al* 1980) and the nitrate reductase activity of milk xanthine oxidase (Sergeev *et al* 1985). These studies link with the growing background of information on the similar structures found in xanthine oxidase and assimilatory nitrate reductase and the nitrogen fixing enzyme nitrogenase, the common active site being a molybdopterin co-factor. In fact the molybdenum cofactors had been isolated and transferred from

XO enzyme to a non-active nitrate reductase enzyme from *Neurospora crassa* to produce an enzyme capable of the aerobic reduction of nitrate to nitrite (Hawkes and Bray 1984).

Experiments describing the formation of urate under hypoxic conditions also led to a re-evaluation of the mechanism and reactions of XO. Reinke *et al* (1987) were able to measure increased 1-methyl urate production in plasma and brain effusate after intra-peritoneal injection of 1-methyl xanthine to hypoxic rats. They presented data that suggested the presence of oxidising substrates other than oxygen and NAD+ which were capable of maintaining XO activity during hypoxia. Elsayed *et al* (1993) used isolated perfused rat lungs to show uric acid as a marker of oxygen tension. Comparing 95, 21 and 0% oxygen concentrations the urate levels generated were far greater in the 0% oxygen perfused lungs than in the normoxic and hyperoxic lungs. Serum urate levels have also been measured in chronic heart failure and show an inverse correlation between serum urate and functional capacity in patients with cardiac failure compared to controls (Leyva *et al* 1997).

2.1.2 Determination of nitric oxide

Various methods for the detection of nitric oxide exist. They range from the detection of nitric oxide gas directly (Glover 1975 and Menon *et al* 1989) to assays of the known effects of nitric oxide. These include the oxidation of oxyhaemoglobin to met-haemoglobin (Kelm *et al* 1988), relaxation responses in isolated blood vessels (Palmer *et al* 1987), anti-aggregation responses of platelets (Moncada *et al* 1988) or the measurement of cGMP generation in NO treated cells (Radomski *et al* 1987).

In experiments on the generation of NO in aerobic conditions the measurement of nitrite has been used. Nitric oxide reacts with oxygen to produce a variety of stable

end products including nitrite and nitrate (Beckman *et al* 1990). The routine measurement of nitrite is to follow the diazotisation of sulphanilamide and N-1(-naphthyl)ethylenediamine dihydrochloride (NED) in the presence of nitrite, the so-called Griess reaction.

Many basic scientific and clinical studies have used this assay system to determine the effect of NOS inhibitors or the prevalence of NO in diseases such as hypertension (Marzinzig *et al* 1997). Many biological fluids can be tested including plasma, serum and urine and also culture medium from cells expressing nitric oxide generating systems (Granger *et al* 1999).

However, to measure nitric oxide under reduced oxygen conditions, this approach is not applicable due to the lack of available oxygen and therefore the generation of nitrite.

Spectrophotometric assays are also used for the measurement of NO reactions with oxyhaemoglobin. This is based on the stoichiometric conversion by NO of oxyhaemoglobin to methaemoglobin. With this assay the formation of NO can be continuously monitored by time dependent recording of the absorbance changes in the Soret band associated with oxyhaemoglobin oxidation at 411nm (Kelm *et al* 1997).

Biological assays of NO release and action can also be used (Moncada et al 1989). Blood vessels or vascular beds are excised and prepared for pressure measurements induced by various treatments. The vessels are constricted by the addition of an agonist and the pressure change noted. The effect of NO on these constricted vessels can be seen as a decrease in pressure as the vessels relax. In this thesis, preliminary experiments were run to assess the effectiveness of preparations under reduced oxygen as classically all preparations have been run in media flushed with 95% oxygen. Their response to various treatments including

XO, organic and inorganic nitrate addition and the effect of allopurinol on the response to various NO donors was also measured.

The use of a membrane-covered amperometric NO sensor (World Precision Instruments, WPI) was also investigated. The basic principle of the sensor is that NO diffuses through the gas permeable membrane and is then oxidised by an electric current in the probe. The magnitude of the current created by the NO oxidation can be related to the concentration of NO in the sample because the rate of oxidation is dependent on the rate of diffusion of the NO to the electrode surface. The rate of diffusion is directly dependent on the partial pressure of NO in the sample.

Initial experiments using this probe allowed for the measurement of NO in solution by forming NO from acidified nitrite in the presence of potassium iodide (KI). This probe, however, had a high signal to noise ratio and slow response times compared to other methods and was not used further in this study. A WPI electro-chemical NO probe has since been used to show NO generation in the presence of xanthine oxidase (Trujillo *et al* 1998).

For the determination of NOS activity, substrate depletion or product accumulation assays have been used. These include L-citrulline production as the by-product of L-arginine breakdown. Also used was the rate of reduction in NADPH absorbance at 340nm, which is also relative to the rate of enzyme turnover. The rate of NADH depletion in the presence of nitrates and nitrites was assessed for xanthine oxidase in the light of its previously described NADH oxidising activity (Sanders *et al* 1997). For experiments where NADH was replaced by another electron donor, an alternative assay was required.

To allow the determination of specific activity a real time NO assay was used. For many years the measurement of NO in the gas phase has been performed in

studies on NO as a pollutant in the atmosphere from industrial output and from car exhausts (Fontijn *et al* 1970). A sensitive method of analysing the volatile gas NO was developed around the reaction of ozone with NO. This reaction follows the equations (9) and (10) below.

$$NO + O_3 \longrightarrow NO_2^* + O_2 \quad (9)$$

$$NO_2^* \longrightarrow NO_2 + hv \quad (10)$$

The formation of electronically excited nitrogen dioxide leads to the decay of that species and the emission of light. The specific emission wavelength is in the red and near infra red wavelengths and is detected by a photomultiplier tube (PMT) through a 600nm band pass filter.

For the determination of NO concentration in the gas phase a calibration gas of known NO content can be purged through the analyser. The signal strength is then used to prepare a standard curve of signal to NO concentration and unknown NO gas concentrations can be calculated. The sensitivity of the instrument in use for these experiments was reported to be below 1ppb (10^{-9}) for NO in the gas phase.

The generation of superoxide and hydrogen peroxide from XO is well known from both purine substrates and NADH. The effect of oxygen on the NO generating capacity of this enzyme is important from the fact that previous studies show a need for strict anaerobic reaction for the reduction of nitrates to nitrite (Fridovich and Handler 1962 and Sergeev *et al* 1985). The possibility exists that this enzyme may generate both reactive oxygen and nitrogen intermediates the reaction of which may lead to the formation of peroxynitrite.

2.2 Methods and materials

2.2.1 Nitrate reductase assay

The activity of nitrate reductase was assessed by following the rate of reduction in absorbance at 340nm of NADPH in a spectrophotometer. The reaction followed the basic principle outlined in equation (11) below.

$$\beta\text{-NADPH} + \text{Nitrate} \xrightarrow{NR} \beta\text{-NADP} + \text{Nitrite} + H_2O \quad (11)$$

Using a final volume of 1ml the reagents were added in the following order (shown as final concentrations, all chemicals used were purchased from SIGMA, UK unless otherwise stated). Buffer - 50mM PBS at pH 7.2, FAD 5μM, β–NADPH 200μM, potassium nitrate 10mM and NR (NAD[P]H: Nitrate oxidoreductase; EC 1.6.6.2 from *Aspergillus sp*, SIGMA, UK) or XO (Xanthine oxidoreductase, EC 1.1.3.22 from bovine buttermilk, Biozyme, UK) enzyme. Two sets of blanks were used, Blank A was made up without the addition of enzyme which was replaced by an equal volume of buffer and Blank B was made up with enzyme but without potassium nitrate which was replaced by buffer. All solutions were freshly dissolved in PBS and remained on ice until required. The reaction was carried out in air-saturated buffer at 25°C and followed in a spectrophotometer (Kontron) with a 1cm light path in 1ml plastic cuvettes at 340nm.

The initial rate of reaction was measured as the linear slope of the absorbance readings. Activity was expressed by using the extinction coefficient for β-NADPH of 6.22 mM^{-1} cm^{-1}.

2.2.2 Nitrite assay

Nitrite was assayed by a modification of Griess assay (Bredt and Snyder 1994). The principle behind the assay relies on a diazotization reaction in the presence on nitrite to give a purple magenta colour, the absorbance of which is proportional to the nitrite concentration (See equation (12) below).

Solutions of unknown nitrite content were reacted with an equal volume of a 1% solution of sulphanilamide made up in the respective buffer and acidified with 1M HCl at pH1. This mixture was allowed to stand at room temperature protected from light for 10 minutes. To this mixture was added an equal volume of 0.1% N-1(-naphthyl)ethylenediamine dihydrochloride (NED) and the mixture allowed to stand at room temperature protected from light for a further 10 minutes. Following incubation, the absorbance at 550nm was measured in a spectrophotometer with a 1cm light path or in a 96-well plate-reading spectrophotometer.

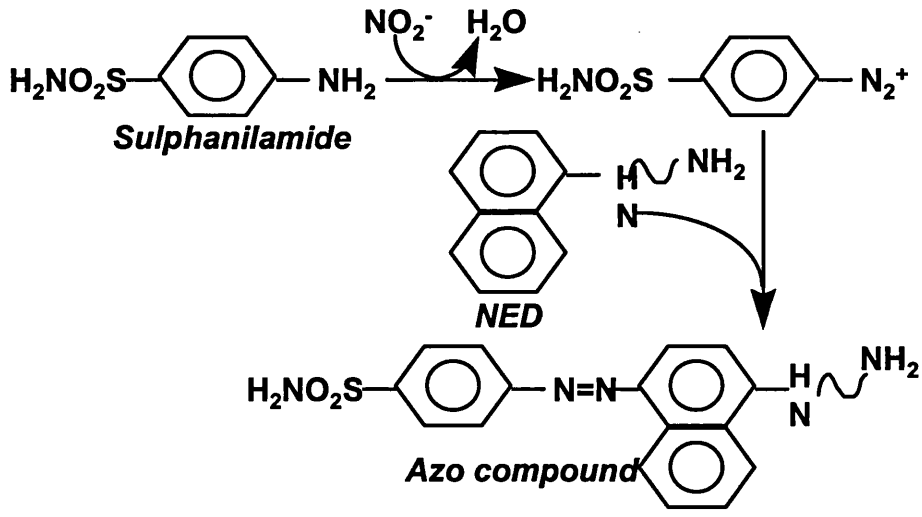

(12)

For each nitrite determination a standard curve of known nitrite concentrations was generated using a serial dilution of a 1mM sodium nitrite stock solution made fresh daily in diluent media. The absorbance of unknown nitrite solutions was related to

the absorbance of the standard nitrite curve using a linear regression equation and a graphical data fitting program (Prism™, GraphPad Software, USA).

The Greiss assay was used in both 1ml and 150μl assay formats. The sensitivity for both assays was ~ 1μM nitrite.

2.2.3 The measurement of oxygen saturation

As the concentration of oxygen is important in the response of cells to their environment, a suitable method of measuring oxygen saturation was required. For all of the experiments recorded in this thesis, requiring oxygen saturation measurements, a Clark type oxygen micro-electrode was used. This type of probe has a small diameter cathode and as a result its consumption of oxygen is low. The resulting oxygen tension gradient is located beneath a membrane which reduces the effect of stirring on the readings. The electrode consists of two platinum wires embedded in glass which form the cathode with the anode being formed by a silver band wrapped around the glass. During use, a voltage is applied across the anode and cathode. This causes the oxygen in the media adjacent to the cathode to be reduced which results in electron flow. It is this flow of electrons that produces a current which is read on the oxygen meter. Diffusion of oxygen occurs into the membrane of the electrode to replenish that lost by reduction. The amount and rate of diffusion is low for this type of electrode and therefore the replenishment of oxygen on the outside of the membrane takes place at normal diffusion rates as opposed to a Clark type macro electrode which requires vigorous stirring.

2.2.3.1 Calibrating the oxygen electrode

The electrode must be calibrated to yield reproducible results. Using media saturated with gases of known oxygen concentration compared to a zero oxygen saturated media, the relative oxygen saturation of a particular unknown media can be determined.

After long storage the electrode was allowed to equilibrate in media for 2 hours prior to calibration. Calibration was carried out using media at the same temperature as that of experimental conditions, typically 37°C. Fist, the zero setting was calibrated using a solution of sodium borate (10mM) to which was added a pinch of sodium sulphite. This drives off the oxygen for 5 to 10 minutes, dependent on stirring velocity, allowing the zero oxygen saturation to be set.

The electrode was then washed in PBS and the 100% oxygen saturation was measured using media gassed with pure oxygen for ~ 20 minutes (All gases were purchased from BOC). Once the readings had stabilised a final calibration check was made by mixing media vigorously to cause air saturation. This should read ~21% oxygen saturation. If the readings were far from those expected, the zero and 100% calibration points were repeated until the air-saturated media was ~ 21% saturation. This occurred on numerous occasions however once calibrated the readings were free from drift for up to 12 hours. Gasses for calibration and in all experiments were prewarmed by passing through heated water at 37°C.

In all experiments the level of zero calibration by the chemical method described above was similar to (± 0.1%O_2sat) the oxygen saturation measured after gassing with 5% CO_2 balanced nitrogen (n = 6). This was the detection limit although this type of nitrogen gas apparently carries some oxygen.

2.2.4. Experimental reaction vials

2.2.4.1 Glove box experiments.

Experiments including cellular incubation and 96-well plate determinations were carried out in a sealable glove box. This chamber allowed for the delivery of a range of gas mixtures and the manipulation of a large number of reactions at one oxygen concentration. The glove box could also be environmentally controlled including temperature and humidity adjustments.

The efficiency of gassing media inside the glove box was assessed in a range of plastic plates at a range of media surface areas and volumes. Figure 2.1 shows the effect of gassing on the oxygen saturation of air-saturated media exposed to 5% CO_2 balanced nitrogen in the glove box.

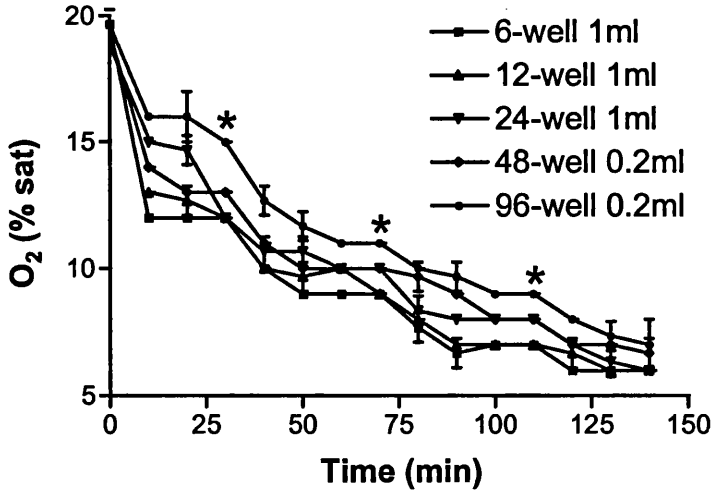

Figure 2.1. The effect of gassing on the oxygen saturation of PBS in a range of plastic vessels. The glove box was gassed - 5% CO_2 balanced nitrogen was allowed to flow through the cabinet displacing atmospheric air - for 10 minutes prior to the introduction of 5 different tissue culture plates with air-saturated PBS at a range of volumes. The oxygen saturation of each well was measured using an oxygen microelectrode (Strathkelvin Instruments,

Glasgow) calibrated as previously described within the glove box every ten minutes. Once the oxygen saturation had stabilised the cabinet was purged with 5% CO_2 balanced nitrogen for a further ten minutes-*. This protocol was repeated and the results of readings taken in triplicate are expressed as means ± SD (n = 1).

The oxygen saturation of each type of plastic vessel is shown to fall over time. The rate of fall is dependent on the amount of oxygen in the glove box, the air-saturated media and the surface area to volume ratio (SAVR) of the respective vessels. The SAVR of 1ml PBS in a 6 well dish is such that the levels of oxygen saturation fall more quickly than in the 96-well plates. As 96-well plates were to be used in experiments the volume was kept at 200µl but the glove box was purged continually for 1 hour prior to starting experiments.

2.2.4.2 The use of sealable 7ml plastic bijou bottles

Further experiments required the use of a reaction vial to allow oxygen variations, temperature control, mixing and ease of access. For single reaction experiments, plastic disposable bijou bottles were used. The oxygen saturation of media within these vessels was measured whilst the media was gassed. Figure 2.2 shows a representative graph of the effect of 5% CO_2 balanced nitrogen gassing on the oxygen saturation of 1ml of PBS at 37°C. The rate of degassing meant that experiments requiring zero oxygen saturation were gassed with 5% CO_2 balanced nitrogen for at least 2 minutes before being introduced to the reaction chamber.

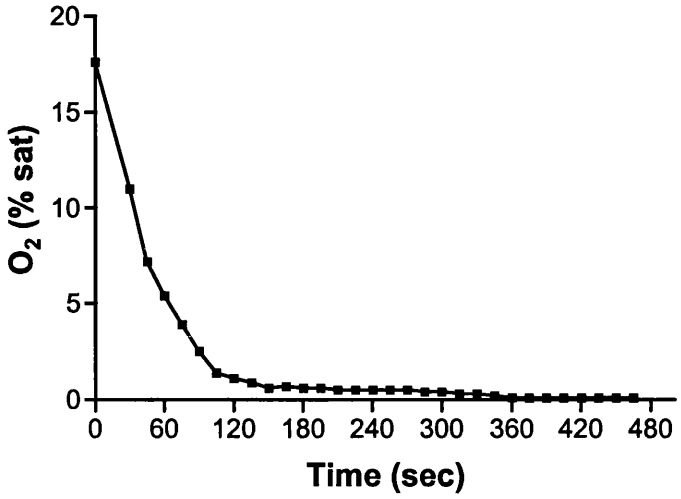

Figure 2.2. The effect of gassing with 5% CO_2 balanced nitrogen on the oxygen saturation of 1ml PBS at 37°C in a 7ml bijou bottle. Measurements were made with a microelectrode as described above and a representative trace is shown.

2.2.5 Xanthine oxidase-mediated generation of nitrite from nitrate

Experiments to determine the nitrate reductase activity of xanthine oxidase were carried out using a 96-well plate format with a final volume of 200µl. All buffers were subjected to gas purging in a glove box at 37°C for 1hour to remove oxygen. Experiments were set up *in situ* without the introduction of atmospheric air, all manipulations being carried out within the glove box. Reactants were mixed by pipetting before the introduction of enzyme that had been gassed separately outside of the glove box. Experiments were terminated by the addition of 1% sulphanilamide inside the glove box which was then assessed for the formation of nitrite by following the nitrite assay protocol detailed in 2.2.2.

2.2.6 The measurement of nitric oxide generation

2.2.6.1 The relaxation response of perfused mesentery

This assay involves the perfusion, via the superior mesenteric artery (SMA), of an excised rat mesenteric vascular bed with Krebs-Henseleit solution (KHS) gassed with known gas mixtures. By perfusing at a constant flow of 5ml min^{-1} and monitoring the perfusion pressure changes it is possible to record alterations in vascular resistance. In order to examine the relaxation response, the tissue must be first constricted using phenylephrine at a final concentration of 10nM in the perfusion buffer. The protocol was carried out as follows:

Rats, female Wistar (~ 250g) from the University of Bath animal house were euthanised by a single injection of Sodium pentobarbitone BP (Euthatal, Rhone Merieux, France) at 200mg kg^{-1} into the peritoneal cavity followed by cervical dislocation. The rat was then dissected by opening along the abdominal midline. The SMA was located by its relationship to the position of the left renal vein, which becomes visible after moving the intestine to the right of the animal. The connective tissue was removed to the right of the renal vein to expose the descending abdominal aorta. The colic artery was identified at the base of the colon and tied off using suture thread. A thread was tied loosely around the SMA close to its origin and an incision made into the descending abdominal aorta opposite to the origin of the SMA. The SMA was then cannulated via the incision using a portex cannula of ~ 2cm with a Luer fitting which attached to the perfusion system. When the cannula was in place it was secured by tying a double knot with suture thread.

Once the mesentery was cannulated, the intestine was removed from the fine branches of the SMA. This was achieved by cutting small blood vessels away from

the colon end of the intestine. The intestine was then gently pulled to remove it from the mesentery all the way to the stomach. The mesentery was then cut free of the stomach and aorta and immediately placed into the perfusion system shown in figure 2.3.

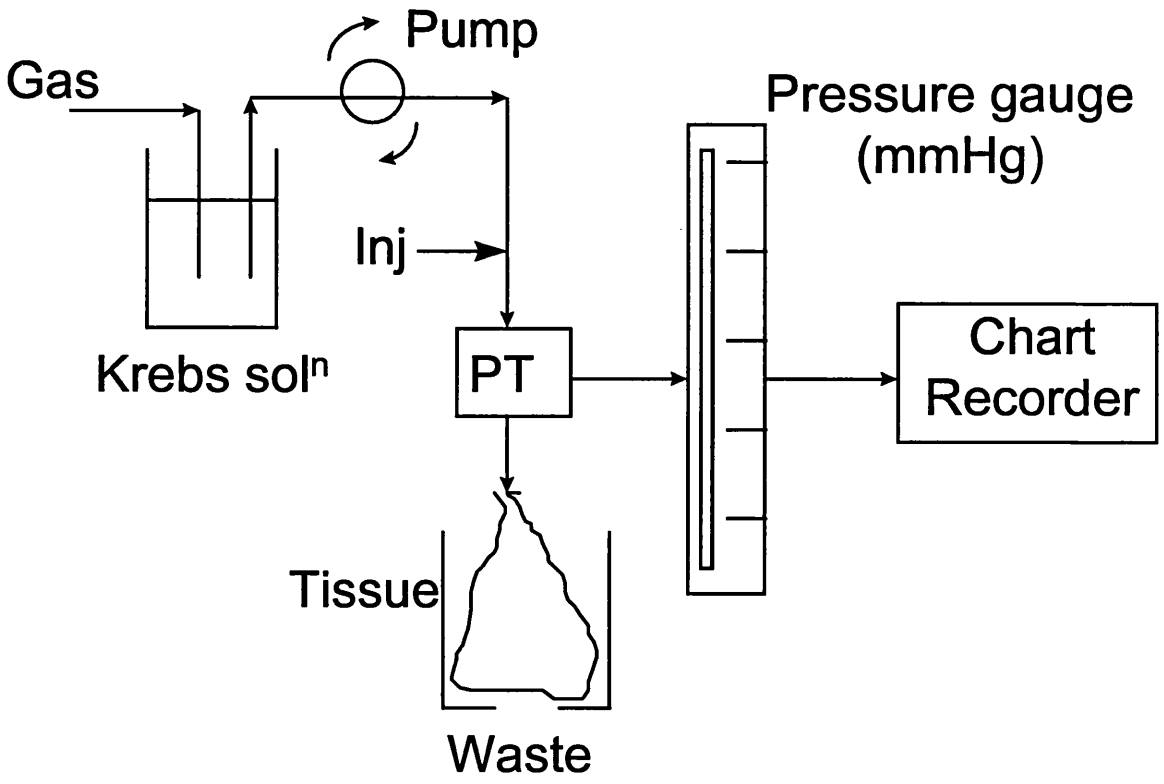

Figure 2.3. The apparatus set up for the determination of relaxation responses of constricted rat mesentery. Inj = injection port, PT = pressure transducer.

Blood was initially removed from the mesentery by perfusion of KHS at 37°C and the preparation left to stabilise for 20 minutes. The mesenteric arteries were then constricted by the addition of phenylephrine to the perfusion media and the change in perfusion pressure was recorded on the chart recorder. This was then left for 20 minutes to stabilise.

Following the experiments each mesentery was fixed in formal saline and prepared for histological section by dehydration in ethanol and xylene and embedded in wax.

Sections, 5μm, were cut using a sledge microtome and the tissue attached to polished glass slides before being baked at 50°C. These sections were then stored at room temperature until processed (see appendix I)

2.2.6.2 The chemiluminescence reaction of NO with ozone

NO release from various enzyme reactions was monitored in the gas phase using an ozone-enhanced chemiluminescence (OEC) analyser. The apparatus was set up as described in figure 2.4. A carrier gas of known oxygen content was purged through the apparatus to gas the reaction cell and to carry the generated NO to the analyser. This gas was first bubbled through water containing activated charcoal in a water bath at 37°C. The OEC analyser (NOA 280, Sievers, USA) required a continual flow rate of gas equal to 200ml min^{-1}. The flow rate of the carrier gas equalled the required uptake rate of the analyser in this sealed system. The reaction cell consisted of a 7ml sterile plastic bijou bottle (Sterilin, UK) which was capped and housed a stirring bar. The cap of the reaction vessel had three holes cut into it to allow the carrier gas in, the gas out to the analyser and a third hole for the injection of substrate and enzyme. This third port was also used for the determination of oxygen saturation using the oxygen micro electrode.

The reaction cell was housed within a water bath with circulating water at 38°C. The temperature was measured in 1ml of PBS inside the reaction cell and was 37°C ± 0.2°C.

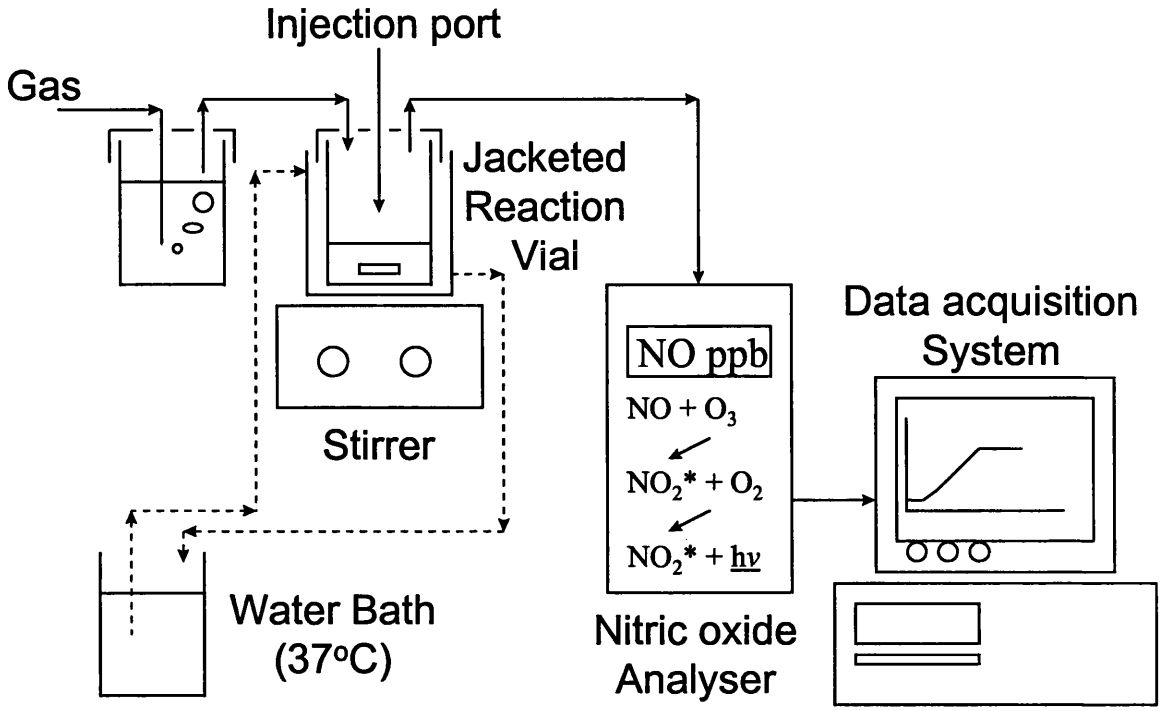

Figure 2.4. The apparatus set up for the detection of NO from various reaction mixtures.

NO was measured continually by the reaction with ozone described above and the results recorded using proprietary software on a personal computer.

The NO analyser was calibrated using gas of 90ppm NO and the internal calibration software of the analyser.

2.2.7 The measurement of peroxynitrite generation

To assess the generation of ONOO- in various systems and the effectiveness of ONOO- scavengers, two assays were employed.

2.2.7.1 Oxidation of Dihydrorhodamine to rhodamine

From the work of Kooy *et al* (1994) and Crow *et al* (1995) it was evident that authentic ONOO- could cause the oxidation of dihydrorhodamine (DHR – Molecular Probes, Inc) to rhodamine which had an absorbance peak at 500nm with a high

molar extinction coefficient (74500 M^{-1} cm^{-1}). This enabled this process to be followed spectrophotometrically. In experiments on the generation of ONOO- by XO the following assay procedure was used.

Reaction solutions were made up fresh from frozen DHR solutions to give final concentrations of 50μM DHR, 0.1mM Diethylenetriaminepentaacetic acid (DTPA) in 1ml of 50mM PBS. This was then placed into a spectrophotometer at 37°C and the absorbance at 500nm was measured over time with a 1cm light path.

This assay was also modified for use in a 96 well plate format. All final concentrations remained the same only the volume was reduced to 200μl. The absorbance was read through a 492nm GG filter over time at 37°C.

2.2.7.2 The peroxynitrite-mediated luminol and lucigenein chemiluminescence

Following the work of Radi *et al* (1993), the use of luminol (5-amino-2,3-dihydro-1,4-phthalazinedione) chemiluminescence with peroxynitrite made for an assay of the ONOO- scavenging effect of various compounds. It was suggested that the reaction of ONOO- with luminol lead to the excitation of aminophthalate as the emitting species. As the formation of aminophthalate is dependent on decomposition of the luminol endoperoxide it is thought that the reaction of ONOO- with luminol must generate this unstable intermediate which then follows the light emitting pathway.

The following protocol was used:

Luminol was dissolved in 1M NaOH and diluted in PBS before the pH was adjusted to 7.3 and then used at a final concentration of 500μM, was injected in to the wells of a black walled 96-well plate. Chemically generated peroxynitrite (See appendix I), at a range of concentrations, was then injected in to the same wells of a 96-well

plate. The resultant chemiluminescence reaction was followed using a plate reading chemiluminescence analyser measuring light emission above 405nm.

The addition of possible scavenging compounds was carried out before the injection of the ONOO- at a range of concentrations in PBS buffer at pH 7.2. The light emission data were relayed to a computer and the maximal light emitted in arbitrary light units (ALU) was taken as the fastest reaction rate.

The effect of peroxynitrite on the chemiluminescence derived from lucigenin (bis-N-methylacridinium nitrate) was also assessed in the same manner using 500μM lucigenin.

2.3 Results

2.3.1 The nitrate and nitrite reductase activity of xanthine oxidase

2.3.1.1 Comparison to Nitrate reductase enzyme

The reduction of nitrate by xanthine oxidase was followed using a variety of methods.

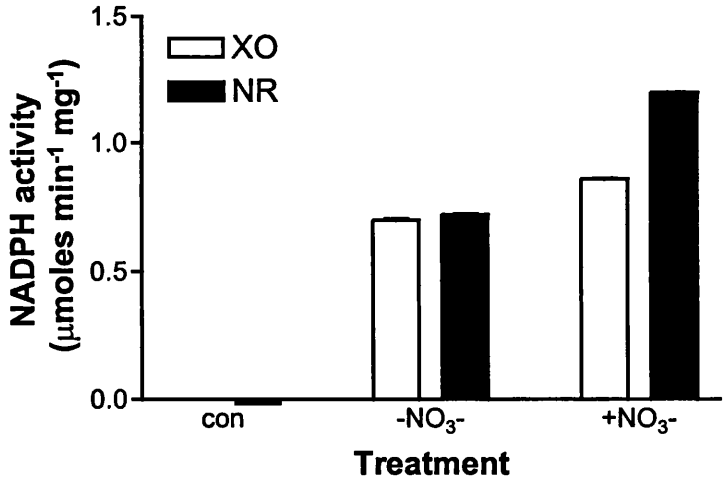

Figure 2.5. The oxidation of NADPH by xanthine oxidase and nitrate reductase in the presence and absence of 10mM potassium nitrate under aerobic

conditions. Experiments were carried out in duplicate cuvettes and the mean ± SEM of three independent experiments is shown.

Both enzymes showed significant reduction of NADPH in the absence of nitrate compared to the auto oxidation of NADPH in the control cuvettes. The addition of nitrate to the reaction was also shown to increase the rate of NADPH reduction. XO enzyme showed a smaller increase in reduction rate compared to NR on the addition of nitrate but similar reduction rates were seen in the absence of added nitrate. Following the reduction of NADPH, the levels of generated nitrite were measured using a modification of the Greiss assay.

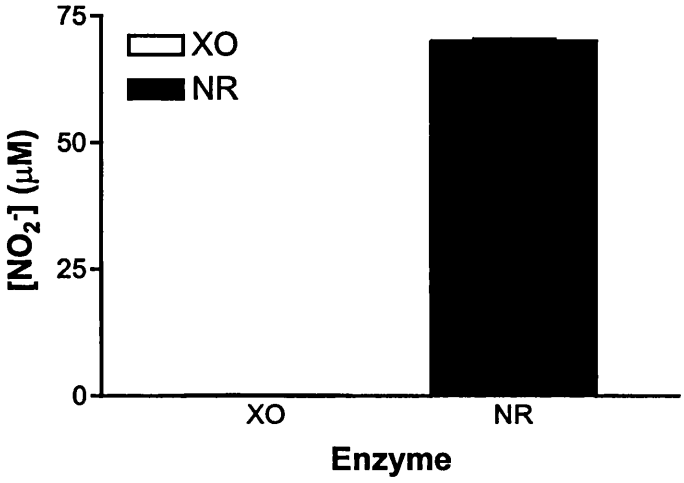

Figure 2.6. The nitrite generated by the aerobic reduction of inorganic nitrate by XO and NR in the presence of NADPH as measured by the Greiss assay. The conditions were as described for figure 2.5. The reactions in the cuvettes were allowed to run for 1 hour to remove excess NADPH and an aliquot was taken from each cuvette and run against a standard curve of known nitrite concentrations.

The apparent nitrite generation by NR in the presence of nitrate is shown to be ~ 70μM. In the case of XO there was no detectable nitrite above the control values by this assay method.

2.3.1.2 The generation of nitrite under reduced oxygen conditions

Following the information given by Fridovich and Handler (1962) and Segeev *et al* (1985) the reaction of XO with nitrate was carried out under reduced oxygen conditions in the presence of xanthine. Experiments were set up in the glove box under 5% CO_2 balanced nitrogen so that the assay was run in reverse by initiating the reaction by the addition of enzyme to the longest time point. The termination of each reaction therefore occurred at the same time and nitrite concentration was then assayed. Figure 2.7 shows the effect of time and nitrate concentration on the generation of nitrite with XO in the presence of inorganic nitrate and xanthine.

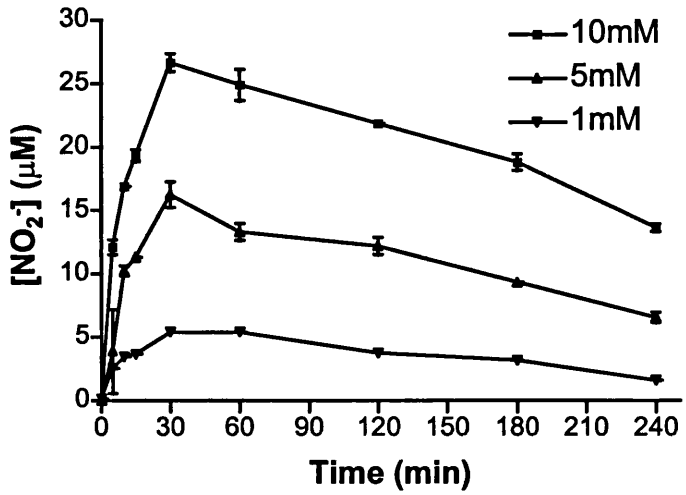

Figure 2.7. The time-resolved generation of nitrite from XO, 53.2μg in the presence of xanthine, 100μM at a range of KNO_3 concentrations in a reduced oxygen atmosphere. The experiments were carried out inside a temperature-regulated (37°C) glove box which was gassed with 5% CO_2 balanced nitrogen. All reagents were allowed to equilibrate inside the glove box for one hour before the initiation of reaction by the addition of XO enzyme. Assay conditions were as follows: Using 50mM PBS pH 7.2 throughout, 100μM xanthine, 1, 5 and 10mM KNO_3 and 53.2μg XO in a humidified atmosphere

under 5% CO_2 balanced nitrogen. A blank without enzyme or without xanthine was also run and gave no measurable nitrite. Graph shows the mean ± SEM (n = 3) in triplicate.

From the graph, the generation of nitrite increases over the fist 30 minutes followed by a reduction in the amount of nitrite assayed. The peak height for each concentration of nitrate was after 30 minutes incubation ~ 5, 15 and 25μM nitrite 1, 5 and 10mM nitrate respectively by this assay method.

2.3.1.3 The effect of pH on nitrite generation

The optimal pH for the reduction of nitrate to nitrite by this system was assessed. Figure 2.8 shows the effect of buffer pH on the generation of nitrite from inorganic nitrate

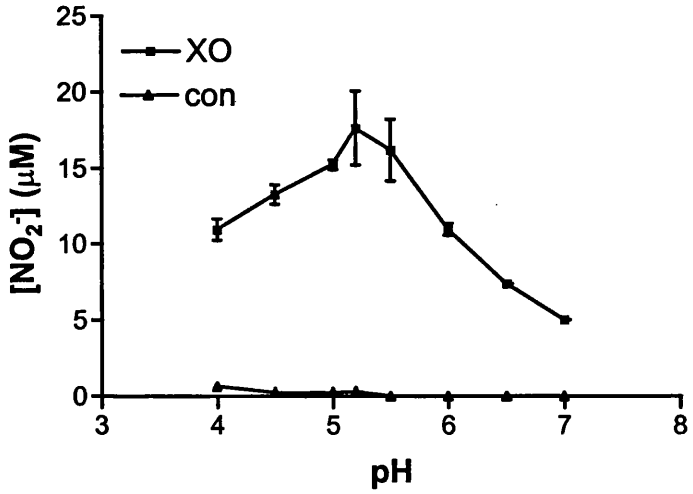

Figure 2.8. The effect of pH on the generation of nitrite from nitrate in the presence of XO and xanthine. Buffer solutions of potassium phosphate buffered saline were generated to give a range of pH values. Using 1mM nitrate, 100μM xanthine and 53.2μg enzyme the reaction was carried out under the conditions previously described for 30 minutes after which the levels of generated nitrite were measured. Results are the mean ± SEM (n = 2) carried out in triplicate.

The effect of lowering the pH was to enhance the generation of nitrite in this system. The pH optimum for this reaction lies between pH 5.5 and 4.5 which is in good accord with Segeev *et al* (1985) who gave a pH optima of 5.2 and similar to Fridovich and Handler (1962) who gave a pH value of 4.6.

2.3.1.4 The effect of known XO inhibitors on the nitrate reductase activity of XO

The effect of known specific XO inhibitors, oxypurinol and BOF-4272 was assayed against a positive control reaction. In Figure 2.9 the effect of both inhibitors is to reduce the measurable nitrite formed compared to uninhibited controls. The inhibitory dose that caused 50% inhibition of the control (IC_{50}) is for BOF-4272, 1.504μM and for oxypurinol 24.74μM.

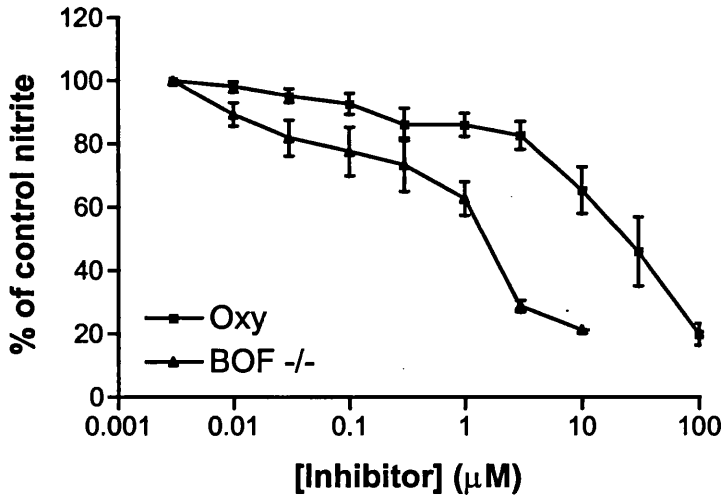

Figure 2.9. The effect of the xanthine oxidase inhibitors oxypurinol and BOF-4272 on the generation of nitrite from nitrate by XO in the presence of xanthine. Experiments were carried out as described in figure 2.3 with the following additions. Oxypurinol or BOF-4272 at a range of concentrations (100μM-0.03μM) were added to the reaction mixture. The reaction was initiated by the addition of XO and followed for 30 minutes after which the levels of nitrite

generated were assayed. The graph shows the percentage nitrite of each treatment compared to a positive control reaction. Results are ± SEM (n = 3) carried out in triplicate.

Diphenyliodonium (DPI) has been used as an inhibitor of NADPH oxidase activity in neutrophils and to inhibit the NADH activity of xanthine oxidase. Its effect on the nitrate reductase activity of XO was assessed here as one of the battery of inhibitors in use.

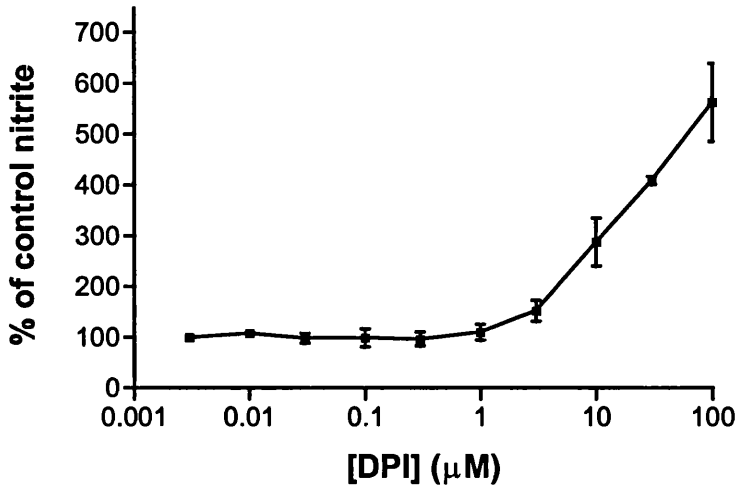

Figure 2.10. The effect of DPI on the nitrate reductase activity of bovine xanthine oxidase. Experiments were as described in figure 2.9. Results are the mean ± SEM of 5 individual experiments carried out in triplicate.

The effect of DPI in this system was not to inhibit but to enhance the measurable nitrite. This was not due to the DPI itself containing nitrite as a control of DPI at all concentrations with enzyme in the absence of xanthine showed no measurable nitrite formed under the same conditions.

This experiment was repeated under 5% CO_2 balanced air conditions with DPI and the results shown as total nitrite generated under the conditions described in figure 2.9. Also shown is the control experiment where xanthine was removed from the reaction mixture.

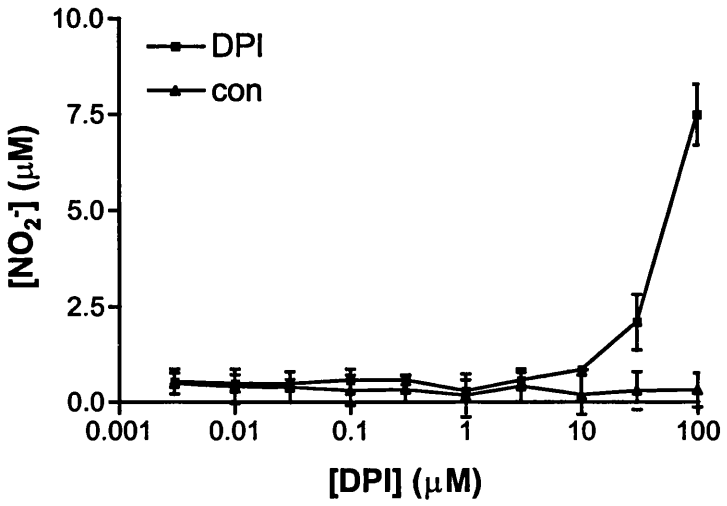

Figure 2.11. The effect of DPI on the nitrate reductase activity of xanthine oxidase under 5% CO_2 balanced air. Experimental protocol as for Figure 2.9. Results are shown as ± SEM (n = 3) in triplicate.

The effect of the DPI is to enhance the XO nitrate reductase activity to generate measurable nitrite under saturated air conditions.

2.3.1.5 The use of organic nitrate substrates

The medicinal use of organic nitrates makes them of particular interest in the study of the nitrate reductase activity of XO. Using commercially available medicinal preparations of both glyceryl trinitrate (GTN) and isosorbide dinitrate (ISDN) (David Bull Laboratories, UK), their effectiveness as substrates for reduction to nitrite by XO was assessed using the protocols previously described for inorganic nitrate. Figure 2.12 shows the initial experiments on the reduction of organic and inorganic nitrate to nitrite by xanthine oxidase in the presence of xanthine and the absence of oxygen.

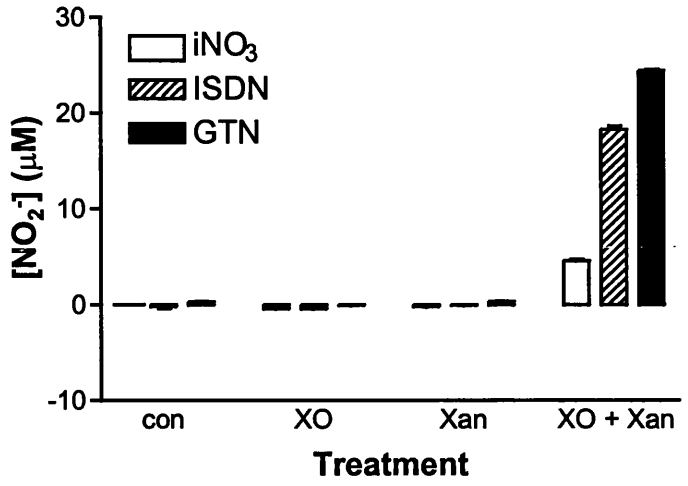

Figure 2.12. The generation of nitrite from the organic nitrates, glyceryl tri nitrate (GTN) and isosorbide dinitrate (ISDN). Experiments were carried out as previously described in figure 2.5 using 1mM nitrate for 30 minutes under reduced oxygen conditions. Results are expressed as mean ± SEM (n = 3) in triplicate.

The generation of nitrite from both organic and inorganic nitrates was observed above control values. Both GTN and ISDN at equimolar concentrations gave significantly more nitrite formation under the conditions described than inorganic nitrate ($p<0.01$ by students t-test comparing ISDN and GTN to inorganic nitrate and $p<0.05$ comparing GTN to ISDN).

2.3.1.6 The effect of XO inhibitors on the reduction of organic nitrates to nitrite by XO

The effect of oxypurinol and DPI on the nitrate reductase activity of XO using organic nitrate substrates GTN and ISDN was assessed as described in figure 2.9. Figure 2.13 shows the effect of oxypurinol addition on the generation of nitrite from GTN and ISDN.

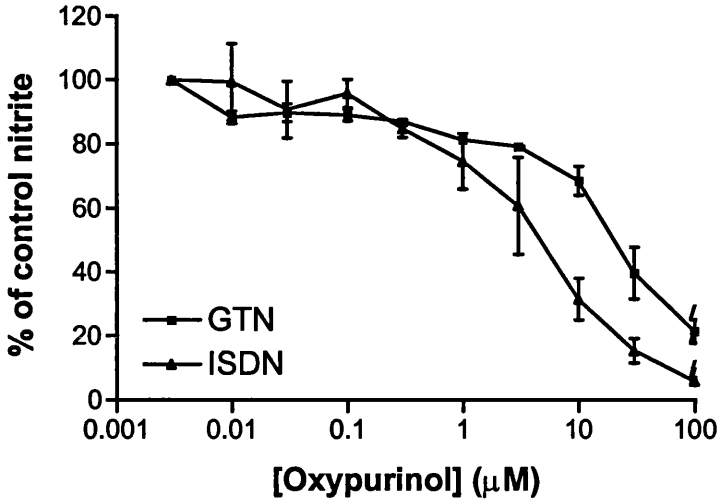

Figure 2.13. The effect of the xanthine oxidase inhibitor oxypurinol on the reduction of organic nitrates GTN and ISDN to nitrite by XO in the presence of xanthine and under limited oxygen conditions. Experiments were carried out as detailed in figure 2.9. Results are shown as the mean ± SEM (n = 3) carried out in triplicate.

Oxypurinol is shown to reduce the measurable nitrite generated from GTN and ISDN. The IC_{50} values for GTN and ISDN are 19.95μM and 4.64μM respectively.

In the light of the results shown previously for DPI and inorganic nitrate, the effect of DPI was assessed with organic nitrates as substrates. As can be seen from figure 2.14, DPI has an inhibitory effect on the reduction of organic nitrate to nitrite in this assay system. The DPI IC_{50} values for GTN and ISDN are 9.620μM and 2.037μM respectively.

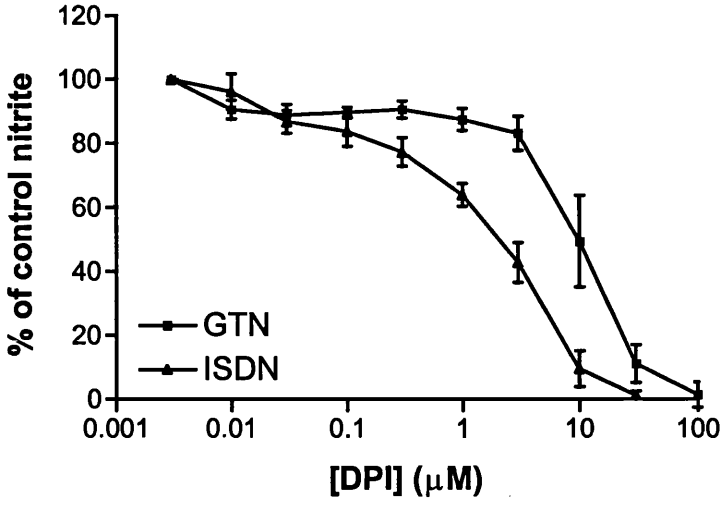

Figure 2.14. The effect of DPI on the nitrate reductase activity of XO using the organic nitrates GTN and ISDN. Experimental protocol and results expressed as detailed in figure 2.5, ± SEM (n = 3) in triplicate.

2.3.1.7 The reduction of nitrite

The proposed mechanism of action of the organic nitrates is via the generation of NO and then the subsequent relaxation of smooth muscle (see introduction 2.1). It was decided to examine the further reduction of nitrite in this system following the results shown in figure 2.3 where nitrite concentration began to decline after 30 minutes of incubation with XO and xanthine. Figure 2.15 shows an attempt to characterise the loss of nitrite as a measure of nitrite reductase activity. It was shown that an initial rapid reduction in measurable nitrite occurred compared to the control and the known starting concentration. This initial rapid reduction is followed by a slower reduction up to 30 minutes, after which there is very little change in the overall nitrite concentration. The maximal reduction is ~ 6μM compared to the control nitrite concentration which remains constant throughout the rest of the assay.

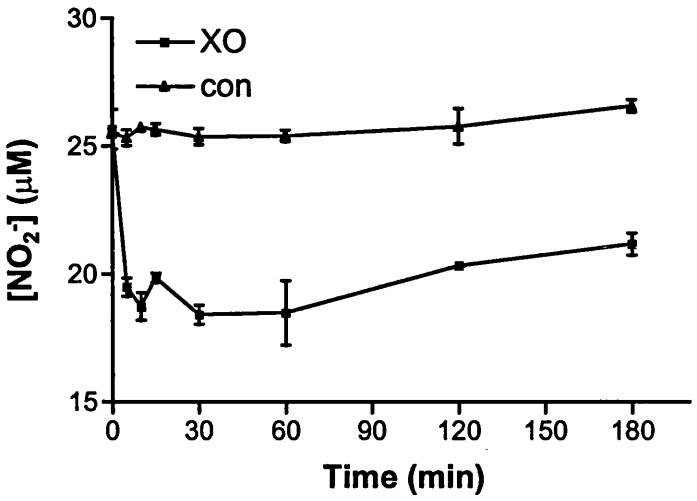

Figure 2.15. The reduction of inorganic nitrite in the presence of XO and xanthine. Experimental protocol was as described for figure 2.5 with the introduction of 25μM sodium nitrite ($NaNO_2$) in place of KNO_3. A control of nitrite with enzyme in the absence of xanthine was also used. Results are mean ± SEM (n = 3) in triplicate.

2.3.2. The measurement of nitric oxide

2.3.2.1 Nitric oxide generation from organic and inorganic nitrates

As discussed in the introduction to this chapter, a variety of techniques can be used to detect NO generation.

2.3.2.1.1 Mesenteric relaxation

The effect of various nitrates and nitrite on the relaxation response of contracted rat mesenteric vessels was measured by monitoring pressure changes in the perfused mesentery. The effect of low oxygen concentration on relaxation was also measured using this system.

Figure 2.16 shows the relaxation response mediated by GTN, nitrate or nitrite at a range of concentrations in the presence of 95% O_2 saturated (normoxic) or 5% CO_2

balanced nitrogen saturated (hypoxic) perfusion media. Relaxation is shown as a positive change in perfusion pressure as opposed to contractions which are shown as a negative change in perfusion pressure.

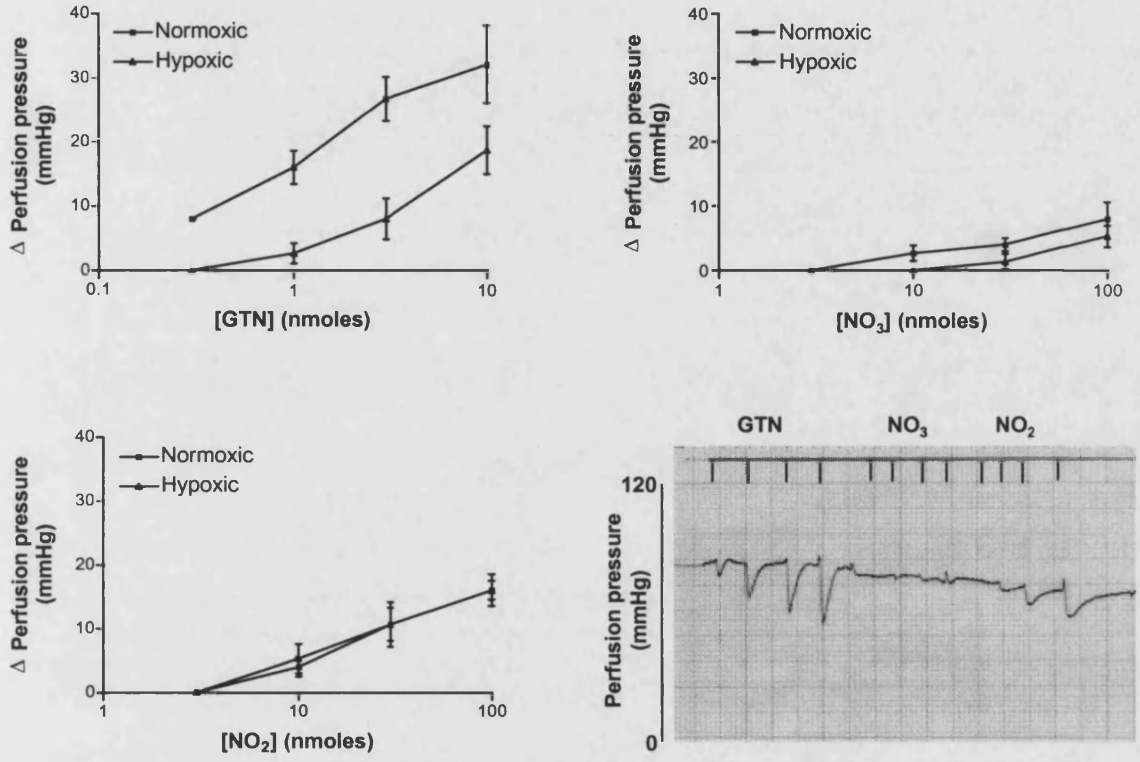

Figure 2.16. The relaxation of constricted rat mesenteric vessels. Rat mesentery was constricted with a continual perfusion of Krebs-Heinslet solution containing 10μM phenylephrine perfused at 5ml min^{-1}. GTN, nitrate or nitrite was injected into the perfusion media and the pressure change recorded on a chart recorder in mmHg. Data are from mean ± SD from 1 experiment in duplicate from two animals.

GTN, nitrate and nitrite caused a dose-dependent reduction in the perfusion pressure of the constricted rat mesentery. GTN caused relaxations that were of greater magnitude than nitrite or nitrate using lower concentrations. Nitrite gave a greater magnitude of relaxation than nitrate of similar concentrations. The

relaxation response of GTN and nitrate was greater in the 95% O_2 saturated perfusion media compared to the 5% CO_2 saturated media: 32.09 ± 5.95 compared to 18.73 ± 3.74mmHg for GTN and 8.02 ± 2.6 compared to 5.34 ± 1.65mmHg for nitrate at 10 and 100nmoles, 95% O_2 to 5% CO_2 balanced nitrogen respectively.

The relaxation response to nitrite however was not affected by the oxygen saturation of the perfusion media with relaxations of 16.04 ± 1.5 compared to 16.04 ± 2.5mmHg at 100nmoles nitrite in 95% O_2 and 5% CO_2.

The effect of allopurinol on the GTN mediated relaxation of phenylephrine contracted 5% CO_2 balanced N_2 saturated perfused rat mesentery was investigated. The change in perfusion pressure on the addition of various concentrations of GTN was measured and compared to the response to the same stimuli in the presence of 100μM allopurinol in the perfusion media. Figure 2.17 shows the results of this experiment.

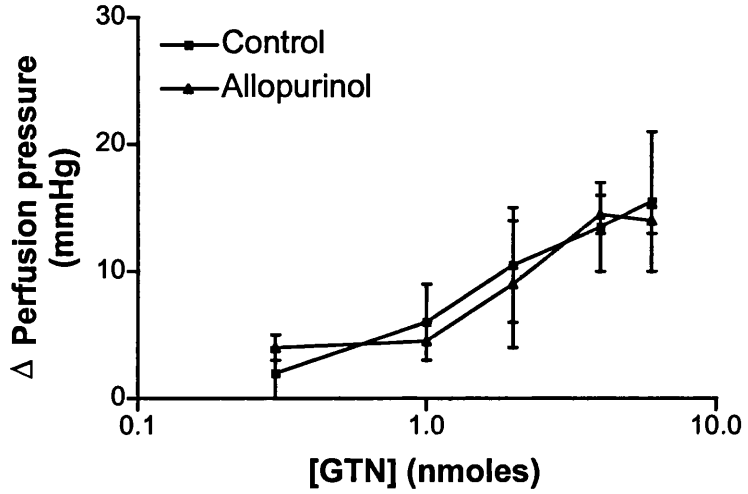

Figure 2.17. The relaxation response to GTN of perfused mesentery in the presence and absence of 100μM allopurinol. Data are mean ± SD from 1 experiment in duplicate from two animals.

Allopurinol at this concentration had no effect on the GTN mediated relaxation of the rat mesentery.

The fixed tissue was sectioned and stained with haematoxylin and eosin and also stained for xanthine oxidase using a polyclonal antibody raised against bovine xanthine oxidase in rabbits (Chemicon, USA). Figure 2.18 shows the H+E staining (A) and the antibody staining (B) for one representative rat mesentery.

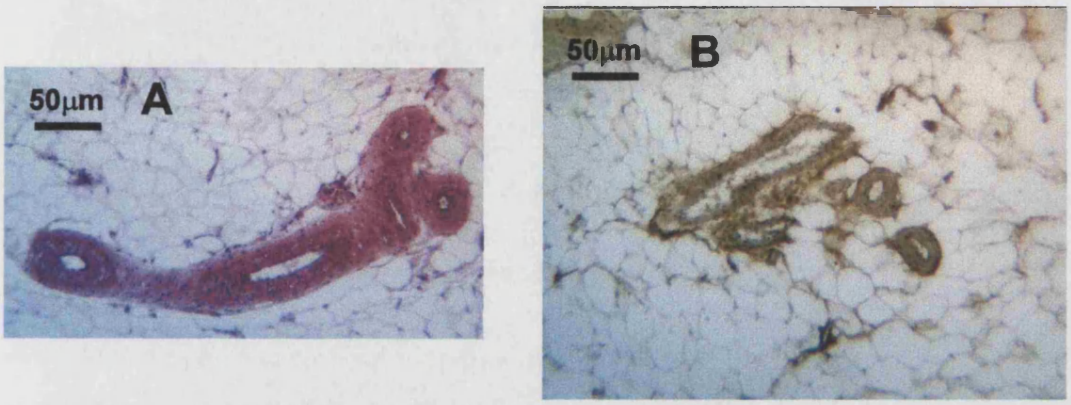

Figure 2.18. The staining of rat mesentery for Xanthine oxidase. Slides were prepared and stained as described in appendix I.

Vessels were observed in a lattice of adipocytes following the removal of lipids in xylene. On staining for XO, it was difficult to interpret positive staining compared to background due to the lack of surrounding cell types. Some possible staining was seen in the smooth muscle layers surrounding the vessels and seemed to be absent from the endothelium. However the results were inconclusive with this antibody.

2.3.2.1.2 Ozone chemiluminescence

The following experiments utilised the ozone enhanced chemiluminescence (OEC) reaction with nitric oxide to measure NO generation from a variety of substrates and XO. The following experiments utilised this method in the determination of NO generation.

The previous experiments on the reduction of nitrates to nitrite and the reduction of nitrite were all carried out in the presence of xanthine. In the following experiments NADH was used in place of xanthine as the electron donor. Figure 2.19 shows a typical NO generation curve derived from GTN, XO and NADH.

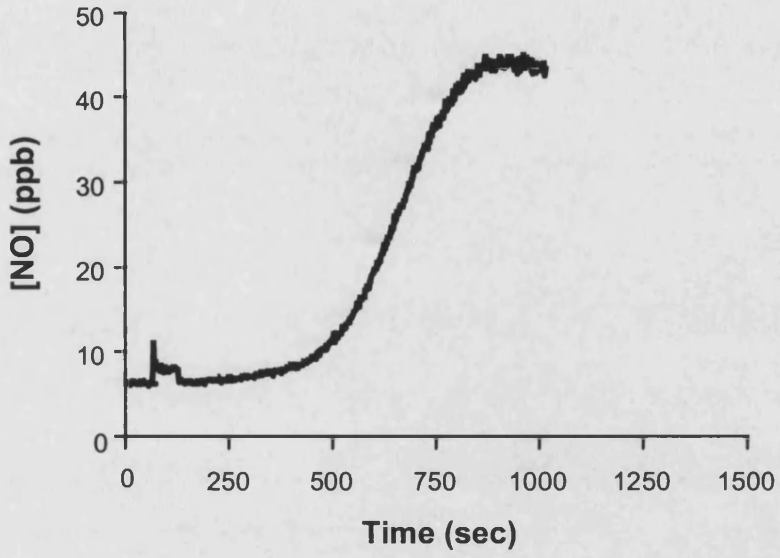

Figure 2.19. The generation of NO from GTN mediated by XO in the presence of NADH. Substrates were gassed with 5% CO_2 balanced nitrogen for 2 minutes prior to their introduction into a reaction vial. NADH and GTN were incubated together prior to the addition of enzyme. The NO generated was followed continually by the chemiluminescence analyser until a plateau was reached. The rate of NO generation was then read as the NO generation in ppb per second.

The graph shows a real time detection of NO from the apparatus setup outlined in figure 2.4. In chemiluminescence reactions the fastest rate of production is given by the peak height of OEC. In the figure above the data prior to the plateau are pre-steady state kinetics where the rate of reaction is continually increasing, i.e. acceleration. At the plateau, the rate of NO production is constant and at its

greatest and is said to be in steady state. The rate of NO production in the figure shown is approximately 45ppb sec^{-1}. Note the time taken from the injection of enzyme ~ 100 seconds to reaching steady state NO generation ~ 770 seconds.

2.3.2.2 The effect of XO inhibitors

The generation of NO from GTN and NADH in the presence of XO and under 5% CO_2 balanced nitrogen was assessed in relation to the inhibitors oxypurinol, BOF-4272 and DPI. The maximal rate of NO generation in a reaction without inhibitor was used as the 100% positive control. The same reaction mixture was then run in the presence of a range of inhibitor concentrations. The maximal rate of NO generation in the presence of inhibitor was then related to the uninhibited maximal rate. Figure 2.20 shows the effect of the inhibitors on NO generation from GTN.

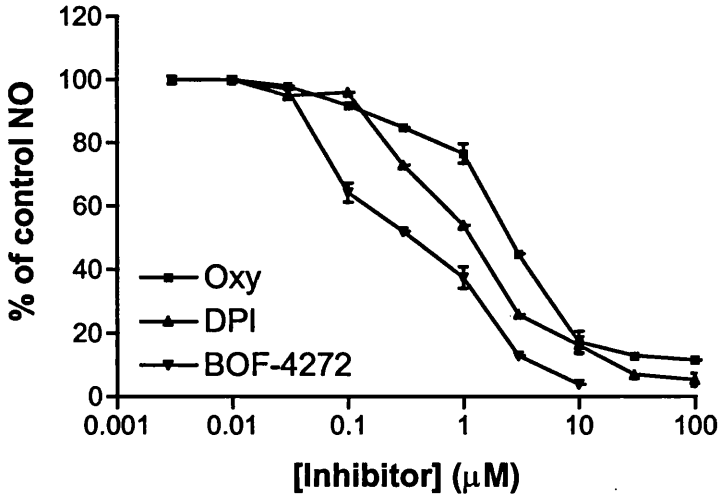

Figure 2.20. The effect of XO inhibitors on the generation of NO from GTN. Using 3mM GTN, 300μM NADH and 212.8μg of XO under 5% CO_2 balanced nitrogen. Results shown are mean ± SEM (n = 3) in duplicate.

All three inhibitors reduce the generation of NO below that of the non-inhibited control. The IC_{50} values for oxypurinol, BOF-4272 and DPI are 2.464μM, 0.348μM and 1.165μM respectively.

In the same manner as described for figure 2.19, the NO generating capacity of XO in the presence of GTN and methylene blue was assessed. Methylene blue caused a dose-dependent reduction of NO generation from GTN and gave an IC_{50} value of 0.6945μM.

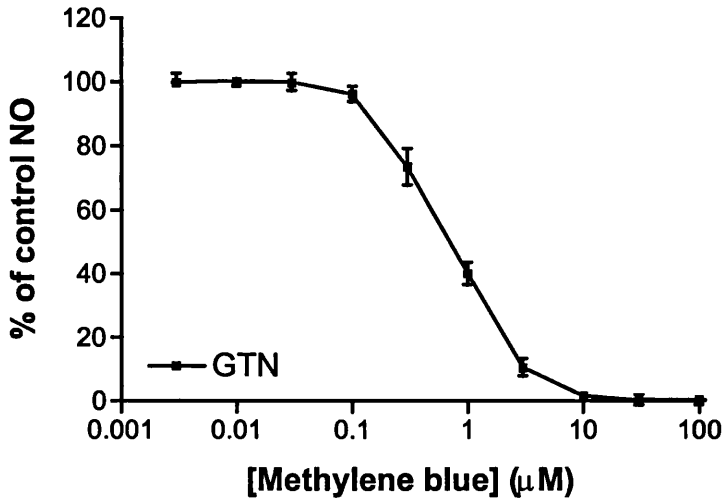

Figure 2.21. Effect of methylene blue incubation on the NO generating capacity of XO in the presence of GTN and NADH. The experiments were carried out as described previously and the graph shows mean values ± SEM (n = 3) in duplicate.

2.3.3 Kinetic determinations

In order to determine the specific activity, the maximal rate and a possible Michaelis constant (K_m) for these reactions, the kinetic parameters were measured. This took the form of the oxidation of NADH in the presence of XO and a range of substrates in the absence of oxygen and the measurement of NO generation in the presence of a range of electron donors and electron acceptors.

2.3.3.1 Measurement of NADH oxidation by XO

XO is known to oxidise NADH to NAD+ in aerobic systems with the concomitant generation of superoxide radical (Sanders *et al* 1997). The rate of NADH oxidation in the absence of any other electron acceptor is dependent on the concentration of dissolved oxygen in the reaction mixture. The rate of NADH oxidation was therefore monitored at a range of oxygen concentrations.

Figure 2.22 shows the effect of oxygen concentration on the rate of NADH oxidation in the presence of XO.

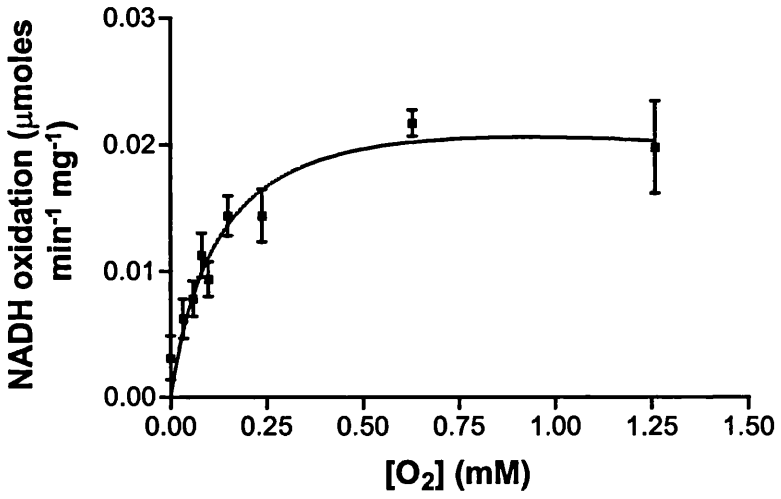

Figure 2.22. The rate of NADH oxidation compared to oxygen concentration. Solutions of NADH and buffer were gassed for 5 minutes with fractional mixtures of 100% oxygen and 5% CO_2 balanced nitrogen to generate a range of oxygen concentrations. XO was also gassed with the same gas mixture and then added to a 1ml cuvette that was sealed with an airtight cap where the oxidation of NADH was followed in a spectrophotometer at 340nm. The initial rate of each oxidation in the presence of 300μM NADH was calculated and the results plotted against oxygen concentration in moles per litre as taken from

oxygen saturation tables (Carpenter 1966 and Green and Carritt 1967). (Data are shown as ± SEM (n=3) in duplicate).

The rate of NADH oxidation is proportional to the concentration of oxygen. This is then saturated at higher oxygen concentrations and follows the law of mass action. The kinetic parameters were calculated by plotting the concentration [S] divided by the initial rate v against the initial concentration of substrate, in this case oxygen, to generate a Hanes-Woolf plot. From the graph shown in figure 2.23, the maximal rate of reaction v_{max} and the Michaelis constant K_m can be calculated.

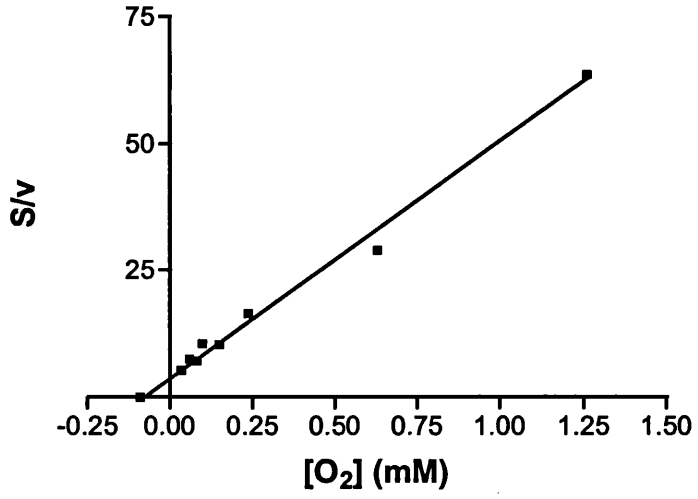

Figure 2.23. The Hanes plot of data from figure 2.22. The slope gives the reciprocal of v_{max} and the x-axis intercept is equal to $-K_m$. Experimental conditions were as described in figure 2.22.

The kinetic values derived from Figure 2.23 give the v_{max} = 0.0214 μmoles min^{-1} mg^{-1} and K_m of 73μM for oxygen.

This assay system was then used to measure the rates of NADH oxidation in the absence of oxygen and in the presence of various electron acceptors.

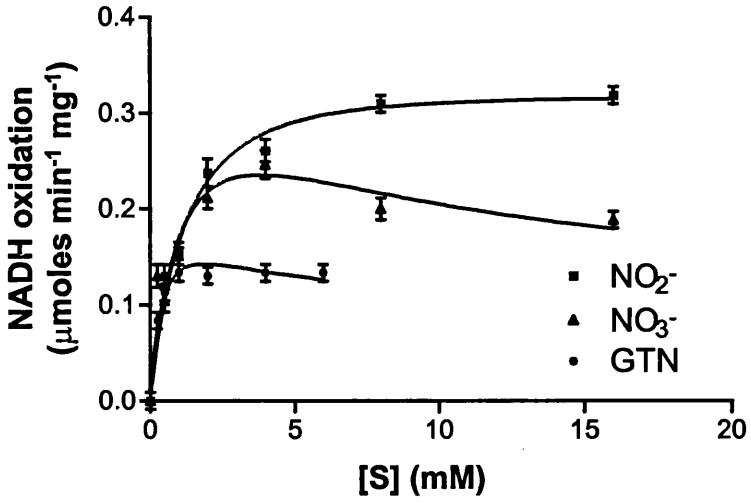

Figure 2.24. The rate of NADH oxidation in the absence of oxygen and in the presence of alternative electron acceptors. The oxidation of 300μM NADH was followed as described in figure 2.21 using buffer gassed with 5% CO_2 balanced nitrogen in capped 1ml cuvettes with XO. (Data show mean ± SEM (n = 3) in duplicate).

All electron acceptors used followed similar kinetic parameters with saturation occurring first in GTN, nitrate and then nitrite. The Hanes-Woolf plot of these data is shown in figure 2.25.

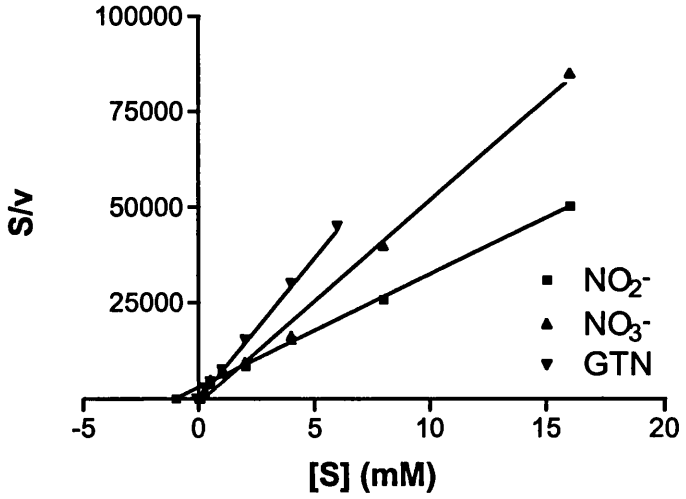

Figure 2.25. The Hanes-Woolf plot of NADH oxidation in the presence of initrate, GTN or initrite.

The kinetic parameters derived from this plot are shown in table 2.1

Substrate	K_{app} (mM)	V_{max} (nmoles min^{-1} mg^{-1})
Oxygen	0.073	21.4
GTN	0.656	135
NO_3^-	0.340	192
NO_2^-	0.723	332

Table 2.1. The kinetic parameters for the oxidation of NADH by a variety of electron acceptors in the presence of XO at 300μM NADH.

To validate this assay, the effect of oxypurinol was assessed. Oxypurinol has no effect on the oxidation of NADH in the presence of oxygen (Sanders *et al* 1997 and Zhang *et al* 1998) but will inhibit substrates which derive their electrons by binding at the molybdenum site. Figure 2.26 shows the effect of oxypurinol at a range of concentrations on the oxidation of NADH in the presence of nitrite.

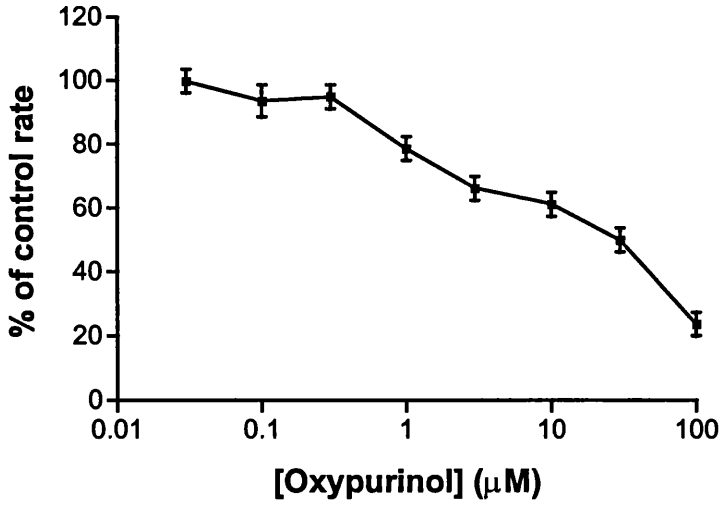

Figure 2.26. The effect of oxypurinol on the oxidation of NADH by XO. In the absence of oxygen using 300mM NADH and 8mM nitrite. Data are ± SEM (n = 2) in duplicate.

Oxypurinol is seen to inhibit the oxidation of NADH in the presence of nitrite with an IC_{50} value of 28.4μM.

2.3.3.2 Kinetic determinations using NO measurements

The use of NO determination allows for the measurement of the end product of reactions and allows the utilisation of alternative electron donors and acceptors all within the same assay protocol.

2.3.3.2.1 Using NADH as the electron donor

Using NADH and nitrite the enzyme concentration dependence of NO generation was measured using the ozone chemiluminescence assay.

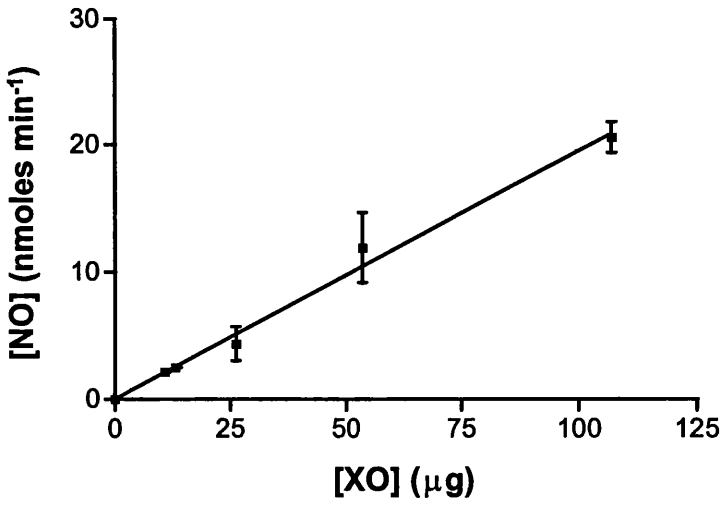

Figure 2.27. The Xanthine oxidase concentration-dependent generation of nitric oxide from nitrite and NADH. NO_2^- at 1mM and NADH at 300μM under 5% CO_2 balanced nitrogen. Data are mean ± SEM (n = 3) in duplicate.

The generation of NO was proportional to the enzyme concentration at fixed substrate concentrations.

The initial rate of reaction was measured for the NO generation from inorganic nitrate at a range of concentrations against a fixed concentration of NADH (300μM). The resultant data were plotted as the rate of reaction (v) against substrate (S) concentration – v/S, curve and then subjected to a linear transform in the form of the Hanes-Woolf plot and is shown in figure 2.28.

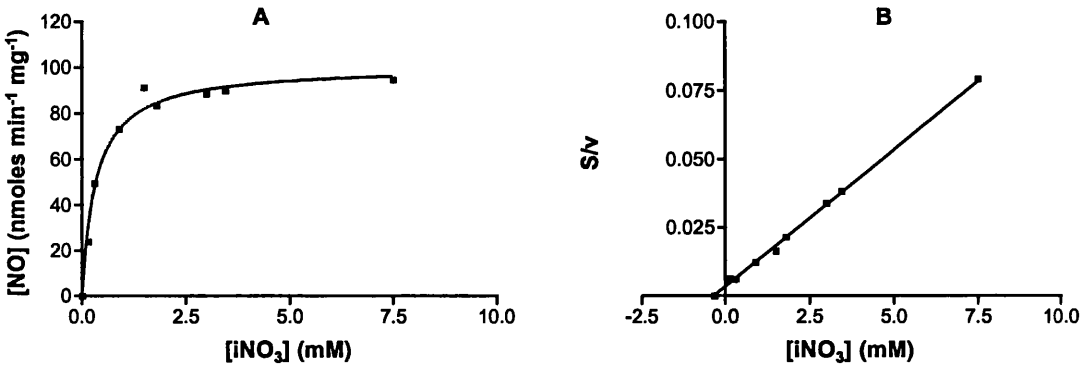

Figure 2.28. The NO generation from inorganic nitrate.

The generation of NO from inorganic nitrate varies hyperbolically with substrate concentration which is indicative of Michaelis-Menten kinetics. Linear transformation of the data in figure 2.28**A** gave a straight line with intercept on the x-axis K_m 0.321mM with a slope v_{max} 98.89nmoles min^{-1} mg^{-1} 2.28**B**. This was repeated for organic nitrate in the form of glyceryl-tri-nitrate (GTN) and the results shown in figure 2.29.

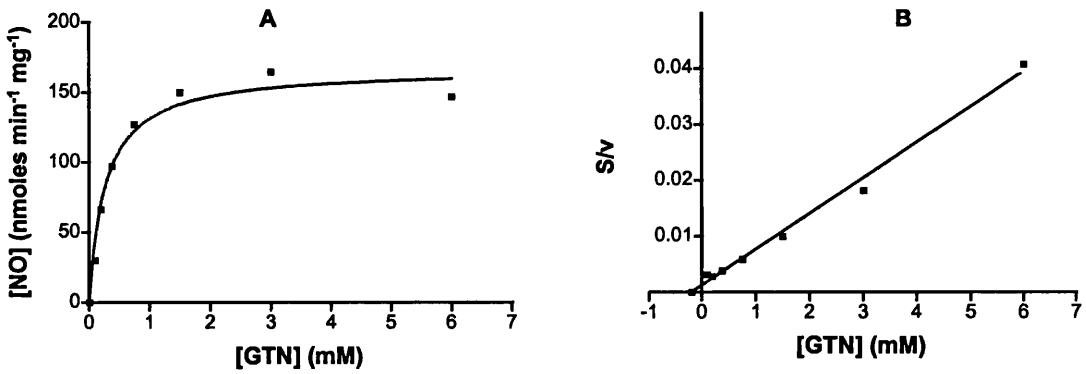

Figure 2.29. The v against S curve for GTN in the presence of 300μM NADH.

In the presence of GTN the generation of NO followed Michaeli-Menten kinetics (2.29**A**) and the linear transform (2.29**B**) gave intercept at K_m 0.194mM and slope v_{max} 156.65nmoles min^{-1} mg^{-1}.

For the generation of NO from nitrite in the presence of NADH, both nitrite and NADH were varied at fixed concentrations of the second substrate (NADH or nitrite respectively).

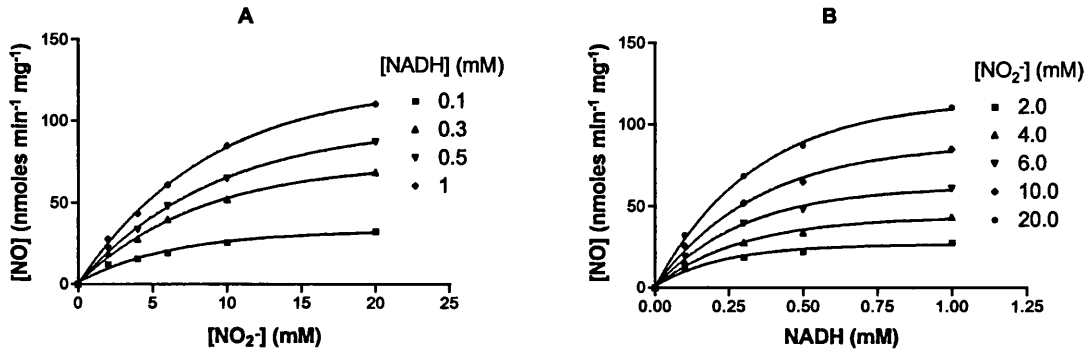

Figure 2.30. The v against S plots for NO generation from nitrite against NADH concentration (2.30**A**) and NADH against varying nitrite (2.30**B**).

For both treatments the reaction followed Michaelis-Menten kinetics. The data were then subjected to linear transform and plotted in figure 2.31.

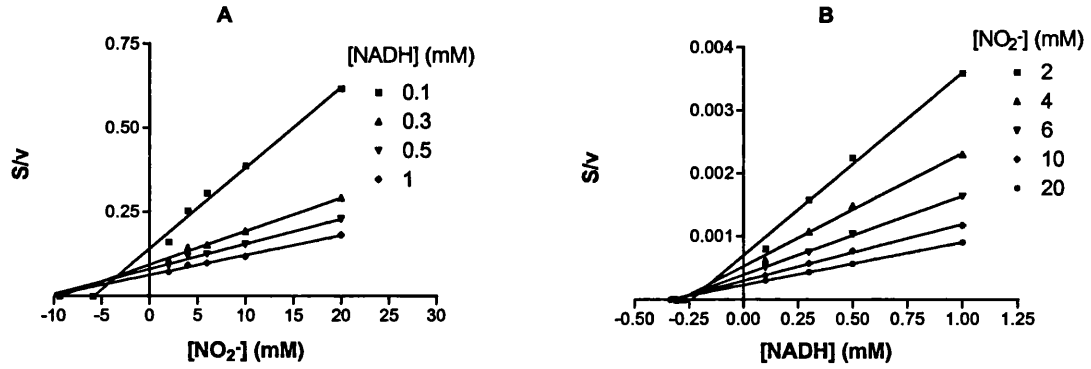

Figure 2.31. Hanes-Woolf plots for nitrite **A** and NADH **B** from the data shown in figure 2.30.

This treatment of data generates variables that can then be subjected to secondary plotting, generating K_m and v_{max} data over a range of substrate concentrations for both substrates.

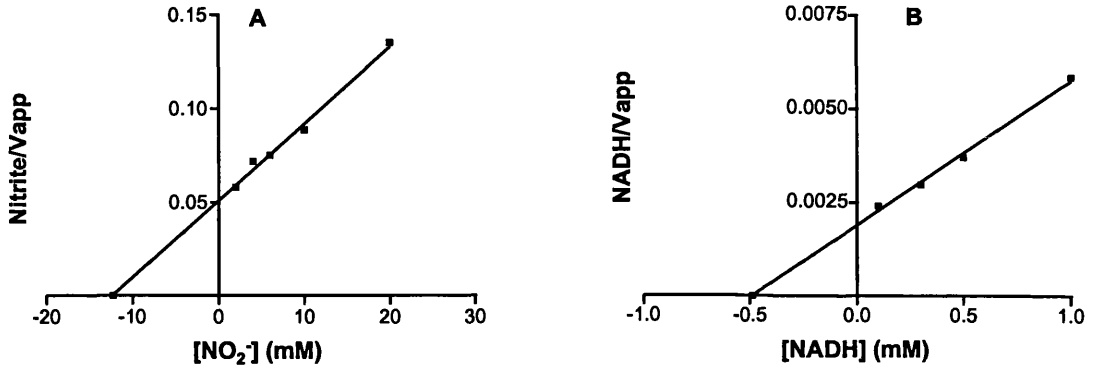

Figure 2.32. The secondary plots for nitrite **A** and NADH **B**.

The x intercept gives the K_m for nitrite as $K_{Nitrite}$ 12.29mM and the K_m for NADH at K_{NADH} 0.488mM. The maximum rate of reaction is given by the slope and is equal to v_{max} 240.98nmoles min^{-1} mg^{-1} and 257nmoles min^{-1} mg^{-1} respectively.

Table 2.2 summarises the kinetic analysis for nitrate and nitrite substrates in the presence of NADH and XO.

Substrate	K_m (mM)	v_{max} (nmoles min^{-1} mg^{-1})
INO_3^- (300μM NADH)	0.321	98.89
GTN (300μM NADH)	0.194	156.65
INO_2^- (NADH range)	12.29	241
NADH (Nitrite range)	0.488	257

Table 2.2. The Kinetic parameters derived from XO mediated NO generation from the ozone chemiluminescence assay.

The Hanes-Woolf plots show non-parallel lines with progressively smaller intercepts on the x-axis as the concentration of fixed second substrate is increased and

suggests that the reaction mechanism follows a ternary complex formation of enzyme and substrate.

The effect of the xanthine oxidase inhibitor oxypurinol was measured in the presence of nitrite and NADH. The effect of oxypurinol was to inhibit the measurement of NO from this reaction mixture in a dose-dependent manner. Figure 2.33 shows the effect of oxypurinol on NO generation from nitrite and NADH.

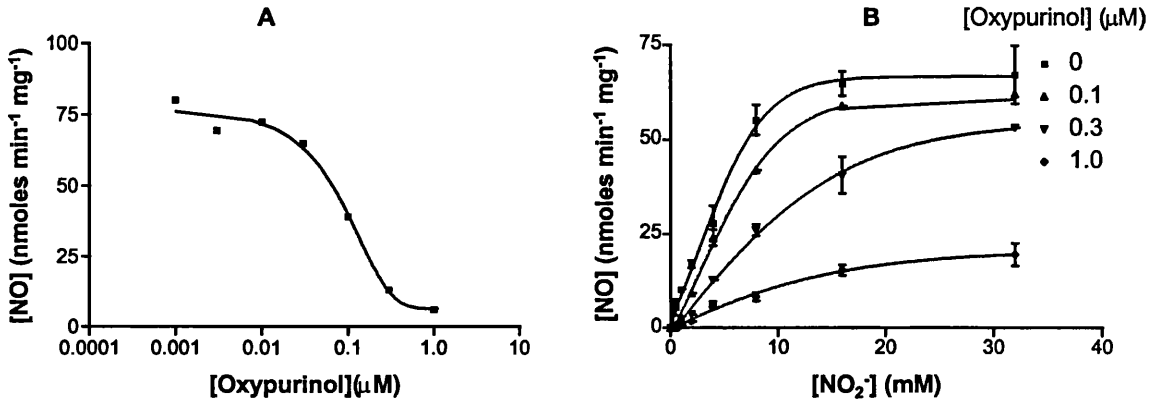

Figure 2.33. The effect of oxypurinol on NO generation from nitrite and NADH. **A** nitrite 20mM and NADH 300μM. **B** nitrite range and NADH at 300μM.

At a range of nitrite concentrations and three fixed oxypurinol concentrations the measurement of NO generation was followed. From the data generated the apparent K_m (K_{app}) for each set of results in the presence or absence of inhibitor was calculated. The secondary plot of K_{app} values against oxypurinol concentrations was plotted to generate the inhibitory constant (K_i).

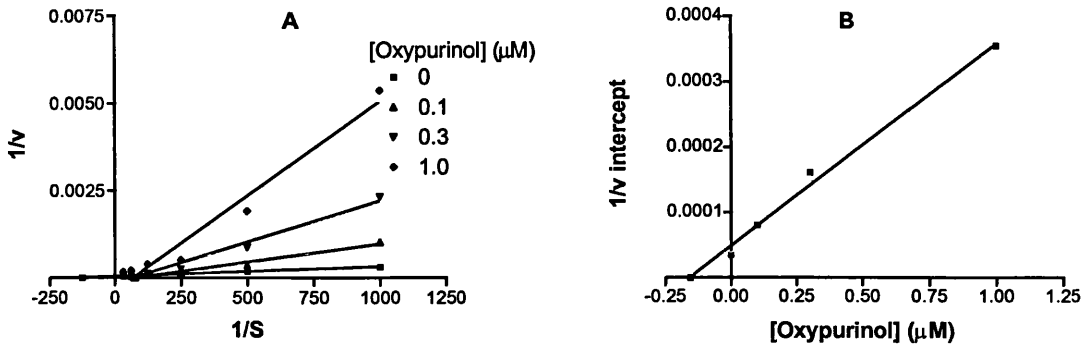

Figure 2.34. The K_{app} (**A**) and K_i (**B**) determinations by linear transformation and secondary plot of data in figure 2.34.

The calculated K_i for oxypurinol in the presence of nitrite and NADH for XO was K_i 0.155μM. The increase in slope of the plot shown in figure 2.34A is suggestive of competitive inhibition for oxypurinol and nitrite.

2.3.3.2.2 Using alternative electron donors

From the original observation that XO could reduce nitrate to nitrite in the presence of xanthine, this reaction was followed measuring the NO generation from nitrite in the presence of a range of xanthine concentrations.

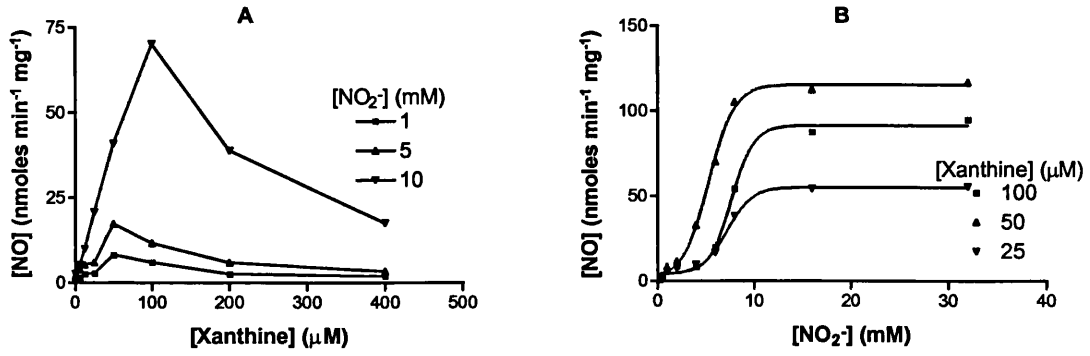

Figure 2.35. The NO generation from nitrite in the presence of XO and xanthine at varying xanthine (**A**) and nitrite (**B**) concentrations.

Varying xanthine concentration at fixed nitrite concentrations shows a point at which NO generation is reduced at high xanthine concentration > 50μM compared to low < 50μM xanthine. This is suggestive of substrate inhibition at high

concentrations of xanthine. The variation of nitrite against xanthine gives somewhat sigmoid shaped curves, which are indicative of non Michaelis-Menten kinetics. This is shown further in figure 2.36 with the upward turn of the Hanes-Woolf plot indicative of substrate inhibition.

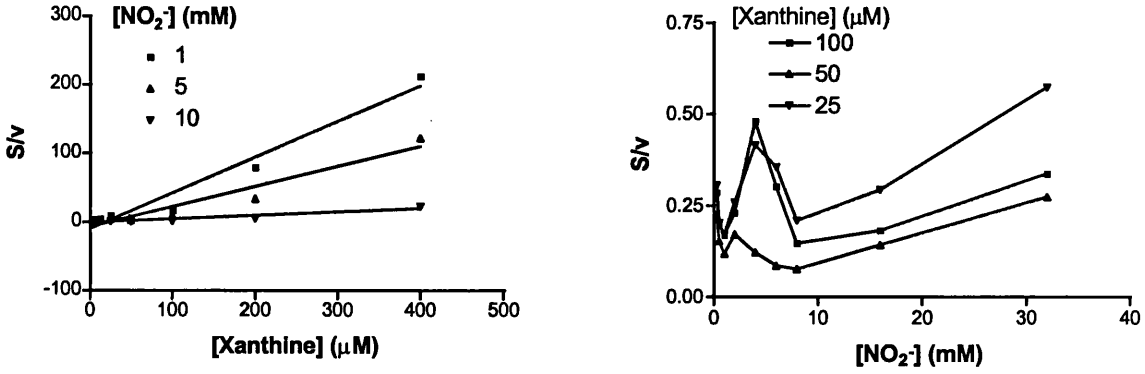

Figure 2.36. The Hanes-Woolf plots of data derived for NO generation mediated by XO in the presence of xanthine and nitrite.

Due to the non-Michaelis-Menten kinetics shown only working estimates of the rate constants are given for reference to relative reaction rates. From the v against S plots the apparent v_{max} and Michaelis constants, K_{app} for xanthine and nitrite are v_{app} 75 and 110nmoles min^{-1} mg^{-1} and K_{app} xanthine ~ 50μM and K_{app} nitrite ~ 7mM.

The use of the purine 1-methylxanthine was also assessed in the same manner as described above for xanthine.

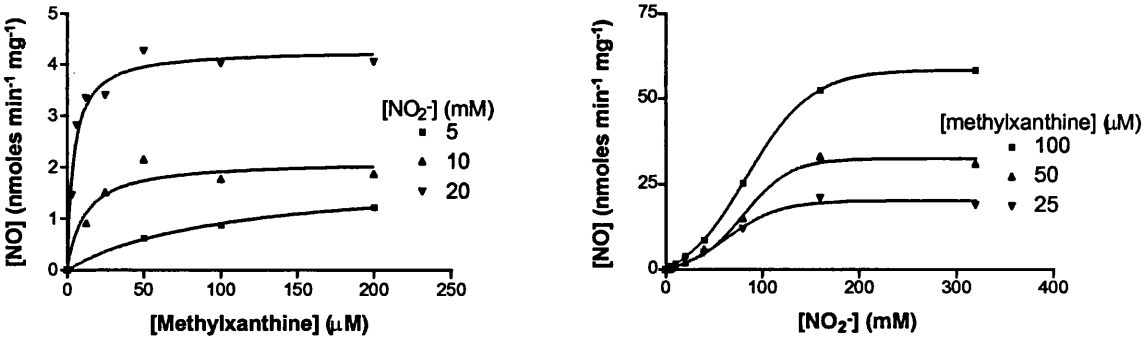

Figure 2.37. The v against S plots for NO generation from nitrite and methylxanthine in the presence of XO at 0%saturation oxygen.

In the presence of nitrite and 1-methylxanthine, xanthine oxidase was able to generate nitric oxide to give rectangular hyperbolas when varying methylxanthine concentration. On varying nitrite concentration, sigmoid like curves were generated and required relatively high nitrite concentration (up to 300mM nitrite) to reach saturation rates.

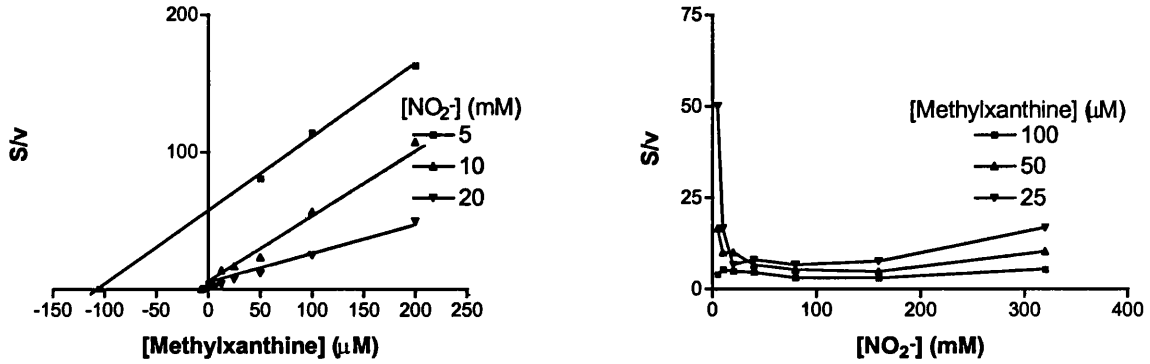

Figure 2.38. The Hanes-Woolf plot of the data generated for methylxanthine and nitrite.

Following analysis by Hanes-Woolf plots, deviations were seen from Michaelis-Menten kinetics whilst varying nitrite concentration similar to those seen for xanthine and varying nitrite concentrations.

From the v against S plot the K_{app} nitrite is given as ~ 25mM and the v_{app} as 8.77nmoles min^{-1} mg^{-1}. The K_{app} methylxanthine is given as ~ 20μM.

The ability of hypoxanthine to act as a substrate in XO mediated NO generation from nitrite was assessed as described above for xanthine.

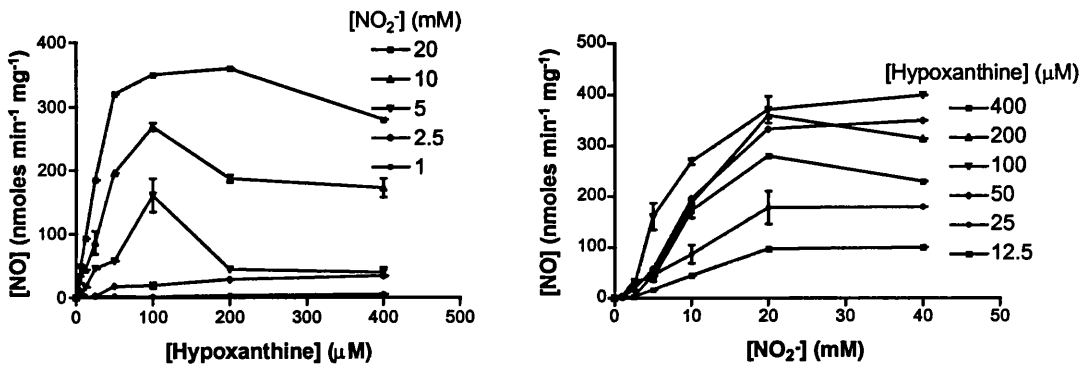

Figure 2.39. The v against S curves for nitrite and hypoxanthine.

At concentrations of hypoxanthine below 100μM, NO generation increases with increasing hypoxanthine and nitrite concentrations. Above 100μM hypoxanthine at low nitrite concentration the NO signal is reduced. However at the highest nitrite concentration the effect of increasing hypoxanthine concentration follows a rectangular hyperbola.

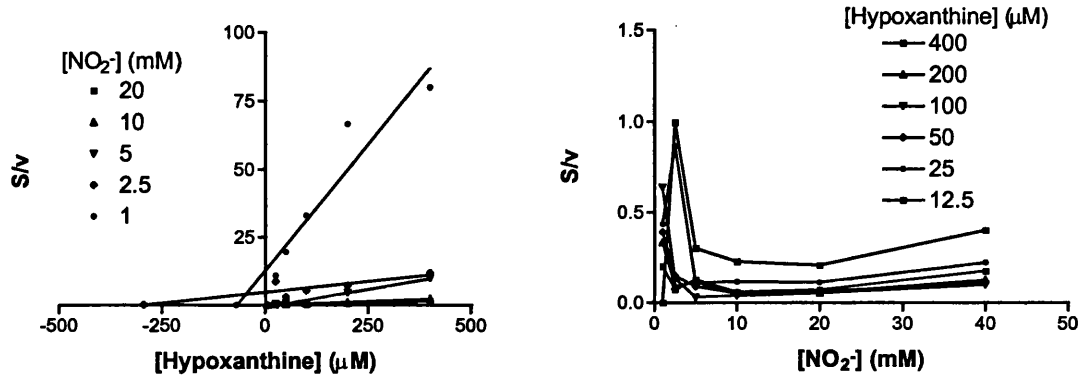

Figure 2.40. The Hanes-Woolf plots varying hypoxanthine A and nitrite B.

Similar Hanes-Woolf plots were generated for hypoxanthine / nitrite as those seen for the other purine substrates used previously suggesting substrate inhibition as shown by upward curves when varying nitrite against fixed purine substrate concentrations. The apparent rate constants from the v against S plots were v_{app} 370 and 400nmoles min^{-1} mg^{-1} with K_{app} nitrite ~ 20mM and K_{app} hypoxanthine ~ 25μM.

2.3.3.3 The relative NO generation from varying electron donors

The generation of NO from nitrite by xanthine oxidase in the presence of a range of electron donors was measured to assess the effects on NO generation following the peak height measurements. Using equimolar amounts of enzyme and substrates the figure 2.41 was generated.

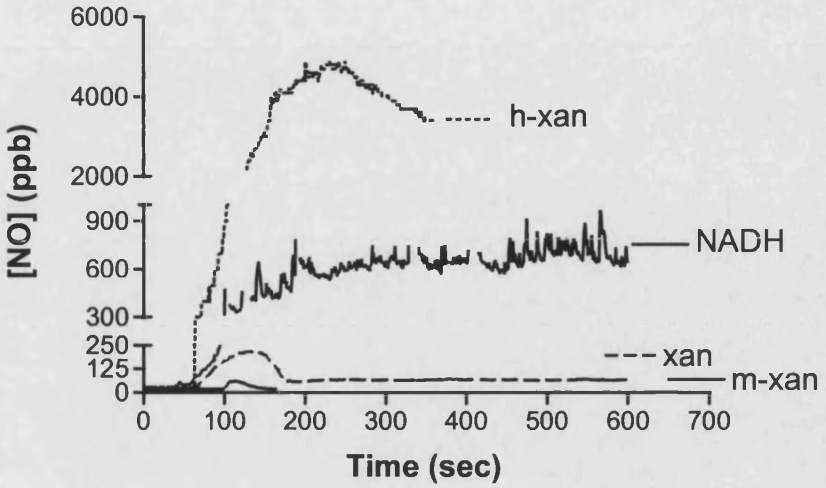

Figure 2.41. The NO generation from nitrite mediated by XO in the presence of a range of electron donors. XO 52.3μg, nitrite 10mM, hypoxanthine, NADH, xanthine and methylxanthine 100μM. Figure shows a representative trace for each electron donor.

The peak height data followed the order Hypoxanthine > NADH > Xanthine > Methylxanthine. Both xanthine and methylxanthine showed a fast initial response which was relatively short lived before the NO signal dropped but remained above the base line for up to an hour. Hypoxanthine showed an initial sharp rise in NO generation which became reduced over time but at a rate slower than xanthine and methylxanthine. NADH showed a relatively slow rise in pre steady state NO generation before reaching a plateau which was kept constant for greater than an hour. The NO generating capacity was eventually reduced back to base line levels after ~ 2 hours with the peak height reducing steadily.

2.3.3.4 Effect of DPI on xanthine-mediated NO generation from nitrite

Due to the effect of DPI on the enhanced generation of nitrite from nitrate such that aerobic nitrite generation was observed (2.3.1.6) the effect on NO generation from nitrite in the presence of xanthine and diphenyliodonium was measured. Xanthine

oxidase enzyme was mixed with xanthine, nitrite and DPI at a range of concentrations under a reduced oxygen atmosphere as previously described. Figure 2.42 shows the effect of this treatment on the OEC for nitric oxide generation.

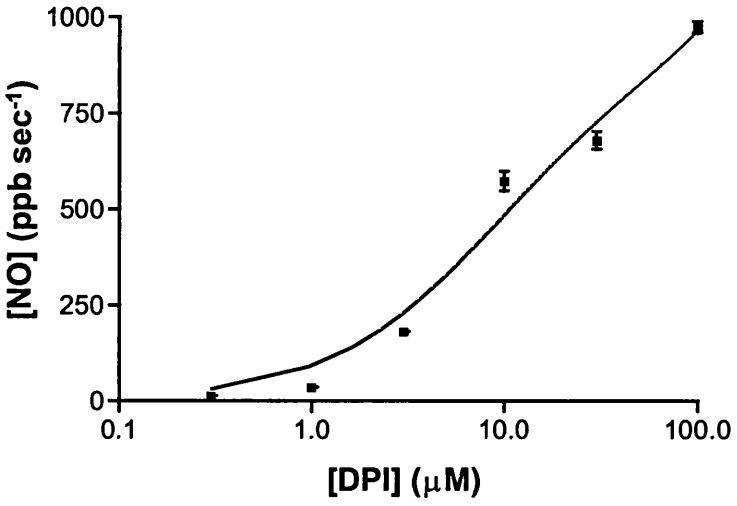

Figure 2.42. The NO generation from nitrite in the presence of XO, 53.2μg, xanthine, 50μM, nitrite, 1mM and DPI at a range of concentrations under low oxygen conditions. Results are mean ± SEM of two experiments in duplicate.

The effect of DPI was to increase the measurable NO from XO, xanthine and nitrite in a dose dependent manner with a significant increase in NO generation above the control without DPI added at concentrations above 1μM in this assay under these conditions.

To assess the possible aerobic generation of NO from this system the experiment was repeated at 21% oxygen saturation of the reaction mixture in figure 2.42 with 100μM DPI. Figure 2.43 shows the results of this study.

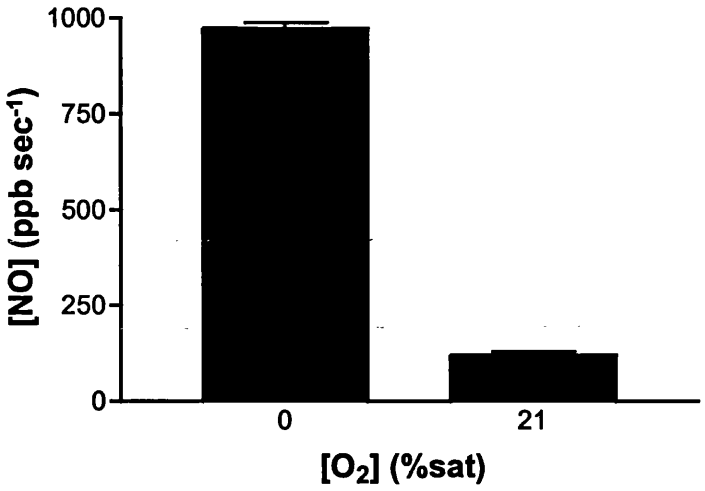

Figure 2.43. The NO generation from nitrite in the presence of XO, 53.2μg, xanthine, 50μM, nitrite, 1mM and DPI 100μM in air-saturated or nitrogen saturated buffer. Data are mean ± SEM (n = 3) in duplicate.

There is a significant increase ($p<0.05$) in the measurable NO in aerobic conditions in the presence of 100μM DPI compared to a control in the absence of DPI. The NO signal in air with 100μM DPI compared to the NO generated in 0% oxygen saturated media in the presence of DPI is significantly reduced ($p<0.01$) with an apparent 10 fold reduction (1000 ppb sec^{-1} in 0% oxygen compared to ~ 100 ppb sec^{-1} in air).

2.3.4 Effect of oxygen on NO generation from nitrite

Oxygen has effects on the measurement of NO by the ozone chemiluminescence system using XO as the catalyst. To determine the effect of oxygen on the measurement of NO, a range of experiments utilising various oxygen concentrations was carried out.

2.3.4.1 In the presence of NADH

NO was generated from a standard assay protocol for the reduction of nitrite by XO to NO in the presence of NADH and the absence of oxygen. The reaction rate was followed and the peak height measured. This protocol was repeated in the presence of known oxygen saturations and the results plotted as rate of NO generation against oxygen saturation. Figure 2.44 shows the effect of oxygen saturation on the rate of NO generation as measured in the ozone chemiluminescence reaction in the presence of 1mM nitrite, 53.2μg XO and 300μM NADH.

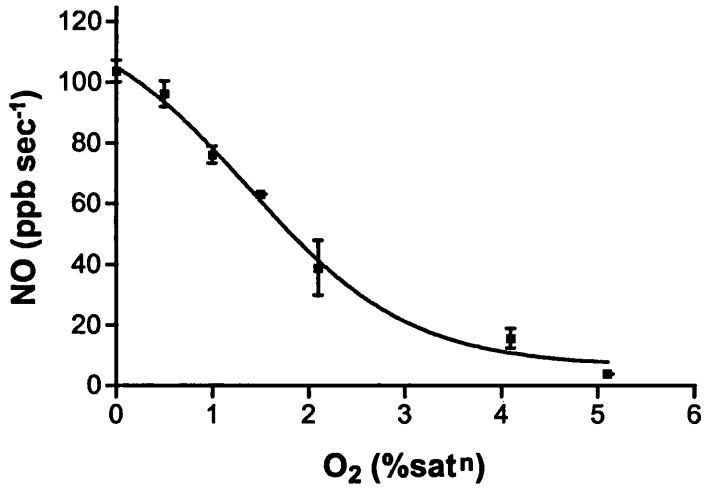

Figure 2.44. The effect of oxygen concentration on the measurement of NO from nitrite. All substrates were gassed using a mixture of 5% CO_2 balanced nitrogen and 100% oxygen. The rate of reaction was measured using the ozone chemiluminescence detection assay. Data are mean ± SEM from 2 experiments in duplicate.

The measurement of NO by this assay is dependent on the oxygen saturation of the media. The reaction rate is inversely proportional to the oxygen concentration. The half-maximal NO generation rate for this concentration of nitrite, NADH and XO

occurs at 1.8% oxygen saturation and the base line readings, where no more NO generation can be detected occurs at ~ 5% oxygen by saturation.

This experiment was repeated in the presence of 10mM nitrite and the results are shown in figure 2.45.

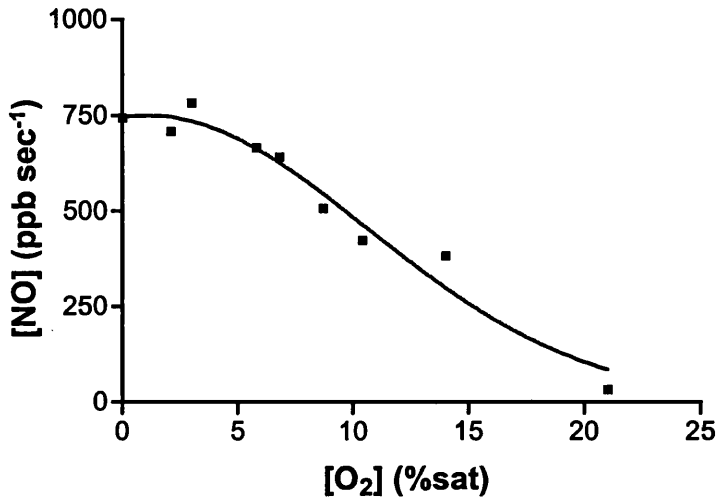

Figure 2.45. The effect of oxygen concentration on the measurement of NO from nitrite. All substrates were gassed using a mixture of 5% CO_2 balanced nitrogen and 100% oxygen. The rate of reaction was measured using the ozone chemiluminescence detection assay. Data are mean ± SEM from 2 experiments in duplicate.

The measurement of NO by this assay is dependent on the oxygen saturation of the reaction, this being inversely proportional to the measured rates. The half-maximal NO generation rate for this concentration of nitrite, NADH and XO occurs at 12.3% oxygen saturation and the base line readings, where no more NO generation can be detected occurs at ~ 21% oxygen by saturation.

At 10mM nitrite NO generation is detectable at higher oxygen saturations than compared to 1mM nitrite 12.3% compared to 1.8% oxygen saturation to give half maximal rates, with the curve being right-shifted.

2.3.4.2 In the presence of hypoxanthine

The effect of oxygen concentration on the generation of NO in the presence of hypoxanthine was also measured. Figure 2.46 shows the effect of oxygen on the NO signal from the ozone chemiluminescence analyser.

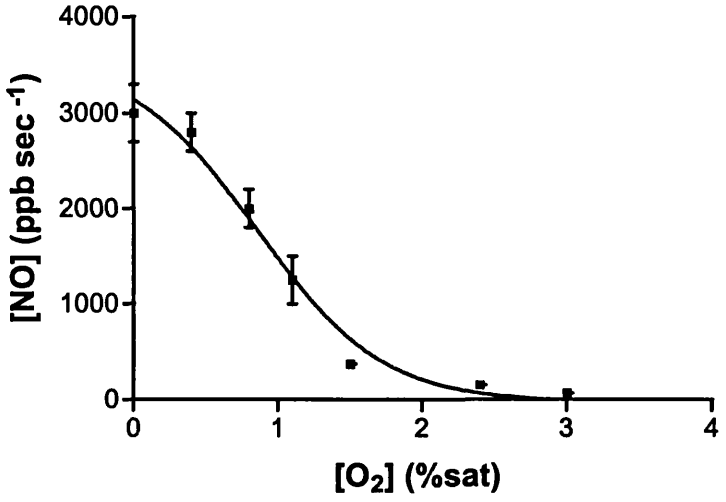

Figure 2.46. The effect of oxygen on the NO signal generated from XO, 53.2μg, nitrite 5mM and hypoxanthine 100μM. Data are mean values ± SEM of two experiments in duplicate.

The measurement of NO by this assay is dependent on the oxygen saturation of the reaction, this being inversely proportional to the measured rates. The half-maximal NO generation rate for this concentration of nitrite, NADH and XO occurs at 1% oxygen saturation and the baseline readings occur at ~ 3% oxygen by saturation.

2.3.4.3 In the presence of superoxide dismutase.

The generation of NO from XO and nitrite with hypoxanthine was measured at a range of oxygen concentrations with and without the addition of bovine superoxide dismutase from bovine erythrocytes (Bohringer, Germany). Figure 2.47 shows the effect of this incubation on the signal generated in the chemiluminescence reaction.

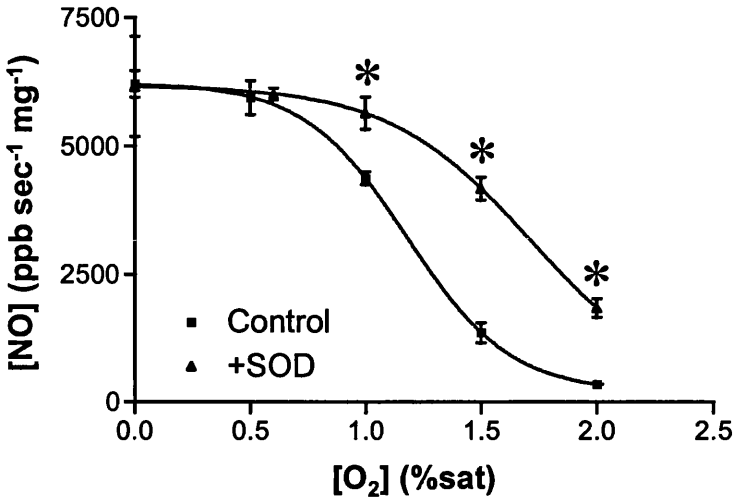

Figure 2.47. The NO generation from XO, nitrite and hypoxanthine in the presence and absence of 250U SOD. The peak heights of reaction rates were taken and compared to the oxygen concentration. Mean and ± SEM of 2 experiments in duplicate. * show significant deviation from the control $p<0.01$.

The chemiluminescence signal generated by the XO/nitrite/hypoxanthine system is reduced as the oxygen concentration increases with a half-maximal response of 1.19%. The signal generated from the same system in the presence of SOD is increased over the control level with a half-maximal response at 1.73%. The addition of SOD gives a statistically significant increase in the measurable signal from the NO generating system as the oxygen increases.

2.3.4.4 In the presence of Diphenyliodonium (DPI)

The effect of DPI was to enhance NO generation from nitrite in the presence of XO and hypoxanthine at low oxygen concentration. Under atmospheric oxygen concentrations, the generation of NO was followed using ozone chemiluminescence in the presence of increasing concentrations of DPI. Figure 2.48 shows the effect of DPI concentration on the NO signal from XO, hypoxanthine and nitrite.

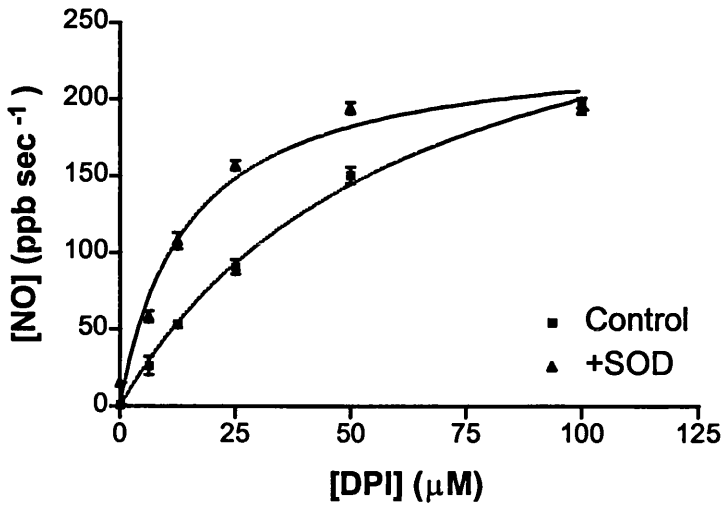

Figure 2.48. The effect of DPI on the NO signal generated from XO (53.2μg), hypoxanthine (100μM) and nitrite (1mM). Also in the presence of bovine SOD (250U). Results are mean ± SEM (n = 2) in triplicate.

The effect of DPI was to allow measurement of the NO signal from hypoxanthine and nitrite under atmospheric air oxygen concentrations. SOD also enhanced the NO signal at lower levels of DPI; half maximal DPI concentration ~15μM in the presence of SOD compared to 30μM in its absence, but there was no further enhancement of NO signal at 100μM DPI with this concentration of SOD.

2.3.5 The measurement of peroxynitrite generation

2.3.5.1 Oxidation of dihydrorhodamine

SIN-1 at a range of concentrations was added to DHR and DTPA in PBS and the absorbance change at 500nm followed in a spectrophotometer. Figure 2.49 shows the absorbance over time for SIN-1 at a range of concentrations.

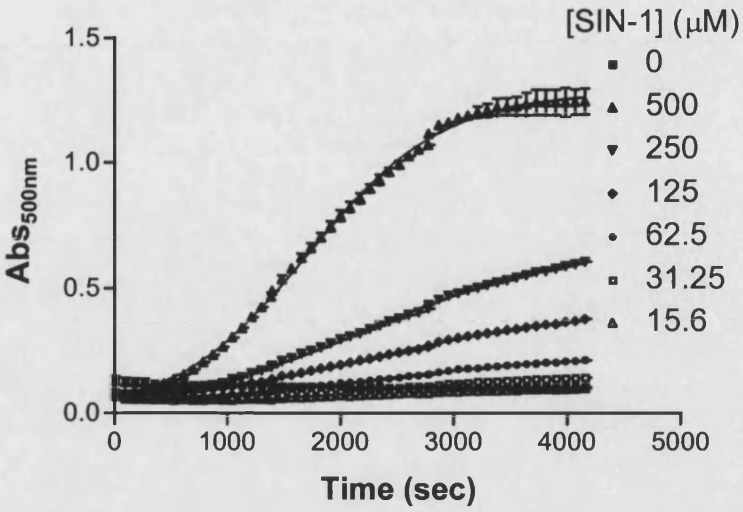

Figure 2.49. The absorbance of DHR following the addition of SIN-1. The blank consisted of DHR, DTPA and PBS at 37°C.

The dose-dependent increase in absorbance over time in the presence of SIN-1 follows sigmoidal kinetics in the highest concentration range. There is an initial lag phase in DHR oxidation to rhodamine followed by an increasing rate of change in absorbance until a plateau is reached. The fastest rate of change in absorbance was measured and the rate of generation of ONOO- calculated using the extinction coefficient of 75000 M^{-1} cm^{-1} for the oxidation of DHR by peroxynitrite and a correction factor of 2.2 as the efficiency of oxidation is ~ 45% (Crow *et al* 1995).

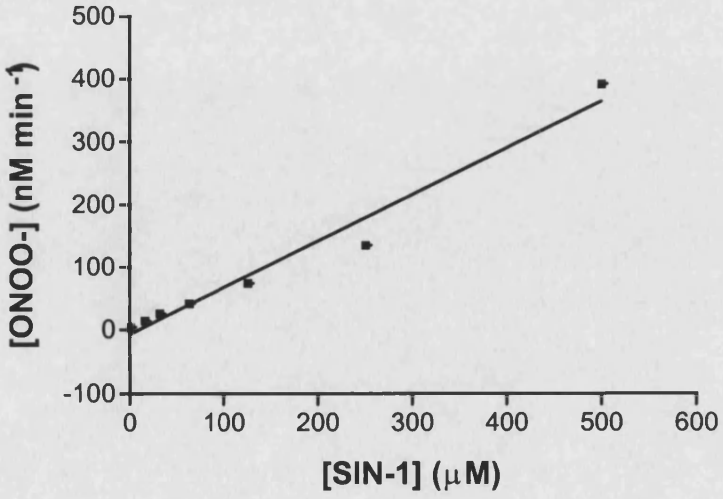

Figure 2.50. The dose-dependent generation of ONOO- from SIN-1 in solution.

Preliminary experiments in the presence of XO, nitrate and NADH in air-saturated buffer showed increasing absorbance of rhodamine at 500nm in both the control and experimental cuvettes. Figure 2.51 shows absorbance over time of DHR in the presence of XO, NADH and DTPA and in the presence or absence of 1mM nitrate.

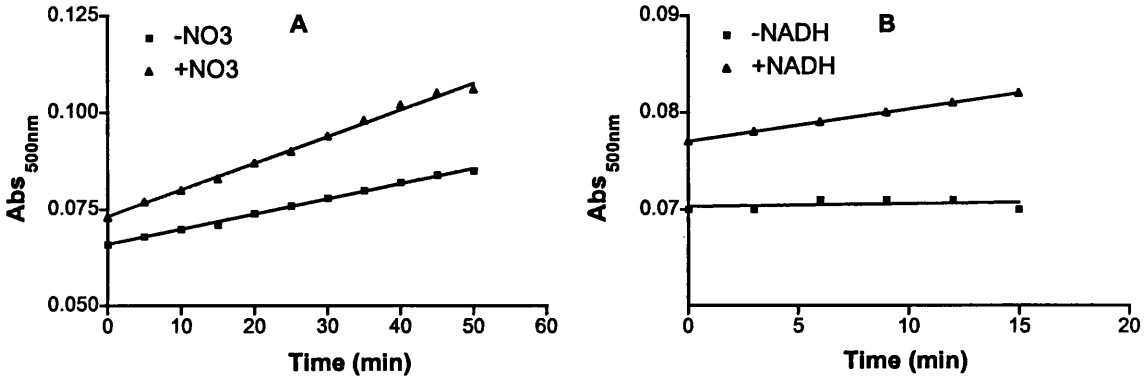

Figure 2.51. The absorbance at 500nm of rhodamine followed over time in the presence or absence of nitrate **A** or NADH **B**.

The rate of rhodamine formation in the presence of nitrate was 0.000691Abs_{500nm} min^{-1} compared to 0.000395 Abs_{500nm} min^{-1} in the absence of 1mM nitrate. The experiment was then repeated in the absence or presence of NADH. Figure 2.51B shows the rhodamine formation at 500nm in the presence of XO, DTPA, DHR and with or without 300μM NADH. Without NADH there is little change in absorbance over time (0.000029 Abs_{500nm} min^{-1}). However in the presence of NADH the rate increases to 0.000333 Abs_{500nm} min^{-1}.

To determine the susceptibility of the rhodamine to oxidation by compounds other than ONOO-, the effect of the oxidant nitrite was measured, as this can be used in the generation of NO by XO.

In the presence of DTPA and DHR, a range of nitrite concentrations was added to the system and the absorbance at 500nm was followed over time. Figure 2.52

shows the effect of increasing nitrite concentration on the rate of oxidation of DHR to rhodamine.

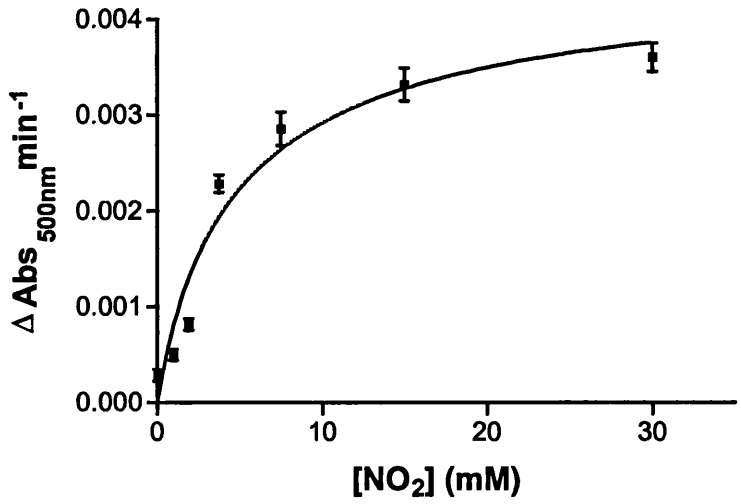

Figure 2.52. The effect of nitrite on the rate of oxidation or DHR to rhodamine. The maximal rate of change in absorbance was measured for each concentration of nitrite and the results plotted against nitrite concentration. Data are mean ± SEM (n = 3) in triplicate.

The effect of the nitrite was to increase the oxidation of DHR to rhodamine in a dose-dependent manner which began to plateau at ~ 30mM nitrite.

This experiment was then repeated by adding back NADH at a constant 30mM nitrite concentration in the presence of DTPA, DHR and PBS and again following the rate of change in absorbance at 500nm. Figure 2.53 shows the results of these analyses.

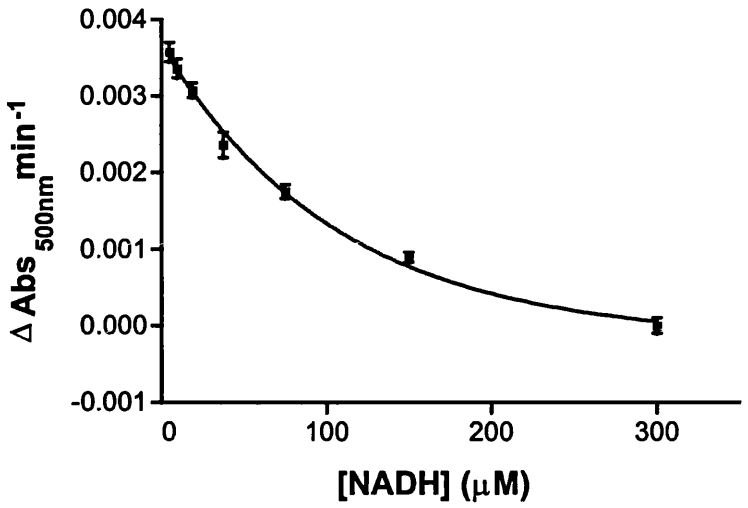

Figure 2.53. The effect of NADH on the nitrite mediated oxidation of DHR to rhodamine. Data are mean ± SEM (n = 3) in triplicate.

NADH addition to the DHR and nitrite mixture causes a dose-dependent decrease in absorbance and therefore oxidation of the DHR to rhodamine, which is sufficient to stop the detection of rhodamine oxidation in the presence of nitrite.

2.3.5.2 Oxidation of luminol and lucigenin

The report by Radi *et al* (1993) on the use of luminol to measure ONOO- generation was used as the basis of the following experiments.

SIN-1 was used to determine the possible use of luminol chemiluminescence as a probe for ONOO- generation. Figure 2.54 shows the luminol-enhanced chemiluminescence from SIN-1 degradation at 37°C.

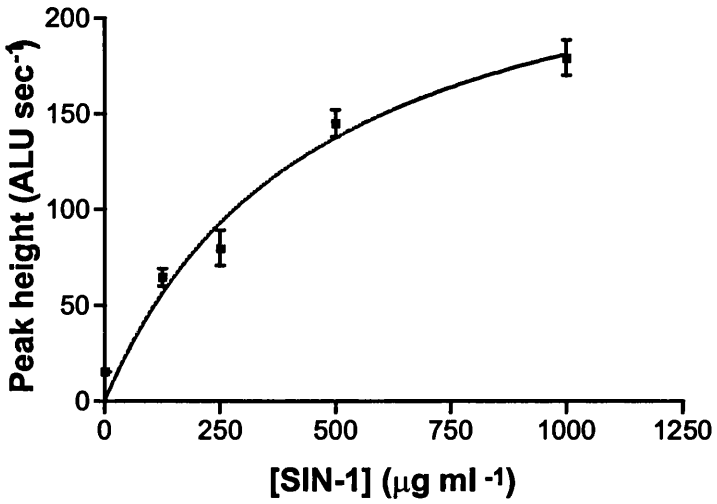

Figure 2.54. The luminol-enhanced chemiluminescence produced by SIN-1 degradation in PBS at 37°C. SIN-1 was injected at a range of concentrations into the wells of a 96-well plate followed by luminol at a final concentration of 500μM and the light generated over time was measured using a 405nmGG filter in series with a photomultiplier tube. Data are mean ± SEM from 3 experiments in triplicate.

The signal generated by the luminol / SIN-1 reaction leads to a peak height measurement which is proportional to the concentration of SIN-1 in solution until ~ 500μM. The signal begins to saturate above this concentration of SIN-1.

Using authentic peroxynitrite, the chemiluminescence signal generated by its reaction with luminol was followed in the same manner as described for SIN-1. The results in figure 2.54 A show the chemiluminescence of a single well followed over time. The peak height measurements were taken for a range of ONOO- concentrations and shown in figure 2.54 B.

The chemiluminescence reaction of luminol with ONOO- is fast as seen in 2.55 A. The peak height measurements show a proportional concentration-dependent increase in chemiluminescence over the concentrations of ONOO- used.

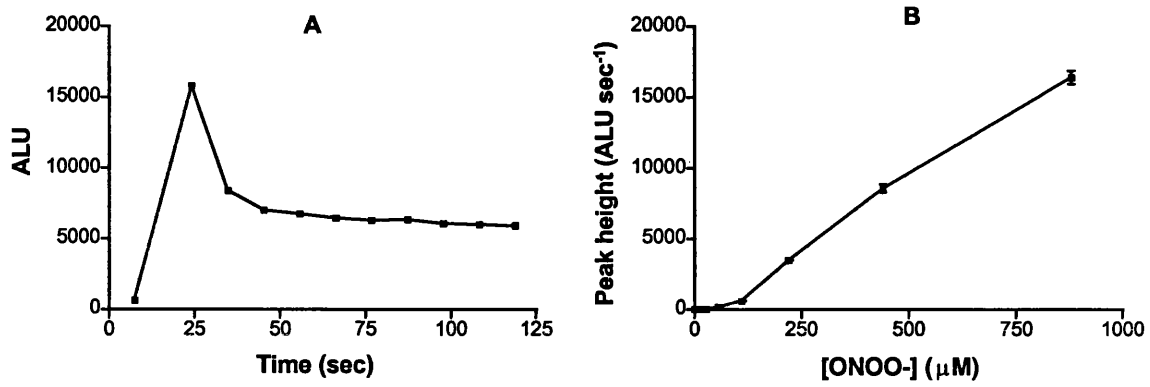

Figure 2.55. The luminol chemiluminescence of authentic peroxynitrite. Luminol (500μM) and a range of ONOO- concentrations were reacted together and the chemiluminescence generated was measured in a chemiluminometer. Data were generated using one well of a 96-well plate as the reaction time to produce peak height measurements was short (figure 2.55 A). Peak height measurements were used to construct figure 2.55 B for a range of ONOO- concentrations. Data for A are from one representative well measured over time and data for B are the means ± SEM of 3 individual experiments carried out in triplicate.

The signal generated by ONOO- and luminol is very large in comparison to the signal from SIN-1and also to the signal generated by XO NADH (see below).

To determine the effect of possible ONOO- scavengers, this assay was used with the inclusion of a range of concentrations of the flavanoid quercetin following the work of Haenen *et al* (1997) to allow further elucidation of the radical species generated.

Figure 2.56 shows the effect of quercetin on the chemiluminescence of 100μM ONOO- and luminol.

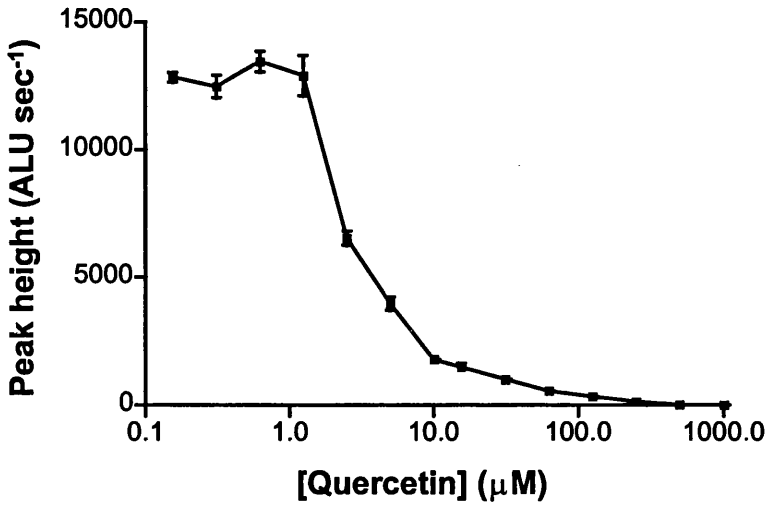

Figure 2.56. The effect of quercetin on the ONOO- mediated luminol-enhanced chemiluminescence (LuEC). Quercetin at a range of concentrations made up in PBS was added to the wells of a 96-well plate. ONOO- was injected into each well to give a final concentration of 1mM and immediately followed by the injection of luminol. The chemiluminescence generated was measured over time and the peak height plotted against quercetin concentration. Data are mean ± SEM of two experiments in triplicate.

Quercetin is shown to reduce the ONOO- mediated LuEC in this assay over the concentration range shown. The half-maximal inhibition occurs at ~ 2.5μM quercetin for ONOO- at 100μM.

As the chemically generated ONOO- requires H_2O_2 for its synthesis and following MnO_2 treatment to remove H_2O_2 it is still possible that the chemiluminescence generated comes from species other than ONOO-. Therefore the effect of ONOO- on the oxidation of lucigenin was also measured as a possible alternative.

Peroxynitrite was again injected into wells of a 96-well plate and reacted with 500μM lucigenin and the chemiluminescence followed over time in a chemiluminometer as previously described. Figure 2.57 Shows the

chemiluminescence signal from ONOO- mediated LEC and the concentration dependent chemiluminescence of ONOO-.

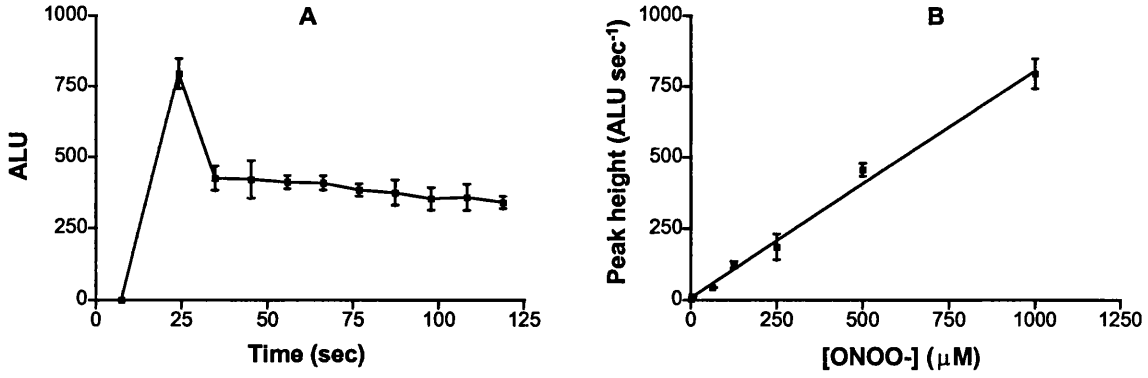

Figure 2.57. The chemiluminescence from ONOO- and lucigenin reactions. Data are mean ± SEM from 2 individual experiments performed in triplicate.

The signal generated from ONOO- and lucigenin compared to luminol-enhanced chemiluminescence is reduced ~ 750 ALU sec^{-1} for 1mM ONOO- compared to ~ 15000 ALU sec^{-1} for 880μM ONOO- with an equimolar concentration of luminol and lucigenin. The reaction follows similar kinetics for both enhancers requiring the experiments to be carried out on single well readings over time rather than in batches.

The response to quercetin was also monitored for ONOO- and lucigenin. Figure 2.58 shows the results of this experiment.

Quercetin is again shown to reduce the ONOO- mediated chemiluminescence with lucigenin with a half-maximal effect at ~ 4μM quercetin with 1mM ONOO-.

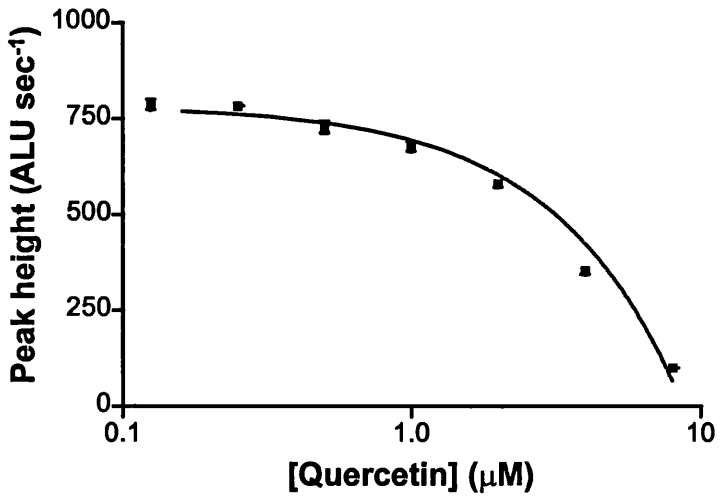

Figure 2.58. The effect of Quercetin on the ONOO- enhanced LEC. The experiment was carried out as described for figure 2.57. Data are mean ± SEM (n = 2) in triplicate.

2.3.5.3 The effect of xanthine oxidase derived radical species

To assess the effect of XO derived superoxide and NO from nitrate and nitrite, LEC was used as a method for the detection of radical generation. Following the method of Crow *et al* (1995), which utilised the iron-chelator DTPA to stop Fenton type reactions of iron and superoxide which generate H_2O_2, the effect of DTPA was assessed in a superoxide generating system using XO and NADH mediated LEC. Figure 2.59 shows the effect of various concentrations of DTPA on the XO NADH mediated LEC. DTPA is shown to dose-dependently reduce the chemiluminescence signal from XO NADH derived species above ~ 100μM. Half-maximal reduction of peak height occurs at ~ 700μM. DTPA was therefore included in the following experiments at a concentration of 100μM.

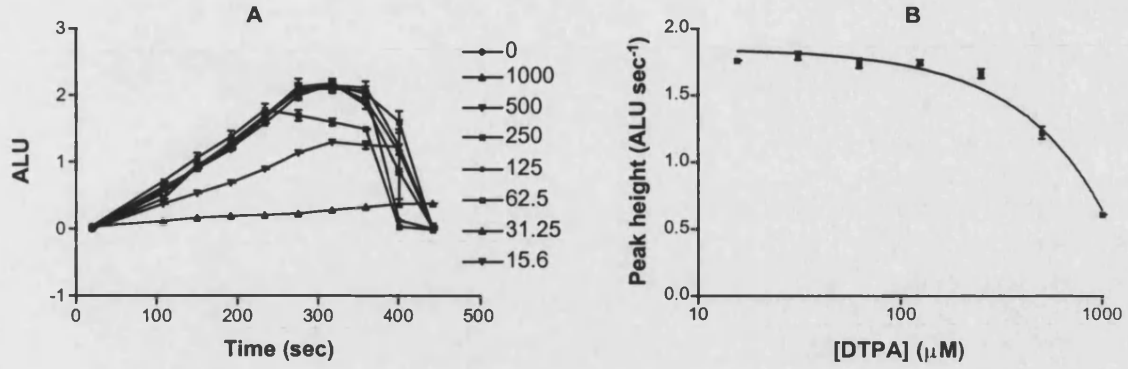

Figure 2.59. The XO, NADH-mediated LEC in the presence of DTPA. XO 10μg, NADH 500μM lucigenin 500μM and DTPA at a range of concentrations were mixed (NADH and lucigenin by injection) in the wells of a 96-well plate. The resultant chemiluminescence from the reaction of XO with NADH and superoxide with lucigenin was measured over time as previously described. Figure 2.59 **A** shows the data mean ± SD from one representative experiment in triplicate while figure 2.59 **B** shows the mean peak height ± SEM of 3 experiments in triplicate.

The effect of inorganic nitrate incubation on the XO, NADH mediated LEC was assessed by the addition of various amounts of nitrate to the chemiluminescence reaction mixture. Figure 2.60 shows the effect of nitrate on the XO NADH mediated LEC.

Nitrate is shown to have little or no effect on the XO NADH LEC under the assay conditions described with 100mM nitrate ~ 1.4 ALU sec^{-1} compared to 1.35 ALU sec^{-1} in the absence of nitrate.

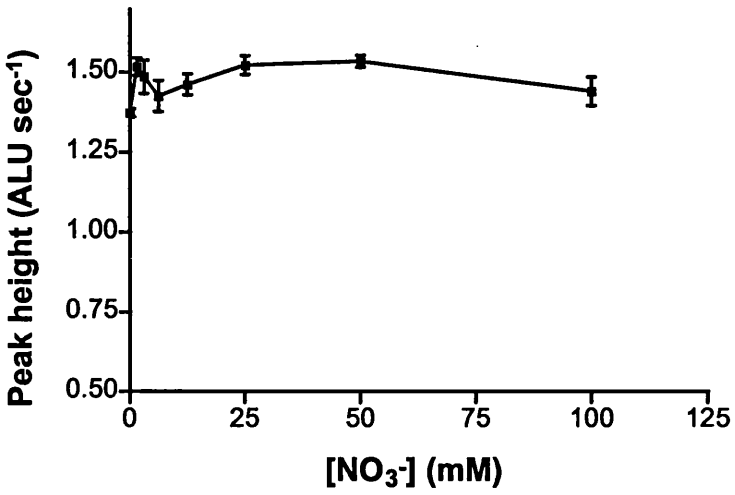

Figure 2.60. The effect of nitrate on the XO NADH LEC.

The effect of nitrite incubation on the XO, NADH-mediated LEC was assessed by the addition of various amounts of nitrite to the chemiluminescence reaction mixture. Figure 2.61 shows the effect of nitrite on the XO NADH-mediated LEC. Nitrite shows a dose-dependent increase in XO NADH LEC up to ~ 10mM nitrite after which increasing the nitrite concentration has little effect on the peak height signal. The control wells show no chemiluminescence in the absence of NADH.

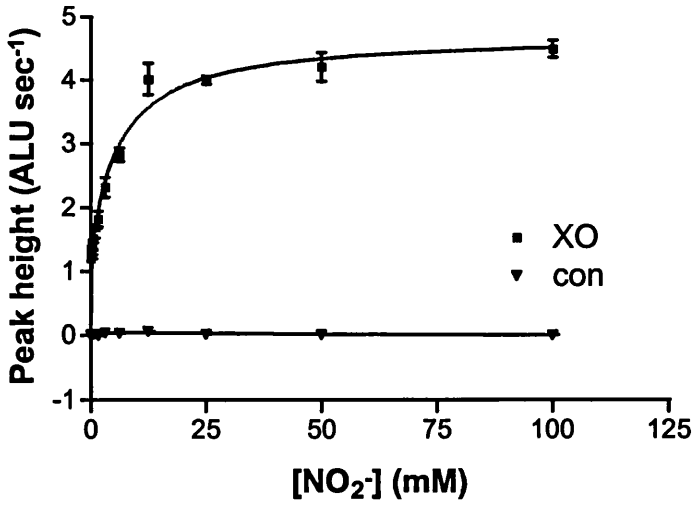

Figure 2.61. The effect of nitrite on the XO NADH-mediated LEC. Nitrite at a range of concentration was added to the wells of a 96-well plate. Which also

contained 10μg of XO. NADH and lucigenin were injected into the wells and the chemiluminescence followed over time. The control wells contained XO, nitrite, DTPA and PBS without the addition of NADH. Data mean ± SEM (n = 3) of three individual experiments.

To determine the contribution to the LEC of XO derived metabolites oxypurinol was added as the known inhibitor of the molybdenum active site. The XO, NADH-mediated LEC in the presence and absence of nitrite was measured in the presence and absence of oxypurinol at a range of concentrations. Figure 2.62 shows the effect of oxypurinol on the XO NADH LEC with and without nitrite.

Oxypurinol reduces the XO NADH mediated LEC only in the presence of nitrite. The half-maximal reduction in LEC is > 100μM oxypurinol in this protocol. Oxypurinol has a small effect on XO NADH LEC at 100μM in the absence of nitrite with the % of control value of 93.5 ± 3.2.

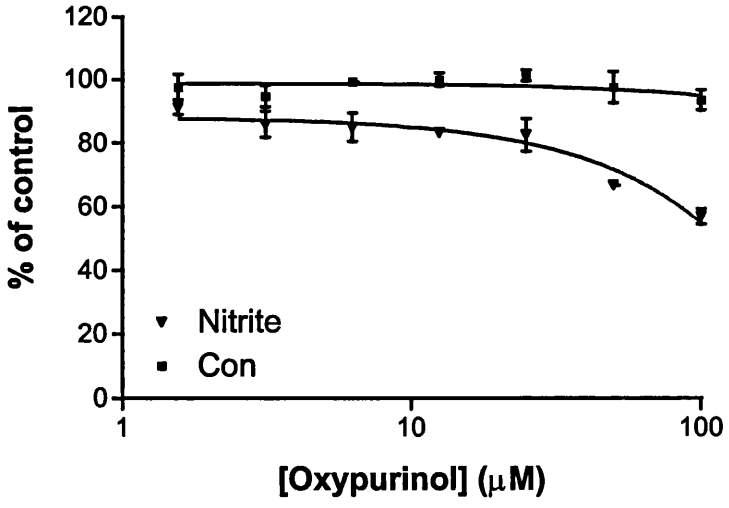

Figure 2.62. The effect of oxypurinol on the XO NADH-mediated LEC in the presence and absence of nitrite. XO 0.1mg, NADH 500μM, nitrite 10mM lucigenin 500μM and DTPA 100μM. Data are mean ± SEM (n = 3) in triplicate.

The effect of quercetin on the superoxide detection by this system was studied along with its effect on the enhanced chemiluminescence signal shown for nitrite and XO NADH. Figure 2.63 shows the data from these experiments.

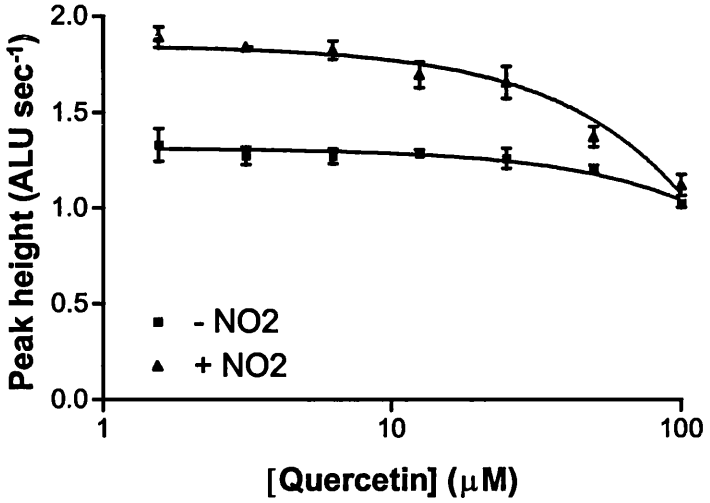

Figure 2.63. The effect of Quercetin at a range of concentration on the XO 10μg, NADH 500μM, lucigenin 500μM and with or without nitrite 1mM LEC. Data are ± SEM (n = 3) in triplicate.

Quercetin reduces the LEC for the signal with the addition of nitrite from ~ 1.8 ALU sec^{-1} to 1.25 ALU sec^{-1} a reduction of ~ 30% of the total LEC. It shows some effect on the LEC in the absence of nitrite at 100μM, a reduction of ~ 24%. However, at 100μM, quercetin has reduced all of the nitrite-enhanced LEC signal back to the non-nitrite-enhanced chemiluminescence.

2.4 Discussion

The oxidation of NADPH by nitrate reductase and XO is seen in the absence of nitrate and is enhanced on the addition of nitrate only in the case of nitrate reductase in the presence of atmospheric air. It was also only possible to measure

the generation of nitrite from nitrate by the nitrate reductase in the presence of NADPH and atmospheric air.

The nitrate reductase activity of XO in the presence of nitrate, xanthine and atmospheric air was not detectable in terms of nitrite generation. Nitrite was detectable however when the oxygen was removed by incubation of the reaction under a reduced oxygen atmosphere. This confirms the results of Sergeev *et al* (1985) and Fridovich and Handler (1962) where anaerobicity was required for the generation of nitrite by XO from nitrate.

When this nitrite generation was followed over time it was observed that nitrite was generated from nitrate and the rate of production was dependent on the concentration of the nitrate added. As the reaction proceeds the concentration of nitrite becomes reduced in what appears to be a two-phase reaction where nitrite is first generated and then lost from the reaction. These two observations, the generation and loss of nitrite only under reduced oxygen point towards a possible mechanism involving XO in the reduction of nitrate and nitrite in the absence of oxygen.

It has long been known that XO can gain electrons from a variety of substrates including purines and aldehydes via an active site containing a molybdenum co-factor. The mechanism has been proposed for electron transfer around the enzyme to a variety of sites and electron stores. Once the enzyme has received electrons from a donor substrate it is not possible for more substrate to be utilised until the electrons can be lost. For this, the use of various electron acceptors allows enzymic turnover. In the case of many enzymes this electron acceptor is molecular oxygen. In its absence however other acceptor molecules can be utilised to allow enzymic turnover. Nitrate and nitrite are two such electron acceptors with the ultimate reduction of nitrate to nitrite and nitrite to nitric oxide.

Thus, nitric oxide is a by-product of enzymic turnover just as superoxide generation is when oxygen is the electron acceptor.

The model system draws parallels from the nitrate reductase enzymes that contain similar active sites and facilitate the reduction of nitrate to nitrite. These enzymes also contain a molybdenum cofactor and gain their electrons from the oxidation of NADH or NADPH. The enzyme, once reduced, will donate its electrons to nitrate in a two electron donation to generate nitrite and this can occur in air. This now generates a possible paradox in the use of nitrate reductase enzymes as the model for XO nitrate reductase activity. The lack of nitrite generation in air by XO suggests that the donated electrons are lost to molecular oxygen with the generation of oxygen radicals. The relative concentration of nitrate and oxygen will serve to control the competition for electrons, with the most likely result being that, at equimolar amounts of oxygen and nitrate or nitrite, oxygen will gain the electrons due to the higher affinity for oxygen that the enzyme possesses. However, if the nitrate reductase enzymes utilise NADH by binding to a FAD moiety to generate $FADH_2$, then is it possible that in air the electrons will be lost to molecular oxygen and the generation of oxygen radicals? In fact this has been shown by Barber and Kay (1996) in assimilatory nitrate reductase (EC 1.6.6.2) a molybdopterin, FAD and cytochrome b_{557}-containing enzyme. Using *Chlorella sp* nitrate reductase and NADH, this group were able to demonstrate the reduction of molecular oxygen and identified the molybdopterin as the primary site of oxygen reduction resulting in the production of superoxide radical.

Here again a difference is seen in the utilisation of oxygen to form superoxide between the NR and XO enzymes. In the presence of NADH and oxygen the addition of cyanide to NR enzyme inhibited the reduction of molecular oxygen. In the case of NADH oxidase enzymes cyanide has no effect on the reduction of

oxygen when NADH is the electron donor (Iverson *et al* 1977 and Morre and Brightman 1991) which is probably the case for xanthine oxidase NADH oxidase activity in the presence of oxygen.

The K_m for oxygen for this *Chlorella sp* NR in the presence of NADH was calculated to be 586μM, much higher than the oxygen concentration in air-saturated buffer (~250μM at 37°C). For bovine XO, Fridovich and Handler (1962) gave a figure of 27μM for the reduction of oxygen in the presence of hypoxanthine and from this thesis in the presence of NADH a K_{app} of ~ 70μM. The affinity for oxygen then is greater for XO than NR in the presence of NADH suggesting that the available electrons are more likely to be donated to oxygen in the case of XO than in the case of NR. It is for this reason that nitrate is utilised by NR as the electron acceptor and the generation of nitrite in atmospheric air.

For XO, the removal of oxygen using a nitrogen atmosphere still allows the donation of electrons to the enzyme and the addition of an electron acceptor in the form of nitrate allows enzymic turnover and the generation of nitrite.

Nitrite itself has been shown to be reduced under a low oxygen atmosphere. The possible fates of nitrite on reduction include the generation of nitric oxide. The utilisation of nitrite measurements allowed the loss of nitrite to be measured over time, which suggested a further reduction and possible generation of nitric oxide. From nitrate, the time resolved reduction to nitrite also showed a loss of nitrite after ~ 30 minutes of generation. This may lead to a possible mechanism of nitrate reduction to NO requiring an intermediate nitrite step. This parallels the reduction of nitrate by denitrifying bacteria that utilise nitrate and nitrite reductase enzymes for the eventual generation of dinitrogen. The intermediates of nitrate reduction to

dinitrogen by denitrifying enzymes include nitrite, nitric oxide and nitrous oxide (Ye *et al* 1994).

It is possible then that XO can show both a nitrate and nitrite reductase activity liberating in order from nitrate: nitrite and nitric oxide. As a model system the nitrite reductase enzymes differ quite markedly from XO in their active sites. To investigate the involvement of the particular active sites involved in the nitrate and nitrite reductase activities of XO, a range of specific inhibitors were utilised.

Taking the nitrate reductase activity first, in the presence of xanthine as the electron donor, this thesis shows that nitrite generation from inorganic nitrate is inhibited by the known molybdenum site inhibitors oxypurinol and BOF 4272. The nature of this inhibition however is not an indication of molybdenum site involvement in the reduction of nitrate to nitrite. As xanthine is the electron donor, the addition of oxypurinol or BOF 4272 will inhibit xanthine binding to the molybdenum active site and therefore the availability of electrons for the reduction of nitrate.

In the presence of DPI, a non-molybdenum site inhibitor however, the generation of nitrite from inorganic nitrate is enhanced in a dose-dependent manner. This enhancement was to such a large extent that the experiment was repeated in the presence of air-saturated buffer. In this case there was also a dose-dependent generation of nitrite from inorganic nitrate and was the first evidence of nitrate reductase activity by XO in air.

This led to the proposal of a working hypothesis based on previous work on the nature of DPI inhibition and the known utilisation of oxygen as the preferred electron acceptor.

Hypothesis. In the absence of oxygen, an electron rich (reduced) XO enzyme could pass its electrons on to a suitable electron acceptor and cause a reduction of

that acceptor to another species. In the presence of oxygen, this would act as the electron acceptor and compete for the available electrons and this competition would be dependent on the relative concentrations of the two acceptors. In the presence of DPI the leak of electrons to molecular oxygen was inhibited and therefore more electrons were available for the reduction of inorganic nitrate to nitrite thereby increasing the nitrate reduction.

The importance of organic nitrates in therapeutic use made these compounds important to study in this context. Using GTN and ISDN it was possible to measure nitrite evolution over time. The amount of nitrite generated over time from the organic nitrates was significantly greater than that generated with equimolar amounts of inorganic nitrate in the presence of xanthine. The effect of oxypurinol was to inhibit the evolution of nitrite in a dose-dependent manner as seen for the inorganic nitrates. However, on the introduction of DPI to the system a potent inhibitory effect was seen which was the opposite of the effect of DPI in the case of inorganic nitrate.

The inhibition of NO generation has been shown previously by Trujillo *et al* (1998). In the presence of XO and xanthine and the absence of oxygen the reduction of S-nitrocysteine (CysNO) was inhibited by DPI at ~ 80% at 40μM compared to ~ 10μM for 80% inhibition in the presence of GTN (this thesis). It was suggested that the flavin site was therefore involved in the catalysis of CysNO. It is not known why the inorganic and organic nitrates should behave in such a different manner. The effect on inorganic nitrite was again a dose-dependent enhancement of NO generation in the presence of xanthine and the absence of oxygen. In the presence of oxygen the DPI allowed the evolution of NO from the reaction at a level ~ 10x reduced compared to oxygen free buffer.

Following the time resolved generation and then loss of nitrite, the effect on the reduction of nitrite as the initial starting substrate was measured. An initial rapid loss of nitrite from the standard was seen which reached a plateau after only a short time. This suggested that the reduction of nitrite was limited by the products formed. It also suggested that some reduction species of nitrite was produced during enzymic turnover with the possibility of NO generation. It was also possible that in the original experiments using nitrates, the nitrite formed was due to the reaction of NO with oxygen to form nitrite in solution. However as all experimental procedures were carried out in the glove box and the fact that the reaction of NO and molecular oxygen is slow in aqueous solution, with a half-life of several hours (Wink *et al* 1993), this explanation does not account for the nitrite generated.

Initial experiments to measure nitric oxide release utilising nitrates and xanthine were unsuccessful and because of the possibility that both xanthine and the nitrate were being oxidised and reduced at the same active centre an alternative electron donor was used.

NADH is able to donate electrons to the enzyme and under atmospheric air, enzymic turnover donates these electrons to molecular oxygen. In the absence of oxygen the electrons once again may be given up to an oxidising agent. It was possible to generate NO in this manner from organic and inorganic nitrates. The effect of the known XO molybdopterin site inhibitors was to reduce the measurable NO in a dose-dependent manner, which is in agreement with the reduction of nitrate at this centre. Here again this confirms work by Sergeev *et al* (1985) and Bray (1984) which utilised the molybdopterin centre either removed completely or isolated from XO and added back to a nitrate reductase enzyme devoid of this active site.

The effect of DPI was also to inhibit the measurable NO generation in a dose-dependent manner, which is to be expected when NADH is used as the electron donor. Stopping the gain of electrons by the enzymes will stop the donation on to the nitrate and therefore inhibit its reduction.

The organic nitrates have been utilised for many years therapeutically and their method of action has been suggested to be via their donation of NO to vascular smooth muscle cells. The mechanism of breakdown has been followed by HPLC revealing a denitration of the compounds in the case of GTN to generate glyceryl di nitrate (GDN) and glyceryl mono nitrate (GMN). This suggests that the generation of NO from GTN follows a nitrite intermediate step to give the reaction shown below.

$$NO_3^- \longrightarrow NO_2^- \longrightarrow NO \qquad (13)$$

This complicates the measurement of NO from nitrates as the reaction to generate NO must be dependent on the rate of nitrite formation and then on nitrite reduction to NO. This led to the study of the reduction of nitrite, being the relatively more simple reaction to follow.

On generating NO from nitrite it was clear from the data that nitrate gave a longer lag time before reaching peak NO generation compared to the nitrite tested. This follows the suggestion that nitrite is an intermediate step in nitrate reduction and the rate of NO generation is dependent on the rate of nitrite formation from nitrate.

The inhibition of NO generation from nitrite by oxypurinol in the presence of NADH also suggests that the molybdopterin site is the part of the enzyme where the electrons are taken from. A conflict now arises as to the possible competition between nitrate and nitrite for the available electrons. At the start of the reaction the concentration of nitrate far outweighs nitrite in the solution. As nitrates are

reduced to nitrite the relative concentrations of the two compounds changes in favour of the nitrites. When the concentration of nitrite is sufficiently high, the available electrons will be donated to nitrite to give NO. The lag time comparison detailed earlier suggests this to be the case. This situation is also supported by earlier experiments using nitrate and xanthine where, over time, following nitrite generation, an initial increase in nitrite is seen followed by a loss of nitrite.

The kinetics of these reactions lead to the suggestion that the molybdenum site is the active domain for donation of electrons from all substrates used. Inhibition was seen with oxypurinol and in the presence of purine substrates, substrate inhibition was seen which complicated the kinetic analysis. The purines are known to be hydroxylated at the molybdenum site and because of the close similarity with the nitrate reductase molybdenum enzymes this is the most probable site of nitrate and nitrite reduction.

All the above determinations occur in the absence of competing oxygen. It is important therefore to assess the effect of oxygen on the generation of NO especially by the methods chosen.

By following the oxidation of NADH in a kinetic assay it was possible to show that the XO-mediated NADH oxidation was dependent on the concentration of dissolved oxygen in the buffer. This assay was then also used to determine kinetic parameters in the absence of oxygen for a variety of electron acceptors the nitrates and nitrite. This assay however is not specific for either oxygen reduction or nitrate, nitrite reduction and so the generation of NO was followed over a range of oxygen concentrations. At two concentrations of nitrite in the presence of NADH, increasing oxygen concentration caused a dose-dependent decrease in measurable NO. The effect of oxygen was less pronounced with the higher nitrite concentration, where greater oxygen concentrations were required to reduce the

NO signal. This was also the case in the presence of hypoxanthine although the point at which the half maximal NO generation occurred was reduced at equimolar nitrite concentrations for hypoxanthine compared to NADH as the electron donor. The possible reasons for the loss of NO signal are,

I. Reaction of NO with oxygen in the aqueous phase

II. Generation of superoxide radical in stead of therefore reducing the available electrons for NO generation

III. Reaction of NO with oxygen in the gaseous phase to produce species not detectable in this assay

IV. Reaction of superoxide radical with NO to generate reactive nitrogen species which are again not detectable by this assay.

As has been shown by Wink *et al* (1993) the reaction of NO with oxygen in solution is slow and rules it out as a possible mechanism in this assay. However points II – IV are possibilities.

To test these points the assay was run in the presence of superoxide dismutase (SOD) which would scavenge any superoxide formed. The results of this experiment showed that the inclusion of high concentrations of SOD could enhance the NO measured from nitrite reduction in the presence of hypoxanthine. This rules out point II and suggests that simultaneous generation of NO and superoxide occurs as the oxygen concentration is increased from 0% saturation. From the work of Beckman *et al* (1990) and Kissner *et al* (1997) the reaction of NO and superoxide is diffusion limited and the most likely reaction to occur. This peroxynitrite generation could account for the loss of NO signal as the oxygen concentration is increased.

Point III, however, is less easy to prove either way and depends on the reaction rates of NO with the available oxygen.

The possibility then exists that peroxynitrite is generated over a range of oxygen concentrations by the simultaneous reduction of nitrite and oxygen. Various methods for the detection of peroxynitrite formation have been utilised. Using SIN-1 as a simultaneous generator of both NO and superoxide and using chemically synthesised peroxynitrite, it was possible to screen assays for enzymic peroxynitrite generation.

The commonly used oxidation of dihydrorhodamine (DHR) gave a positive result in the presence of SIN-1. When used in conjunction with XO and nitrates in air-saturated buffer the control reactions showed a change in absorbance over time which was independent of the nitrate concentration. In fact on addition of increasing concentrations of nitrite the rate of DHR oxidation was increased in the absence of added XO enzyme. Repeating this experiment in the presence of increasing NADH concentrations, the oxidation of DHR was reduced suggesting a competition between the strong oxidant (nitrite) and the strong reductant (NADH). In accordance with Crow *et al* (1995), XO and xanthine had no effect on DHR oxidation, but this assay was not used further due to the problems encountered with the substrates to be used.

Luminol had previously been shown (Radi et al 1993) to give chemiluminescence in the presence of authentic peroxynitrite. It was possible to use this assay in a multi-well set up. Authentic ONOO- caused a dose-dependent increase in the chemiluminescence caused by reaction with luminol and this was inhibitable by the inclusion of the known ONOO- scavenger quercetin (Haenen *et al* 1997). Lucigenin was also shown to luminesce on addition of authentic peroxynitrite and was also inhibitable by the addition of quercetin.

Lucigenin-enhanced chemiluminescence was used for the determination of XO mediated ONOO- generation due to the ease of use of the multi-well format. In the

presence of nitrate, the chemiluminescence signal is not enhanced over that generated in the presence of NADH, XO and oxygen alone. Nitrite however shows a dose-dependent increase in LEC that is not due to nitrite alone. The possibility is that at atmospheric oxygen concentrations, NO is being generated at the high concentrations of nitrite used and this reacts with the superoxide generated to produce LEC. It is possible though that the reaction of superoxide with nitrite at such high concentrations may mediate the LEC seen. Trujillo and colleagues (1998) were able to show the decomposition of s-nitrosothiols mediated by xanthine oxidase. They stated that this effect could been seen by two distinct mechanisms with the generation of peroxynitrite. The reactions showed XO/xanthine induced decomposition of s-nitrosothiols in air-saturated buffer due to the participation of superoxide. The NO generated could then react with a second superoxide to form peroxynitrite as a bystander reaction: mediated but not catalysed by the enzyme. The high concentrations of nitrite used here could also generate NO spontaneously which would add to the signal but would not be enzymic.

To clarify this point, oxypurinol was added at a range of concentrations and shown to inhibit significantly the nitrite enhanced LEC, with little effect on the XO/NADH mediated LEC at the concentrations used, suggesting catalytic reduction of nitrite. Further evidence of ONOO- generation came with the inhibition of the lucigenin signal in the presence of quercetin where only the nitrite enhanced signal was affected.

It is possible then that under the conditions described XO and a range of electron donor substrates in the presence of nitrite at a range of concentrations could generate both superoxide and NO simultaneously with the eventual generation of peroxynitrite.

Chapter 3

The antibacterial activity of peroxynitrite and xanthine oxidase derived reactive species

Chapter 3

This chapter deals with the susceptibility of bacteria to oxidants generated either enzymically or by chemical means. It looks to determine the radical generating capacity of XO in a situation where the oxygen tension is variable and to assess the possible antibacterial action of metabolites from a milk-derived enzyme.

3.1 Introduction

3.1.1 Xanthine oxidase, peroxynitrite and bacterial viability

The study of free-radicals and their generation has gone on for many decades (Edwards and Plumb 1994). However, their role in physiology has usually been seen as a pathological one, with the dogma being that radicals were so reactive and unselective that they could not be involved in normal biochemical processes (Pryor and Squadrito 1995). Free radical publications of the time were limited to the situations where high concentrations of radicals were produced from exposure to high-energy radiation or toxins such as carbon tetrachloride.

Arguably, it was only when the enzyme superoxide dismutase (SOD) was described by McCord and Fridovich in 1969 that the idea became accepted that free-radicals could be generated by many cell types in normal physiology and controlled by yet further cellular mechanisms (McCord and Fridovich 1969a and b).

3.1.1.1 The antibacterial activity of NO and superoxide

Free radicals have previously been implicated in bacterial cytotoxicity (Akaike *et al* 1992, Bowdy *et al* 1990, Pabst et al 1982) and especially in the respiratory burst of macrophages and neutrophils (Morel *et al* 1991, Miller and Britigan 1997 and Hampton *et al* 1998). The range and variety spans singlet oxygen and superoxide

from the oxidation of NADPH in the neutrophil membrane to the generation of "bleach" in hypochlorous acid generation by myeloperoxidase in phagosomes within a restricted environment (Byun *et al* 1999 and Saran *et al* 1999). Chemically generated hypochlorite has also shown its efficacy as an antibacterial agent (Rusin *et al* 1998).

Nitric oxide is generated by a variety of cell types including macrophages that have been stimulation with interferon gamma and *E. coli* lipopolysaccharide (Marletta *et al* 1988). The macrophage has also been shown previously to generate oxygen radicals even under resting conditions (Drath and Karnowsky 1975) which was significantly enhanced following phagocytosis (DeChatelet *et al* 1975). Tsunawaki and Nathan (1984) described a NADPH-dependent oxidase that could generate superoxide from macrophages which was also associated with the membrane in the guinea pig macrophage (Pick *et al* 1987).

Other organisms have also been shown to have susceptibility to nitric oxide. Long *et al* (1999) demonstrated the mycobacteriocidal actions of exogenous nitric oxide treatment and suggested this as a possible therapy in patients with pulmonary tuberculosis. Saura *et al* (1999) and Persichini *et al* (1999) produced evidence to show antiviral properties of NO and the inhibition of HIV-1 virus replication.

Inflammatory situations and bacterial infections, which are rich in exuded inflammatory cells, therefore contain a range of free radical-generating systems in the form of activated cells.

Intragastric levels of NO have been measured to be between 10 and 100ppm and this is suggested as having biological effect in the stomach (Weitzeberg and Lundberg 1998). Acidified nitrite has also been shown recently to kill various gut pathogens much more efficiently than acid alone (Benjamin *et al* 1994 and Dykhuizen *et al* 1996).

Nitrates are generally excreted in the urine at higher concentrations compared to the low level of measurable nitrites (Green *et al* 1981). However bacteria that cause urinary tract infections (UTIs) may convert nitrate to nitrite using a nitrate reductase enzyme and the detection of nitrite in urine has been used as a diagnostic tool for UTIs. Acidification and vitamin C intake have been used as treatment against UTIs (Weitzeberg and Lundberg 1998). The ingestion of 2g of vitamin C for two days induced a seven-fold increase in NO release from nitrite-containing urine from healthy volunteers. It was further shown that addition of nitrite to acidified urine dose-dependently decreased the *in vitro* growth of *E. coli* (Lundberg *et al* 1997). This may lead to the nitrate reducing bacteria participating in the production of the necessary substrates for their own destruction.

3.1.1.2 Bacterial survival and antioxidant mechanisms

The individual cytotoxicity of nitric oxide and superoxide relies on the susceptibility of the target organism to the stress derived from these free radical species. Nunoshiba *et al* (1992 and 1995) have shown that nitric oxide signals *E. coli* through the same transcription factors as superoxide and the genes induced by nitric oxide are those essential for the protection against oxidative damage. Also in *Salmonella typhimurium* Crawford and Goldberg (1998) have shown that a flavohaem protein regulates gene expression on stimulation by nitric oxide. It has also been confirmed in *E. coli* that a flavohaem affords protection from NO. Specifically, the haem serves a dioxygenase function that produces mainly nitrate. These studies identify enzymes with reactions that were thought to occur only by chemical means. It was also emphasised that the reactions of NO with haemoglobins were evolutionarily conserved and have been adapted for cell-specific functions (Hausladen *et al* 1998).

The presence of oxygen radical detoxification systems in bacteria is well documented (Fee 1991 and Nunoshiba 1996). *E. coli* possess a superoxide dismutase-like enzyme which generates hydrogen peroxide. This species is then detoxified by a catalase-like enzyme to oxygen and water (McCormick *et al* 1998). The importance of SOD in the defence of bacteria against superoxide generation was assessed by Gort and Imlay (1998). They controlled the expression of cytoplasmic SOD within the *E. coli* to show the relative amounts of superoxide generation that were required to cause enzyme inactivation, growth deficiencies and DNA damage. These studies showed a graded response to the loss of SOD in the cells. At small reductions in SOD activity, a substantial reduction in the activity of labile dehydratases was seen. An increase of more than four-fold superoxide generation measurably impaired growth and a five-fold increase sensitised cells to DNA damage.

Schwartz *et al* (1983), however, showed the cytotoxicity of neutrophils to bacteria and suggested that even though the bacteria contained the protective antioxidant enzymes, under the conditions within the phagosome, the flux of superoxide and hydrogen peroxide generated was sufficient to overwhelm the cells antioxidant mechanisms.

Other proteins have been associated with antioxidant mechanisms. Lundberg *et al* (1999) suggested that Glucose-6-phosphate dehydrogenase is required in *S typhimurium* resistance to reactive oxygen and nitrogen species. The DNA repair enzyme formamidopyrimidine-DNA glycosylase was also essential to antioxidant defence from *E. coli* treated with high levels of hydrogen peroxide (Alhama *et al* 1998).

It is clear then that bacteria and viruses can be susceptible to free radical attack but also have some relevant antioxidant enzymes to survive particular stresses.

Xanthine oxidase has been shown previously to generate superoxide and, in this thesis, nitric oxide. Xanthine oxidase-derived superoxide and hydrogen peroxide have been indicated in antiviral activity by causing apoptosis in the infected cells (Skulachev 1998), in association with duodenal ulcers and *Helicobacter pylori* infections (Ben-Hamida *et al* 1998) and *in vitro* susceptibility of *Mycobacterium leprae* to oxygen-mediated damage (Dhople 1996).

However the effectiveness of either superoxide or nitric oxide alone has been questioned in the light of their possible reaction products.

3.1.2 The role of peroxynitrite

Reactions and effects that were once attributed to either NO or superoxide may now be reassessed. The evidence comes from the combination of the radicals forming the strong oxidant peroxynitrite (Beckman *et al* 1990 and Beckman and Koppernol 1996). This reaction leads to the modulation of the effect of each individual radical. For example, superoxide can reduce the effects of nitric oxide by causing the generation of ONOO- (Gryglewski *et al* 1986 and Rubbo *et al* 1994). In the same manner the capture of superoxide by nitric oxide has been suggested as the modification of actions previously described for superoxide alone (Bautista and Spitzer 1994 and Wink *et al* 1994).

The ability of ONOO- to cause nitration reactions with a variety of residues has been suggested as one of the methods leading to pathology (Beckman and Koppernol 1996). ONOO- reacts with tyrosine residues to generate nitro-tyrosine and can also react with DNA to generate nitrated bases and strand breakage (Szabo and Ohshima 1997).

Following strand breakage a secondary effect has been suggested involving the activation of the nuclear enzyme poly(ADP-ribose) synthetase (PARS) and

apoptosis. Single (not double) strand breakage is an obligatory signal for PARS activation. PARS causes the ADP-ribosilation of a number of important proteins involved in repair including topoisomerase I and II, DNA polymerase α and β and DNA ligase 2. This ribosylation tends to decrease their activity and therefore has an effect on the cell function (Szabo *et al* 1996).

Activation of PARS can also deplete cell energy stores by using up the electron transport substrate, NAD+, which can then go on to cause acute cell dysfunction. The ability of ONOO- to cause DNA damage in bacteria was therefore studied as a measure of the oxidative damage that may be the cause of ONOO- bacterial killing. Peroxynitrite has been shown previously to be formed by macrophages during bacterial engulfment (Ischiropoulos *et al* 1992) and to have an effect as a bactericidal agent (Zhu *et al* 1992 and Brunelli *et al* 1995).

The following experiments were designed to assess the effect of ONOO- on bacterial viability and the possible generation of this species by XO leading to a novel anti-bacterial system.

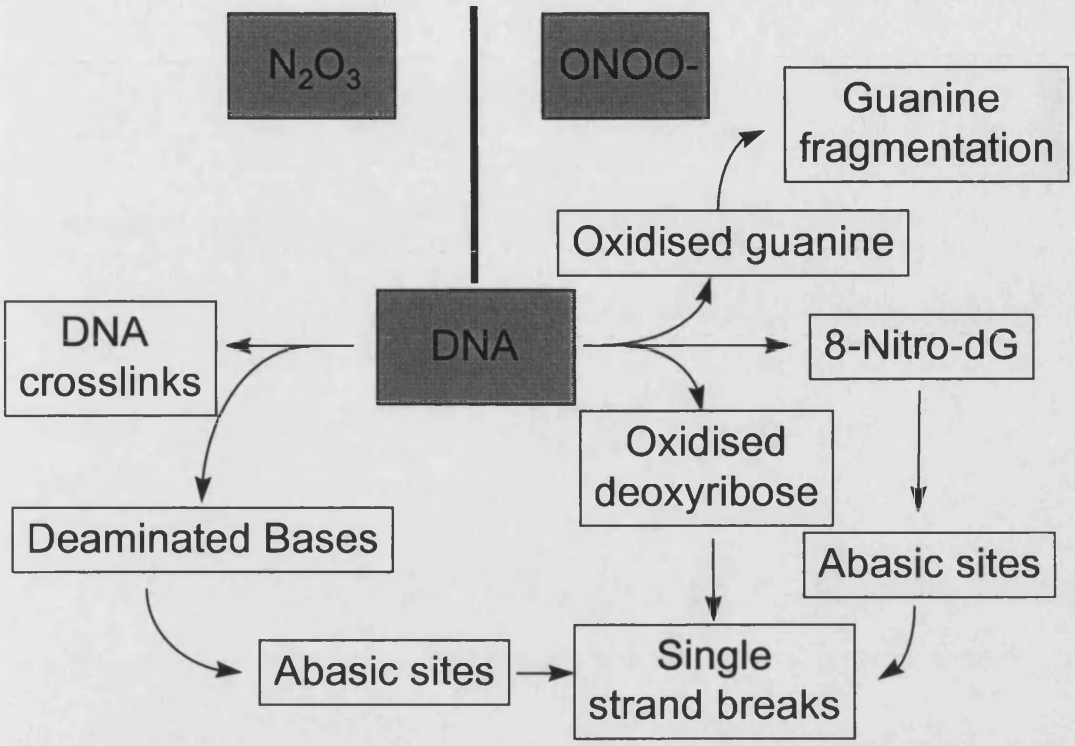

Figure 3.1. Summary of the possible effect of NO derived species on DNA damage.

3.2 Method and materials

3.2.1 Enzyme activity in bovine and human milk products

The activity resident in non-purified milk samples from both bovine and human sources was measured. Bovine milk was taken from commercially produced sources following pasteurisation. Also samples of raw milk were taken from cows and assessed in the same manner. Human samples were taken at various time points post partum and stored frozen at –20°C in a domestic fridge freezer for over a year before being assayed. Commercially produced infant feed formulas were also used as packaged by the manufacturer. Commercially produced Golden Churn (St Ivel) spread was assessed for activity as this is made with 20% buttermilk.

3.2.2 Lucigenin-enhanced chemiluminescence measurements

The generation of superoxide radical from various enzyme sources was measured using the oxidation of lucigenin as a marker. Superoxide radical reacts with lucigenin in a radical – radical addition reaction to yield an unstable dioxetane; the decomposition of which produces the excited state acridone. Decomposition of this acridone to the ground state emits light which can then be detected using a photomultiplier tube (PMT) (Faulkner and Fridovich, 1993 and Liochev and Fridovich, 1997).

These experiments were completed using a 96-well plate-reading chemiluminometer (Anthos, Lucy 1) with the capability to vary the chamber temperature and wavelength of measured light. As the peak light emission for lucigenin is 500nm, to remove unwanted non-lucigenin-emitted light, a green glass bandpass filter of 492nm (GG492nm) was used for lucigenin enhanced chemiluminescence (LEC).

Chemiluminescence (CL) enhancement was also used in the measurement of hydrogen peroxide (H_2O_2) and peroxynitrite (ONNO-). For luminol-enhanced chemiluminescence (LuEC) the peak-emitted wavelength is 425nm therefore a green glass 405nm (GG405nm) bandpass filter was used.

Xanthine oxidase has been show previously to generate superoxide radical using xanthine or NADH as substrates with oxygen as the terminal electron acceptor. The CL assay therefore provides a quick and reproducible method for obtaining information on the activity of a range of samples, from purified enzyme to human plasma samples and cultured cells.

3.2.2.1 Basic assay protocol

Assays were performed usually in triplicate in a final volume of 200μl. Lucigenin was made up to a stock concentration of 2mM in PBS. Substrates were made up at a range of concentrations in PBS. Samples were added to plates at a final volume of 100μl either as neat solutions or the volume difference made up to 100μl in PBS. Each plate was allowed to equilibrate to 37°C by placing the plate into the closed reaction chamber of the chemiluminometer (Lucy) for 5 min. The reactions were initiated by the injection of 50μl volume of substrate followed by 50μl of lucigenin into the wells of a 96-well plate.

Each particular protocol had its own-programmed routine of injection and luminescence readings. Typically, each well was measured with an integration time of one second sequentially before the initiation of the reaction. Injections of the substrate and enhancer were followed immediately by a second measurement. Once all the reactions had been started, the luminometer made readings in each well sequentially to follow the CL reaction. Due to the time taken for injection, reading and integration of each well, experiments were restricted to 24 wells (eight sets of triplicates) to allow the reaction to be followed. Measurements of the peak height of reaction were made, as this is where the reaction rates were at their maximal. On occasions the reaction rates were particularly fast which meant that the cycle time for each reading had to be reduced. This was accomplished by reducing the number of samples down to a suitable level allowing the measurement of peak height data.

Inhibitors were added into the plates prior to the initiation of the reactions so that the volume did not exceed 100μl, the final concentrations being in a range of dilutions from 100μM.

3.2.3 Western blot analysis

To determine the XO protein content of milk and other samples an antibody raised against bovine butter milk XO was used to detect immobilised proteins by Western blot analysis. Typically, proteins were electrophoresed through a SDS polyacrylamide gel under reducing conditions before transfer to a nitrocellulose membrane. This membrane was then probed for the appearance of XO protein using the anti-XO antibody and a chemiluminescence detection technique. The appearance of a 150KDa band was indicative of XO protein but some preparations would also show the typical degradation products of this enzyme.

This assay system allows the determination of individual proteins from a mixture by separating them according to molecular weight. Proteins in a solution of negatively charged detergent (SDS) are unfolded and negatively charged. The addition of a reducing agent such as mercaptoethanol or dithiothrietol breaks di-sulphide bonds. Applying a current across the gel causes the charged proteins to migrate toward the positive anode with the larger proteins being retarded by the gel which is dependent on the gel concentration relative to small proteins

3.2.3.1 Protocol

Proteins for analysis were isolated by a variety of means and the absolute protein concentration measured by a modification of the Bradford assay. An eight percent sodium dodecyl sulphate polyacrylamide gel (SDS gel) was prepared (See appendix II) and allowed to set before the addition of a five percent stacking gel to form running wells. Proteins which had been previously denatured in stacking buffer were loaded on to the gel in equal volumes. A voltage of 120V was applied to the gel, typically for 1 and a half hours before the gel was removed for protein

determination by blotting onto nitrocellulose or staining the gel itself in Coomassie blue.

3.2.3.2 Coomassie blue stain

A solution of 1% Coomassie blue was made up by dissolving Coomassie brilliant blue dye in 55% glacial acetic acid 10% methanol made up in ddH_2O. SDS gels were added to square plastic staining dishes in the presence of Coomassie blue for 45 minutes. The gel was then destained with a solution of Destain (7.5% glacial acetic acid, 5% methanol in ddH_2O) for 1 hour. This Destain was then replaced by fresh Destain and the gel left overnight at room temperature.

3.2.3.3 Gel blotting

The blotting apparatus was set up for wet blotting. Gels for blotting onto nitrocellulose were layered onto two pieces of Whatman 3mm blotting paper cut to size and soaked in blotting buffer (see appendix II) inside a blotting cassette. Onto this was layered a piece of Hybond-C nitrocellulose paper soaked in blotting buffer with the air bubbles removed by rolling a 10ml pipette over the paper. Onto this was layered a further 2 pieces of blotting paper and the blotting cassette closed to hold the layers in place. This cassette was then removed to the blotting apparatus where a current of 150mA was applied to the gels for 2 hours.

3.2.3.4 Probing the blots

Following blotting, the nitrocellulose was blocked by incubation with 5% non milk-fat protein (Marvel) made up in PBS/0.5% Tween 20 (MPT) for 1 hour. Specific primary antibodies were then added to the nitrocellulose for between 1 hour and overnight incubations. The nitrocellulose was washed 6x 5 minutes in PBS/0.5% Tween 20 (PT) before the addition of secondary Horseradish peroxidase (HRP)-

labelled antibodies in MPT for 2 hours at room temperature or overnight at 4°C. The blots were then washed for a further round of 6x 5 minutes in PT before the detection of reaction products.

3.2.3.5 Chemiluminescence detection of reaction products.

Antigenic proteins were detected by the utilisation of a light-emitting non-radioactive method and x-ray film detection. Only proteins bound by the primary and secondary antibodies will be detected by the utilisation of the hydrogen peroxide/HRP oxidation of luminol. The oxidised luminol emits light at a wavelength of 425nm which is detected by blue light sensitive autoradiography film. Using this system blots were soaked in luminol/H_2O_2 solution for two minutes before drying on paper towels. In a dark room, under safe light conditions, the blots were exposed to autoradiography film for a range of time points. The films were then processed to reveal the reaction products in an automated processor.

3.2.4 Bacterial culture and preparation

The infective bacterial strains *Escherischia coli* NCTC 86 (*E. coli*), *Salmonella enteritidis* DV 232 (*S. enteritidis*), *Lactobacillus casei* 6375 and *Staphylococcus aureus* 6751 were cultured on nutrient agar at 37°C by streaking out using a flamed tungsten loop from frozen stock cultures kept at the University of Bath. Colony formation usually occurred with overnight incubation. These stock cultures were used for subsequent experiments including sub-culturing in nutrient broth (NB Lab Lemco broth, Oxid, UK) and plating onto nutrient agar weekly.

Strains of *Micrococcus sp* and *Bacillus sp* were isolated from commercially pasteurised semi skimmed bovine milk onto nutrient agar and identified by morphological examination of colonies and by Gram's stain.

Experimental overnight cultures of bacteria were set up by inoculating 25ml of sterile NB with a single bacterial colony taken by a sterile loop from an inoculated agar plate. Cells were cultured at 37°C in sterile conical flasks with shaking at 100 revolutions min^{-1}. Cells were harvested by centrifugation at 400g and resuspended in either sterile NB or sterile PBS. Counts were performed by adding 10µl of cell suspension into 990µl of either NB or PBS in a plastic cuvette. The absorbance of this mixture was then measured at 470nm in a spectrophotometer with a 1cm light path against a blank of NB or PBS alone. The absorbance was then related to a standard curve which had been previously determined under the same conditions of absorbance against viable count for each cell type used (See figure 3.2). Final working cell concentrations were then produced by using the appropriate dilutions in either nutrient broth or PBS.

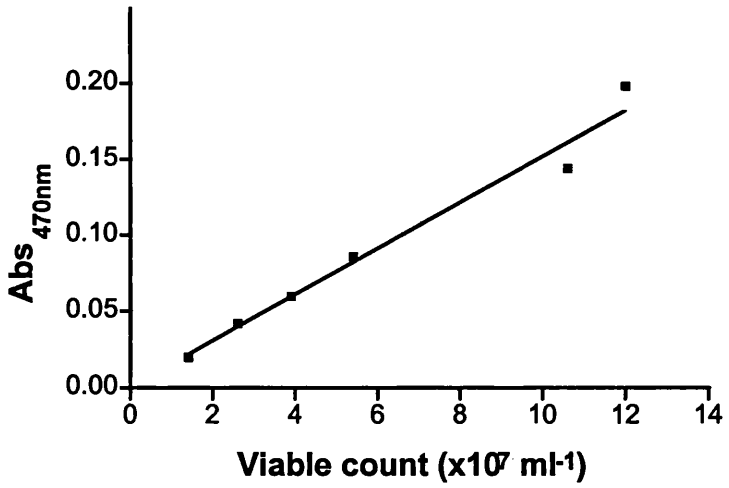

Figure 3.2. The correlation of absorbance at 470nm against viable count for *E. coli* NCTC86 grown in NB with shaking at 100 revolutions min^{-1}.

Viable counts were performed by plating bacteria onto agar and incubating over night at 37°C. Colonies were seen as glassy white plaques against the agar background. The number of colonies counted per plate (Colony forming units, CFU) was related to the absorbance of the seeding population R-value = 0.991

from n = 6. The cell count can be taken directly from the graph or by multiplication of the absorbance with the slope of the line (Viable count $x10^7$ ml^{-1} = Abs_{470nm} x 64.64).

3.2.5 Viability assay

The viability of control and treated bacteria was assessed by viable count of colony forming units (CFU).

Agar plates were set up by fist dissolving 28g agar in 500ml of Ultra pure H_2O. This solution was then subjected to sterilisation by autoclaving for 15 minutes at 121°C under pressure. The still molten agar solution was poured into sterile plastic petri dishes (Sterilin) and allowed to cool. On cooling, the agar solidified to form a gel that was then covered by the petri dish lid and the plates kept at 4°C until use, which was typically within one week.

Prior to use, the agar plates required air drying to remove condensation that formed within the petri dishes during storage. This was achieved by inverting each plate and removing the lid in a warm room (37°C). The plates were allowed to dry until all signs of condensation had been removed which was typically within 30 minutes. The plates were then recovered with their lids and stored at room temperature before use which was within 4 hours of air drying.

Plates were inoculated using sterile technique in the presence of a Bunsen flame and under a class I safety cabinet by the addition of cells in 100µl of either NB or PBS. Following inoculation, cells were spread onto the agar using an ethanol-flamed, glass spreading rod. The inoculated plates were incubated at 37°C overnight. Each batch of incubated cells also had a non-inoculated plate that had undergone the air drying procedure to show the level of background contamination.

This contamination tended to be low with a maximum of 0-2 colonies formed per plate.

3.2.6 Cell growth assay

The rate of cell growth was assessed by utilising the change in absorbance over time of cells in NB as a modification of the cell counting assay. Two procedures were used incorporating a manual and an automatic assay.

The manual assay used a spectrophotometer with a 1cm light path and 1ml plastic cuvettes. NB (990μl) was inoculated with 10μl of a known number of cells as assessed by the standard curve assay and the absorbance at 470nm was measured every 15 minutes against a blank of NB until a plateau in absorbance measurements was reached. The cuvettes were kept sealed with Parafilm™ (Parafilm "M", American National Can, USA) in a water bath at 37°C.

This assay was automated using a plate reading chemiluminometer (Anthos, Lucy) using it in an absorbance measurement mode. This was achieved using a GG492nm filter and clear bottomed sterile plastic 96-well plates. The chemiluminometer was temperature-controlled at 37°C and the plates were left *in situ* during the experiments. A final volume of 200μl was used throughout the experiments using this automated technique. A program of measurement steps was written for the Lucy to follow, including multiple readings and incubation wait times of 15 minutes between each measurement.

This automated technique allowed for large throughput experiments to be carried out in triplicate with little intervention once the assay was running.

Figures 3.3 and 3.4 show the growth of *E. coli* as followed in both assays at a range of inoculum concentrations.

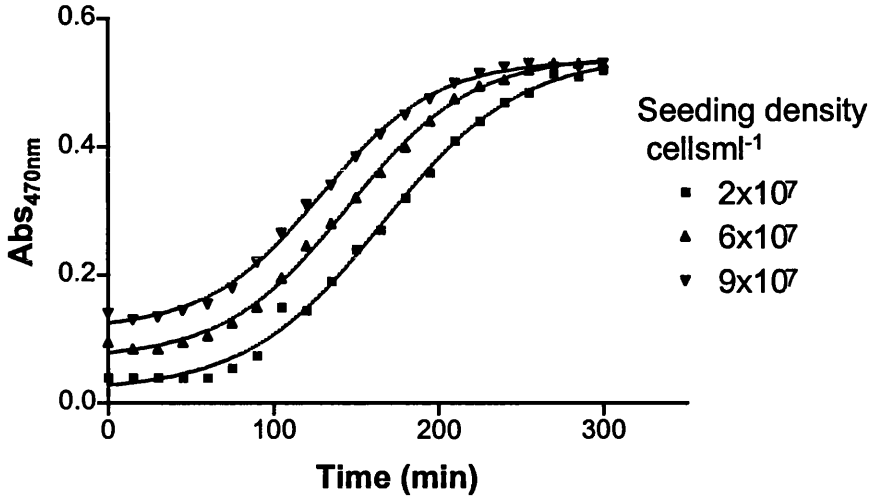

Figure 3.3. The manual assay for growth of *E. coli* at a range of seeding densities.

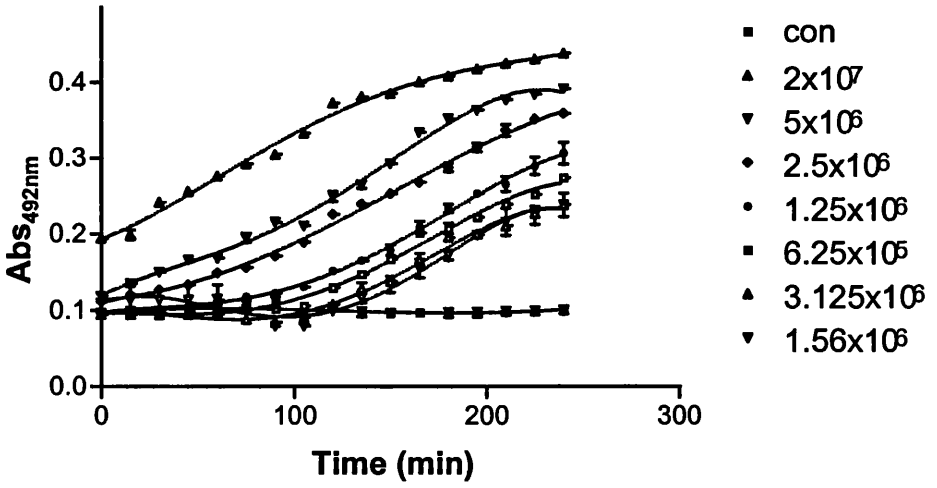

Figure 3.4. The change in absorbance caused by inoculating NB with *E. coli* at a range of seeding densities assessed by using the automated 96-well plate assay as described above.

The two assay protocols show similar growth curves for *E. coli*. The manual assay was hindered by the fact that it was labour intensive for multiple replicate samples and that the spectrophotometer in this case did not have a water jacketing set up to control temperature fluctuations.

The automated assay however removed both of these obstacles and allowed the possibility for many more readings to be taken. The difference in final volume 1000µl – 200µl made little difference to the overall outcome and growth rates seen. The smaller volume in use with the automated assay could have caused problems with concentration of cells due to increased evaporation of media from the wells, since the plates were not sealed as was the case for the manual assay. The plates were set up so that the wells around the edge of the plate contained 200µl sterile water to reduce edge effect evaporation in an effective "water jacket" for the bacterial cultures. No evidence of evaporative loss was seen in the experimental wells for the duration of these experiments.

All experiments into the effect of various treatments on bacterial growth were carried out using one or both of these assays.

3.2.6.1 The effect of hypoxia on growth rate

The effect of low oxygen concentration on growth rate was measured to characterise this parameter during further experiments that required a hypoxic approach. Both *E. coli* and *S. enteritidis* are facultative anaerobes, being able to utilise a range of electron donors other than oxygen in its absence.

Cells were cultured overnight as described previously and then added to fresh nutrient broth in 1ml cuvettes which were either saturated with room air or gassed with 5% CO_2 balanced nitrogen. The oxygen concentration was measured with the oxygen probe and then the cuvettes sealed with Parafilm. The absorbance at 492nm was measured over time to compare the growth rates.

Figure 3.5**A** shows the effect of oxygen tension on the growth rate of *E. coli*.

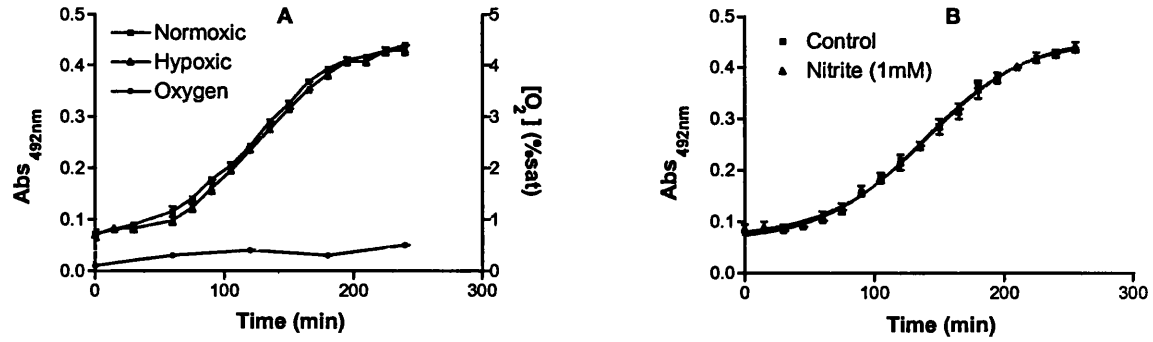

Figure 3.5. The effect of low oxygen and concentration and nitrite on the growth rate of *E. coli* in nutrient broth.

The growth rate of *E.coli* was not affected by the removal of oxygen from the nutrient broth. The oxygen concentration remained low <0.5% saturation throughout the time of the experiment.

This experiment was also repeated in the presence of 1mM sodium nitrite. Figure 3.5**B** shows the effect on *E. coli* growth rate with added nitrite under reduced oxygen conditions. Nitrite has no effect at 1mM concentration on the growth rate of *E. coli* in the absence of oxygen.

3.2.7 Peroxynitrite generation

Various methods for the generation of ONOO- now exist and are routinely used (Crow *et al* 1995, Pryor *et al* 1995 and Uppu *et al* 1996). For the experiments shown here a modification of the technique described by Crow *et al* (1995) was used.

Peroxynitrite was generated using a quenched flow reaction apparatus as described by Reed *et al* (1974). An aqueous solution of 0.6M sodium nitrite ($NaNO_2$) was rapidly mixed with an equal volume of 0.7M hydrogen peroxide (H_2O_2) containing 0.6M hydrochloric acid (HCl) and immediately quenching with the same volume of 1.5M sodium hydroxide (NaOH). All reaction solutions were kept

on ice. The concentration of peroxynitrite was determined spectrophotometrically at a wavelength of 303nm in 0.3M NaOH using an extinction coefficient of $1670M^{-1}$ cm^{-1} (Hughes and Nicklin 1968). Solutions of freshly synthesised peroxynitrite ranged from 150 – 200mM (~ 95% yield). Stock solutions of ONOO- were stable for several weeks (Crow *et al* 1995) at -20°C. However stock ONOO- was generated weekly and ONOO- was not used after 7 days of synthesis.

This method leads to some residual nitrite and hydrogen peroxide contamination. The hydrogen peroxide was removed by reacting solutions of chemically formed ONOO- with manganese dioxide (MnO_2) for 5 minutes followed by filtration through 0.22μm filter (Haenen *et al* 1997). Also ONOO- was allowed to decompose (dONOO-) at room temperature for 3 days to be used as the control for the residual nitrite/nitrate and NaOH (Bauer *et al* 1992 and Pfeiffer *et al* 1997). Sufficient buffering and dilution in PBS reduced the effect of the residual NaOH further.

3.2.8 The effect of peroxynitrite addition on cell growth in bovine milk

Commercially generated bovine milk was incubated with ONOO- and dONOO- before being plated onto nutrient agar and incubation overnight with viable counting. Each day a 1ml aliquot was removed and mixed with 100μM ONOO- or the equivalent dONOO- dilution. The viability of naturally occurring bacteria was assessed over time.

3.2.9 The effect of hypoxanthine addition to bovine milk.

Commercially produced pasteurised bovine milk was incubated in the presence of hypoxanthine and the viability of infecting organisms was assessed by viable count on nutrient agar in the same manner as described for peroxynitrite effects on bovine milk.

3.2.10 the effect of hydrogen peroxide and ONOO- on cell growth

Monocultures of bacteria isolated from milk or from stock cultures kept at the University of Bath were incubated in the presence of hydrogen peroxide or ONOO- and the growth rate determined using an automated assay as described in 3.2.6.

3.2.11 The effect of XO metabolites on bacterial viability

Xanthine oxidase was used as a generator of radical species in the presence of bacteria and its effect was measured on the viability of two bacterial species, namely *E. coli* and *S. enteritidis*.

Bacterial cultures were grown overnight in NB as previously described. Aliquots of $2x10^7$ cells ml^{-1} were taken and incubated with a reaction system consisting of bovine xanthine oxidase (XO, 53.2 $\mu g ml^{-1}$), nicotinamide adenine dinucleotide in reduced form (NADH, 300μM) or hypoxanthine or xanthine (100μM), sodium nitrite, ($NaNO_2$, 1-10mM) and oxygen at a range of concentrations as described in section 2.2.6.2. The initial reaction chamber set up was modified for the reaction and environmental control of reactions with bacteria. Figure 3.6 shows the modified water bath and the experimental set up for four reaction chambers. This allowed for greater numbers of reactions to be followed simultaneously.

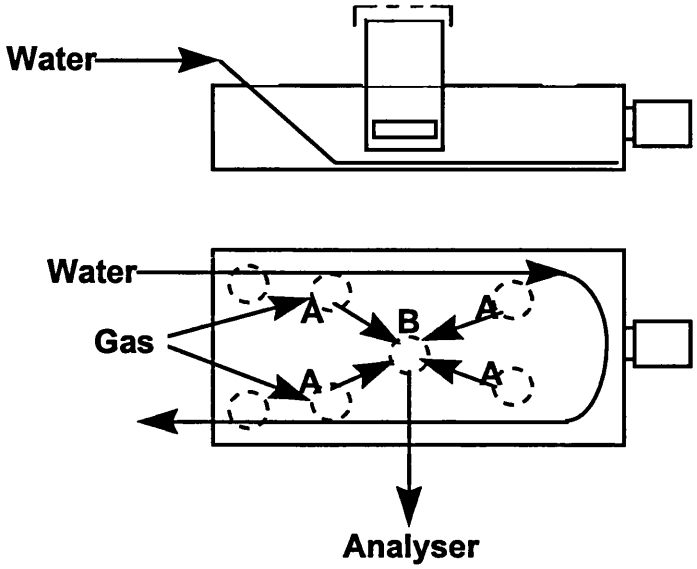

Figure 3.6. The modified reaction cell set up. Shown is the water jacketing system and the gas flow from four reaction cells (**A**) into a fifth cell (**B**) which was linked to the analyser.

This reaction mixture was followed at 37°C for 30 minutes with mixing before an aliquot was taken and plated onto agar and incubated overnight as described. Viable cell counts were performed in triplicate and the results expressed as a percentage viable count related to a non-enzyme control.

This procedure was repeated using xanthine and hypoxanthine as electron donor substrates and the results were expressed in the same manner.

3.2.12 The effect of XO metabolites on cell growth

Various bacterial isolates were grown in monoculture over night in nutrient broth. Sterile nutrient broth was inoculated with $2x10^7$ cells $well^{-1}$ of a 96 well plate. To each well was added either xanthine oxidase enzyme, hypoxanthine or a mixture of the two and the growth rate in each well calculated by following the change in absorbance over time at 492nm at 37°C in a plate reading spectrophotometer.

3.3 Results

3.3.1 Enzyme activity of various milk-derived sources

3.3.1.1 Bovine milk

The superoxide generating capacity of milk-based products was measured using lucigenin-enhanced chemiluminescence (LEC). Superoxide can be measured from xanthine or NADH in the presence of xanthine oxidase and oxygen. The superoxide generating capacity of raw bovine milk was assessed in this manner for both substrates. Figure 3.7 shows the effect of milk dilution in PBS on the chemiluminescence signal.

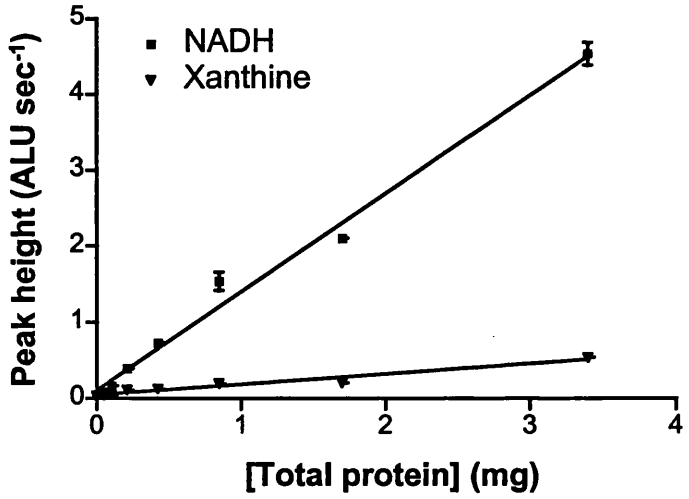

Figure 3.7. The lucigenin-enhanced chemiluminescence of raw unpasteurised bovine milk. Aliquots of milk were mixed with NADH, 500μM or xanthine, 250μM and lucigenin, 500μM and the chemiluminescence was measured in a 96-well plate reader as described in 3.2.2. Data are mean ± SEM (n = 3) in triplicate.

The chemiluminescence signal is proportional to the amount of total protein in each sample. NADH gives a larger signal compared to xanthine in this assay.

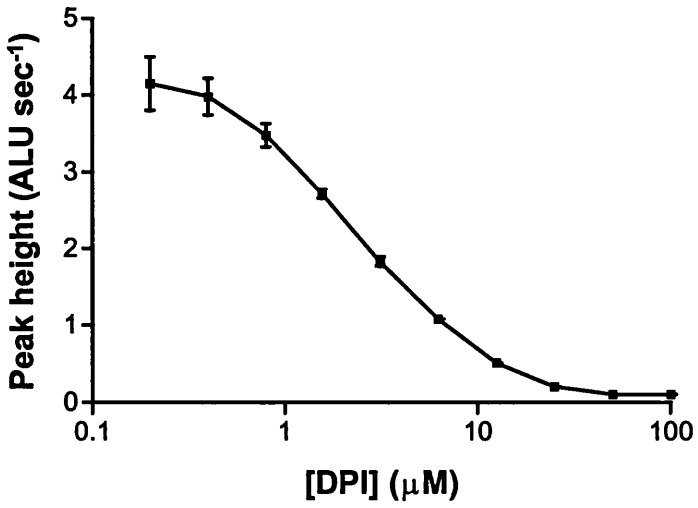

Figure 3.8. The effect of DPI on the NADH-mediated LEC from raw bovine milk. DPI was dissolved in PBS and added to the wells of a 96-well plate by using a doubling dilution in PBS before the addition of raw bovine milk at 3.4mg well^{-1}. The reaction was started by the addition of NADH and lucigenin and the chemiluminescence measured over time. The data are means ± SEM (n = 3) in triplicate of the peak height chemiluminescence.

The effect of DPI is shown in figure 3.8. DPI inhibited in a dose-dependent manner the LEC derived from the raw milk in the presence of NADH and gave an IC_{50} value in this protocol of 2.45μM.

The xanthine-mediated LEC was assessed in the presence of a range of oxypurinol concentrations. Figure 3.9 shows the effect of oxypurinol on the xanthine-mediated LEC of raw bovine milk.

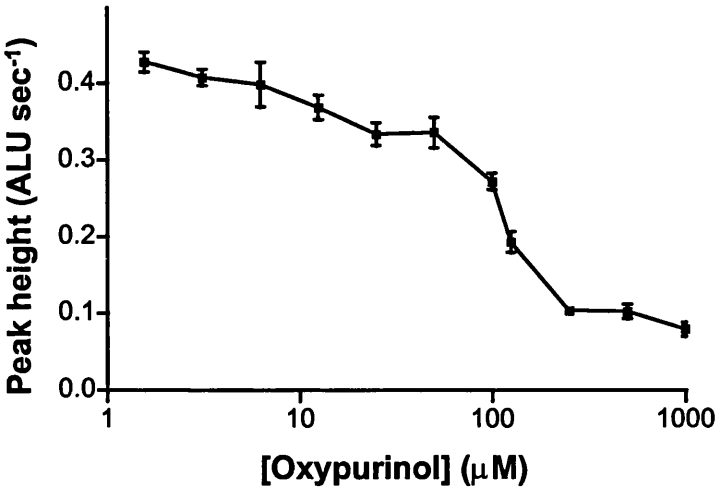

Figure 3.9. The effect of oxypurinol on the xanthine-mediated LEC of raw bovine milk. The assay was carried out as described in figure 3.2 where xanthine, 250μM was substituted for NADH and oxypurinol for DPI. Data are mean ± SEM (n = 3) in triplicate.

Oxypurinol caused a dose-dependent inhibition of the xanthine-mediated LEC of raw bovine milk and gave an IC_{50} value in this protocol of 117.5μM.

The effect of pasteurisation and fat content of milk was assessed by measuring the NADH-mediated LEC of full fat (FF) and semi-skimmed (SS) pasteurised milk. Figure 3.10 shows there to be no significant difference between the signal LEC generated from FF compared to SS milk. However, when compared to the raw milk in figure 3.7, the peak height signal generated under the same conditions for NADH is reduced in both FF and SS milks ~ 2.2 ALU sec^{-1} compared to ~ 4.5 ALU sec^{-1} for raw unpasteurised milk at the same total protein content.

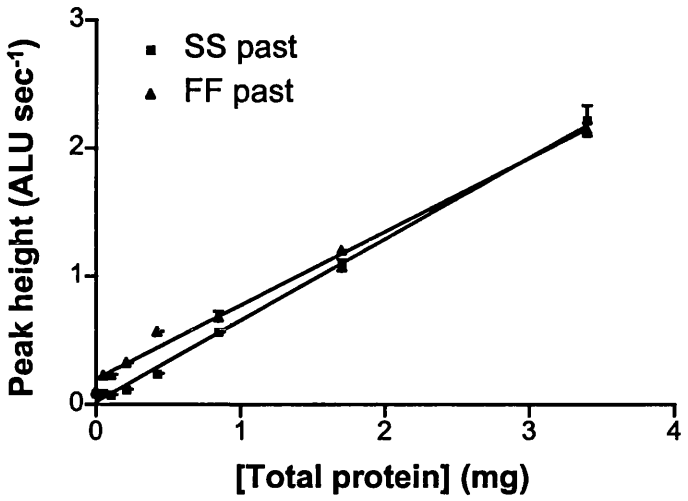

Figure 3.10. The NADH-mediated LEC of full fat and semi-skimmed pasteurised milk. The activity of these milks was measured as described in figure 3.7.

The difference between raw and pasteurised milk may suggest an effect of the pasteurisation process although the samples tested were not from the same herd. The measured activity of raw bovine milk was therefore treated by microwave exposure to show the effect of heating on the activity and temperature.

3.3.1.2 The effect of microwave treatment

To determine the effect of the commonly used microwave method of reheating human milk and to assess the effect of temperature on activity, raw bovine milk was subjected to microwave radiation and XO activity studied. 200ml of raw unpasturised bovine milk were subjected to microwave radiation on full power (900W) over time in an open glass container. At each time point a 300µl aliquot was removed from the milk and added to the wells of a 96-well plate. At each time point the temperature of the milk was measured using a mercury thermometer after shaking to homogenise the milk. This process was repeated for 120 seconds of microwave exposure and the aliquoted milk was allowed to warm or cool to room temperature. The milk was then tested for its NADH-mediated LEC as a measure

of the superoxide generating activity in the milk. Figure 3.11 shows the effect of microwave treatment on NADH-mediated LEC.

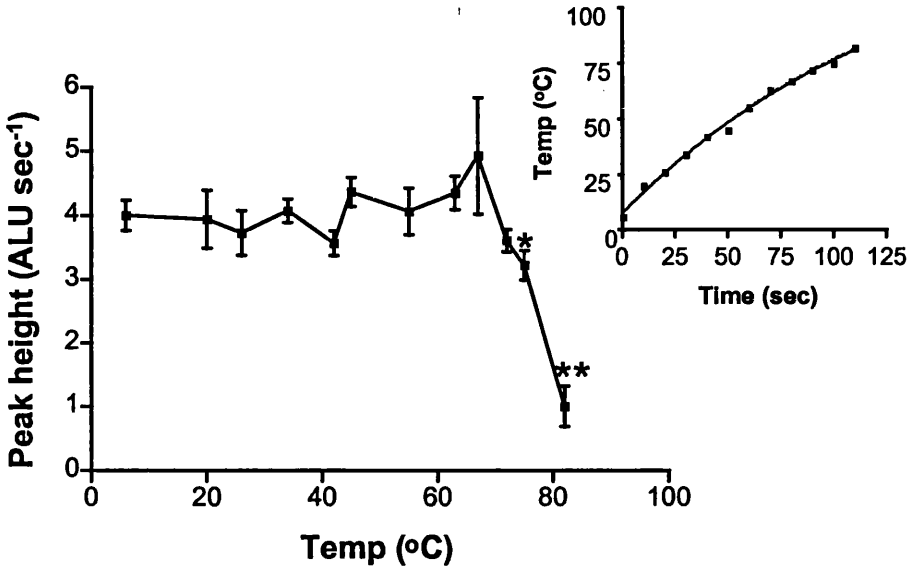

Figure 3.11. The effect of microwave treatment on the NADH-mediated LEC from bovine milk. NADH 500μM with lucigenin 500μM enhancement run at 37°C. Data show the activity against temperature of bovine milk whilst the inset shows the effect of microwave time on the temperature of the milk. Data are mean ± SEM (n = 2) in triplicate.

Microwave treatment causes the temperature of the milk to increase proportionately to the time of microwave exposure. The NADH-mediated LEC from the temperature-matched samples remains constant until the temperature exceeds ~ 70°C after which the LEC is reduced significantly * at 76°C ($p<0.05$) and ** 86°C ($p<0.01$) compared to the activity in untreated milk (~ 6°C).

3.3.1.3 Human milk

The NADH and xanthine-mediated LEC of human milk were measured in the same manner as for bovine milks. Figure 3.12 shows the NADH and xanthine-mediated LEC from a sample of human milk.

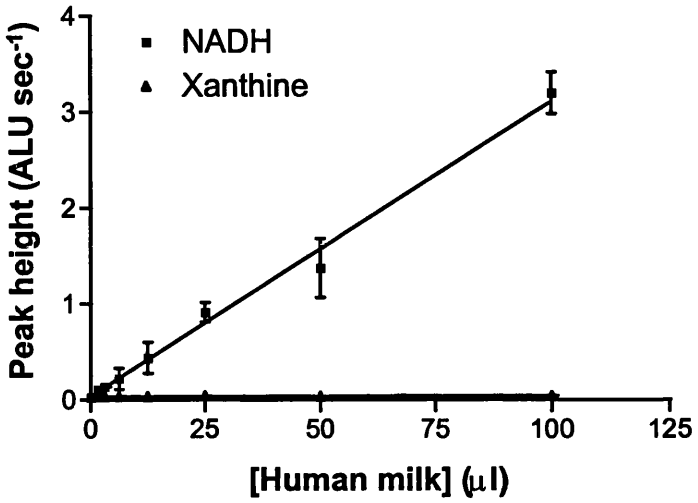

Figure 3.12. Human milk-mediated LEC in the presence of NADH or xanthine. Data are shown as described in figure 3.7 for human milk 30 days post partum. Experiments were run on three consecutive days and show mean ± SEM (n = 3) in triplicate of one sample from one mother.

Human milk shows a proportional increase in activity for NADH LEC. The xanthine-mediated LEC however is not detectable by this method with values similar to a PBS blank.

3.3.1.4 Infant milk formula

The activity of infant milk formulas was assessed in the same manner to determine both xanthine and NADH activity. Pre-formed formula feeds were added to the assay system as described previously at a range of concentrations. Feeds used were Aptamil® first with Milupan™ (Milupa, UK), SMA Gold® (SMA Nutrition, UK) and Cow and Gate Premium® (Cow and Gate, UK) and were all marketed as first feeds from birth.

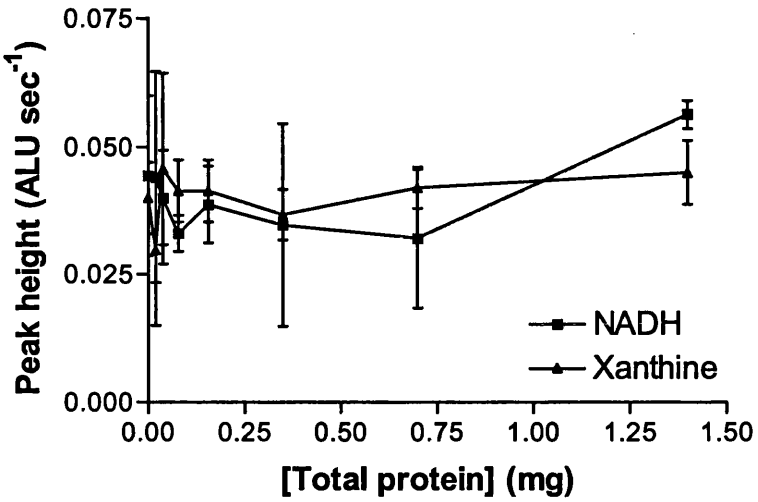

Figure 3.13. The NADH and xanthine-mediated LEC in infant milk formula Aptamil. For Aptamil, Cow and gate and SMA Gold infant milk there was no measurable activity above background counts in this assay system (See also figures 3.14 and 3.15) for both NADH and xanthine.

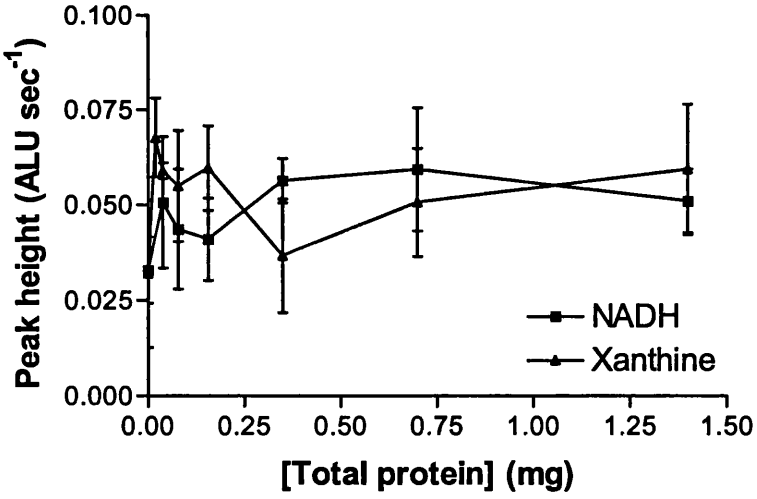

Figure 3.14. The NADH and xanthine-mediated LEC for infant milk formula Cow and Gate. Data shown as ± SEM (n = 3) in triplicate.

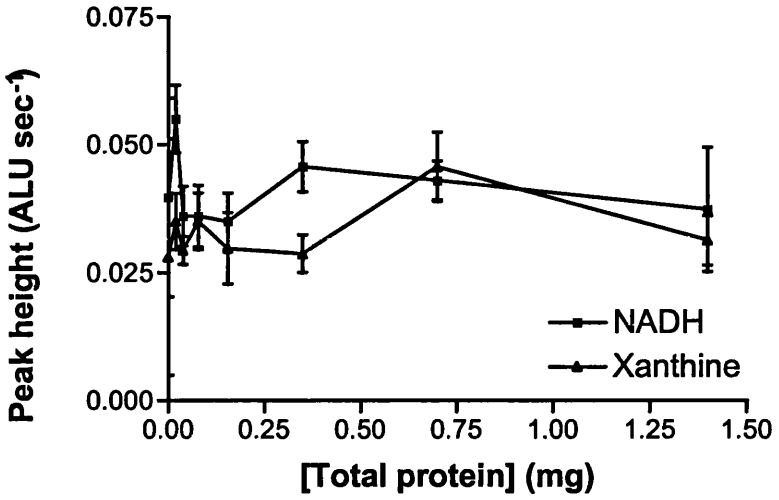

Figure 3.15. The NADH and xanthine-mediated LEC of infant formula SMA Gold. Data shown as ± SEM (n = 3).

3.3.1.5 Buttermilk from Golden churn

Some commercially produced spreads contain a potential source of XO activity in that they are supplemented with bovine buttermilk. The NADH-mediated LEC of Golden Churn spread which contains 20% buttermilk was tested. From a solid at room temperature, the spread forms a bilayered system when heated to 40°C. The upper layer consists of sunflower and vegetable oils whereas the lower phase contains proteins. Both phases were tested for their NADH-mediated LEC activity. Figure 3.16 shows the NADH-mediated LEC of the two phases of Golden Churn

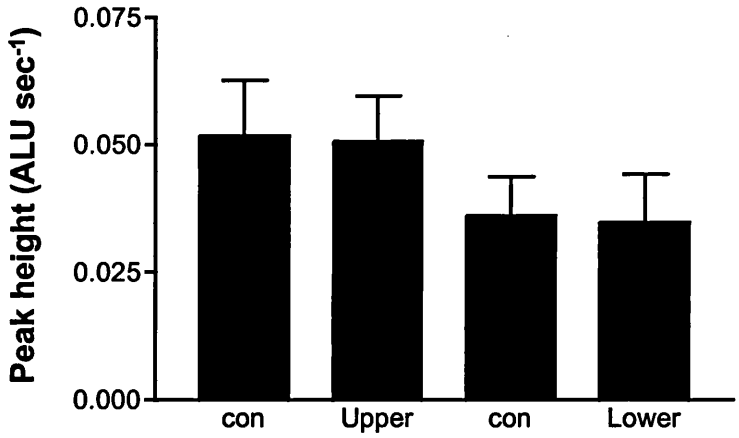

Figure 3.16. The NADH-mediated LEC from the two-phase system of heated Golden Churn spread. Data are ± SD (n = 1) of triplicate results.

Using this system it was not possible to detect NADH-mediated LEC.

The buttermilk was then assessed for its ability to generate NO from nitrite and NADH under a nitrogen atmosphere using the OEC assay. Figure 3.17 shows the effect of buttermilk addition and oxypurinol addition on the NO generation from nitrite and NADH.

NO was measured from buttermilk in the presence of nitrite and NADH and this activity was inhibited by the addition of oxypurinol.

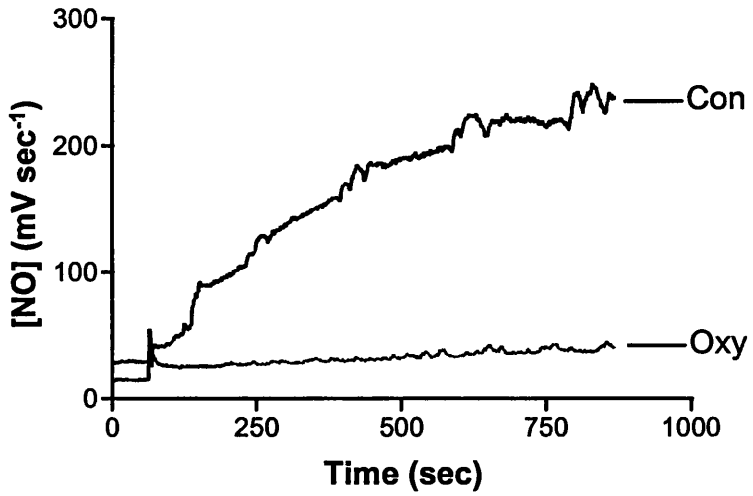

Figure 3.17. The NO generated from buttermilk. Buttermilk was isolated from St Ivel Gold spread as described above. Using 500µl buttermilk, 1mM NADH, 10mM nitrite and 100µM oxypurinol under a nitrogen atmosphere.

3.3.2 Protein analysis of various milk sources

To determine the XO content of a range of sources, each milk product was subjected to gel electrophoresis and Western blotting.

3.3.2.1 Protein gel of milk products

A gel was run of human and bovine milk, Aptamil and Cow and Gate infant formulas and Golden Churn spread. Figure 3.18 shows the proteins in each of these preparations by Coomassie blue stained gel.

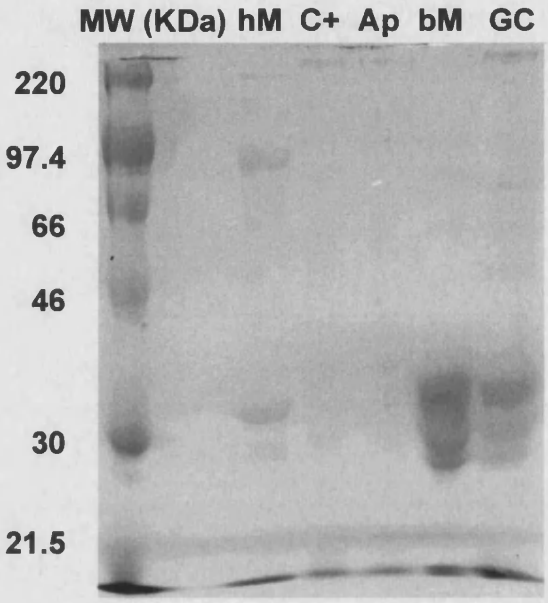

Figure 3.18. The protein gel for various milk based products. MW = molecular weight markers in KDa, hM = human milk, C+ = Cow and Gate, Ap = Aptamil, bM = bovine milk and GC = Golden Churn spread.

The milk products were also blotted onto nitrocellulose and probed for the appearance of XO. Figure 3.19 has the results of this analysis.

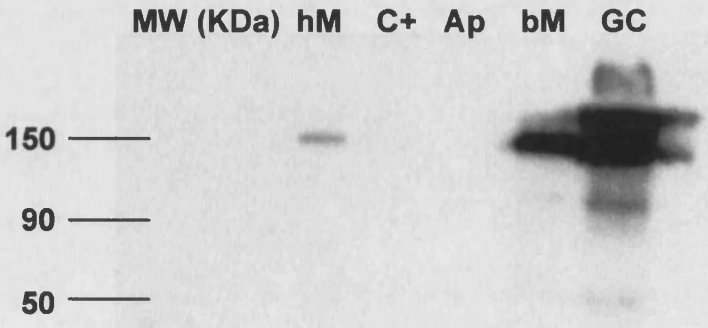

Figure 3.19. The response of various milk products to probing for XO.

Human and bovine milk both show strong staining at 150KDa and bovine milk and the Golden Churn protein shows degradation products at ~ 90 and ~ 50KDa. Both the Cow and Gate and Aptamil milk formulas show no reactivity towards the anti-XO antibody in this preparation.

3.3.3 Human milk XO protein

To assess the levels of enzyme secreted in human milk a study was undertaken to measure the activity and specific protein content of human milk post partum. Five samples were collected on days 7, 30, 36, 66 and 158 days post partum from a mother who gave birth to a full term healthy baby and was herself generally fit throughout the time of the collections. Milk was collected during spontaneous expression with the aid of a breast pump at times when the infant was not feeding.

3.3.3.1 Total protein determination

The total protein content of the human milk samples was measured using a modification of Bradford's assay (see appendix II). Figure 3.20 Shows the effect of time post partum on the total protein content of the human milk.

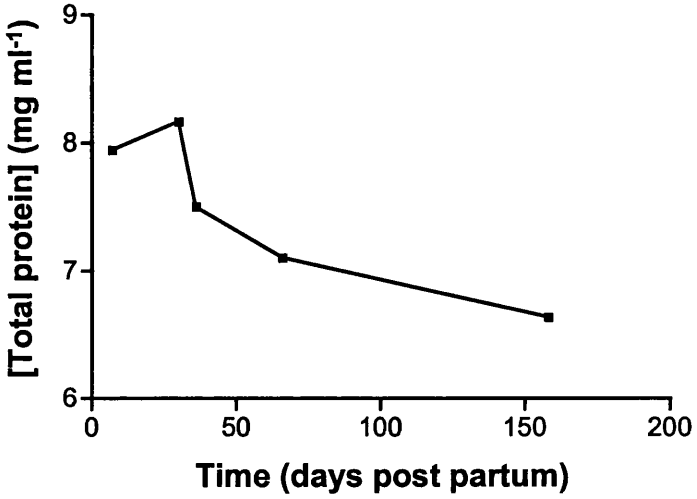

Figure 3.20. The total protein content of human milk post partum.

The total protein content of the human milk varies post partum with a general downward slope. The visual inspection of the milk samples showed that when homogenised by mixing the general turbidity of the milk on visual inspection decreased as the post partum time increased.

3.3.3.2 XO protein measurements

To assess the relative activities of enzymic action the amount of XO protein as opposed to the total protein amount was measured. This information linked with the activity will show changes in activity corrected for enzyme concentration and will possibly show changes in relative activity over time. This was determined by the use of Western blot analysis.

Milk samples at 10μg total protein per well were subjected to SDS page electrophoresis on an 8% gel as described in section 3.2.3, run in duplicate with one gel stained with Coomassie blue and the other gel used for Western blot analysis. Figure 3.21 shows the Coomassie blue stained gel

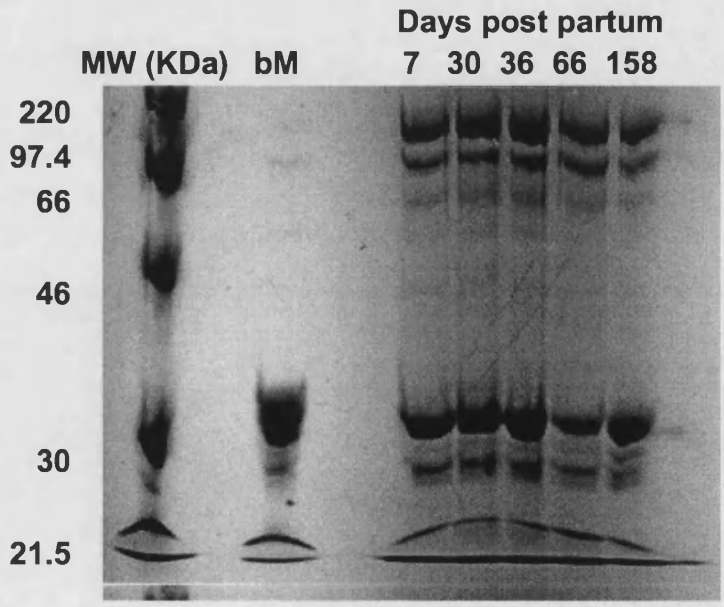

Figure 3.21. Human milk samples following SDS PAGE electrophoresis and staining for protein with Coomassie blue. Also shown are the molecular weight marker and **bM** (bovine milk).

The nitrocellulose blot was probed using anti-bovine XO antibody raised in rabbits with a secondary swine anti-rabbit HRP-labelled antibody. Figure 3.22 shows the staining pattern seen for these milk samples.

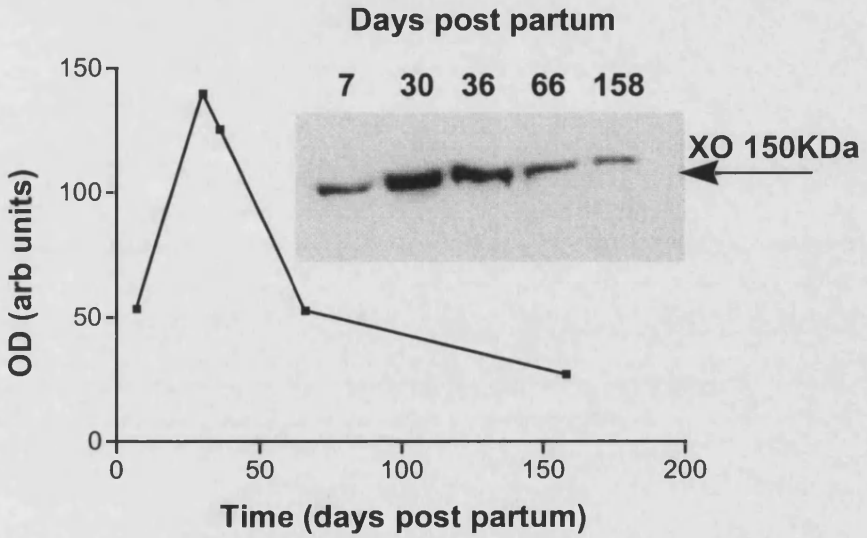

Figure 3.22. The staining of human milk for XO

This was repeated with the addition of purified human milk XO of known protein concentration. The optical density of the 150KDa band was measured and related to the known dilution series. The concentration of the unknown milk protein was then calculated and is shown in figure 3.23.

The reactivity of the immobilised protein shows changes over time post partum. There is reactivity in all samples, the optical density measurements of which increase from day 7 to 30 and thereafter begin to fall to levels below that of 7 days by 158 days post partum. On longer exposure of the membrane further degradation products begin to appear which are indicative of XO protein.

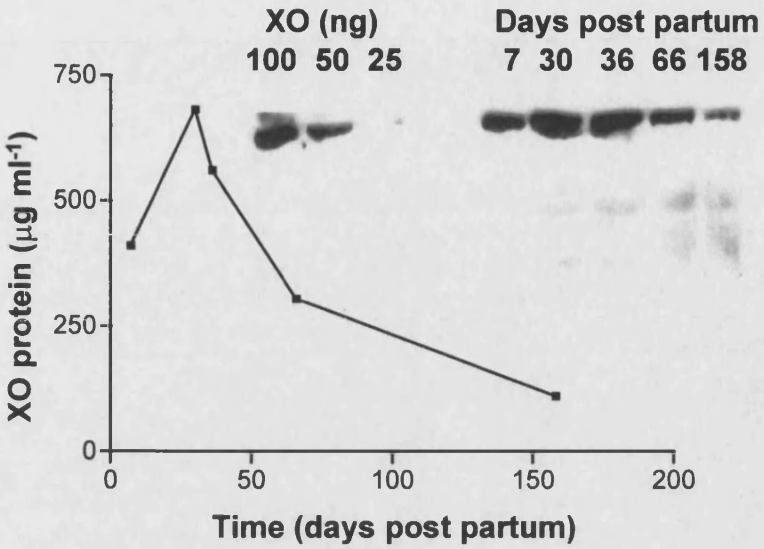

Figure 3.23. Repeat of Western blot of human milk samples with purified human XO as internal standard.

3.3.3.3 XO enzymic activity

The enzymic activity of human milk was assessed by measuring the NADH and xanthine-mediated LEC and correcting for XO enzyme content as measured in 3.3.3.2.

Figure 3.24 shows the NADH and xanthine-mediated LEC of human milk.

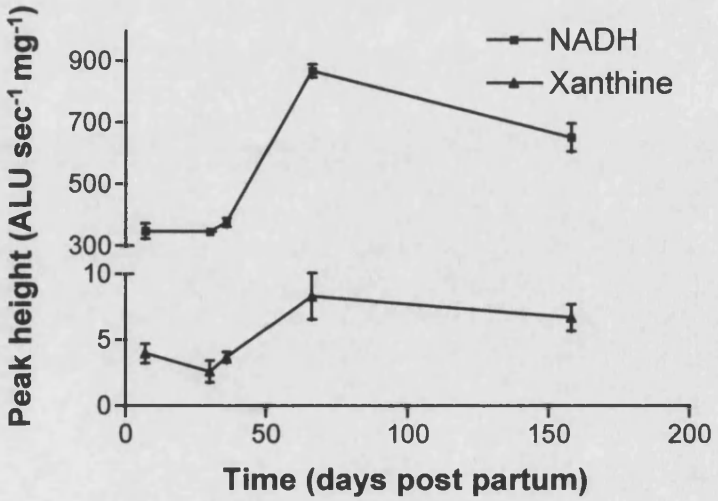

Figure 3.24. The response of human milk with NADH and xanthine in LEC. Data are mean ±SEM (n = 2) of triplicate values corrected for amount of XO enzyme present.

The activity of the human milk is shown to increase relative to the amount of enzyme present. A straight line over time would show that the enzyme generated had the same activity throughout the lactation period. These data however show that as the time post partum increases the activity of the enzyme found in milk increases.

The conversion of pterin to isoxanthopterin by human milk xanthine oxidase was measured using a fluorimeter with excitation at 345nm and emission at 390nm in quartz cuvettes with stirring at 25°C. Figure 3.25 shows the rate of product formation for each time point post partum.

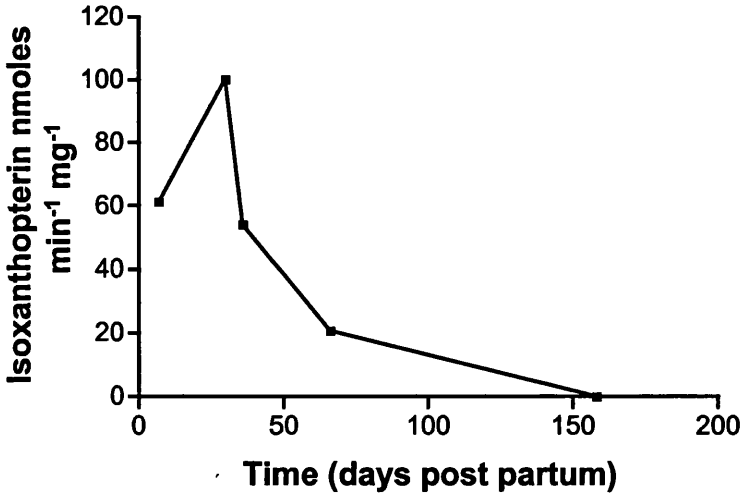

Figure 3.25. The XO activity of human milk samples as assessed using the rate of production of isoxanthopterin from pterin substrate. Rates were taken in the presence of 500µl human milk and 200µM pterin made up to a final volume of 1ml in PBS. Results are means of two experiments performed on consecutive days.

Human milk was found to metabolise pterin to its fluorescent oxidation product isoxanthopterin. The rate of reaction varied across the time post partum but gave a peak activity at ~ 30 days.

The NO generating capacity of human milk was determined using the Ozone enhanced chemiluminescence (OEC) analyser. Human milk was reacted with nitrite and NADH under reduced oxygen conditions as described in section 2.2.6.2. Figure 3.26 shows a typical trace of the NO generated from human milk under the conditions detailed.

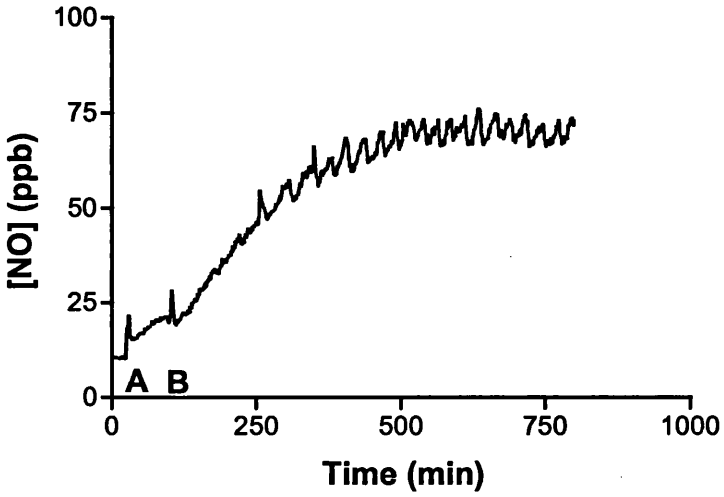

Figure 3.26. The generation of NO from nitrite (10mM), NADH (1mM) and human milk (500µl) day 7 post partum in the absence of oxygen. All reactants were gassed with 5% CO_2 balanced nitrogen and added to the reaction chamber sequentially, NADH at time zero, nitrite at **A** and human milk at **B**.

The milk gave a typical reaction curve with the exception that the signal showed some variation and was pulse-like. It was noted at the time that the impellar caused the reactants to foam, forming bubbles. As the bubbles burst the stored NO would be seen as a spike in the readings. The average of the top of a spike and its associated trough was taken as the rate of NO generation per second.

This procedure was repeated for all the post partum milk samples and is shown in figure 3.27 with the amount of XO protein per milligram measured by the Western blot analysis.

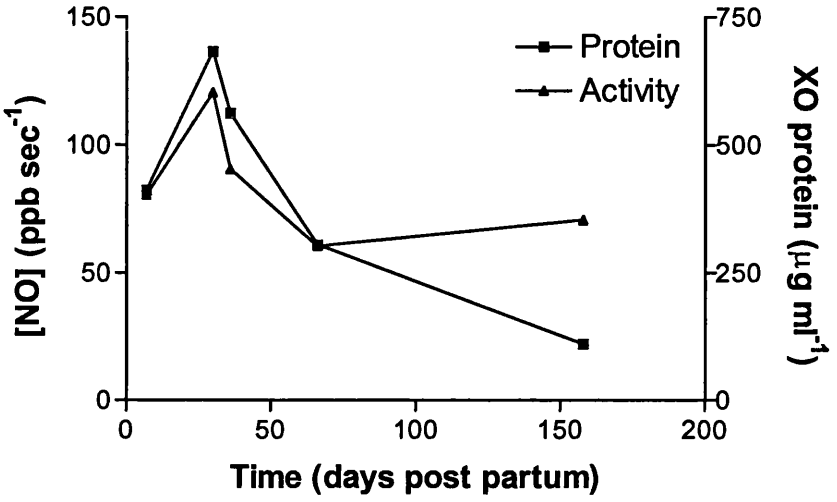

Figure 3.27. The NO generating capacity of human milk in relation to time (days post partum) for one mother.

The NO generating capacity of the human milk correlates to the amount of XO enzyme in each sample as estimated from the Western blot analysis over the first 4 time points. Following 158 days post partum there is a deviation in the activity relative to the amount of enzyme, which also mimics the total protein measurements (section 3.3.3.1). By calculating the NO enzyme activity to XO protein the relative activity over the 6 months post partum milk samples can be shown. Figure 3.28 shows the NO enzyme activity corrected for XO protein.

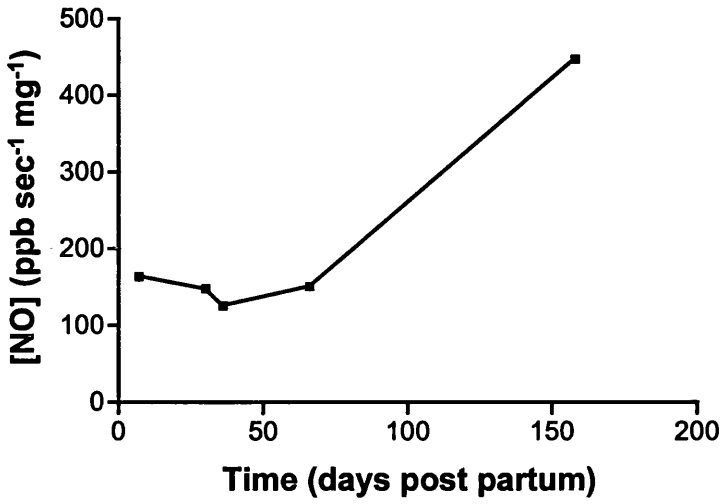

Figure 3.28. The data from figure 3.25 Transformed to show activity of human milk samples per milligram of XO protein.

The NO generating activity in the human milk samples stays relatively constant over the first 66 days post partum. At 158 days post partum, as the total protein content of the milk drops, the amount of estimated XO enzyme also falls. However at this 6 month time point the activity of the milk is increased relative to the amount of protein present.

3.3.4 Peroxynitrite effect on cell viability

3.3.4.1 Bolus additions to stationary phase bacterial cultures.

Peroxynitrite at a range of concentrations was added to cultures of *E. coli* and *S. enteritidis* of known cell concentration and the cells then plated onto agar for viable count determination. Figure 3.29 shows the effect of ONOO- addition and also the effect of dONOO- on cell viability.

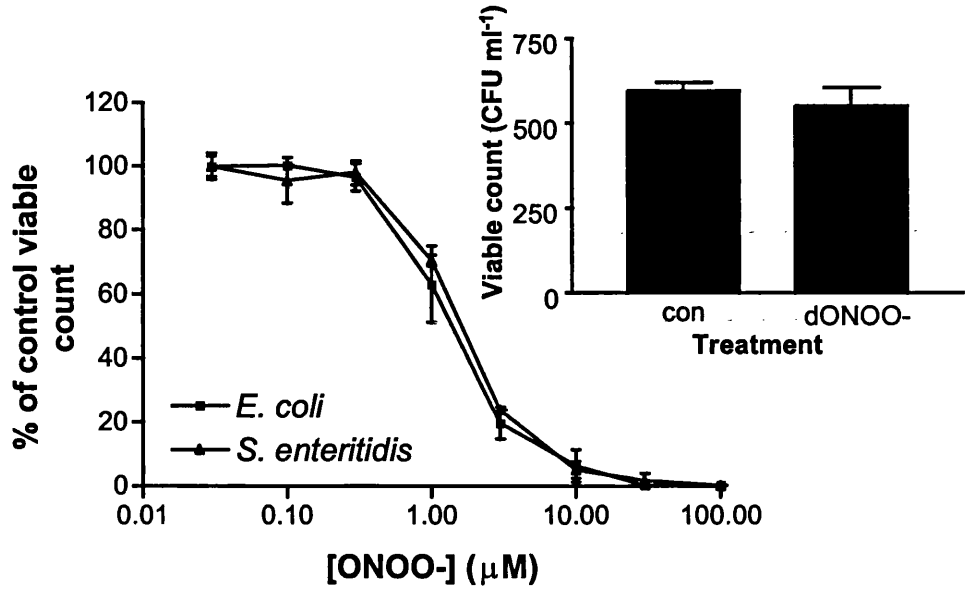

Figure 3.29. The bolus addition of ONOO- to *E.coli* and *S. enteritidis*. Cells were diluted to suitable working concentrations (10^7 – 10^8 cells ml^{-1}) in sterile phosphate buffered saline (PBS). ONOO- at a range of concentrations was added as a bolus dose to cells and incubated at room temperature for ten minutes. Aliquots were taken from the treated cells, plated on to nutrient agar and incubated in a warm room at 37°C overnight. Viable counts were performed as described previously and the number of colonies formed was related to a control consisting of decomposed ONOO- diluted in the same manner as 100μM ONOO-. Shown in the inset is the effect of decomposed ONOO- (dONOO-) on cell viability against control cells in PBS. Graphs show mean ± SEM (n = 2) experiments in triplicate.

The effect of ONOO- is to significantly reduce viability in both cell types compared to the dONOO- and naive controls. The IC_{50} value for ONOO- in this experimental set up was for *E. coli* and *S. enteritidis* 1.402 and 2.026μM respectively.

3.3.4.2 Effect of peroxynitrite addition to bovine milk

To assess the effectiveness of peroxynitrite as an anti-bacterial agent in milk, bolus additions of ONOO- were made to commercial sources of semi-skimmed milk. The milk was treated in a manner similar to general household use in that it was kept at 4°C during the period of the experiments.

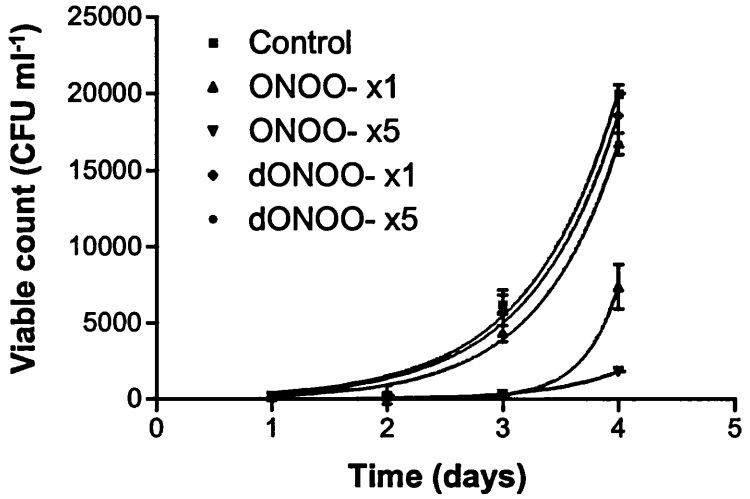

Figure 3.30. Effect of peroxynitrite addition to bovine milk. Aliquots were taken on day one of experimentation and plated onto nutrient agar for viable count determination. Treatments consisted of milk, milk plus a single bolus addition of 100μM ONOO- or dONOO-, and milk plus bolus additions of ONOO- or dONOO- daily for 5 days. Data show mean ± SEM (n = 2) in triplicate

ONOO- addition to semi-skimmed milk showed a time-dependent retardation of colony forming units on plating on agar. A single bolus addition of ONOO- significantly ($p<0.01$) reduced the CFU ml^{-1} compared to control values at all time points. Multiple additions of ONOO- also significantly reduced CFU ml^{-1} ($p<0.01$) compared to control values and also showed a significant reduction ($p<0.05$) compared to a single bolus dose (by students t-test).

3.3.4.3 Effect of hypoxanthine on bacterial growth in bovine milk

Semi skimmed and pasteurised bovine milk was incubated at 4°C for seven days. Each day an aliquot of 1ml was removed and incubated at 37°C for 30 minutes. This aliquot was then plated onto agar and incubated overnight at 37°C. Any colonies formed were counted and expressed as colony forming units per ml of milk against time. From the same milk, an aliquot was taken on day 0 and 100μM sterile hypoxanthine was added and then incubated and treated as described for the untreated milk. Figure 3.31 shows the effect of hypoxanthine treatment on bacterial viability.

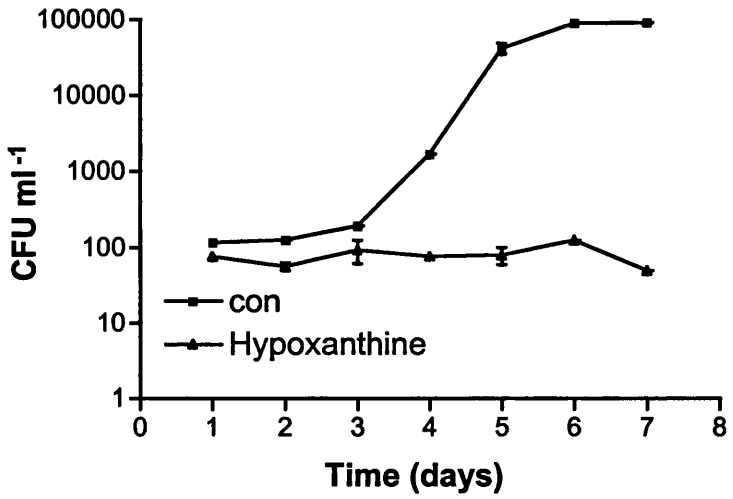

Figure 3.31. The effect of hypoxanthine on the naturally occurring flora in commercially generated pasteurised semi-skimmed milk. Results are mean ± SD in triplicate from one experiment.

Hypoxanthine has the effect of reducing the number of viable colonies when grown on agar compared to the untreated controls.

Assessment of the colonies by Grams stain (see appendix II) picked out Gram positive rods and Gram positive cocci in bunches shown in figure 3.32.

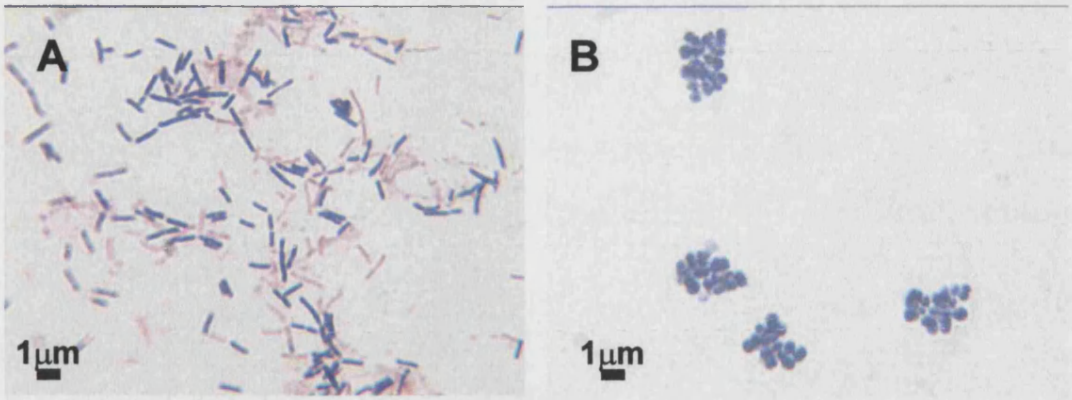

Figure 3.32. The Gram stain of colonies cultured on agar from bovine milk. Individual colonies were inoculated into nutrient broth and incubated at 37°C overnight with shaking. The resultant monocultures were Gram stained and viewed using a microscope with oil immersion. **A** Gram positive rods and **B** Gram positive cocci in bunches.

3.3.4.4 Peroxynitrite effect on cell growth.

The apparent difference in killing effectiveness seen by the bolus addition of ONOO- in figure 3.30 was assessed using the absorbance growth assay described for *E. coli*.

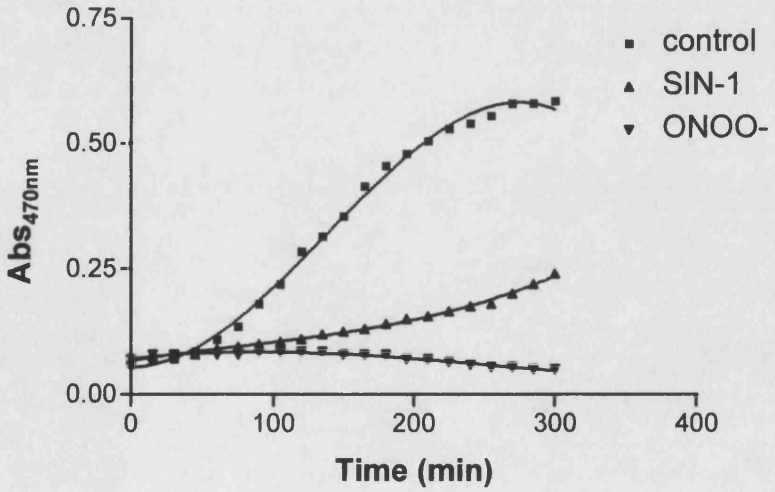

Figure 3.33. ONOO- effects were measured following the bolus addition of 100μM ONOO- at various time points in the growth of cells. Also, continuous production of ONOO- was assessed in this system using a 1mg ml^{-1} solution of 3-morpholinosydnonimine (SIN-1) which releases both superoxide and NO simultaneously on hydration.

Figure 3.33 shows the effect of continuous ONOO- generation on bacterial growth. SIN-1 addition causes the reduction in growth compared to the control. The serial addition of ONOO- causes the greatest effect but the concentration of ONOO- required is far in excess of that generated continually by SIN-1 (~1μmole min^{-1} mg^{-1}) (Crow *et al* 1995)

This effect was further investigated by the addition of 100μM ONOO- at single time points throughout the growth phase. Figure 3.34 shows that addition of ONOO- one hour after seeding causes a significant reduction in absorbance compared to the additions at time 0, 2 and 3 hours following seeding. An effect of each addition can be seen in the reduced total absorbance following seven hours of incubation.

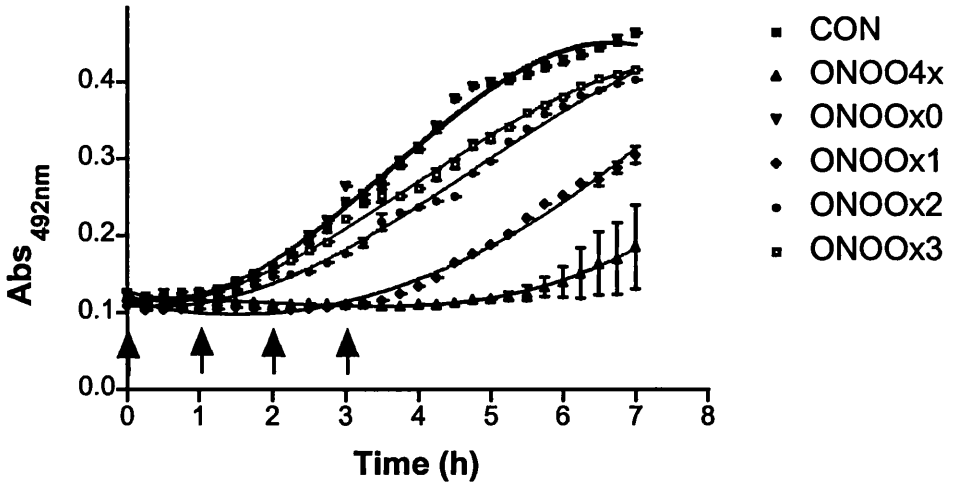

Figure 3.34. The effect of growth phase on bacterial susceptibility to ONOO-. *E. coli* were seeded into the wells of a 96-well plate in NB and their growth followed by measuring absorbance. ONOO- was added at various time points

after seeding 0,1,2,3 hours respectively. Also a control of untreated cells was run for comparison with cells treated every hour (CON and ONOO4x). Data are mean ± SEM of 2 experiments in triplicate.

To assess the effect of ONOO- addition to a range of bacteria the automated absorbance assay was used. By calculating the growth rate constant for each cell type in the absence and presence of a range of concentrations of oxidants it was possible to determine the growth rate relative to an untreated control.

Using equation (15) below the growth rate constant was calculated.

$$\mu = \frac{(\log_{10} N_{t1} - \log_{10} N_{t0}) \times 2.303}{(t1-t0)} \qquad (15)$$

Where μ = the growth rate constant, N_{t1} the absorbance at t1, N_{t0} the absorbance at t0, t1 time in minutes in exponential growth and t0 time in minutes at the start of exponential growth.

Using *Staphylococcus aureus*, *Lactobacillus casei*, *Bacillus sp* and a *Micrococcus sp*, *E. coli* and *S. enteritidis*, the effect of ONOO- addition was assessed. Figure 3.35 shows the effect of ONOO- addition on the growth rate constant related to a control treated with decomposed ONOO-.

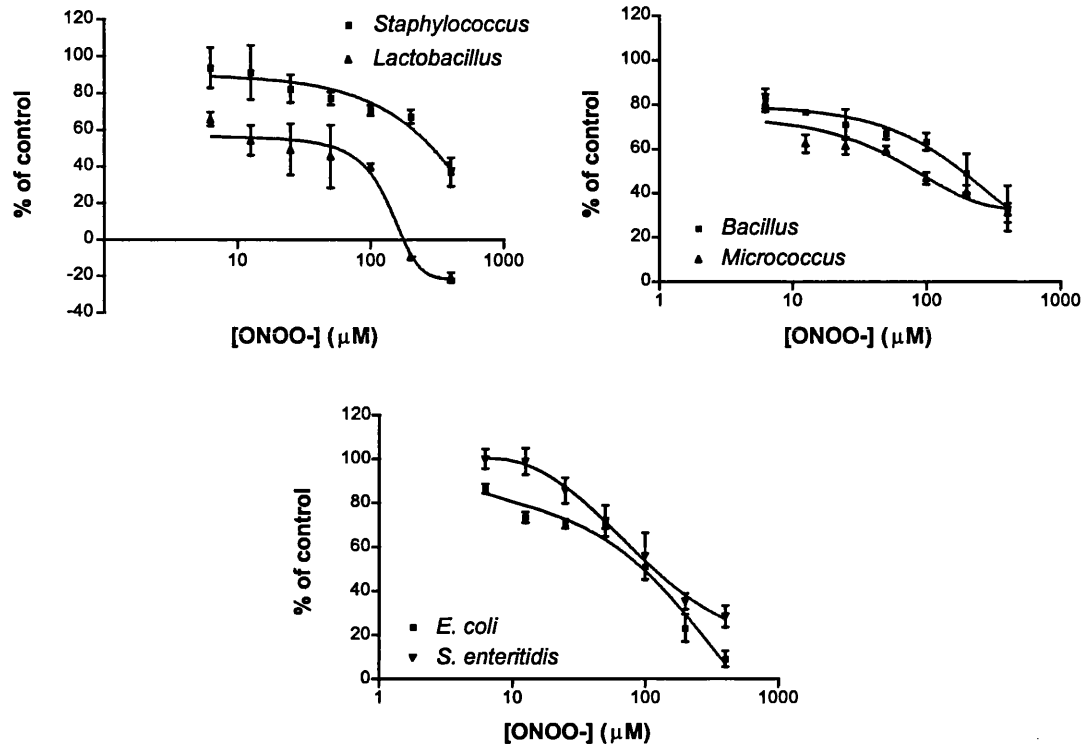

Figure 3.35. The effect of ONOO- on the growth rate of various bacteria. Cells were seeded into fresh nutrient broth after over night culture at $2x10^7$ cells $well^{-1}$. ONOO- was added at the start of the exponential growth phase for each species. Results are mean ± SEM of three individual experiments carried out in triplicate.

The effect of ONOO- addition reached significant difference for *Staphylococcus* at 25μM ONOO-, at 25μM for *S. enteritidis* whereas significant deviation $p<0.05$ was reached for the other four bacterial species at all concentration of ONOO- used in this experiment (Students t-test)

This experiment was repeated using hydrogen peroxide and the results are shown in figure 3.36.

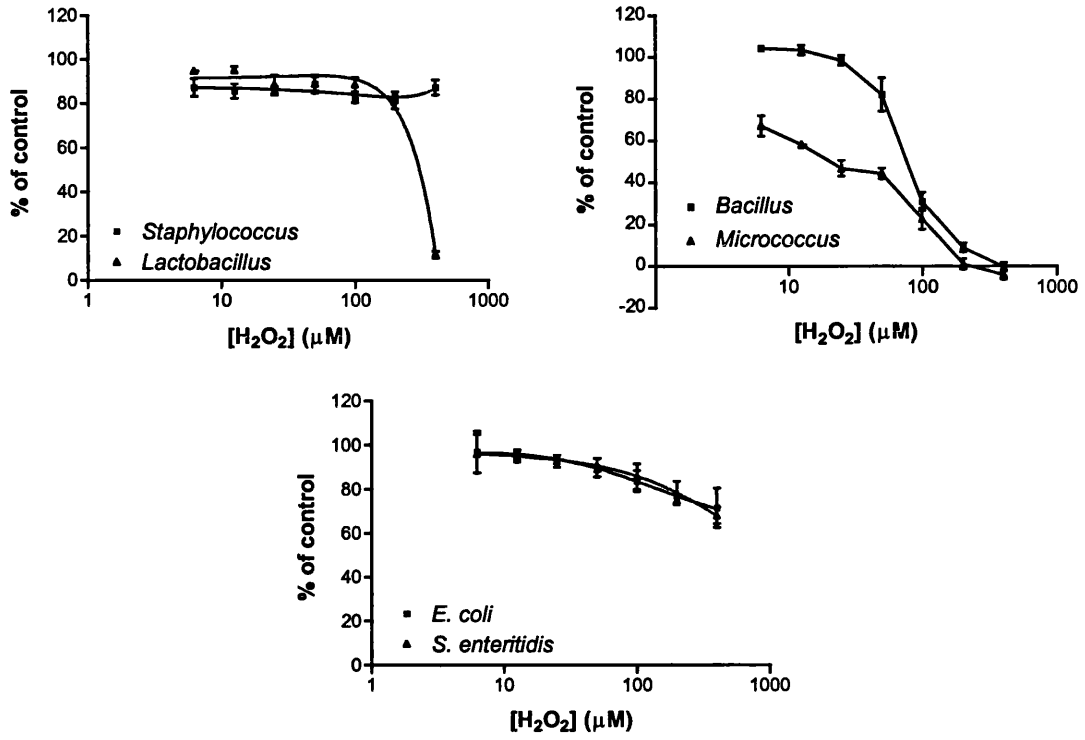

Figure 3.36. The effect of H_2O_2 on growth rate of various bacteria. Protocol as described in figure 3.35. Results are ± SEM of three individual experiments carried out in triplicate.

There was no significant deviation from the control for *Staphylococcus* at the concentrations tested and only concentrations of 200 and 400μM H_2O_2 were significant $p<0.05$ and <0.01 respectively for *Lactobacillus*. For *Bacillus* and *Micrococcus* species both show significant reduction in growth rate: *Bacillus* significance reached at >50μM H_2O_2 and *Micrococcus* at all concentrations tested by students t-test. Both *E.coli* and *S. enteritidis* showed significant deviation ($p<0.05$) from the control at concentrations above 12.5μM H_2O_2.

The dose of ONOO- and H_2O_2 at which 50% reduction in growth rate is observed for each species is shown in table 3.2.

Species	ONOO- (μM)	H_2O_2 (μM)
Lactobacillus	55	304
Micrococcus	57	19.5
Bacillus	70	77.6
E. coli	96.1	-
Salmonella	114.6	-
Staphylococcus	290	-

Table 3.2. Summary of the half maximal growth rates of bacteria exposed to ONOO- and H_2O_2.

3.3.5 Effect of xanthine oxidase-derived metabolites on cell viability

3.3.5.1 Effect of Hypoxanthine and xanthine oxidase in air

To asses the effect of enzyme derived metabolites, monocultures of various bacteria were grown overnight in nutrient broth and then grown in the presence of purified bovine xanthine oxidase and hypoxanthine. This was assessed by calculating the growth rate constant for each cell type in the absence and presence of a range of concentrations of enzyme and substrate as previously described for ONOO- and H_2O_2.

Figure 3.37 shows the effect of increasing hypoxanthine concentration at 30μg XO protein compared to a control containing 200μM hypoxanthine.

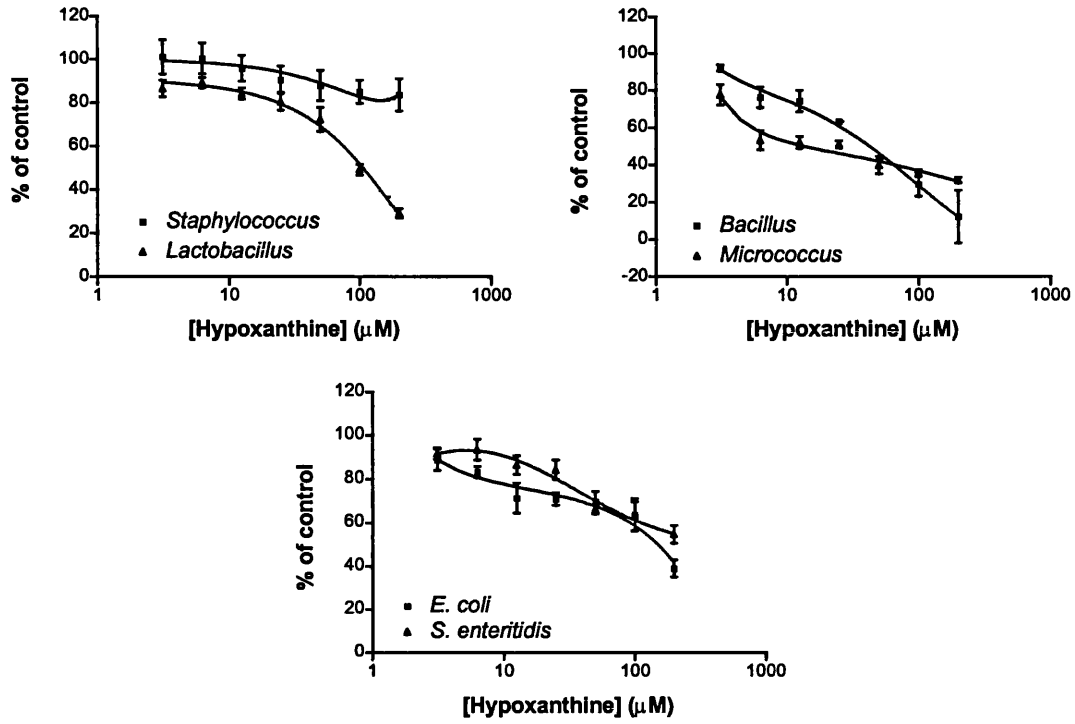

Figure 3.37. The effect of XO and hypoxanthine on the growth rate of various bacterial species. Protocol as described for ONOO- effects except that all substrates and enzyme were added at time 0 minutes. Results are mean ± SEM of three individual experiments in triplicate.

The addition of hypoxanthine alone at 200µM caused no significant deviation from cells grown in the absence of hypoxanthine. Significant reduction in growth rate ($p<0.05$) was measured for all six bacteria with the half maximal concentration of hypoxanthine and is summarised in table 3.3.

Species	Significance p<0.05 (μM hypoxanthine)	Half maximal growth rate (μM hypoxanthine)
Staphylococcus	>50	-
Lactobacillus	>12.5	103.5
Bacillus	>6.25	39.8
Micrococcus	>3.125	25.1
E. coli	>3.125	151
Salmonella	>12.5	-

Table 3.3. The summary of XO / hypoxanthine effect on bacterial growth rate in atmospheric air.

All growth rates were significantly reduced compared to control cells. The reduction in growth rate to the half maximal level was seen in all species except *Staphylococcus* with maximal reduction in growth of ~ 20% at the concentration of enzyme and hypoxanthine used.

3.3.5.2 Effect of oxypurinol on XO and hypoxanthine mediated growth effects

Oxypurinol was added to the wells of a 96 well plate as part of a growth assay for *Lactobacillus casei.* The effect of 30μg XO and hypoxanthine at 100μM was to reduce growth rate significantly in this bacteria. The addition of oxypurinol was to determine the enzymic nature of the growth retardation. Figure 3.38 shows the effect of a range of oxypurinol concentrations on the growth of *Lactobacillus.* Oxypurinol in the absence of XO and hypoxanthine had no effect on the growth rate of *Lactobacillus* at the concentrations used.

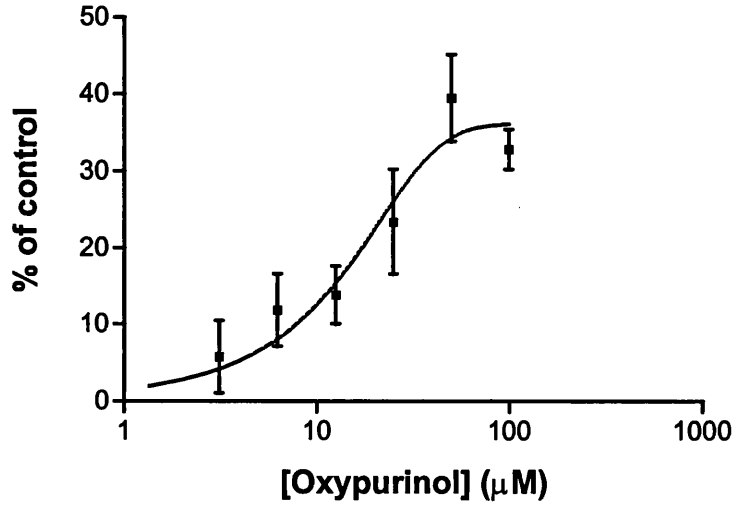

Figure 3.38. The effect of oxypurinol on the XO, hypoxanthine mediated growth retardation in *Lactobacillus*. Cells were grown in a 96 well plate format and exposed to XO and hypoxanthine. Oxypurinol was added at a range of concentrations and results are shown as the % of control growth rate from cells in the absence of XO but in the presence of 100μM hypoxanthine. Results ± SEM (n = 3) in triplicate.

Oxypurinol reversed the inhibition of growth rate mediated by XO / hypoxanthine in a dose dependent manner.

3.3.5.3 The effect of oxygen concentration on bacterial viability

As the type of oxidant generated is dependent on the oxygen concentration of the reaction mixture, the effect of oxygen was assessed on the viability of bacteria in the presence of nitrite, XO and an electron donor. It was not possible to run the experiments using the automated assay so cells were incubated with radical generating systems for 30 minutes before plating onto agar for viable count determination as described in section 3.2.8. Figure 3.39 shows the effect of oxygen concentration on the viability of *E. coli* and *S. enteritidis* following 30 minute incubation in the above reaction mixture.

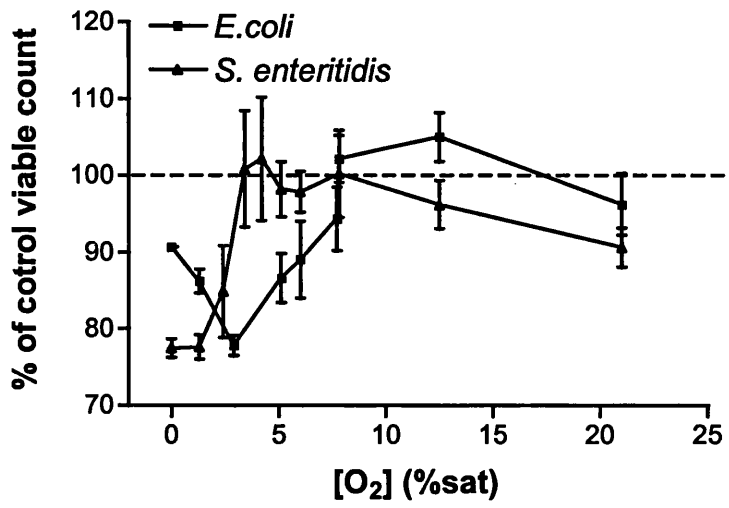

Figure 3.39. The viability of bacterial strains in the presence of XO metabolites. $2x10^7$ cells ml^{-1} were added to XO, 53.2μg, NADH, 300μM and nitrite, 1mM and incubated for 30 minutes under defined oxygen concentrations. Data are mean ± SEM (n = 2) in triplicate shown as percentage against control cells in the absence of NADH.

For both cell types viability is reduced compared to controls incubated under the same conditions. Viability varies with oxygen concentration in the media. *S. enteritidis* is more susceptible to the metabolites at 0% oxygen (viability ~75% compared to ~ 90% viability for *E. coli*). The peak killing oxygen concentration for *E. coli* and *S. enteritidis* is 2.9% and 0% respectively. As the oxygen concentration increases the viability of both bacterial strains increases with little or no killing above ~ 8% oxygen. However there does seem to be some killing at higher oxygen concentrations with ~ 10% and 5% killing for *E. coli* and *S. enteritidis* respectively at 21% oxygen.

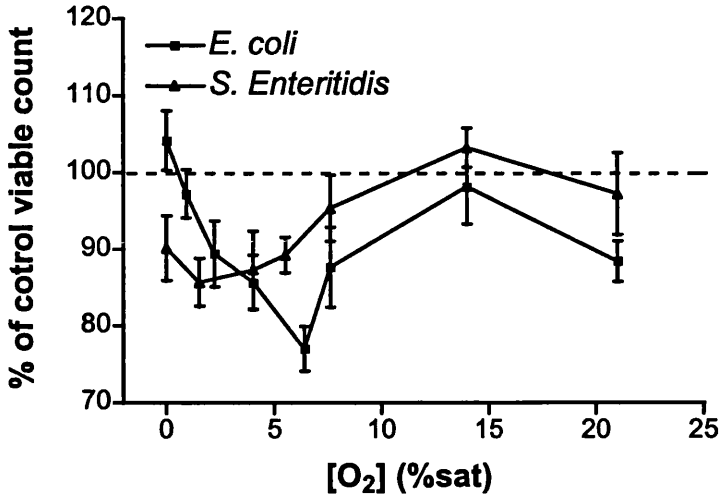

Figure 3.40. The effect of hypoxanthine on the viability of bacteria. Exposure to a range of oxygen concentration in the presence of XO 53.3μg, hypoxanthine 100μM and nitrite 2.5mM. Data are mean ± SEM (n = 2) in triplicate.

The peak killing for *E. coli* and *S. enteritidis* in the presence of hypoxanthine was seen at 6.4% and 1.5% respectively. Some killing was also seen at 21% oxygen for both bacterial strains but was only significant for *E. coli*.

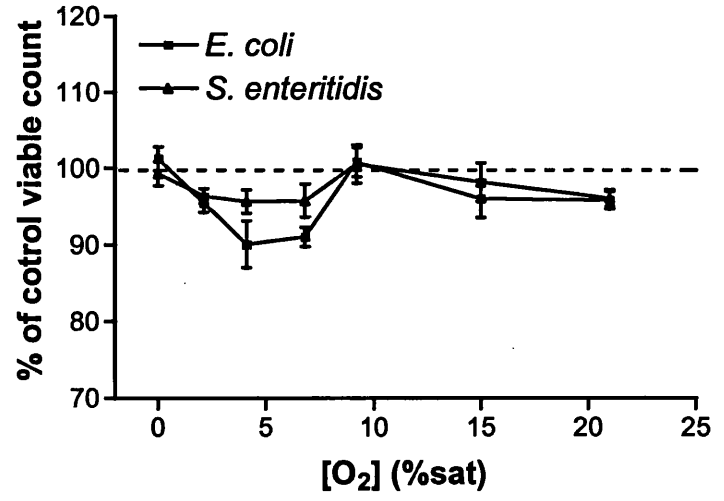

Figure 3.41. The effect of xanthine as electron donor on bacterial viability. Exposure to a range of oxygen concentrations in the presence of XO 53.3μg, xanthine 100μM and nitrite 2.5mM. Data are mean ± SD (n = 1) in triplicate.

The effect of xanthine was small compared to control levels at all concentrations of oxygen utilised.

3.4 Discussion

In the light of the oxygen and nitrogen radical-generating capacity of XO and its high concentration in mammalian milk, the possibility of its utilisation as an antibacterial enzyme has been studied.

XO enzymic activity was assessed in a variety of milk products to compare them with milk formulas often used as a substitute to maternal milk in feeding neonates. Bovine and human milks both contain large amounts of NADH active enzyme. The xanthine activity of human milk was very low compared to bovine milk and this compares well with previously published data on the differences between bovine and human milk-derived XO enzyme (Sanders *et al* 1997). Infant milk formulas showed no NADH or xanthine mediated LEC. However these formulas contain the antioxidants Vitamins C and E which have been shown previously to reduce LEC in the presence of superoxide. When probed for XO protein by Western blot analysis these formulas were found to be lacking in this reactive protein using this antibody.

In the case of butter milk derived from Golden churn a similar lack of LEC was seen for both substrates. However, the butter milk was active when tested for NO generating activity and this activity was also oxypurinol inhibitable. With Western blotting there was also a strong signal for the 150KDa band when probed with the Chemicon anti-xanthine oxidase antibody. This preparation also contains antioxidant vitamins and it is possible that it was these factors that reduced the LEC even when active enzyme was available.

In the light of evidence suggesting that breast milk confers protection on the infant from enteritis compared to infants fed formula preparations, it is a possibility that

xanthine oxidase-derived radicals may play a role in protecting the infant from enteric infections.

Human milk showed activity in both xanthine and NADH-mediated LEC, pterin mediated activity and also as a generator of NO in low oxygen conditions in the presence of nitrite and NADH. The human milk also showed a variation in activity data over time post partum. When corrected for XO protein, the activity per mg of protein remained relatively constant over 66 days. Only at ~ 6 months had the protein content per millilitre fallen but the enzyme activity per milligram was increased over the previous time points per milligram of XO protein. It is possible that the activity of the enzyme is controlled such that on reduced protein generation the activity is increased in some way to confer more radical generating capacity. Also the size of feed and therefore amount of enzyme in the gut is generally increased over time post partum and this may also confer a greater protective effect.

This is the first description of the NO generation from nitrite in the presence of NADH from a human source of XO. From the previously described superoxide generation from both human and bovine milk XO, the possibility exists to generate NO and superoxide simultaneously.

The effect of ONOO- addition to bacterial cultures was to decrease viability and growth rate constant in a dose-dependent manner for all bacteria studied.

Two assays were utilised for the measurement of ONOO- effects on the two Gram negative bacteria, *E. coli* and *S. enteritidis*. The viability assay used where cells were incubated with ONOO- in PBS gave the inhibitory dose of 1μM which is far reduced compared to the growth rate assay which utilises growing cell in culture media. The previously stated IC_{50} values for a different strain of *E. coli* are somewhat higher than the viability assay stated here but are similar to the data

shown in the growth assay (Brunelli *et al* 1995). This may be due to strain characteristics or the state of the cells on addition of peroxynitrite. In this thesis the point of addition of ONOO- has also been shown to greatly effect the outcome for growing cultures suggesting the growth cycle as a possible target for therapy.

The variation in susceptibility to ONOO-, H_2O_2 and enzyme derived metabolites may in part be due to the generation of antioxidant enzymes by the bacteria. The effect of ONOO- addition on early log phase cultures showed the greatest effect and it is at this time that most of the bacteria will not be generating their antioxidant enzymes.

If the radical products of milk XO are to be bactericidal, they must be able to mediate their effects in milk with all the associated proteins and lipids. Using the model of pasteurised, semi-skimmed milk, which contains naturally occurring environmental contamination, the effect of chemically synthesised ONOO- showed a reduction in viability of the species contained in the milk over time. A single dose of ONOO- significantly reduced the viability of contaminating organisms as did the multiple doses of ONOO-.

The single addition of a bolus of hypoxanthine also reduced bacterial growth in milk and it is suggested that this was through the action of xanthine oxidase derived metabolites. Indeed in the XO / hypoxanthine susceptible *Lactobacillus*, the addition of oxypurinol protected the cells and allowed growth.

Recently, it has become of importance to reduce the utilisation of antibiotics as growth supplements in animal feeds and across the spectrum of bacterial infections because of the resistance developed by many bacteria to commonly used antibiotics. Work in pigs fed a diet containing increased lactose has seen a reduction in the amount of antibiotic required for health. This has been suggested to be due to the selection of non-harmful, commensal bacteria such as the

Lactobacilli sp which out-compete possibly harmful bacteria (Oli *et al* 1998). Although *Lactobacillus* were affected by XO / hypoxanthine it is possible that due to an increased lactose diet the effects on growing *Lactobacillus sp* may be to out compete the more infective bacteria even in the presence of the radical generating system with the combination of approaches of synergistic benefit.

The effect of ONOO- on growing cell cultures showed a difference in susceptibility which was dependent on the point of the growth cycle. Cells were more susceptible to ONOO- during the early part of the log phase compared to the lag and stationary phases as assessed by sequential additions of ONOO- to the cultures. The addition of ONOO- at the start of the log phase had the greatest effect on growth. At this point, the cycle time can be as short as 20 minutes between divisions. At this time the production of antioxidant defence proteins such as SOD and catalase are not expressed to such a high extent as seen in the stationary phase. The particular effect of ONOO- addition depends on the mode of action of ONOO- on growth and viability. It has been previously shown (Beckman and Koppenol 1996) that ONOO- has a variety of effects on proteins of particular importance and on DNA (Szabo and Ohshima 1997). Strand breaks in DNA require repair enzymes which themselves can be inhibited by ONOO- which can cause a reduction in growth rate if the breakages are not lethal in nature (Szabo *et al* 1996). It is also known that ONOO- can be transported through membranes either passively in the protonated form or actively using a 4,4'-diisothiocyanatostilbene-2,2'-disulphonic acid (DIDS) inhibitable HCO_3^-/Cl^- ion channel in the anionic form where it can cause nitration of proteins especially of tyrosine residues and inhibit various activities (Denicola *et al* 1998).

The sensitivity of bacterial species must depend on the antioxidant mechanisms that they utilise, and the ability to block the entry of ONOO- into the cell. The form

of the peroxynitrite may also have a differential effect with peroxynitrous acid able to passively diffuse through membranes and may therefore be a more potent intracellular oxidant and nitrating agent.

The viability of bacteria in the presence of XO-derived metabolites varied with oxygen concentration under the conditions used. Using the combined activities of NO and superoxide generation at a range of oxygen concentrations, peak killing activity could be seen in the range of oxygen concentrations where simultaneous generation is expected.

This effect is seen at relatively low enzyme concentrations. From the levels used here (~ 50μgml^{-1}) the concentration of XO enzyme in human milk from this thesis covers the range from 300 – 800μgml^{-1}, greater than a ten fold increase in the amount of available enzyme.

It is possible then that the radical generating activity of xanthine oxidase in the environment of the neonatal bovine or human gut may play a role in mediating the growth and colonisation of bacteria and the onset of infection by pathogenic strains of bacteria.

Further work on the variation in oxygen content on the viability of bacteria in the presence of xanthine oxidase derived metabolites is required.

Chapter 4

The binding of xanthine oxidase to endothelial cells

Chapter 4

This chapter deals with the possibility that XO circulates as an active enzyme in man and can bind to cellular surfaces to allow relocation of active enzyme to sites distant from protein synthesis.

4.1 Introduction

4.1.1 The cellular expression of XO

Previously, the expression of XO had been localised to a variety of organs and this finding spawned the ideas surrounding its possible role in reperfusion injury (McCord 1985). This also suggested that other diseases may be due to or have some component that is due to oxidant stress and the localisation of XO enzyme to a particular tissue may suggest that an oxidant forming role may occur in that tissue. It was surmised that in joint inflammation many oxidant processes were occurring one of which may well be linked to the expression of XO.

Work carried out by Stevens *et al* (1991) and others pointed to a change in the vascularity found between normal and inflamed rheumatoid synovium. By measuring the relative density of the vasculature it was shown that inflamed synovia were relatively poor in blood vessels. The relative hyperplasia of the surrounding tissue had led to an outstripping of the blood supply to the synovium and eventually this would lead to a chronically hypoxic tissue.

Also shown was the expression of XO protein in the synovium. This was localised to the microvascular endothelium that lined the vessels. This produced the proposal that on a primary insult leading to increased pressure in the synovial capsule, phases of acute hypoxia followed by reperfusion of the tissue occurred.

The localisation of the oxidant producing enzyme XO to the EC would cause damage during reperfusion as the oxygen was reintroduced.

4.1.2 Xanthine oxidase binding studies

The apparent functions of xanthine oxidase enzyme and its relative expression among various organs has led to the development of literature that aims to describe its role as an enzyme involved in pathology. From experiments carried out on the inhibition of enzyme activity, it was clear that an intracellular source of the enzyme was responsible for the damage seen. However, further reports suggest that the use of specific inhibitors of XO caused an inhibition of damage at locations far from the target organs. Experiments using allopurinol or by pre-treatment of animals with tungsten to inactivate XO were shown to decrease lung vascular barrier function secondary to splanchnic ischaemia-reperfusion (Terada *et al* 1992 and Koike *et al* 1993). It was also noted that, at allopurinol concentrations lower than those at which antioxidant effects are observed, there was a display of tissue protection in organs apparently low in or devoid of detectable endogenous XO activity (Zimmerman *et al* 1988). Examples of this came from both rabbit and human heart studies where myocardial ischaemia-reperfusion injury was significantly attenuated by allopurinol despite the apparent lack of enzyme activity in these organs (Gardner *et al* 1983, Grum *et al* 1986, Terada *et al* 1988 and Sarnesto *et al* 1996).

The suggested reason behind these findings is the possibility that XO circulates in the blood plasma either as a free protein or complexed with anti-XO antibodies (Benboubetra *et al* 1997). Plasma levels of XO were also shown to rise following ischaemia-reperfusion injury to the splanchnic system or following hypovolemic

shock with further increases seen on perfusion of high levels of intravenous heparin (Terada *et al* 1992, Tan *et al* 1993 and 1995).

This system then, utilising a range of stimuli may allow the release of XO from various organs into the circulation by secretion or other means. The binding of this circulatory form of XO onto the surface of endothelial cells could concentrate the enzyme at specific points where its reaction products may have their actions.

Previously, XO has been shown to associate with the endothelium and also to bind to heparin-sepharose 6B complexes *in vitro* (Radi *et al* 1997).

Recently it has also been observed in isolated and cell line derived endothelial cells that XO can localise to the cell surface. It was also observed that the staining pattern of individual cells was polarised with accumulation of antigen at specific sites on the cell, often on pseudopod like processes abutting other cells (Rouquette *et al* 1998).

The apparent affinity of XO for glycosaminoglycans may be used to exploit the radical generating capacity of the enzyme. Virulent strains of bacteria must often bind to a substrate to allow invasion particularly in gut associated pathogens. This adhesive process has been shown to involve certain matrix proteins including fibronectin, collagen and fibrinogen. It has also been noted that certain glycosaminoglycans (GAGs) can mediate bacterial and virus binding.

Heparin is a sulphated GAG known for its anti-coagulant activity that is exclusively produced by the mast cell and is not usually a part of the extra cellular matrix. However, it has close structural relationship to heparan sulphate which is found in the extracellular matrix and on the surface of most animal cells. Heparin is more sulphated than heparan sulphate and a basic protein that nonspecifically binds the strong polyionic heparin may not necessarily have an affinity for heparan sulphate (Ortega-Barria and Pereira 1991 and Frevert *et al* 1993).

Many microorganisms express heparin binding surface proteins and the internalisation of several viruses involves the binding of the virus to heparan sulphate proteoglycans at the cell surface. *Chlamydia trachomatis* is an obligate intracellular bacterium that requires adhesive processes to enter animal cells. It apparently synthesises a heparan sulphate like GAG that is bound to its surface. The heparan sulphate then serves as a bridge that can bind other heparin binding proteins to the host cell surface (Patti *et al* 1994).

4.1.3 Circulating plasma xanthine oxidase

To study the activity of circulating proteins a range of assays were employed. Using blood from normal healthy volunteers pre and post exercise NADH activity was assessed by NADH mediated chemiluminescence and NADH oxidation. The oxidation of NADH in the absence of oxygen and the presence of nitrite was also measured. Finally Western blots of normal human plasma were run and blotted for xanthine oxidase protein.

The following experiments were designed to further the evidence for the circulating form of XO and the ability of XO to bind on the surface of live cultured endothelial cells and bacteria in the form of *E. coli* cultures. The mechanism by which this occurs was also studied by the measurement on endothelial cell surface heparan sulphate glycosaminoglycan expression and the effect of heparinase treatment. Also the ability of hypoxia to modulate XO binding and heparan GAG expression was also assayed.

4.2 Method and materials

4.2.1 Flow cytometry

4.2.1.1 Introduction

Flow cytometry grew out of various other disciplines used to quantify individual cells or organelles. Techniques such as microfluorimetry, microspectrophotometry and microinterferometry provided a means to quantify DNA, RNA or proteins. Flow cytometry and associated electronic cell sorting offered advances in that it was capable of rapid measurement of several hundreds and thousands of cells per second with high accuracy and reproducibility. This in turn lead to the development of probes for various physiological parameters especially early on in cell cycle analysis (Darzynkiewicz and Crissman 1990).

4.2.1.2 Basic background

The basis behind all flow cytometers is the use of light scattering as a method to visualise particular cell types including size, morphology and granularity within a population. To do this, the cytometers use a focused beam of light usually from a laser that interacts with particles flowing in a stream of fluid. Using a method known as hydrodynamic focussing; a stream of fluid, the sample stream, is encapsulated in a second sheath of fluid where turbulence has been removed. This allows the sample stream to exist within the sheath stream without mixing of the two fluids. The laser is then focussed onto the sample stream and illuminates particles or cells in the stream as they flow (see figure 4.1)

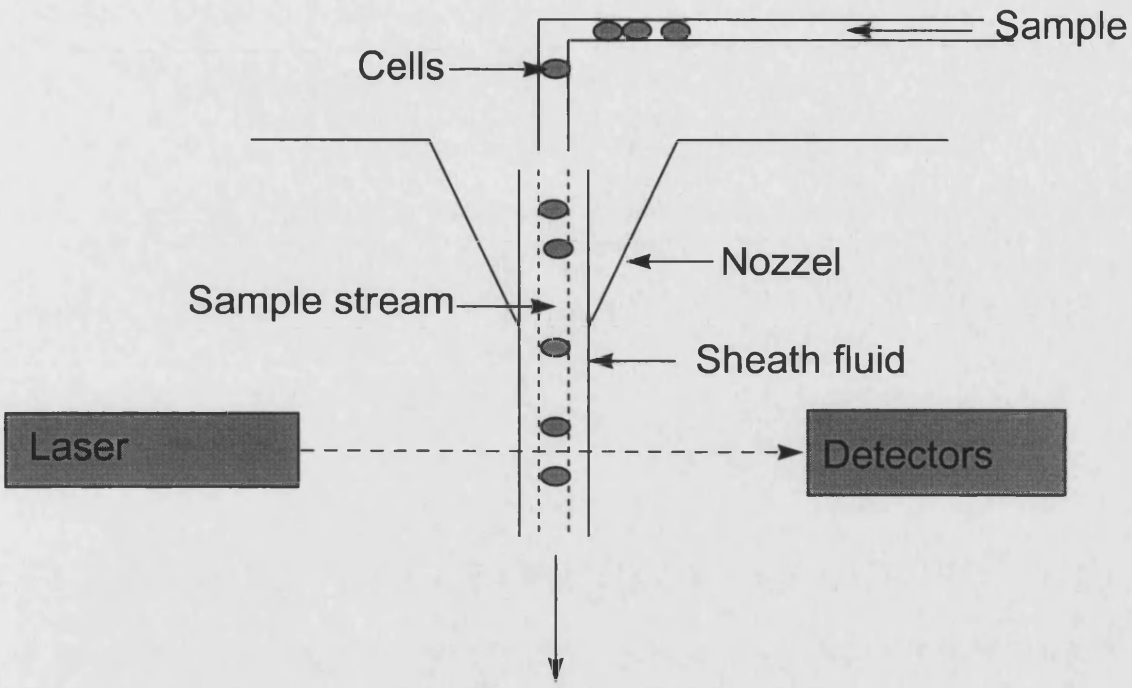

Figure 4.1. The basis behind hydrodynamic focussing.

The subsequent light scattering of the particles is measured using detectors which are set at two points relative to the light direction. These two parameters low angle or forward scatter (FSC) detector is set at ~ 10 degrees deflection from the primary laser beam. The side scatter (SSC) detector is set at 90 degrees to the primary laser beam. With these two parameters it is possible to discern a population of cells from debris and also to discern individual populations such as mononuclear leukocytes and granulocytes from a mixed population of white cells.

Using electronic gating it is also possible to identify a cell population of interest and analyse that population whilst collecting data for the whole sample. This technique is required when cells are to be discerned from debris and other non-cellular contaminants which may cause false positive results. Electronic gating was used in all experiments described below to remove such debris.

Also used was the threshold parameter. This allows the removal of some of the smaller particles before electronic gating. In all experiments with human cells the

laser beam was focused through a neutral density filter which effectively limits the resolution of the cytometer to particles greater than 5 micrometers in diameter. The cytometer used for these experiments had its laser focussed onto the sample stream in air. That is to say that a nozzle of 100μm in diameter is used as the hydrodynamic focussing device. This allows for relatively large cell types such as EC to be used.

4.2.1.3 Cell surface measurements

Cellular antigens can be measured using a range of fluorescent probes. The laser emits light at a particular wavelength, commonly 488nm, which will excite specific molecules such as fluorosceine-iso-thiocyanate (FITC) and propidium iodide (PI) and cause them to fluoresce. Using a range of wavelength filters, multiple probes may be used simultaneously and fluorescent parameters of cell surface and/or intracellular antigens may be measured. Due to the Stokes shift of these fluorescent probes the emission wavelength does not overlap with the excitation wavelength and by using filters of known bandwidth the overlap of fluorochrome emissions can be minimised (See figure 4.2)

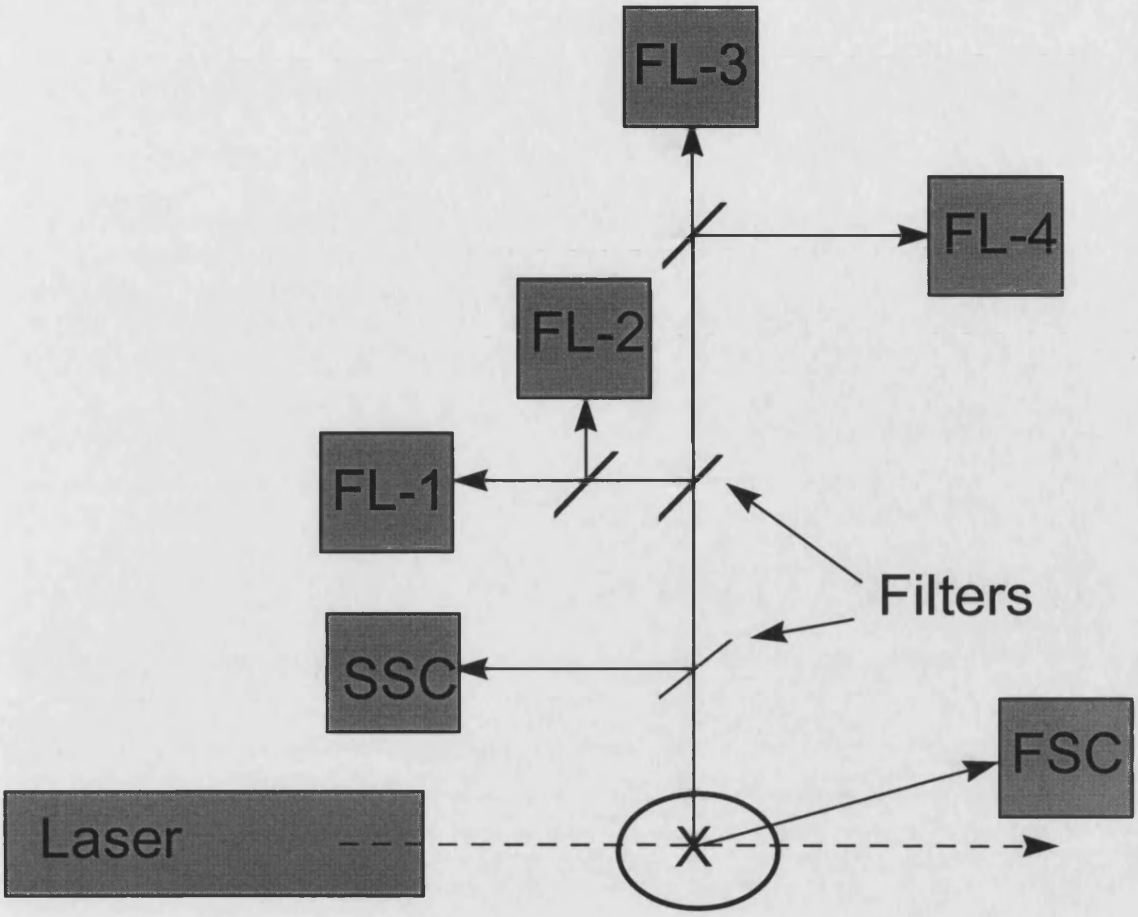

Figure 4.2. The basic set up of the flow cytometer. X is the direction of sample fluid flow down through the page and point of excitation. Shown here are the detectors for multiparameter analysis of up to 4 fluorescence signals and analysis of light scattering parameters. (FL-1 refers to fluorescence channels for the detection of a discreet wavelength of emitted light, FL-2 – 4 being further fluorescence detectors).

Each detector consists of a filter of known band width and a photon multiplier tube (PMT). The particular light that reaches the PMT is coded into a digital signal and amplified. The electronics of the cytometer can then display each parameter event, light scattering and fluorescence as a series of plots.

The sensitivity of the cytometer depends on the voltage being applied to each of the PMTs. These can be varied by the user and is used during routine alignment of the instrument with fluorescent beads.

The information generated can be shown as a series of plots including histogram plots, usually showing event number against measured parameter such as fluorescence and dot plots, showing two parameters simultaneously. To display the data two systems are used: logarithmic and linear scales. Each system lies over 1024 channels (0-1023) and information can be shown as mean channel height which relates to the mean position of the data showing a normal distribution along a particular axis. In the following experiments mean channel height is used as the measure of fluorescence for each of the sets of data generated.

4.2.2 Tissue culture

4.2.2.1 Cell isolation

4.2.2.1.1 Human umbilical vein endothelial cell (HUVEC) isolation

Large vein endothelial cells have been cultured as relatively pure populations since the early 1970s. The following isolation technique is a modification of methods described by Jaffe *et al* (1973) and Gimbrone *et al* (1974).

Human umbilical cords were collected from neonates following birth and stored at 4°C until use, which was typically within 48 hours of delivery. Cords were prepared under sterile conditions in a class II flow cabinet (Microflow biological safety cabinet, MDS, UK) on a dissecting tray previously swabbed with 70% ethanol. The outer surface of the cords were swabbed with pink chlorhexidine gluconate (0.5% w/v in 70% v/v IMS - Depuy® Healthcare, UK) as a disinfectant. Each cord was then inspected for clamp marks caused during the delivery and also for needle

marks which would cause leakage in the following procedure. The vein of each cord, identified by its lack of intimal smooth muscle, was then cannulated using two plastic leur adapters in series which were fastened in the cord by plastic bag ties to produce a tight seal. Phosphate buffered saline (PBS) solution was then flushed through the cords to remove any residual blood remaining in the vein. This was repeated until the PBS ran clear and all the blood had been removed from the vein. The opposite end of the cord was then also sealed with two plastic bag ties to which was added a $0.5mgml^{-1}$ solution of type II collagenase (SIGMA, UK). The cords were then left to incubate at room temperature for 30 minutes to 1hour after which the collagenase solution was removed and PBS flushed through the vein to remove any remaining endothelial cells. The resulting cell suspension was then centrifuged at 400g to pellet the cells which were resuspended in "HUVEC culture medium" (HM) (see appendix III) and plated typically onto $T\text{-}25cm^{-2}$ tissue culture treated culture plates (Falcon, UK) and placed in an atmosphere of 5% CO_2 95% air at 37°C. These cells were then washed in HM on the day following isolation and the media replaced every two to three days.

On reaching confluency, the cells were passaged at a split ratio of 1:5 and used in experiments between passage 1-5. The purity of the isolated population, measured by immunological staining of vWF antigen: a marker for endothelial cells, was consistently over 99% reflecting the lack of contaminating cells from other lineages.

4.2.2.1.2 Synovial microvascular endothelial cell (SMEC) isolation

The methods used to generate cultures of synovial microvascular endothelial cells were based wholly on the work of Abbot *et al* 1992. The method described below is a modification of that published protocol.

Human synovia were collected from the joints of patients undergoing total knee (TKR) or total hip (THR) replacements in the treatment of rheumatoid and

osteoarthritis. The synovia were removed under sterile conditions and stored at 4°C until use which was typically within 12 hours following excision. The microvasculature was removed by dissection of the synovial membrane. Hyperplasic tissue which is villus like and highly vascularised was removed by immersion of the synovium in media which caused the villi to float upward and facilitated dissection. Removed villi were placed into medium and minced with crossed scalpel blades before being incubated for 60-90 min in $2mgml^{-1}$ type IV collagenase (Worthington, UK) at 37°C. Following incubation, the tissue was gently homogenised in a loose fitting siliconised/PTFE homogeniser. The resulting cell suspension was then sequentially filtered through 100 and 40μm sterile filters (Falcon, UK) to further dissagregate the cells and remove cell clumps. Cells are counted and their viability was assessed by the means of trypan blue exclusion. The endothelial cell proportion of the whole cell suspension are calculated assuming that they comprise 3-5% of the total cells isolated. To select the endothelial cells from this heterogeneous population, immuno-magnetic sorting is utilised. This procedure involves the labelling of the endothelial cells with an antibody directed to a surface antigen expressed only on endothelial cells. This antibody then acts as an antigen to a second layer of antibody to which is conjugated a magnetic bead. On binding of the second layer, the cells can be separated by subjecting them to a magnetic field; the labelled cells being dragged out of the suspension towards the magnet.

The following procedures were all carried out at 4°C. Cells were pelleted by centrifugation at 400g for 5min before being resuspended in 1ml PBS/bovine serum albumin (PBS/BSA - 1%). To this was added 10μl of anti-CD31 antibody per 10^6 endothelial cells ($1mgml^{-1}$ mouse IgG1, R and D systems, UK) for ten minutes on

ice. Following incubation, the cells were shaken to resuspend them and a further 10 minute incubation was performed before the cells were washed in PBS/BSA. The second layer sheep anti-mouse IgG1 antibody coated paramagnetic Dynabeads® (Dynal, Sweden) were added to the cell suspension on ice for 15 min at a ratio of 3:1 (beads:cells). Following this incubation, the cells were subjected to a magnetic field which selected out the CD-31 expressing cells. The endothelial cells remained attached to the side of the collection vessel whilst the endothelial depleted cell suspension was removed for a further round of bead labelling. The isolated cells were then washed and subjected to the magnetic field for a second time before being plated onto fibronectin coated (5μgcm^{-2} SIGMA, UK) 6 well plates in SMEC media (SM) (see appendix III).

Cells were grown to confluence before passaging at a 1 in 3 ratio onto fibronectin coated tissue culture plastic. Cells were used up until their 5th passage. Endothelial origin was defined by the positive labelling by anti-vWF antibody. This technique has the capacity to produce a greater than 90% purity of endothelial cells.

4.2.2.1.3 Synovial fibroblast (SF) isolation

Synovial fibroblasts were isolated in a modification of the SMEC isolation procedure. The cells were isolated as the negative (unsorted) population from the CD-31 expressing cells in that they were not attached to magnetic carrier beads and were therefore left behind in the media once the SMEC had been removed. These cells were grown to confluence on T-75cm^{-2} flasks in SF media (see appendix III). The fibroblast nature of these cells was assessed by their spindle shaped morphology and cultures were passaged at a 1 in 5 ratio at confluence.

The purity of such cultures was generally high due to the rapid growth of fibroblasts over any contaminating cells in this media preparation.

4.2.2.2 Culture of cell lines

4.2.2.2.1 Culture of EA hy 926

EA hy 926 cell line was an epithelial / HUVEC fusion. Cells were maintained frozen under liquid nitrogen at –196°C in 50% FCS and 10% DMSO diluted in M199 media. Before use, cells were rapidly defrosted under warm running water and resuspended in HM to dilute the DMSO by mixing 2ml cell suspension into 13ml HM. These cells were pelleted by centrifugation and resuspended in HM and seeded onto T-75 cm^{-2} tissue culture flasks. Cells were grown to confluence as described for HUVEC and passaged at a 1:5 ratio.

4.2.2.2.2 Culture of HTB4 human mammary epithelial cell line

These cells were cultured as described for EA hy 926 cell (4.2.2.2.1) and grown to confluence in fibroblast media.

4.2.3 Cell characterisation

4.2.3.1 Endothelial cell immunoreactivity to vWF

Localisation of vWF was one of the first specific criteria to characterise the lineage of endothelial cells (Jaffe *et al* 1973). More recently however, Chung-Welch *et al* (1989) have shown vWF in mesothelial cell but not in certain microvascular endothelial cells in vitro (Shaw *et al* 1984).

The expression of vWF in HUVEC, SMEC, and EA hy 926 was conducted on the cells in culture following the protocol below. This forms part of a standard staining procedure for cultured and fixed cells.

Confluent passage 1 cells were seeded either onto Thermanox® cover slips in 24 well or 4 well plates or onto 4 or 8 well glass chamber slides (Falcon, UK). Cells were allowed to adhere for up to four hours before the wells were flooded with the appropriate media. Following overnight culture the cells were washed three times in PBS before fixation in ice cold acetone:methanol (1:1 ratio) for 3 minutes. The cells were then washed a further 3 times in ice cold PBS/0.5% tween 20 (PT).

Cells were then blocked with the addition of 5% Marvel PT (MPT) for one hour at room temperature. Primary antibody dilutions were carried out in MPT and added to the cells for 1 – 2 hours incubation at room temperature. For vWF staining either a range of dilutions from 1/500 –1/2000 of rabbit anti-human vWF (SIGMA, UK) in MPT or MPT alone.

The cells were washed 3 times in PT and then the secondary antibody added. 1 drop in 5 ml MPT of goat anti-rabbit HRP conjugated antibody (Vector Labs, UK). Cells were washed 3 times in PT prior to the addition of Vectastain ABC-Alkaline phosphatase which was made up in PT 30 min before addition and added for a further 30 minutes incubation at room temperature. The chromagen used was Fast-Red TR/naphthol AS-MX insoluble Alkaline phosphatase substrate with 1mM Levamisole (SIGMA, UK). This solution, in Tris buffer, was added on to the cells and the reaction was followed by observing colour development using light microscopy. The reaction was quenched by washing the cells in Ultra Pure H_2O.

Counter staining was performed using Mayers haematoxylin. Cells were immersed in haematoxylin solution (SIGMA, UK) for 30 seconds before being washed in running tap water. Cells were mounted in Aquamount® (BDH, UK) and visualised under light microscopy.

4.3 Results

4.3.1 Expression of XO (INTRACELLULAR) in EC

4.3.1.1 In endothelial cells

HUVEC were grown in glass chamber slides and fixed in ice cold methanol/acetone 1:1 for 3 minutes followed by washes 3x in ice cold PBS. The cells were stained for xanthine oxidase using a range of primary antibody concentrations (rabbit anti-bovine xanthine oxidase, Chemicon, USA) in MPT over night at 4°C. The cells were washed 6x 5 minutes in PT followed by incubation with a goat anti-rabbit horse radish peroxidase labelled secondary antibody for 2 hours in PT. Cells were washed 6x 5 minutes in PT before the addition of avidin biotin complex alkaline phosphatase (ABC-AP, Vectastain, Vector Laboratories, UK) for 30 minutes. Cells were washed 6x 5 minutes in PT before the chromagen Fast Red TR/Naphthol AS-MX (SIGMA, UK) was added in tris buffer. The reaction was stopped by the addition of copious amounts of Ultra pure water. Slides were counterstained in Meyers haematoxylin for 5 minutes followed by washing in running tap water before mounting in aquamount. Figure 4.3 shows HUVEC stained for both xanthine oxidase and for vWF for comparison.

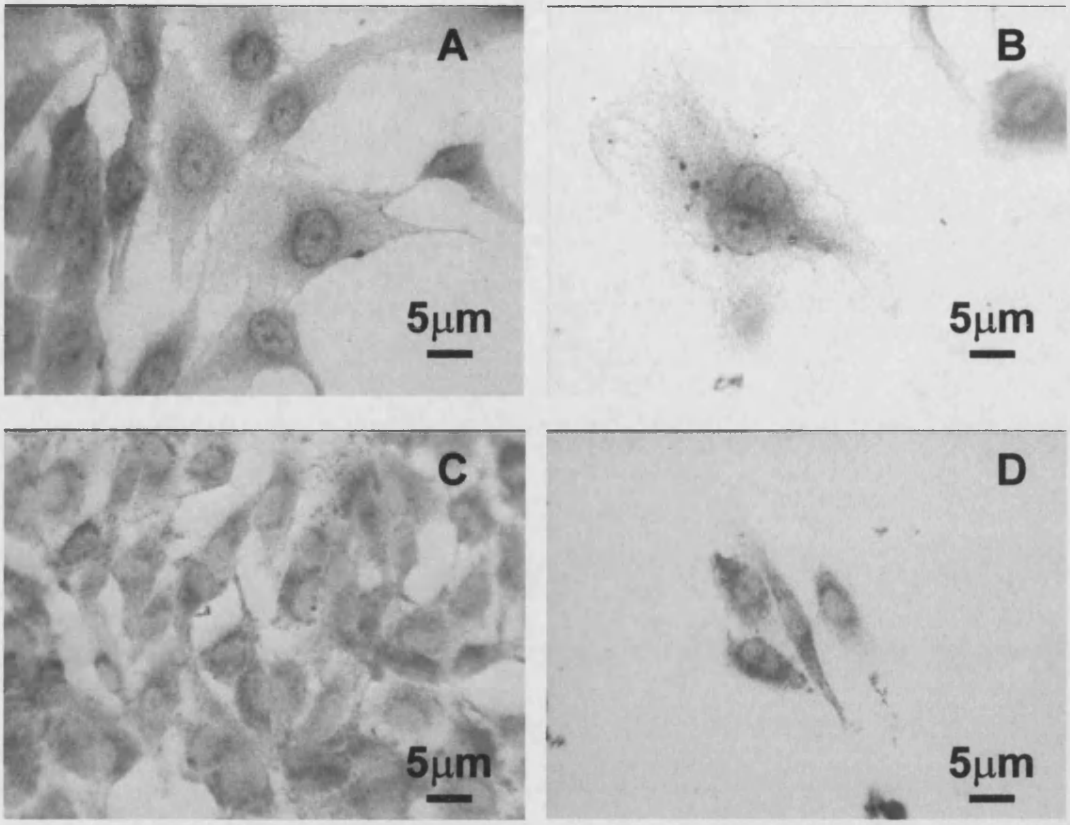

Figure 4.3. The staining of HUVEC for XO (A and B) and vWF (C and D).

HUVEC stained for XO showed both perinuclear and diffuse granular staining when grown to subconfluence as shown. In comparisson, vWF stained HUVEC showed strong granular staining indicative of Weibel-Palade bodies localisation of vWF protein.

4.3.1.2 Effect of hypoxia on cellular enzyme activity

Endothelial cells were cultured to confluence in T-75cm^{-2} tissue culture flasks (Falcon, UK). Cells were then incubated in reduced serum SMEC media (1% FCS, rSMEC) for 24 hours before being washed and the media changed for SMEC media. The cells were then subjected to 24 hours of 5% CO_2 balanced air or 5% CO_2 balanced nitrogen at 37°C in a humidified atmosphere. The cells were then harvested by scraping and washed in PBS containing anti proteinases

(homogenisation wash, HW) and resuspended in homogenisation buffer (HB) (see appendix III). The cell pellets were then homogenised and drawn 3x through a fine gauge needle (18G) using a 1ml syringe. The resulting suspensions were pelleted by centrifugation and stored at -70°C. Enzyme assays were carried out in air saturated PBS in the presence of 20μM pterin and the fluorescence measured over time with excitation at 345nm and the emission wavelength of 390nm. The rate of product formation was measured as the slope of the graphs and calibrated with a known amount of isoxanthopterin fluorescence. Figure 4.4 shows the effect of 24 hour hypoxia on pterin mediated activity from cultured endothelial cells.

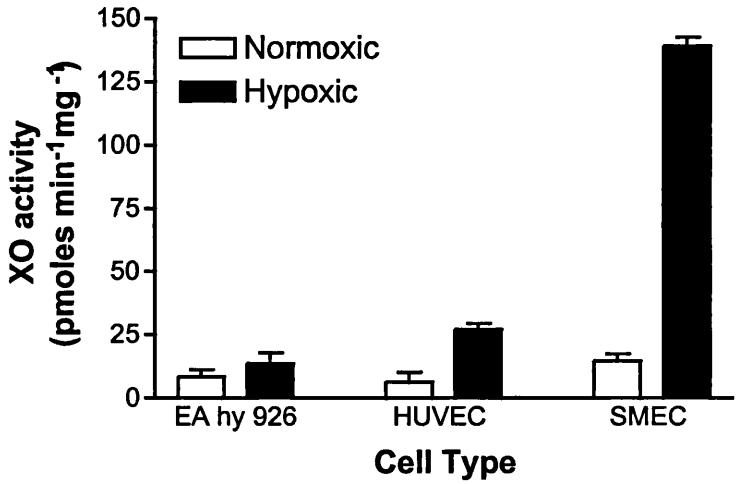

Figure 4.4. The pterin activity of cultured endothelial cells exposed to normoxic or hypoxic environments for 24 hours. Data are mean ± SEM of 3 experiments in duplicate.

Pterin mediated activity is observed in all three cell types following both normoxic and hypoxic incubations. The effect of hypoxia on HUVEC and SMEC was to increase the pterin mediated activity significantly above that of the normoxic exposed cells, HUVEC $p<0.05$ and SMEC $p<0.01$. There was no significant difference between cell types exposed to normoxic conditions and there was no

significant increase in activity of EA hy 926 cells following 24 hour hypoxia. HUVEC showed a small but significant $p<0.05$ increase in activity following hypoxia treatment compared to EA hy 926 cells. SMEC showed strong significant increase in activity over both EA hy 926, $p<0.01$ and HUVEC, $p<0.01$ following 24 hour hypoxia by students t-test.

The samples were also tested for their ability to cause NADH mediated lucigenin enhanced chemiluminescence. Cell homogenates were incubated with NADH (500μM) in the presence of lucigenin (500μm) in a chemiluminometer and the reaction followed over time as previously described for purified xanthine oxidase enzyme. The peak height of reaction was measured and corrected for total protein content and is shown in figure 4.5 as the peak height ALU min^{-1} mg^{-1} for each cell type following 24 hour normoxic or hypoxic exposure.

All cell types showed a significant chemiluminescence signal above a PBS control. There was no significant difference between EA hy 926 and HUVEC in normoxic exposed cells. SMEC showed a significantly greater chemiluminescence, $p<0.01$ compared to both EA hy 926 and HUVEC following 24 hour normoxic exposure. All cell types showed a significant increase $p<0.05$ in NADH mediated LEC following hypoxic exposure compared to normoxic exposed cells.

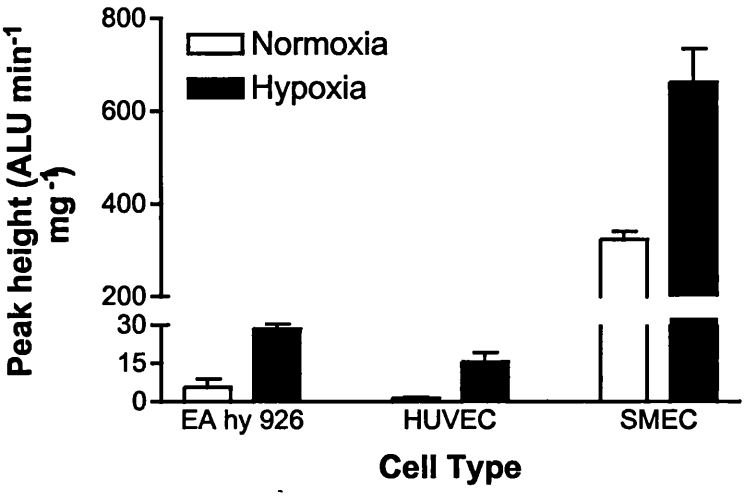

Figure 4.5. The effect of hypoxia on the NADH mediated LEC from endothelial cells. Data are mean ± SEM of 3 experiments in triplicate.

4.3.2 Expression and binding (SURFACE) of endogenous and exogenous XO

4.3.2.1 FACs of surface XO expression

4.3.2.1.1 Determination of antibody concentration

To determine the appropriate antibody dilutions for use in the following experiments, a pilot study was run where HUVEC were stained for XO using a primary antibody raised in rabbits to bovine butter milk XO (Chemicon, USA). This was then labelled with a FITC conjugated goat anti-rabbit IgG (whole molecule) secondary antibody (SIGMA, UK). The protocol was as follows:

HUVEC were isolated as described previously (4.2.2.1.1) and grown to confluence on T25cm^{-2} tissue culture flasks. Cells were harvested by the addition of cell dissociation solution (CDS), typically 2ml in T25cm^{-2} and tapping the side of the flask to dislodge cells. The cell suspension was then added to 13ml HM and centrifuged at 400g for 5min at room temperature to pellet the cells. The CDS/HM supernatant was then removed by aspiration and the cells were resuspended before the addition of 1ml PBS. Cell concentration and viability was then assessed using trypan blue exclusion with a haemocytometer (see appendix III).

Cells were then diluted to 5x10^5 cell ml^{-1} in PBS. The cells were then divided into two sets labelled Chemicon and FITC. To the Chemicon set of cells a dilution of Chemicon antibody (stock at 10mgml^{-1}) was added prior to 10µl of FITC conjugated goat anti-rabbit antibody (SIGMA, UK). To the FITC set of cells 10µl of Chemicon antibody was added as the primary followed by a dilution of the FITC conjugated goat anti-rabbit antibody. Each antibody labelling step was carried out over 20

minutes at room temperature. Between each addition of antibody the cells were washed 2x in PBS by centrifugation and resuspended in PBS. During the addition of the FITC antibody all procedures were carried out under low light and the tubes were wrapped in foil.

As part of the routine flow cytometer set up, a set of control cells was also used. This comprised of completely unstained cells, cells stained with primary antibody alone and cells stained with secondary antibody alone. Using the variable voltage applied to the PMT, the population of HUVEC flowing through the cytometer at ~200 events sec^{-1} was focussed to form a discreet area related to their side and forward light scattering parameters. Figure 4.6 shows a typical dot plot of SSC against FSC for a population of HUVEC.

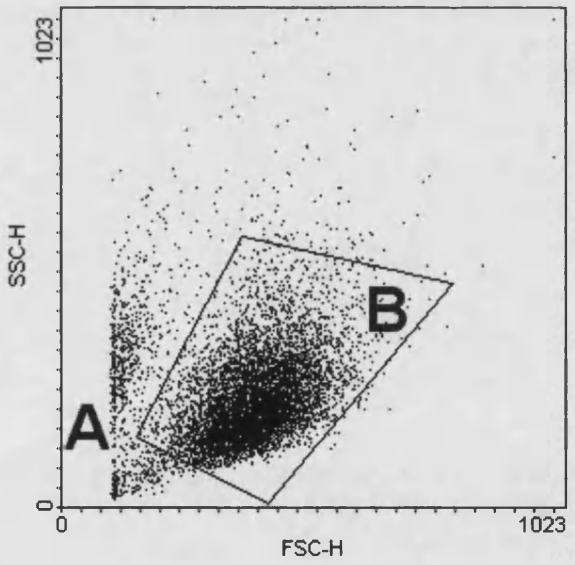

Figure 4.6. A typical dot plot of SSC-H versus FSC-H for a population of passage 3 HUVEC. The area marked as **A** is to show the effect of electronic throsholding on the signal. Area **B** is the population of interest. A total of 10,000 events were measured inside the quadrant area. However the total number of events actually measured may range from 10,000 to 20,000 depending on the

number of events outside of the selected area. This data was accumulated using a 100μm nozzle size with the neutral density filter in place.

The fluorescence parameters of the unstained control cells were measured to set the auto fluorescent background levels. Figure 4.7.shows a typical fluorescence histogram plot for unstained control HUVEC following optimisation.

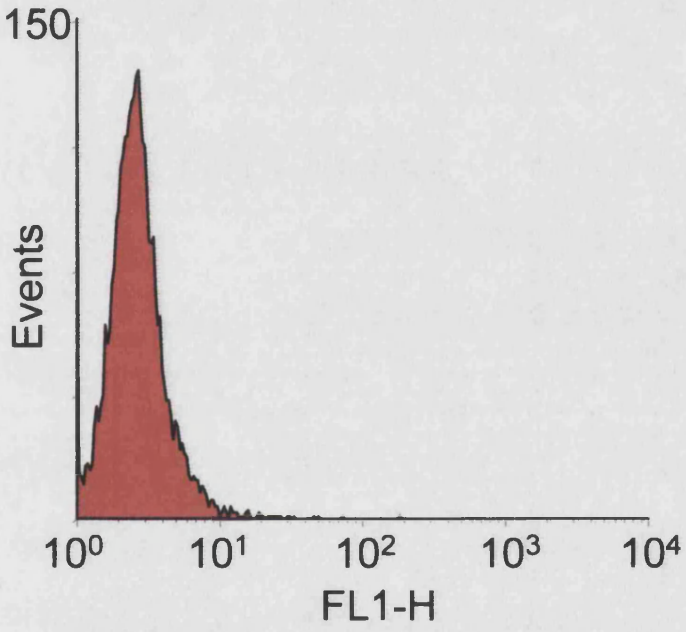

Figure 4.7. A typical histogram plot for unstained HUVEC measuring the fluorescence parameters for emission wavelengths of 510 – 520nm (FL1-H). Shown is the number of events (10,000 from the gated quadrant area shown in figure 4.6) against fluorescence on a logarithmic scale.

Once this process had been completed, the cytometer was not adjusted further throughout the experimental run.

On addition of cells stained with primary antibody alone, no change in fluorescence was observed. This was also the case on the addition of cells stained with

secondary FITC conjugated antibody alone. This is shown in figure 4.8 as overlying plots.

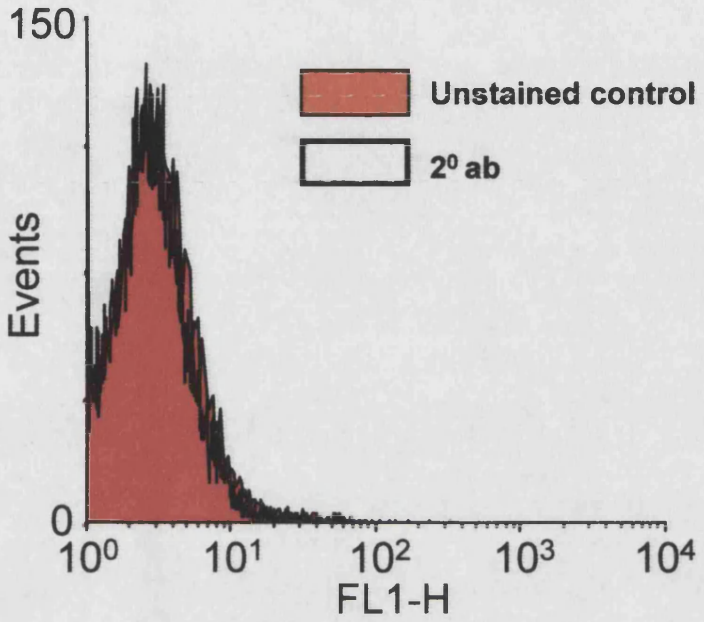

Figure 4.8. Overlaid plots of individual primary (red background) and secondary (heavy black outline) antibody stained HUVEC fluorescence.

This process was repeated for all the antibody concentrations and figure 4.9 shows the fluorescence of control cells overlaid by HUVEC stained with both primary and secondary antibodies using 5μl of each antibody respectively.

The mean channel height for each antibody concentration was measured for each 10,000 event data set and plotted against antibody concentration for each antibody as shown in figure 4.10. This shows a dilution effect in fluorescence that is dependent on the concentration of both antibodies and that the optimum antibody concentration for these unstimulated passage 3 HUVEC to show positive surface staining for XO is to use 5μl per 2.5×10^5 cells. These concentrations were used for all subsequent flow cytometry experiments and eukaryotic cell types.

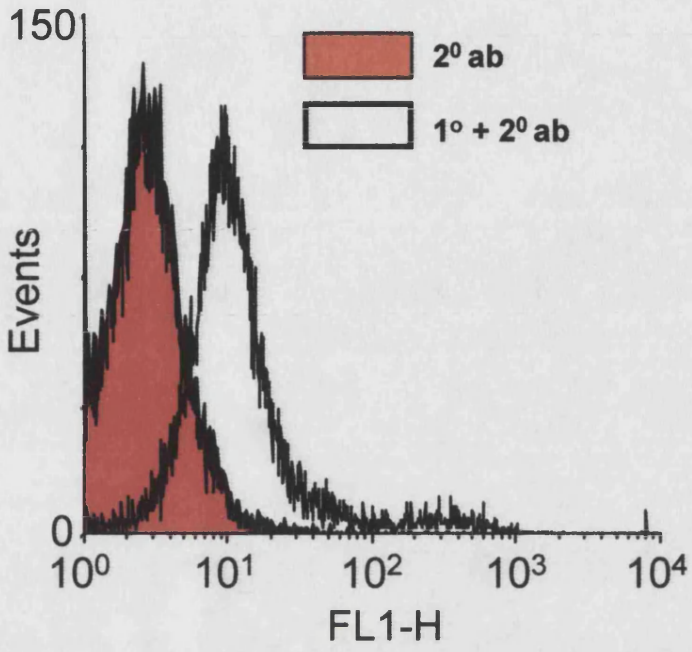

Figure 4.9. The fluorescence of passage 3 control HUVEC (secondary antibody stained – red background) overlaid by HUVEC stained with both primary and secondary antibodies (heavy outline).

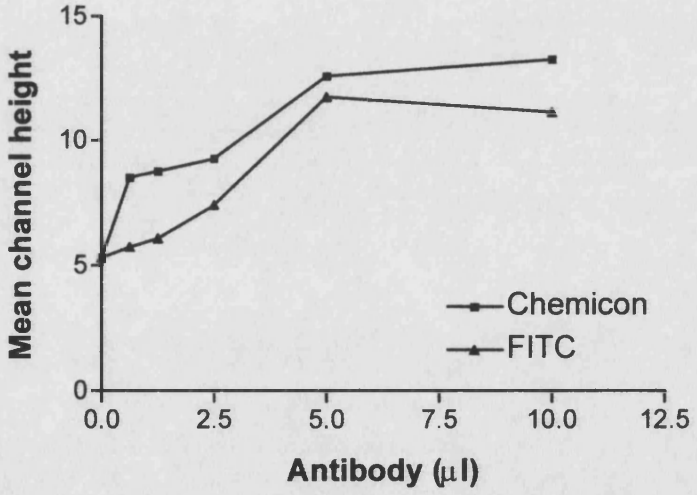

Figure 4.10. The mean channel height of fluorescence for unstimulated passage 3 HUVEC.

The above protocol was repeated for HTB4 cells and human synovial fibroblasts. Figure 4.11 shows the FITC fluorescence of HTB4 cells labelled with anti-XO

antibody and FITC labelled secondary antibody. There is a clear shift of the fluorescent population to the right suggesting increased fluorescence and positively stained cells.

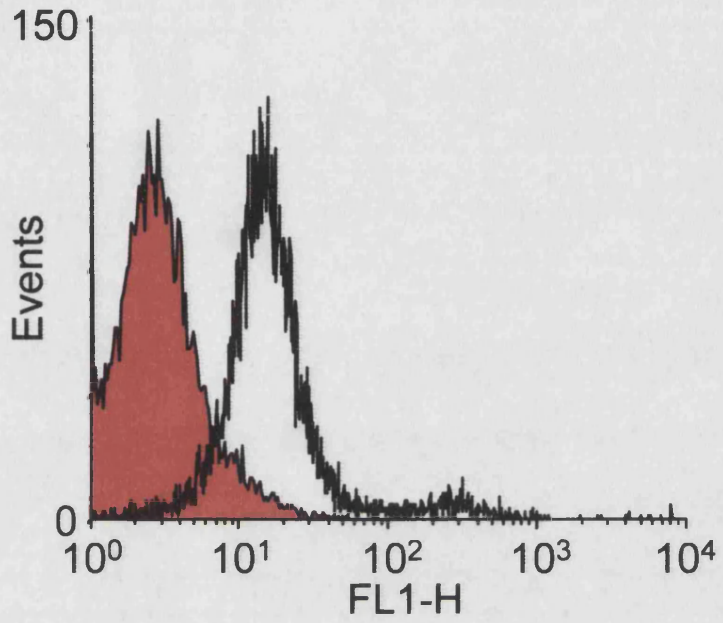

Figure 4.11. The surface expression of XO on HTB4 cells

Human synovial fibroblasts were cultured to confluency and live passage 2 cells were stained for XO. Figure 4.12 shows a fluorescence histogram of the controlled unstained cell population overlaid with cells stained with anti-XO and FITC labelled antibodies.

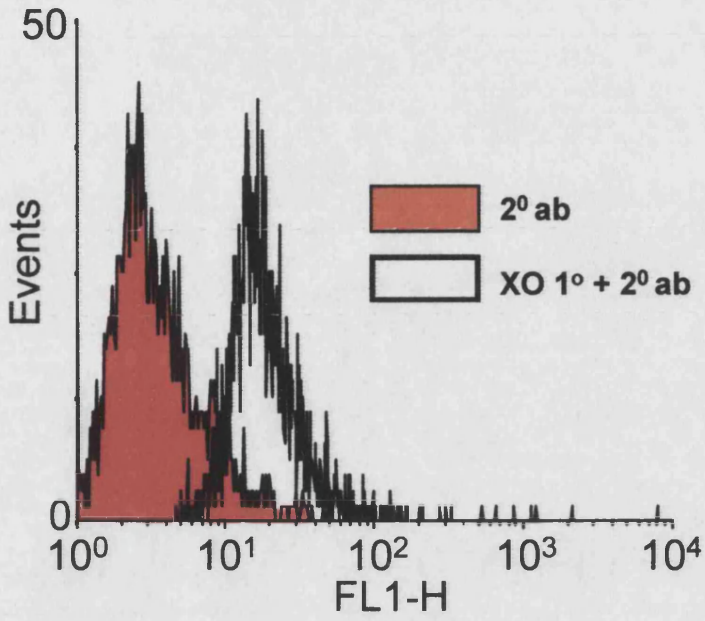

Figure 4.12. The surface antigenicity of passage 2 synovial fibroblasts stained for XO in the same manner as previously described.

There is shown a positive right shift in the fibroblast cell population stained with both antibodies compared to controls suggesting increased fluorescence and positively stained cells.

4.3.2.2 Flow cytometric determination of XO binding to live HUVEC

HUVEC were cultured to confluence and harvested as previously described (4.2.2.1). Cells were then exposed to a range of purified xanthine oxidase enzyme concentrations (1000μg – 10μg $2.5x10^5$ $cells^{-1}$) for 20 minutes at room temperature and washed 2x in PBS. The cells were then stained using anti-XO antibody and a FITC labelled antibody as previously described (4.3.2). The cells were then characterised by flow cytometry measuring their forward and side light scattering parameters and their FITC fluorescence.

Figure 4.13 shows the FITC fluorescence of cells following incubation with a range of XO enzyme concentrations and staining with anti-XO antibody. The control cells

were incubated with the highest concentration of XO enzyme without antibody labelling and were of similar fluorescence to the unstained controls. FITC labelled antibody control with cells incubated with enzyme also showed no increase in fluorescence above unstained controls.

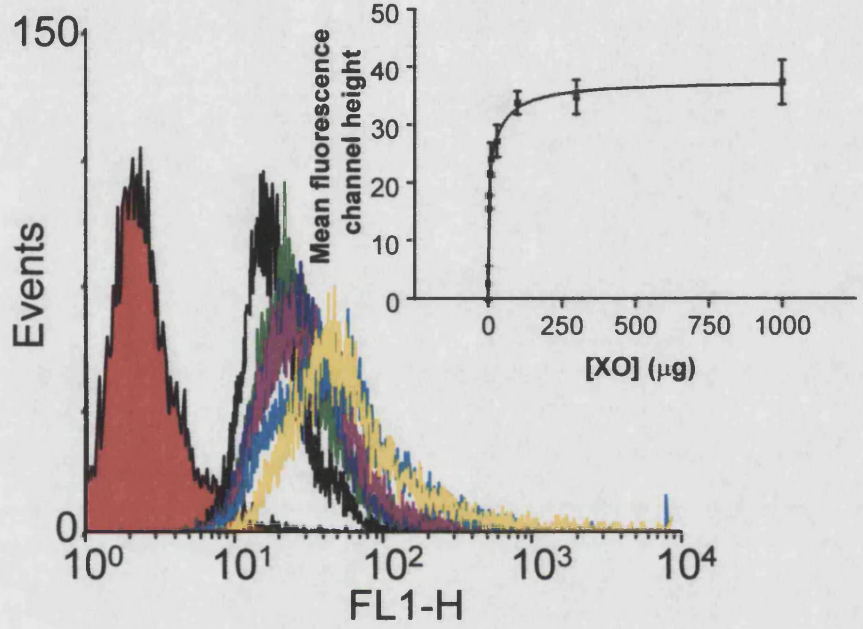

Figure 4.13. Flow cytometry data of surface XO binding. The insert shows the mean fluorescence channel height against enzyme concentration from mean ± SEM (n = 2) in duplicate of 10,000 events.

The fluorescence of each cell population was seen to increase relative to the concentration of XO enzyme with which it had been incubated in a dose dependent manner.

4.3.2.3 The effect of hypoxia on surface expression and binding of XO to HUVEC

HUVEC were exposed to 24 hour hypoxia to assess the effect on the surface expression of XO. Control cells were cultured under 5% CO_2 balanced air mixtures at 37°C in a humidified atmosphere. Cells were made hypoxic by culturing in a 5%

CO_2 balanced nitrogen atmosphere at 37°C in a humidified atmosphere. The surface antigenicity to an anti-XO antibody was measured as previously described using a flow cytometric assay.

Figure 4.14 and inset show the effect of hypoxia on the surface antigenicity to anti-XO antibody of HUVEC.

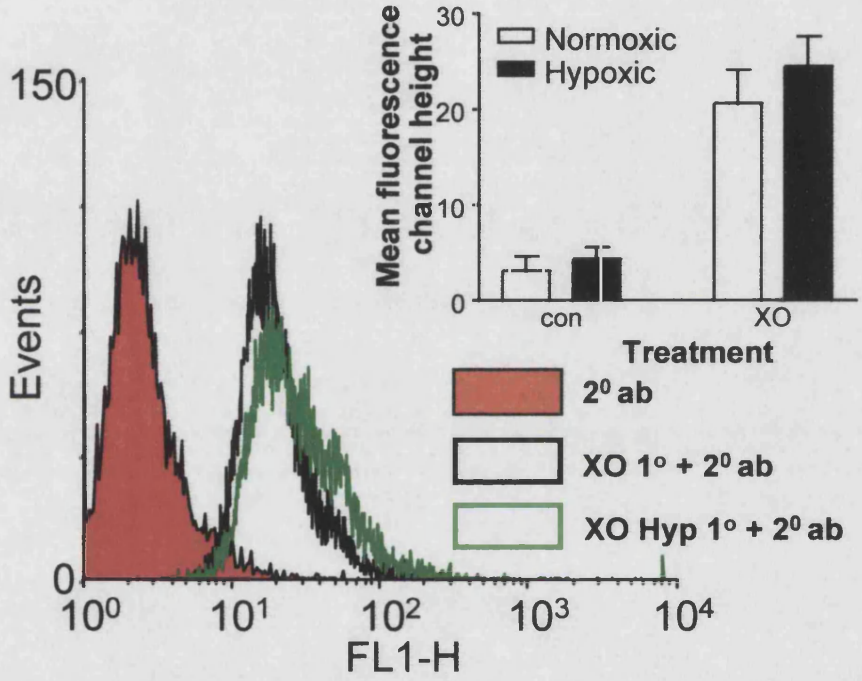

Figure 4.14. Effect of Hypoxia on surface expression of XO.

Both cell populations, hypoxic and control cells, showed positive fluorescence compared to unstained control HUVEC. Hypoxic exposed cells showed a small increase in fluorescence compared to cells exposed to air for 24 hours which was not significant (MFCH 20.6 ±3.56 in air and 24.5 ±3.11 under hypoxic conditions). The hypoxic cell population shows a shoulder on the normal distribution histogram plot compared to the normoxic control cells of higher fluorescence.

Cells that had been made hypoxic for 24 hours were harvested and incubated with a range of XO enzyme concentrations as previously described (4.3.2.2). The

fluorescence of cells stained for XO was measured by flow cytometry and compared to the fluorescence of cells incubated with XO in the same manner having been cultured under 5% CO_2 balanced air conditions.

Figure 4.15 shows the effect of XO enzyme incubation to cells following 24 hour culture in 5% CO_2 balanced air (normoxic) or 5% CO_2 balanced nitrogen (hypoxic).

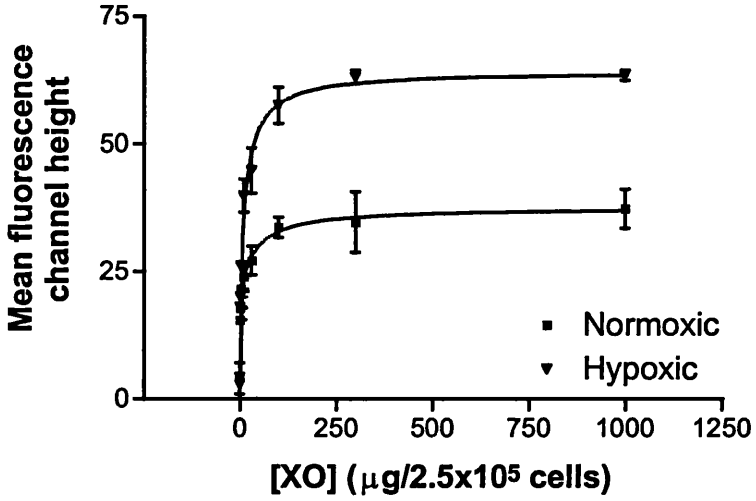

Figure 4.15. Effect of Hypoxia on surface XO binding. Figure shows the mean fluorescence channel height from 2 experiments in duplicate ± SEM using the normal distribution of 10,000 events for each treatment.

Cells from both treatment protocols bind XO in a dose dependent manner and show saturation of XO binding per cell at ~ 100 – 300μgml^{-1}. The cells exposed to low oxygen concentration however show a significant increase in fluorescence $p<0.05$ by students t-test compared to enzyme concentration matched controls.

4.3.2.4 The effect of heparinase I treatment on surface expression and binding of XO in HUVEC

HUVEC were harvested as previously described and exposed to one hour of Heparinase I (EC 4.2.2.7) enzyme treatment (SIGMA, UK) (1U ml^{-1}) or incubation in PBS for 1 hour (control cells). The antigenicity to anti XO antibody was then

assessed in both cell populations using flow cytometry. Figure 4.16 and inset show the effect of Heparinase I treatment on the fluorescence of HUVEC stained for XO.

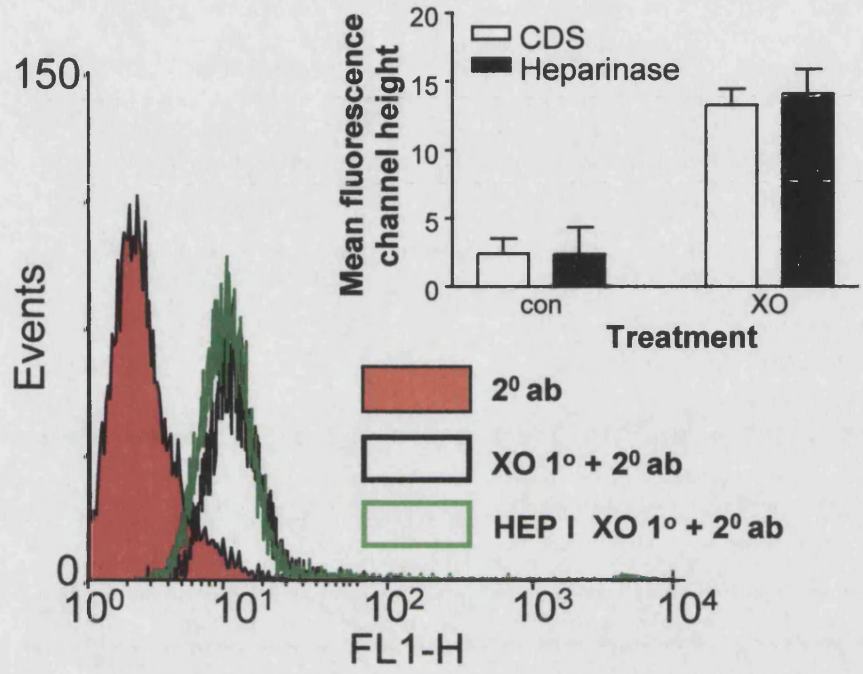

Figure 4.16. Effect of Heparinase I treatment on surface XO expression.

Both cell populations show positive fluorescence for XO labelling compared to the unlabelled control cells. The Heparinase I treatment has no significant effect on the fluorescence of HUVEC stained for XO compared to the untreated cell population.

The effect of Heparinase I treatment on the binding of purified XO to HUVEC was assessed by flow cytometry. Cells were exposed to Heparinase I for 1 hour followed by washing in PBS and incubation with a range of XO concentrations for 20 minutes. The cells were then washed and stained for XO using an anti XO and FITC labelled antibodies as previously described.

Figure 4.17 shows the effect of Heparinase I treatment on the fluorescence of HUVEC following incubation with purified XO enzyme.

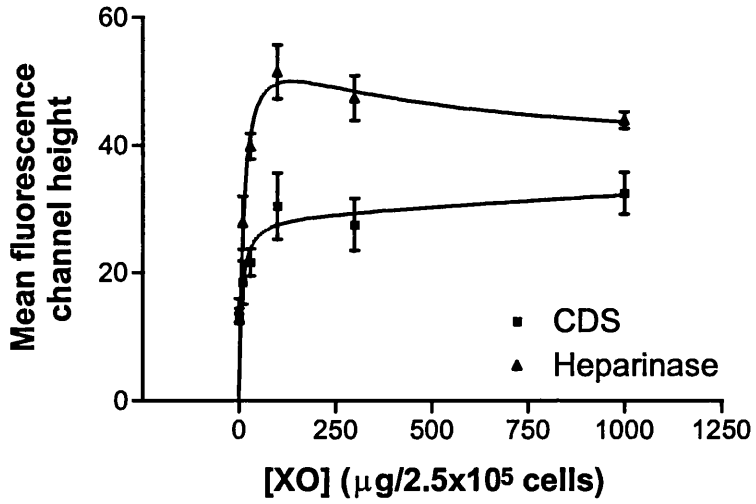

Figure 4.17. Effect of Heparinase I treatment on surface XO binding. Figure shows the mean fluorescence channel height from 2 experiments in duplicate ± SEM from the normal distribution of 10,000 events for each treatment and experiment.

Both treated and control cells show a dose dependent increase in fluorescence relative to the concentration of added enzyme. Both treatments show saturation of the fluorescence at ~ 100μg of added enzyme. The Heparinase I treated cells show significantly increased fluorescence $p<0.05$ by students t-test compared to the equivalent added XO enzyme concentration in non treated cells.

4.3.2.5 The effect of Trypsin on the surface expression and binding of XO to HUVEC

As Trypsin has been shown to cause proteolysis of XO its use as a dissociation solution compared to a non enzymatic cell dissociation solution (CDS) was assessed in terms of the surface expression and binding of XO to HUVEC.

Passage 2 HUVEC were harvested in 2ml Trypsin EDTA (GIBCO, UK)) solution or with 2ml CDS (SIGMA, UK) and washed in PBS. Cells were then either incubated with purified XO enzyme (100μg) and stained for XO or stained for XO as

previously described. Figure 4.18 shows the effect on fluorescence of trypsin treatment of HUVEC in their XO antigenicity with and without added purified XO.

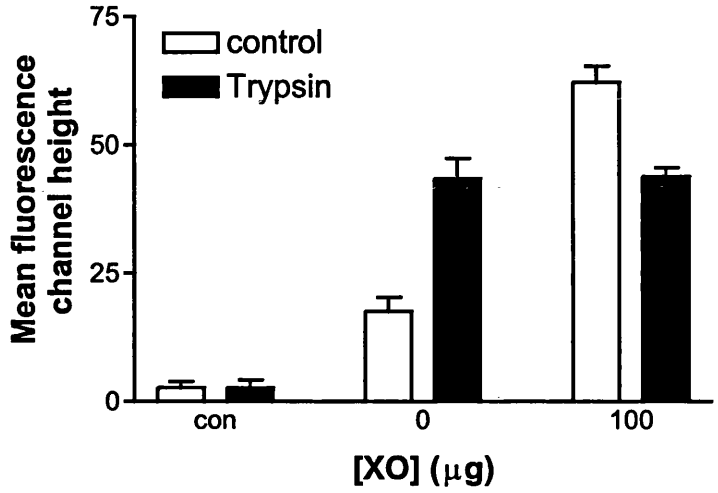

Figure 4.18. Effect of trypsin on surface XO binding. Results are mean ± SD of one experiment in duplicate from 10,000 events

Trypsin is shown to cause an increase in the fluorescence of HUVEC in the absence of added purified XO enzyme compared to CDS treated cells. On the addition of purified XO enzyme the fluorescence of CDS removed cells is increased as was shown previously. The Trypsin treated cells however show no increase in fluorescence over cells without the addition of XO enzyme and the fluorescence signal is reduced compared to the CDS treated XO incubated cells.

4.3.2.6 The surface expression of Heparan sulphate proteoglycan

The surface expression of Heparan sulphate proteoglycan (HSP) was assessed using a monoclonal antibody raised to bovine HSP (mouse anti bovine Heparan sulphate proteoglycan, subclass IgG_1, Chemicon, USA) and a FITC labelled secondary antibody. These cells were then subjected to flow cytometric analysis and the levels of fluorescence compared for labelled and unlabelled cells. As the monoclonal antibody was raised in mouse an isotype control raised in mouse

against keyhole limpet haemocyanin can be used to assess the non-specific binding of the primary antibody.

Figure 4.19 shows the fluorescence of passage 2 HUVEC stained with anti HSP antibody compared to an isotype stained control population.

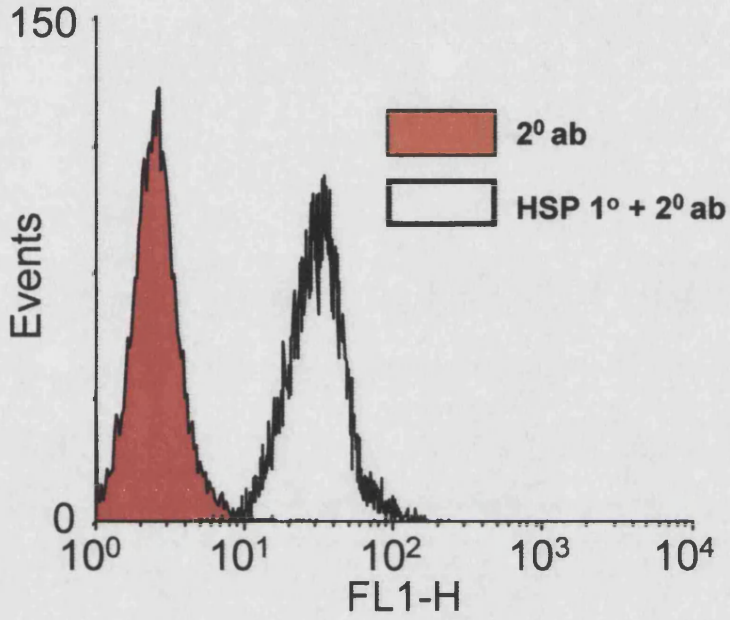

Figure 4.19. FACs of surface Heparan-sulphate GAG expression. Representative of 10,000 events.

The HSP labelled cells show significant ($p<0.01$ by student t-test) positive fluorescence (MFCH 41.3 ±3.44) compared to the isotype control cell population (MFCH 3.6 ±1.12) suggesting the surface expression of HSP in naive passage 2 HUVEC from two experiments in duplicate.

4.3.2.7 The effect of hypoxia on surface expression of Heparan sulphate proteoglycan by HUVEC

Passage 2 HUVEC were subjected to 24 hour hypoxia as previously described (4.3.2.3) and compared in their HSP expression to cells cultured under normoxic conditions.

Figure 4.20 shows the fluorescence histogram of cells stained for HSP following 24 hours normoxic or hypoxic exposure.

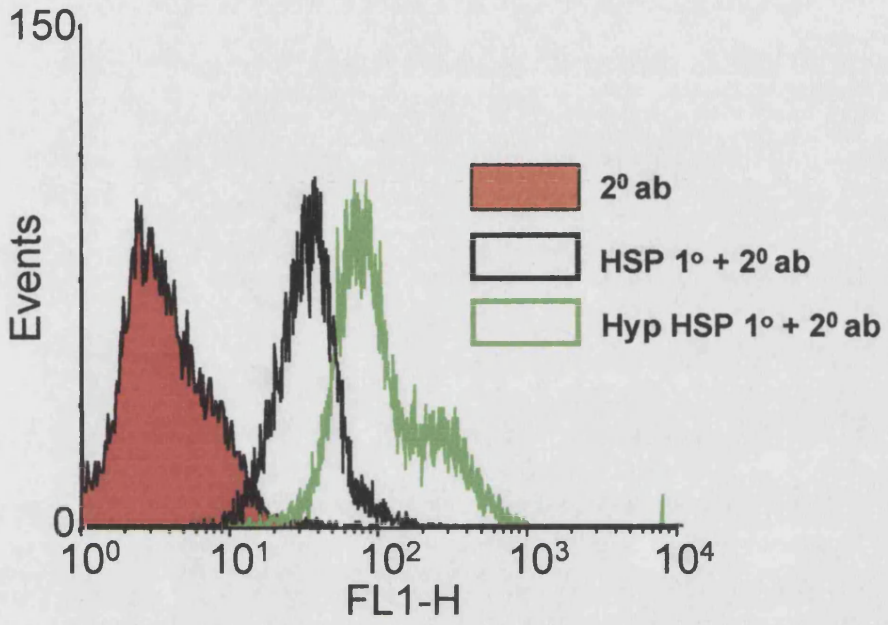

Figure 4.20. Effect of Hypoxia on surface Heparan sulphate GAG expression. Representative histogram of 10,000 events for each treatment. Hyp = hypoxic cells.

HUVEC stained for the expression of HSP under normoxic and hypoxic conditions show positive fluorescence compared to the isotype control. The cells incubated under low oxygen conditions show increased fluorescence compared to the normoxic controls (MFCH 63.2 ±4.12 versus MFCH 41.3 ±3.44 from two experiments in duplicate). The shape of the curve from hypoxia treated cells shows a shoulder not seen in the normoxic controls. This may be due to a sub-population of cells that express greater HSP in response to hypoxia compared to the population as a whole.

4.3.2.8 The effect of Heparinase I treatment on HUVEC Heparan sulphate proteoglycan expression

HUVEC were removed by CDS treatment from tissue culture plates and washed in PBS. Cells were then incubated in Heparinase I (1U ml^{-1}) for 1 hour before washing and staining for HSP and subjected to flow cytometric analysis. Figure 4.21 shows the effect of Heparinase I treatment on the fluorescence of HUVEC stained for HSP.

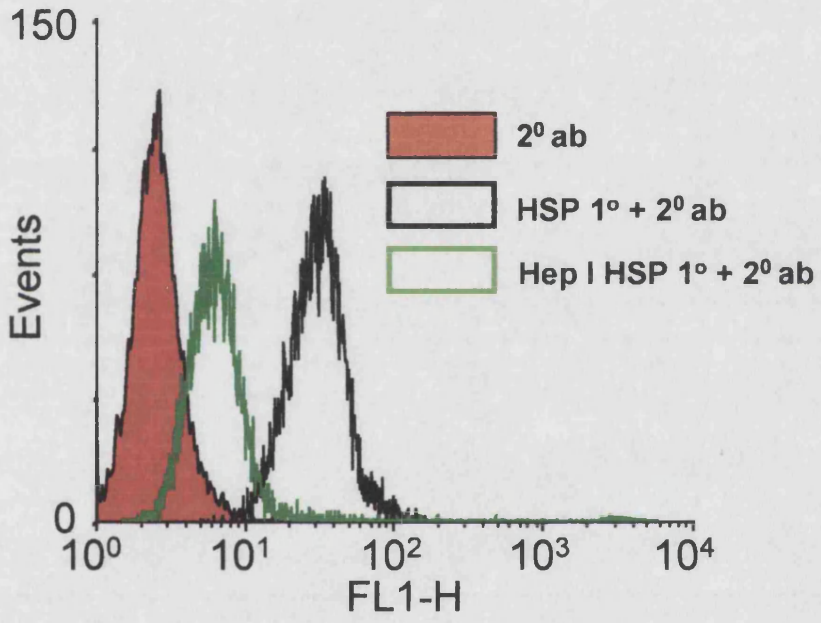

Figure 4.21. The effect of 1 hour Heparinase I treatment on HSP expression by HUVEC. Representative histogram of 10,000 events for each treatment.

HSP stained Control cells were shown to have positive fluorescence compared to the isotype control stained cells. The cells treated with Heparinase I show reduced fluorescence compared to naïve cells stained for HSP but still show greater fluorescence when compared to the isotype control stained cells (MFCH 17.5 ± 2.2 following heparinase treatment compared to non heparinase treated cells MFCH 41.3 ±3.44 and Isotype controls MFCH 5.9 ±4.01).

4.3.3 Xanthine oxidase binding to bacterial cell surface

4.3.3.1 Analysis by enzyme assay

To determine the possibility that XO can bind to the surface of bacteria allowing closer proximity of radical generating systems, bacteria were incubated in the presence of purified enzyme. Following incubation the bacteria were centrifuged at high speed to form pellets and the supernatant removed for analysis of enzyme activity in both the pellet and supernatant.

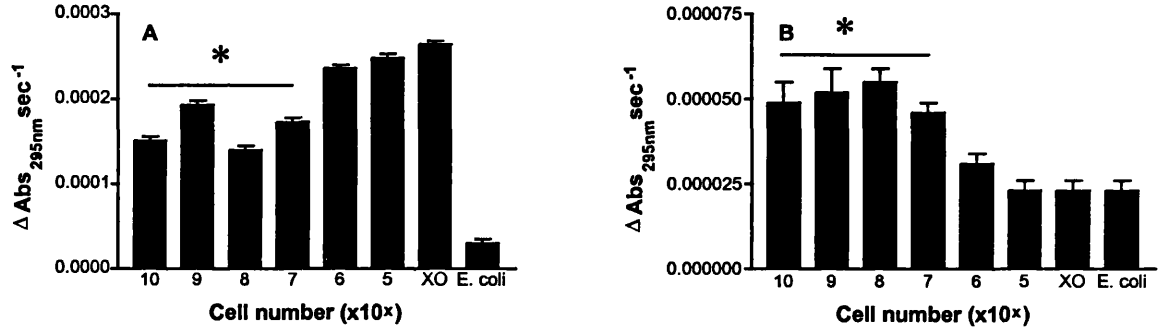

Figure 4.22. The xanthine to urate activity of *E. coli* after incubation with purified XO enzyme at a range of cell densities. *E. coli* were incubated with XO before washing and measurement of the activity contained in the supernatant **A** and pelleted **B** fractions. Mean ± SEM (n = 2) in duplicate. * line indicates significant difference from XO control $p<0.05$ by student t-test.

The amount of activity contained within the supernatant is inversely proportional to the cell concentration previously incubated: activity decreases as cell number increases. The amount of activity found associated with pelleted cells is proportional to the cell number: enzyme activity increases with increasing cell number.

The supernatant was also probed for appearance of XO by staining for protein following 1 dimensional electrophoresis. Figure 4.23 shows the relative proportions

of protein from 10μl of supernatant from each treatment. Here the optical density is inversely proportional to the cell number which mirrors the effect by measuring activity in the supernatant.

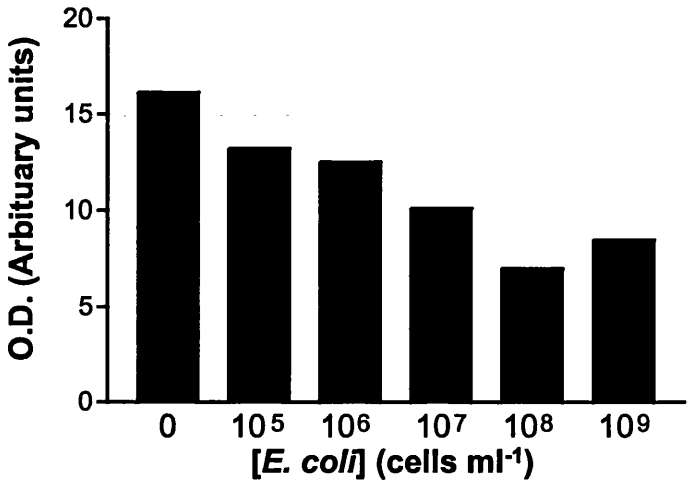

Figure 4.23. The relative amount of protein found in the supernatant after incubation with various concentrations of *E. coli*. The supernatants were electrophoresed on an 8% gel which was then stained with Coomassie brilliant blue stain and fixed in acaetic acid/methanol before being scanned and the relative optical density of the characteristic 150KDa band was measured for each cell concentration.

4.3.3.2 Flow cytometric analysis

The ability of XO to bind to bacterial cell surfaces was assessed using flow cytometric analysis in an adaptation of techniques developed for endothelial cells. The size of the bacteria make their analysis by flow cytometry more difficult to interpret because of the greater signal to noise ratio. To combat this a modification of a technique determined for the study of human platelets was used. This entails the use of logarithmic scales for both SSC and FSC and a removal of the neutral density filter which increases the sensitivity of the instrument to particles of ~ 1μm

and greater. This causes an increase in the signal to noise ratio of the particulate material in the buffer used. To combat this the threshold voltage is increased whilst running only buffer through the instrument until counts per second are below ~ 10 events. The bacteria are then run through the instrument and the SSC and FSC parameters are determined for the particular population of interest. Figure 4.24 shows a typical SSC against FSC dot plot for *E. coli* in solution.

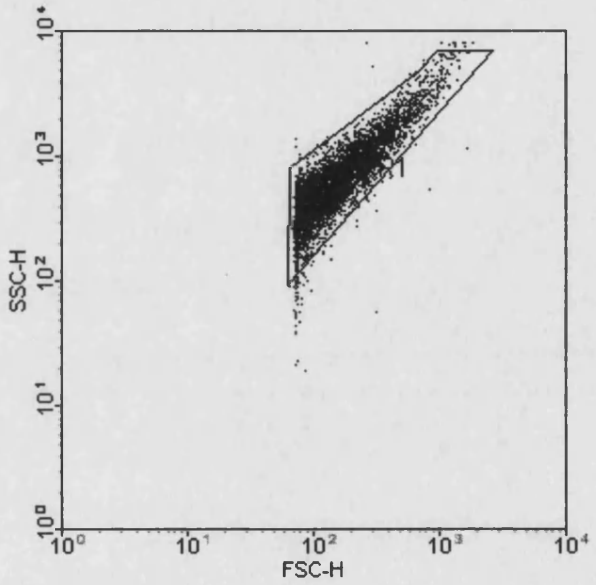

Figure 4.24. The SSC and FSC parameters of unstained *E. coli* in a suspension of PBS. The population was detected using 172mW argon ion laser (Enterprise, Coherent, USA) exciting at 488nm with the threshold set at ~ channel 400 of 1024 (~ 10^3 on the FSC-H scale). Only events lying within the marker region were counted.

The fluorescence characteristics of these bacteria was measured simultaneously. The fluorescence data for the region shown in figure 4.24 is shown in figure 4.25 **A**. The fluorescence signal from unstained bacteria was set as the background auto fluorescence by adjusting the voltage of the fluorescence PMT and the settings were not changed throughout the rest of the experiments. Figure 4.25 **A** shows the

fluorescence signal from unstained control and cells stained with primary antibody and there is no shift in the fluorescence of the population. On the addition of FITC labelled secondary antibody to cells the fluorescence of this population is increased above the background control 4.25 **B**.

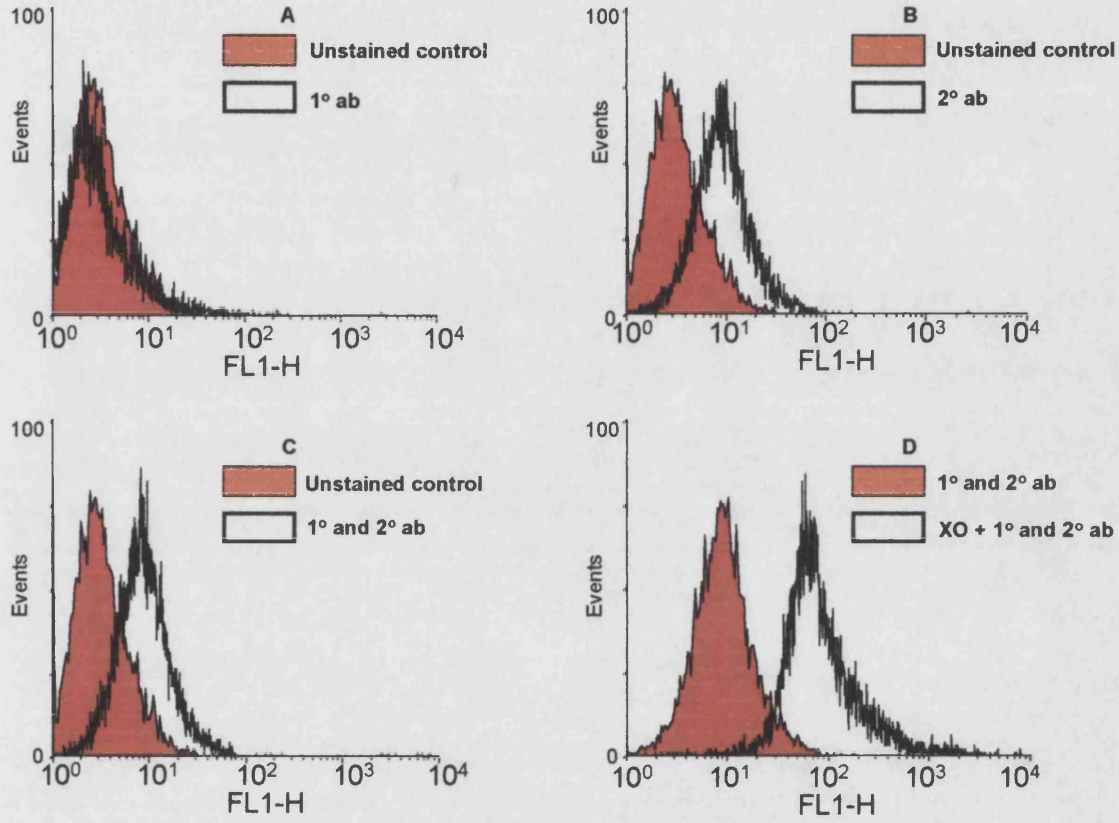

Figure 4.25. The fluorescence associated with *E. coli* stained with various antibodies and with XO added. *E. coli* from an overnight culture were washed in PBS and resuspended in either PBS or PBS and XO protein for 20 minutes at RT. The cells were further washed in PBS and incubated with or without primary antibody for 20 minutes at RT. Further washings were followed by incubations with or without FITC secondary antibody for 20 minutes at RT. The cells were washed finally in PBS and then subjected to flow cytometric analysis.

To assess the binding of primary antibody to the bacteria both primary and secondary antibodies were incubated with the bacteria 4.25 **C**. The fluorescence is enhanced in this population over the control cells but not above the fluorescence signal from secondary antibody labelled cells. Figure 4.25 **D** shows the effect of adding 100μg of purified XO against the primary and secondary antibody fluorescence alone. This population is further enhanced over the unstained control and also the antibody control suggesting that XO protein is associated with the bacteria in a manner that allows labelling with primary and secondary antibodies. The cells incubated with enzyme alone showed no enhanced fluorescence above the control cells 4.25 **A**.

4.3.4 Measurement of plasma activity.

In the circulation of patients with rheumatoid arthritis there is a DPI inhibitable plasma activity that can oxidise NADH and can generate superoxide radical (Benboubetra *et al* 1997 and Zhang *et al* 1998). The activity in apparently healthy individuals was assessed using a variety of assay techniques.

To assess the activity in plasma venous blood was collected by venepuncture in to citrate buffer as an anticoagulant at a 1:9 citrate to blood ratio. The blood was immediately centrifuged to pellet the red cells and leave a supernatant that contained plasma proteins. This upper layer was removed and frozen immediately in 1ml aliquots at –70°C.

4.3.4.1 Plasma NADH oxidation

Plasma was thawed on ice and then added into a 1ml plastic cuvette with PBS and NADH at 100μM final concentration. The rate of NADH oxidation was followed by measuring the absorbance of the reaction mixture at 340nm with a 1cm light path

over time. The initial rate of change in absorbance was measured for dilutions of plasma and related to the total protein content of the plasma as assessed by Bradford's assay as previously described. Figure 4.26 shows the rate of oxidation of NADH at 340nm against total plasma protein for one subject using an extinction coefficient of 6.22 mM^{-1} cm^{-1}.

Plasma causes the dose dependent oxidation of NADH in the presence of saturating air to give a rate of ~ 50nmoles min^{-1} mg of total $protein^{-1}$ in the presence of 100μM NADH.

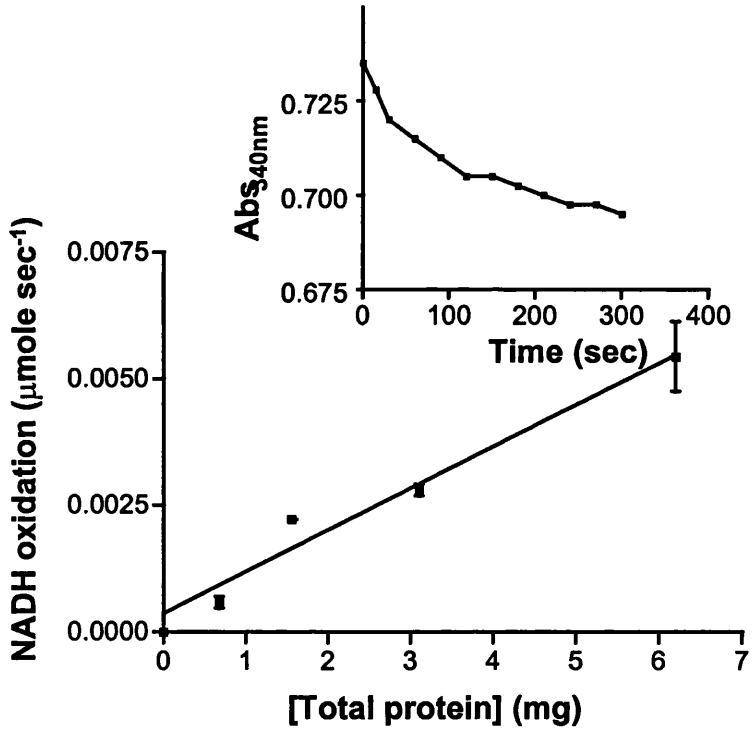

Figure 4.26. The oxidation of NADH by human plasma. Inset shows raw data set for one individual experiment with the main figure showing the oxidation rate against total protein content. Data are mean ± SEM (n = 2) in duplicate of plasma from one volunteer from one sample.

4.3.4.2 Plasma NADH chemiluminescence

The same samples as used in 4.3.4.1 were assessed for the ability to generate superoxide radical from NADH using the oxidation of lucigenin enhanced chemiluminescence. Figure 4.27 shows the NADH mediated LEC of human plasma and the LEC from purified XO protein for comparison.

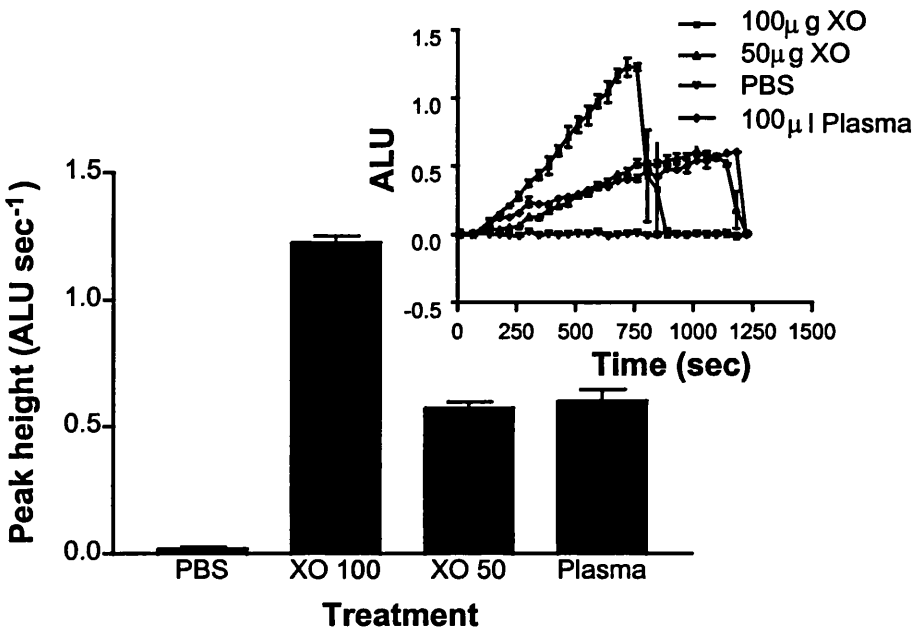

Figure 4.27. The NADH LEC for human plasma and bovine XO protein. Bovine XO at 100 and 50µg in the presence of 500µM NADH and 500µM lucigenin as previously described. Results are mean ± SD for one sample in triplicate.

Plasma caused chemiluminescence in the presence of NADH and lucigenin which was equivalent to the CL signal from ~ 50µg of purified bovine xanthine oxidase.

4.3.4.3 Plasma NADH oxidation in the absence of oxygen and the addition of nitrite

To measure the possible xanthine oxidase activity of plasma, the utilisation of nitrite as the terminal electron acceptor from NADH oxidation was used as an assay. The oxidation of NADH was followed in a spectrophotometer as preciously described.

Cuvettes containing NADH and nitrite were gassed with 5% CO_2 balanced nitrogen and capped with Parafilm™ following the addition of gassed plasma. The rate of NADH oxidation in the presence of nitrite and the absence of oxygen was calculated and is shown relative to air saturated plasma / NADH in the absence of added nitrite.

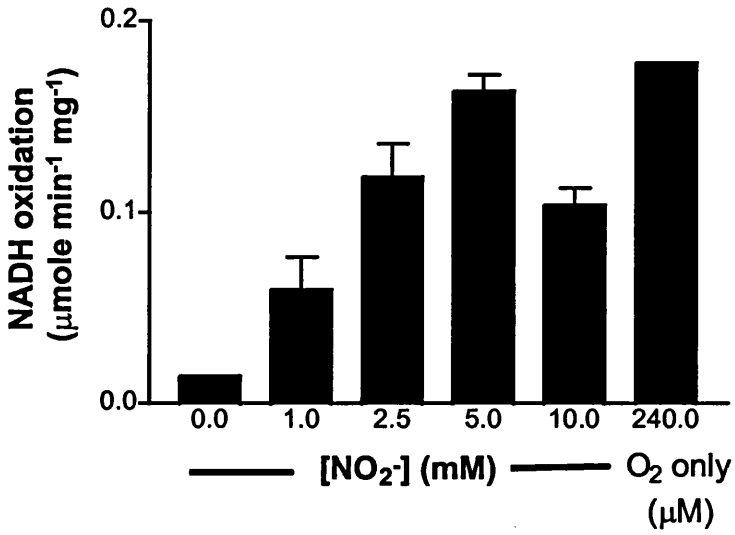

Figure 4.28. The effect of nitrite on the oxidation of NADH by human plasma in the absence of oxygen. Results are mean ± SD of one sample in triplicate.

NADH was oxidised by plasma in the presence of nitrite and the absence of oxygen. The oxidation of NADH was dependent on the nitrite concentration with equivalent oxidation to air saturated media at ~ 5mM nitrite.

4.3.4.4 Plasma NO activity

Following the results in figure 4.28 the possibility that plasma could mediate the reduction of nitrite to NO was assessed. Using ozone enhanced chemiluminescence (OEC), plasma was reacted with nitrite and NADH under reduced oxygen concentrations. Figure 4.29 shows the NO generation from nitrite and NADH in the presence of human plasma.

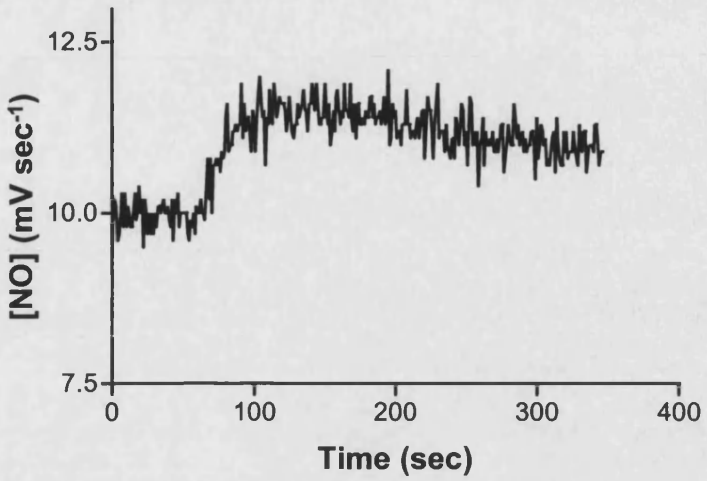

Figure 4.29. The NO generation from human plasma in the presence of nitrite and NADH. NADH, 1mM, nitrite 10mM and 500µl human plasma. Plasma was added at 60 seconds following the injection of Nitrite and NADH at time 0 seconds.

The measurement of NO from plasma in the presence of nitrite was difficult and the figure shows the small response measured in mV sec^{-1} for NADH mediated NO generation (mV sec^{-1} equivalent to ~ 0.5ppb sec^{-1}).

The utilisation of xanthine was also assessed as an alternative electron donor and due to the enhancement in NO generation shown in the presence of DPI this was also added to increase the signal as described in chapter 2. Figure 4.30 Shows the NO generation from human plasma in the presence of xanthine and DPI replacing NADH.

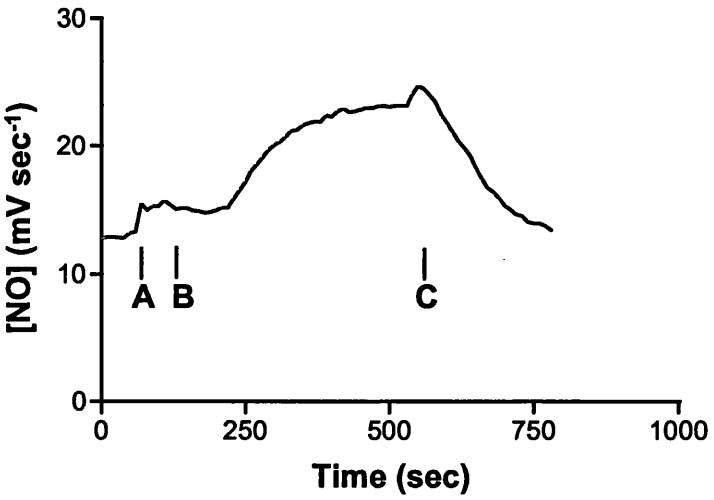

Figure 4.30. The generation of NO from human plasma. In the presence of xanthine, 100μM, DPI, 100μM, nitrite, 10mM and 500μl human plasma at 15mg ml^{-1} to a final volume of 1ml. Plasma was added at **A**, nitrite, DPI and xanthine at **B** and oxypurinol (100μM) was added at **C**.

In the presence of xanthine and DPI an increase in NO generation can be seen with human plasma. On the addition of oxypurinol **C** (100μM) the NO signal is lost and returns to baseline levels.

The effect of xanthine concentration was also measured with the addition of 100μM or 50μM xanthine to the reaction mixture. Figure 4.31 shows the effect of xanthine concentration on the NO generation from human plasma.

Reducing the xanthine concentration reduces the peak height to which the NO generation reaches with 10mV sec^{-1} at 100μM xanthine compared to ~7mV sec^{-1} in the presence of 50μM xanthine (after correction for background NO signal). Both reactions were still generating measurable NO after 2 hours of incubation at the same level as that shown in figure 4.31.

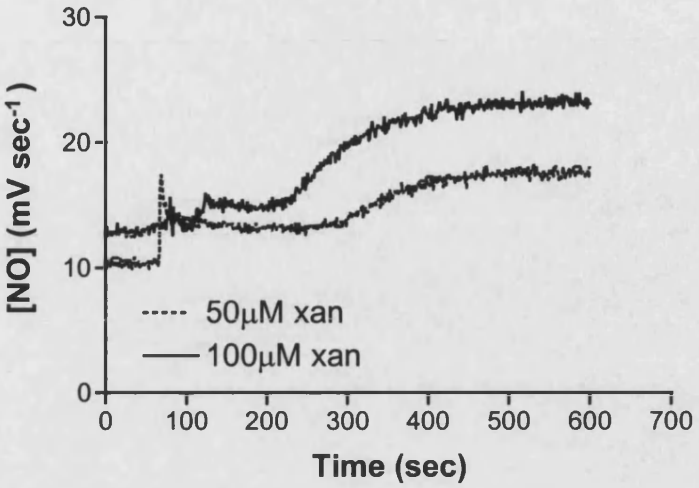

Figure 4.31. The NO generation from human plasma dependent on xanthine concentration. Protocol as for figure 4.30 with the addition of 100 or 50μM xanthine.

4.3.5 The effect of exercise on plasma activity

To assess the effect of exercise and oxygen debt on the activity found in plasma a healthy volunteer was exercised for a total of 12 minutes. The measured heart rate during exercise peaked at 183 beats per minute (bpm) and was above 140 bpm for at least five minutes following cessation of the exercise and above 100 bbp for a further five minutes. Venous blood was taken immediately before exercise and at regular intervals following exercise by intravenous cannulation (20G/32mm Venflon cannulae, Ohmeda, Sweden) with sodium citrate as the anticoagulant. The plasma was produced by centrifugation of the samples and 1ml aliquots were frozen at –70°C. Fresh plasma was assessed for the total protein, NADH oxidation and NADH mediated LEC to determine activity.

4.3.5.1 The effect of exercise on plasma total protein levels

Plasma protein was measured by a modification of Bradfords assay. The results are shown in figure 4.32.

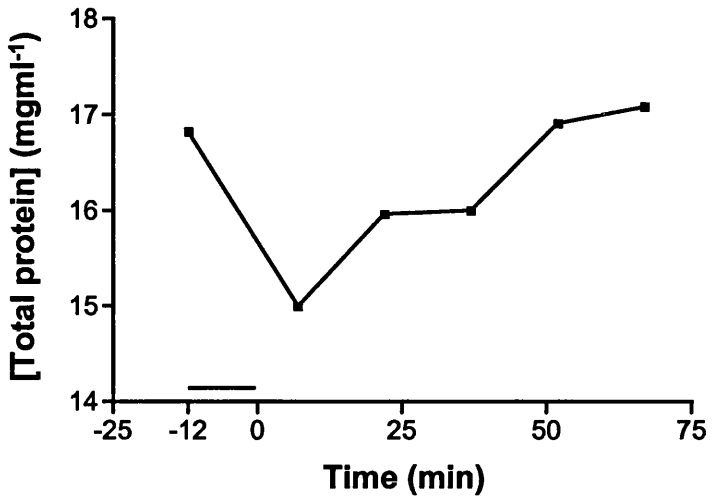

Figure 4.32. The total plasma protein from plasma taken before and immediately following exercise. Bar shows period of exercise.

The plasma protein levels were reduced immediately following exercise compared to pre exercise levels and remained so for some 30 – 40 minutes. By 52 and 67 minutes however the plasma protein concentration had returned to pre exercise levels.

4.3.5.2 The effect of exercise on plasma NADH oxidation

The oxidation of NADH by pre and post exercise plasma samples was followed at 340nm in a spectrophotometer. The results are shown in figure 4.33 corrected for total protein against time.

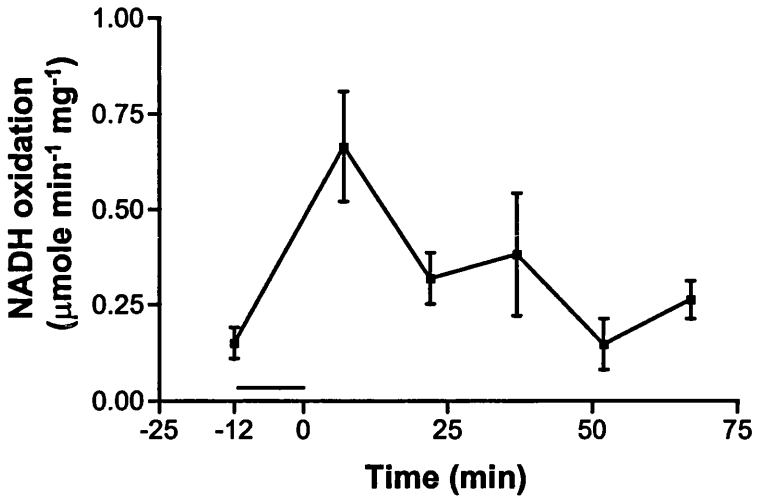

Figure 4.33. The effect of exercise on the oxidation of NADH by plasma. NADH oxidation in the presence of plasma was followed over time and calculated using the initial rate data and an extinction coefficient of $6.22mM^{-1}$ cm^{-1}. Results are mean ± SD (n = 1) in triplicate.

The pre exercise rate of NADH oxidation was ~ 150nmoles min^{-1} mg total $protein^{-1}$ compared to ~ 660nmoles min^{-1} mg total $protein^{-1}$ seven minutes after the cessation of exercise. This activity is increased above pre exercise levels in all but the 52 minute time point. The general trend follows a peak of activity which returns towards pre exercise levels over an hour after exercise.

4.3.5.3 The effect of exercise on plasma NADH mediated LEC

The chemiluminescence mediated by NADH was measured in the pre and post exercise plasma samples and the activity corrected for total protein content. The results are shown in figure 4.34.

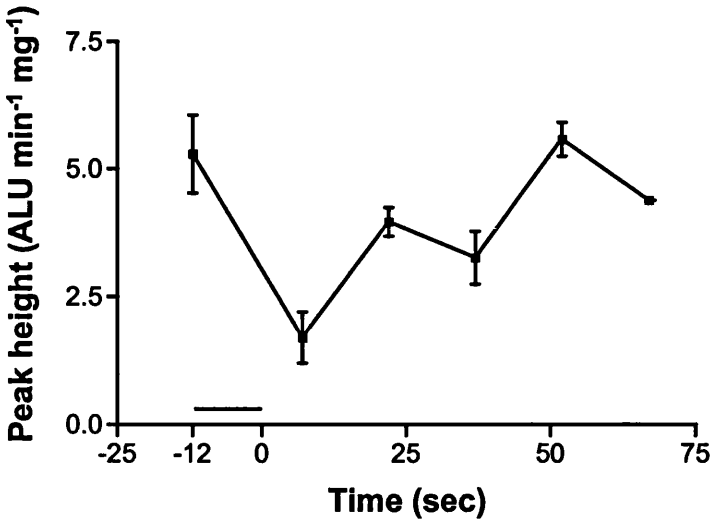

Figure 4.34. The effect of exercise on the plasma NADH mediated LEC. Peak height measurements were measured as previously described. Results are mean ± SD (n = 1) in triplicate.

Human plasma pre exercise was shown to have NADH mediated LEC suggesting the generation of superoxide. The post exercise samples show an immediate reduction in chemiluminescence signal compared to the pre exercise levels. The general trend for activity shows an initial drop which recovers to the pre exercise levels by 52 minutes post exercise.

4.3.5.4 Western blot of exercise plasma samples

Exercise samples were subjected to Western blotting with an antibody raised to bovine xanthine oxidase (Chemicon, USA). Figure 4.35 shows the results of gel electrophoresis and Western blotting for bovine xanthine oxidase and pre and post exercise plasma samples.

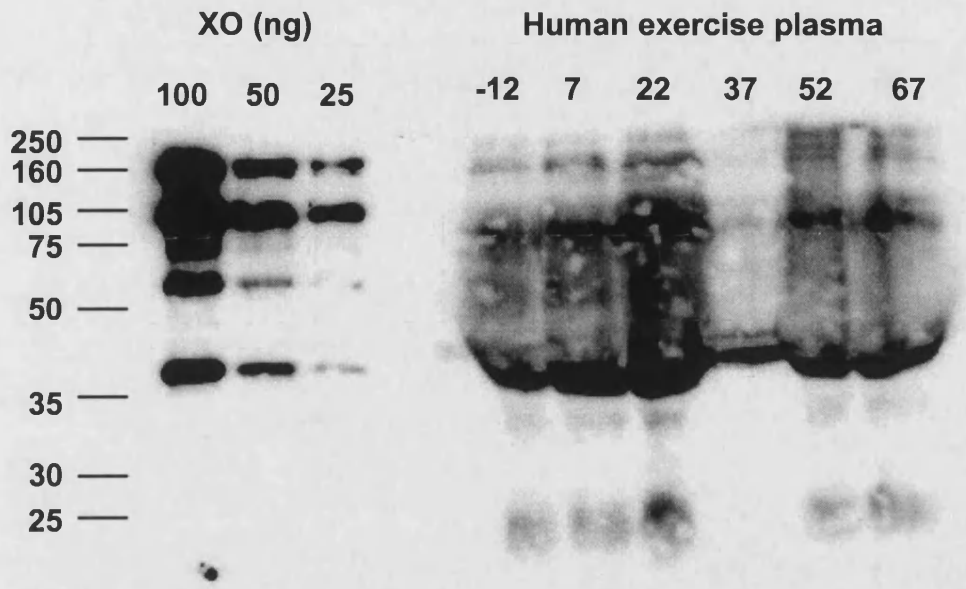

Figure 4.35. The Western blot of human plasma pre and post exercise. Shown are bovine xanthine oxidase of known concentration (XO) against 30μg lane^{-1} of human plasma with times pre and post exercise. Molecular weight markers are shown in KDa to the left of the figure.

The bovine enzyme shows the typical staining gained with this Chemicon antibody. The plasma samples show strong banding patterns at ~ 40KDa, ~ 70KDa and some banding at ~ 150KDa size. There is also an increase in the intensity of staining over the time of post exercise compared to pre exercise levels in all bands apart from 37 minutes post exercise. Measuring the optical density of the apparent 150KDa band it was possible to generate a graph of optical density against time of exercise.

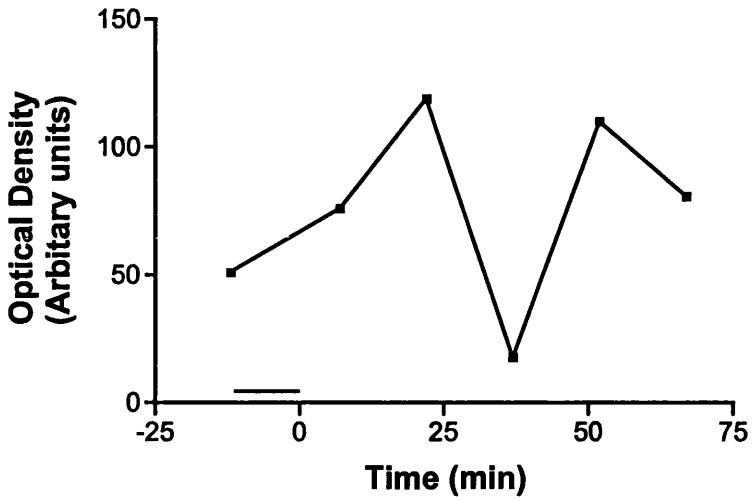

Figure 4.36. The optical density of 150KDa band from human plasma.

The optical density of the 150KDa band increases following cessation of exercise which drops at 37 minutes but is raised again following 52 minutes before being reduced again at 67 minutes.

4.4 Discussion

The release of XO in to the circulation following heparin addition or in a range of pathologic conditions suggest a mechanism as to the effect of enzymic products on a range of tissues which would otherwise be devoid of activity. Previous experiments into the binding of exogenous XO have taken the path of purified binding substrates and enzyme activity measurements to determine the degree of binding. Here an *ex vivo* system has been developed using live endothelial cells and the sensitive and specific measurement of bound enzyme using flow cytometry.

This system utilises the size dependent cut off criteria to avoid false positive results that flow cytometers employ. The fluorescence measurements are related to the concentration of protein and will only be detected when bound to particles greater than 5 microns in diameter. By selecting the endothelial population, non viable

cells and particulate materials are excluded from the analysis. The limit of detection for the flow cytometer used in terms of fluorescence measurements was ~ 800 bound molecules of FITC. The right shifted normal distribution curves suggest that greater than that number of FITC molecules were bound to each individual cell. However it is not possible to determine the binding site number which is related to the number of bound or expressed molecules due to the use of a polyclonal primary antibody. For this reason the relative fluorescence measurements are used.

In the absence of added exogenous XO, primary cultured naive endothelial cells show a right shifted curve suggesting surface expression of antigen(s) recognised by the primary antibody. All other combinations of added antibody were proven to be negative and this suggests that XO protein was expressed on the surface of endothelial cells. However it was not possible to produce a Western blot of endothelial cell protein using the same polyclonal antibody to give a distinct 150KDa band indicative of XO. Also it was not possible to discern whether the protein was expressed from internal stores or was attached in the membrane or attached to the surface from the circulation before isolation.

In the case of exogenously added XO, the purified bovine enzyme used gave the characteristic XO banding pattern on Western blots probed with the polyclonal antibody. Therefore the added enzyme was recognised by the primary antibody and suggests that XO added to endothelial cells binds in a dose dependent manner. As the analysis was of individual cells it also suggests that each cell was capable of binding a finite amount of enzyme as the fluorescence was seen to plateau indicating saturation of the binding sites on the cell.

As hypoxia is an inducer of xanthine oxidase in terms of activity (Terada *et al* 1997) its effects on surface expression of XO protein and XO binding capacity was

assessed. Hypoxia had little effect on endogenously expressed enzyme where as it caused an increase in the enzyme binding capacity compared to cells incubated under atmospheric oxygen concentrations. This suggests that following a period of hypoxia there is a change in the binding capacity of the endothelium which may cause the concentration of circulating proteins and in particular circulating XO.

It has been suggested that the binding of XO to cell surfaces is dependent on the glycosaminoglycans expressed to form the glycocalix and in particular heparan sulphate glycosaminoglycan. Heparinase I treatment of the cells for one hour caused an increase in the binding capacity of each cell. The removal of heparin and heparan sulphate glycosaminoglycan had the opposite effect to that which was expected. If XO bound to the cell via heparan sulphate, its removal should reduce the apparent binding to the cell surface. Previous reports have suggested that XO may bind to other proteoglycans including dermatan sulphate and chondroitin sulphate (Adachi *et al* 1993 and Radi *et al* 1997). It is possible therefore that other binding sites become available or that the overall surface charge of the cell changes to increase the binding of added XO protein.

It has been reported that heparinase treatment reduced the binding of XO to endothelial cells (Adachi *et al* 1993) or had no effect on the binding capacity of endothelial cells (Houston *et al* 1999) whereas chondroitinase treatment reduced binding by up to 50% (Houston *et al* 1999). The discrepancy between all three studies may be due to the different approaches to the measurement of binding. The two published accounts used enzyme activity rather than protein measurement (as is the case in this flow cytometric assay). Radi *et al* (1997) had described a reduction in activity of enzyme bound to heparin sepharose whilst Houston *et al* (1999) measured rates of superoxide production by soluble and cell bound XO and found there to be no difference. By using enzyme activity as the measure of

binding it may be possible to under estimate the amount of bound enzyme due to changes to activity that may occur. The use of both an activity assay and protein concentrations may give more information as to the specific effects of heparinase treatment.

The expression of heparan sulphate glycosaminoglycan was also assessed by flow cytometry in naïve, hypoxic and Heparinase I treated endothelial cells. Endothelial cells showed a right shifted curve suggesting increased fluorescence in naive cells stained with a monoclonal antibody raised against bovine heparan sulphate GAG. On treatment of the cells under hypoxic conditions, the fluorescence was increased over the naïve control cells and also showed a possible greater fluorescent sub-population of heparan sulphate GAG labelled cells. This experiment linked with the increased fluorescence associated with endogenously added XO to previously hypoxic cells suggest that an increase in GAG expression leads to an increased binding potential.

The effect of hypoxia on the GAG expression of endothelial cells has been measured previously. Levine *et al* (1982) showed an increase in synthesis and secretion of dermatan sulphate and heparan sulphate GAGs in porcine aortic endothelial cells following hypoxic treatment. Humphries *et al* (1986) showed a decreased secretion of GAGs but no change in the cell associated GAG expression following hypoxic treatment of bovine aortic endothelial cells. Also in bovine aortic endothelial cells, Karlinsky *et al* (1992) showed reduced incorporation of radiolabelled sulphate into cell layer associated heparan sulphate in hypoxia but the binding of antithrombin III was markedly increased suggesting an increase in affinity. There was also a change in molecular weight of the heparan sulphate GAGs in hypoxic exposed cells.

The change in affinity caused by hypoxic treatment may be reflected in the high fluorescent sub-population seen. This may be due to increased binding or affinity for the antibody in this sub-population along with an increase in the antigen available. It may be possible by using dual labelling techniques to assay the sub-population of high fluorescent cells for their XO binding capacity and select them out by sorting for further evaluation.

It was important to assess the ability of Heparinase treatment to affect the cell surface expression of heparan sulphate GAG expression. Heparinase reduced the fluorescence signal due to cells stained with anti heparan sulphate GAG antibody.

All of these experiments taken together suggest that whilst hypoxia stimulates binding and heparan sulphate GAG expression this may not be the only mechanism for binding of XO. The increase in apparent binding caused by the removal of heparan sulphate GAG suggests an associated mechanism, such as chondroitin sulphate GAG as shown by Houston *et al* (1999).

Other receptors for many proteins are also expressed on the surface of endothelial cells. One such protein is ICAM-1, the receptor for CD11b used for neutrophil binding. ICAM-1 however will also bind to the RGDS binding motif found in fibronectin and other matrix proteins. From the published amino acid sequence (Ichida *et al* 1993) however, XO does not contain an RGDS motif in its primary sequence. The heparin-binding site of XO has been described (Fukushima *et al* 1995) and it is possible that more binding sites will be determined as the secondary and tertiary structure of the enzyme is elucidated.

Recently it has been suggested that XO is endocytosed from the surface of cells to be located in some intracellular compartment (Houston *et al* 1999). The possibility exists that the staining seen in these experiments was not of surface expressed or bound enzyme but of intracellular localised antigen. It is possible that the whole

complex of enzyme, primary and secondary antibody was endocytosed which would generate a similar staining pattern as that produced. However, this would still suggest that a binding event with associated signalling in the cell had occurred prior to endocytosis with endocytosis being a relative fast event compared to the staining procedure used here.

In order to remove the possible problems associated with antibody staining an alternative may be to utilise fluorescently labelled XO enzyme. A population of cells can be monitored in real time using flow cytometry and plotted as fluorescence against time. Unstained cells would show little fluorescence and on the addition of labelled enzyme, only cells binding the enzyme would begin to fluoresce. Commercially available kits utilise the binding of fluorescent dyes to free amino groups. One such kit FluoroLink from Amersham uses a bisfunctinal NHS-ester cyanine dye. With a combination of real time flow cytometry and confocal laser scanning microscopy which allows the optical sectioning of cells, the binding and subsequent movements of the labelled enzyme could be followed.

In the case of XO, this approach may also contain problems in that the apparent enzyme binding is dependent on electrostatic attractions between the enzyme and cell surface components. The use of amino groups on the enzyme to bind dye causes a change in the electrostatic charge over the whole enzyme. This in turn would reduce the binding capacity of the enzyme for its target.

Endocytosis of the enzyme as a mechanism of capture suggests an active event requiring signal transduction pathways. This may be useful in determining the relationship between the binding event and subsequent fate of the bound enzyme. Using cell calcium flux as a measure of interaction may show insights into the events initiated by protein binding especially in an electrostatic manner rather than the more formal receptor-ligand approach.

The binding of XO to GAGs may be of importance in the cytotoxicity displayed to bacteria. Many viruses and bacteria bind to their target via heparin like GAGs as part of their infection strategy (Patti 1994). Foot and mouth disease virus (FMDV) for example will bind integrin molecules on the host cell but the majority of binding occurs through heparan sulphate. The initial binding is to heparan sulphate followed by high affinity binding to integrin receptors (Jackson *et al* 1996).

Using *E. coli* it was possible to show by flow cytometry and enzyme activity the binding of XO to bacteria. This binding may be important in terms of the proximity of enzymic products to the bacteria. It is even possible that the bacteria may provide the substrates for the enzyme to generate the reactive species for bacterial self destruction.

In bacteria the binding characteristics are mediated by a range of surface expressed pili or fimbriae and it has been determined that in clinical isolates *of E. coli* from urinary tract infections, the addition of GAGs can have an anti-adhesive effect (Busolo *et al* 1995). Esosaminoglycan sulphate showed greatest effect against P-fimbriated *E. coli* whilst galactosaminoglucuronglycan sulphate was anti-adhesive on type one fimbriated *E. coli* showing differential effects on a range of adhesive molecules.

Milk itself contains complex carbohydrates, including glycoproteins and glycosaminoglycans. It has been suggested that these compounds offer an anti-adhesive action to bacteria reducing their infective capability (Newburg 1999). In HIV-1 infection GAGs have been implicated in the inhibition of gp120 binding to CD4 which is the first step in HIV infection. XO may therefore not only bind to bacteria to increase the proximity to the target for radical mediated damage but may also reduce infection by a physical impairment of bacterial binding. However it must also be noted that the concentration of enzyme compared to GAGs and

glycoproteins may cause competition for binding sites on the bacteria which may in turn reduce the proximity killing effect. In this thesis XO protein in human milk accounted for ~ 10% of total protein which is variable over time of lactation post partum and also to some extent to the diet and health of the mother.

Intracellular XO expression in endothelial cells was determined by immunolabelling and enzyme assay of isolated and cultured endothelial cells. The reaction product from the peroxidase labelled secondary antibody was localised to the perinuclear region but also with diffuse granular cytoplasmic staining in naïve cells. The subcellular localisation to the cytoplasm in rat hepatocytes has been previously described by Ichikawa *et al* (1992) using electron microscopy techniques. Further to this the same group analysed fractionated cells and found activity in the cytosol but not in cellular organelles.

The staining pattern in endothelial cells showed a slight resemblance to cells that were stained for vWF. This shows a granular staining pattern as the Weibell-Palade bodies are picked out being the organelle of storage for vWF. If XO co-localises in the WPB then this may account for a mechanism of secretion along with vWF and p-selectin translocation to the membrane. As the XO protein does not include a signal sequence to target it for secretion, an alternative mechanism would be required. Alternatively, the endothelial cell has been shown to contain other discrete storage granules which are small and dense and contain tissue-type plasminogen activator (tPA) (Emeis *et al* 1997) that are released on stimulation with thrombin or heparin (Klocking and Markwardt 1994). tPA being part of the coagulation cascade and fibrinolysis is therefore secreted along with vWF on stimulation of the endothelium. Heparin has been shown to cause XO release into the circulation from two patients infused with heparin which was suggested as causing the release of GAG bound heparin (Adachi *et al* 1993). It is also possible

that stored granules containing XO either from intracellular generation or from endocytosis of surface bound XO are secreted on addition of heparin if co-localised with vWF or tPA into the circulation which would not be discernible from the release of surface bound XO.

vWF release is also stimulated by hypoxia (Pinsky *et al* 1996) and hypoxia causes the endothelium to become prothrombotic (Ogawa *et al* 1990). IL-8 secretion is also stimulated by hypoxia and has been localised in a preformed state to the Weibel-Palade bodies (Utgaard *et al* 1998). The effect of hypoxia on endothelial XO enzyme activity was to increase the pterin mediated and NADH mediated activities per milligram of total protein.

Also noted was that on exposure to hypoxia, HUVEC would begin to secrete vWF into the culture media (Pinsky *et al* 1996). This led from earlier observations that vWF staining in synovia did not always pick out the endothelium when it has been the method of choice for EC labelling experiments (Stevens *et al* 1991).

The differences seen in the superoxide generation and NADH utilisation may suggest that the superoxide generating system was not solely responsible for all of the NADH oxidation. Other NADH oxidising enzymes are found circulating naturally and neither of the above assays are specific for xanthine oxidase as such. However, the generation of NO from plasma in the presence of xanthine or hypoxanthine and the absence of oxygen is probably the most specific measure of xanthine oxidase activity as yet there have been no alternative systems described that generate NO in this way.

The simulated hypoxia or oxygen debt endured by high output exercise may have a mediating effect on the circulating xanthine oxidase levels. Further study in to the levels of hypoxia simulating either altitude induced or pressure induced low oxygen may allow for the determination of the importance of this activity for normal subjects

and also for the response to exercise of subjects with inflammation and particularly joint inflammation.

The prevalence of a circulating radical generating enzyme then is important. This is particularly so if this enzyme is a nitric oxide / superoxide generating system that is stimulated by hypoxia and inflammatory cytokines. On the one hand a NO generating enzyme destined for an area that suffers hypoxia may relieve that oxygen debt by supplying endothelial relaxation factor. One the other hand this may eventually lead to the reperfusion of the site causing the generation of superoxide and possibly peroxynitrite which may be deleterious.

Further work to determine the secretion, binding, intracellular location and possible endocytosis of xanthine oxidase is required in order to elucidate its role in pathology and physiology in both inflammatory disease and acute hypoxic episodes.

Chapter 5

General Discussion

Chapter 5

5.1 General discussion

In this thesis the well-established ability of xanthine oxidase to generate oxygen free radicals has been extended to highlight the fact that the particular species generated is dependent on the available substrates and prevailing reaction conditions. As the predominant substrate requirement for the generation of superoxide and hydrogen peroxide is oxygen for the classical activity of XO, the rates of generation are therefore limited by its availability. As oxygen is acting as the oxidising agent, it is itself reduced to superoxide by the addition of an electron donated from a variety of substrates. In the same way, nitrate or nitrite will reoxidise the reduced enzyme whilst becoming themselves reduced to nitrite and nitric oxide respectively. The rate of these reactions is dependent on the concentration of nitrate and nitrite and on the concentration of oxygen. As the oxygen concentration is increased then the rate of measurable NO generation is decreased. In the case of all oxidising substrates, therefore, there is competition for the available electrons.

The reduction in measurable NO seen in previously hypoxic systems where oxygen is reintroduced can be explained by the simple competition between oxidising substrates for electrons. However, simultaneous generation of superoxide and nitric oxide is indicated by the experiments where the addition of superoxide dismutase (SOD) increased the measurable NO signal as oxygen concentration was increased. This strongly suggests that the reaction product of NO and superoxide, peroxynitrite, is formed as the concentration of oxygen is increased in a previously hypoxic system. As the concentration of nitrite is

increased, the concentration of oxygen at which the loss of the NO signal occurred is also increased. Therefore the generation of NO or superoxide is dependent upon the concentration of the oxidising species. It is known that the generation of peroxynitrite is dependent primarily upon the flux of NO and, therefore, as the nitrite concentration is increased the concentration of oxygen at which peroxynitrite generation occurs is shifted to the right of the oxygen curve. The likelihood of peroxynitrite generation is therefore dependent on the flux of NO, which is itself dependent upon substrate availability.

Assays of peroxynitrite that were previously published were not suitable for the measurement of the products of nitric oxide and superoxide generated from nitrite and NADH or xanthine in the presence of xanthine oxidase. The oxidation of dihydrorhodamine is the basis of a commonly used peroxynitrite assay, however, dihydrorhodamine was shown to be oxidised in the presence of nitrite. This oxidation was reduced on the addition of the strong reducing agent NADH and for this reason the signal generated in the presence of enzyme could not be discerned from the controls.

Using chemiluminescence, it was possible to show an enhanced signal that is dependent upon nitrite concentration above that of enzyme and single substrate alone. The precise identity of the luminescent molecule is unknown, but the use of controls containing specific scavengers, strongly suggest the species to be peroxynitrite. This is dependent upon the reaction of peroxynitrite with the scavenger rather than with the luminescent compounds before the luminescence pathway is initiated. It is entirely possible that the reaction of superoxide with nitrite leads to a molecule that reacts with lucigenin to generate luminescence. The suggestion of a bystander reaction has been proposed by Trujillo *et al* (1998) where superoxide reacted with S-nitrosocystene to form peroxynitrite. The use of

specific inhibitors of the enzyme will not necessarily distinguish peroxynitrite generation as both superoxide and nitric oxide would be inhibited by the known xanthine oxidase inhibitors of any of the active sites involved. It is only the use of scavengers that are specific for peroxynitrite, superoxide and nitric oxide alone that will allow the calculation of the products using a reporter assay such as the chemiluminescence assay used here.

Other assays employing antibody staining for nitrated residues may be suggestive of ONOO- generation, such as the immunodetection of 3-nitrotyrosine (3-NT). Although this is not a kinetic assay, this may be used as a marker of ONOO- generation using reporter proteins such as bovine serum albumin. The effect of ONOO- on the activity of human SOD has been used as a measure of ONOO- generation (Macfadyen *et al* 1999). Both the nitration and inhibition of superoxide dismutase activity can be used as the human SOD enzyme contains a tyrosine residue at its active site, the nitration of which causes a loss of activity. This differs in the bovine enzyme as the tyrosine residues are far removed from the active site. The nitration of XO enzyme itself may be useful in determining ONOO- generation and this could be related to the possible inhibitory effect on enzyme turnover. ONOO- has also been shown to inhibit iron-sulphur proteins by disruption of the Fe-S moiety, xanthine oxidase is such a protein. It is possible, therefore, that the generation of ONOO- by the enzyme may lead to a reduction in catalytic activity in a self-regulating manner in a similar manner to the effect of NO binding to the haem iron in nitric oxide synthase self regulation (Abou-Soud *et al* 1995).

Recently it has been suggested that NO binding to xanthine oxidase can cause the desulphuration of the enzyme leading to inactivity (Ichimori *et al* 1999). This may also be a self-regulating mechanism as the nature of the inhibition was reversible by resulphuration of the molybdopterin active site. In this thesis, however, under

enzyme turnover conditions generating NO, no such inhibition was observed. This may be accounted for by the assay used, as the measurement of NO requires the NO to be forced into the gas phase by vigorous stirring which may reduce the effect of NO in solution on the activity of the enzyme.

In a physiological setting, the generation of superoxide from xanthine oxidase would be dependent upon the availability of oxygen in the tissues. At lower oxygen concentrations the superoxide generating capacity would also be lowered. The availability of nitrite has been shown in the plasma to range from low micromolar, ~1μM to over 500μM depending on diet and health of the subject (Baylis and Vallance, 1998). The oxygen concentration is dependent upon perfusion and oxygenation of the haemoglobin. In acute low oxygen it is possible that XO could play a role in the generation of NO from the available substrates to allow for the reoxygenation of hypoxic tissues. As the concentration of available oxygen rises, the flux of NO would be decreased as the generation of superoxide occurs. The further reaction of NO and superoxide to generate peroxynitrite would then occur. To some extent however, endothelial SOD could detoxify this environment by reduction of the available superoxide and enhancement of the nitric oxide flux. At higher concentrations of available oxygen, the activity of SOD as a scavenger of superoxide would be overwhelmed with the subsequent generation of peroxynitrite. This in turn could lead to the inhibition of further SOD activity by inactivation of the enzyme and subsequent exacerbation of the peroxynitrite generating capacity by increasing the oxygen range over which this occurs.

The generation of peroxynitrite is known in a variety of pathological conditions through the use of antibody staining for the nitration product of peroxynitrite and tyrosine residues, 3-nitro tyrosine. The nitration of enzymes has been implicated in

their loss of activity. This has particular importance in the case of the human SOD enzyme where inactivation leads to the loss of cellular function and tissue breakdown (Beckman and Koppernol, 1996). The effect of peroxynitrite on cell replication has also been shown with strand breaks in DNA and inhibition of the repair enzymes by the direct action of peroxynitrite (Burney *et al* 1999).

The possible beneficial effects of reactive species generation on bacterial killing was also tested for this enzyme in the light of its expression in milk of both human and bovine origin. The high concentration present in milk and epidemiological evidence suggested that parental milk feeding to the neonate enhanced survival and fitness compared to milk substitute-fed individuals. It was clear that peroxynitrite and hydrogen peroxide had a negative effect on bacterial survival and that, in the presence of xanthine oxidase and substrate, the survival of bacteria was reduced.

The limited killing effect seen at a range of oxygen concentrations in the presence of nitrite requires further study. The assays used require development to allow large through-put growth assays to be utilised at a range of oxygen concentrations. The development of such a 96-well assay requires the incubation of plates *in situ* with gassed atmospheres of known oxygen content. It is also important to assess the surface characteristics of cells incubated at varying oxygen concentrations, since bacteria cultured under hypoxic conditions generate surface proteins which may allow enhanced binding of enzyme and therefore mediate any killing effect by enhancing the proximity effect of oxidant generation (James and Keevil 1999).

Utilisation of strains expressing a range of surface molecules may help to increase the understanding of the binding characteristics of enzyme to bacteria, and also to

determine whether this is a mechanism in milk and feed stuffs that occurs in the presence of other possibly competing molecules.

The milk mucins comprise an array of anti-adhesive molecules for enteroinvasive *E. coli* and Rotavirus (Newburg 1999). The association with these molecules and the milk fat globule may allow for the close association of enzyme and bacteria, but may also generate a protective bridge between the enzyme and cell surface to reduce the proximity killing effect. The effect of mucins on the protection and or binding of enzyme to bacterial strains could also be assessed using the assays employed above.

The mechanism by which ONOO-, H_2O_2 and xanthine oxidase-derived metabolites have their effect on bacteria was not investigated here. However, both ONOO- and H_2O_2 have been suggested to cause strand breaks in DNA and have an effect on DNA repair enzymes. This was also a similar case to the effect of NO and the final effector molecule could range from the original oxidants to their breakdown products and especially the hydroxyl radical. The utilisation of specific scavenger molecules may help to elucidate the effectors. Measurement of strand breaks in isolated bacterial DNA can be made by agarose electrophoresis, which can also be used for nitration studies by blotting of DNA on to nitrocellulose and probing with anti-nitro base antibodies. The specificity of action could then be discerned for ONOO- and H_2O_2.

The bacterial resistance mechanisms could also differ with the detoxification of hydrogen peroxide following a catalase-like step compared to the ONOO- decomposition, possibly leading to positive identification of the toxic species mediating the killing. However, because of the possibility of other breakdown products, such as the hydroxyl radical from ONOO- and Fenton-mediated H_2O_2 breakdown, the effector molecule may be difficult to determine and may be

dependent upon the bacterial antioxidant systems as to which toxic species is generated.

The apparent toxicity of ONOO- and peroxynitrous acid (ONOOH) have been disputed because of the ionisation of the toxic species ONOO- and therefore its movement through membranes is hindered by charge interactions. However ONOOH can diffuse through membranes and cause nitration of proteins shown by nitration of haemoglobin in erythrocytes (Denicola *et al* 1998). The transport of ONOO- and the diffusion of ONOOH may allow the use of the HCO_3^-/Cl^- transport inhibitor 4,4'-diisothiocyanatostilbene-2,2'-disulphonic acid (DIDS) to elucidate the role of either species in the killing effect seen with bacteria. Reducing the extracellular pH to move the ratio of ONOO- towards ONOOH, the pKa for the equilibrium being 6.8, may enhance the toxicity of the generated species by selecting the protonated form. Those bacterial strains possessing a means of active transport may be more susceptible to ONOO- toxicity than those which can block the entry of or modify the oxidant properties of ONOOH. This may also be strain and species specific.

In certain diseases, circulating xanthine oxidase activity has been identified. How the enzyme is released into the circulation and what its possible function may be are still unclear. It does, however, confer the ability of the enzyme to relocate to tissues via the circulation, suggesting an active mechanism of secretion and recruitment to endothelial cell surfaces. The nature of the nitric oxide-generating activity may suggest a role of radical generation for reoxygenation strategies or the more deleterious role as a reactive oxidant generator.

It has been suggested that following binding of the enzyme to endothelial cells, the active process of endocytosis accounts for the loss of enzyme from the circulation

and the uptake of enzyme into the cell (Houston *et al* 1999). This also suggests some kind of signalling event occurs following binding, however this has yet to be observed. Other bound proteins may give clues as to the mechanism and to the fate of captured enzyme. The association of enzyme with clathrin would point to a clathrin-coated pit event with endosome formation and recycling to alternative membranes as a mechanism for redistribution within cells.

It has also been noted that sulphated proteoglycans are endocytosed in cultured skin fibroblasts suggesting that the mechanism of binding and endocytosis may be mediated by a single event or chain of events initiated by the binding of surface protein (Prinz *et al* 1978).

The initial binding to GAGs by XO may mimic the binding of certain infective bacteria which bind first by electrostatic interaction followed by a stronger receptor ligand binding such as that seen in *Neisseria gonorrhoea* (Duensing and Putten 1998). This infective bacteria binds to vitronectin on the cell via a heparin-binding outer membrane protein OpaA causing the glycosaminoglycan to act as a molecular bridge.

Fibrinogen is a circulating protein that binds to cellular surfaces via the interaction of ICAM-1 and an RGDS binding sequence. This binding also causes calcium flux in the bound cells. Such an arrangement of amino acids is not seen in the published primary sequence data for human xanthine oxidase, which may suggest an alternative receptor interaction if binding occurs, or that the tertiary structure causes the alignment of such amino acid residues to form a recognised binding domain.

Xanthine oxidase possesses two heparin binding domains within its sequence (Fukushima *et al* 1995), which can be located to the 85KDa subunit following

proteolysis. However, as yet the tertiary structure is unknown and it is not possible to suggest that these binding sites are available in the native form of the enzyme. The extracellular bound SOD enzyme also has a heparin-binding motif (Oury *et al* 1996). It has been shown that this motif can be proteolytically cleaved to produce a non-bound inactive form that will diffuse into the surrounding tissue or circulation (Enghild *et al* 1999). It was suggested that this might represent a regulatory pathway effecting distribution and activity and therefore the effectiveness of SOD at particular tissues. It is possible therefore, that the circulating xanthine oxidase may occur as a result of cleavage of the heparin binding domain and that protein not bound by another means could be lost to the circulation. This would therefore preclude further binding of this cleaved enzyme to heparin or heparan GAGs. Proteolysis of extracellular SOD can occur by trypsin treatment and it is well known that trypsin causes the proteolytic cleavage of xanthine oxidase into subunits of 20, 40 and 85KDa where the redox centres, iron-sulphur, FAD and molybdenum domains are located respectively (Nishino 1994). Cleavage of bound enzyme would release the protein from the surface of the endothelium by the loss of heparin binding capacity and the breakdown of the enzyme into its constituent subunits could remove molybdenum-based superoxide activity. However, it is entirely possible that the NADH-oxidising activity would remain intact, as the FAD active site does not require the other redox sites to be available for superoxide formation. As for the molybdenum domain, the NADH-mediated reduction of nitrite to NO would not occur. However, the xanthine and hypoxanthine-mediated nitrite reductase activity is still possible as only the molybdenum active site seems to be involved. From the evidence shown by inhibiting the FAD site with DPI and enhancing the generation of nitrite from nitrate and NO from nitrite suggests this as a mechanism. It is also possible that this active subunit would lose its oxygen-

dependent NO generation and be capable of generating NO at relatively high oxygen concentrations in the presence of suitable substrates.

The binding of proteolysed XO enzyme could also be measured by the use of flow cytometry in a manner as described in Chapter 4 and compared to non-proteolysed enzyme on endothelial cells. The ability of blood plasma to generate NO in the presence of purine substrates and nitrite in air would also point to this mechanism.

It is also possible, however, that the proteolysis of the heparin-binding domain causes the loss of molybdenum-mediated activity as the domain is found within the 85KDa subunit that contains this active site. It was noted, however, that the heparin-binding domain does not overlap the molybdenum binding site and no change in activity was seen in the presence of heparin (Fukushima *et al* 1995). The determination of the specific activity of isolated enzyme subunits may point towards the change in activity seen in plasma samples.

To have a similar strategy of control over oxidant-producing and antioxidant enzymes may suggest a link between XO and SOD expression and activity, as they are closely associated both on the endothelium and in their evolutionary linkage. It has been suggested that xanthine oxidase and superoxide dismutase are linked by virtue of the fact that their genes are inherited together, being located on the same chromosome, as measured by the recombination rate in Western palearctic frogs (Hotz *et al* 1997). These data also suggest that the two enzymes may have been linked, in at least the early vertebrates, some 400 million years ago as they are also linked in teleost fish and mammals and both protein sequences are extensively conserved.

The use of mesenteric perfusion and the effect of hypoxic exposure may allow the testing of enzyme binding from the circulation. Using the perfused mesentery a solution of enzyme could be perfused through the vessels with subsequent staining

with antibody or by activity measurements to show binding of circulating enzyme to vessel endothelium. It is also possible to test the effect of hypoxic exposure on the adhesivness of the endothelium by using rats exposed to chronically reduced oxygen levels.

Also seen in this thesis was the possibility that exercise with associated oxygen debt may cause an increase in circulating radical-generating enzymes. Further work utilising exercise regimens under controlled oxygen conditions in an isolation chamber, the oxygen concentration of which is reduced compared to atmospheric concentrations, may show increased levels of oxidant-generating enzymes in the plasma. This technology is already available as a method of training elite athletes by simulating exercise at altitude in such a chamber giving all the benefits associated with altitude training. The possibility therefore exists that an oxygen debt exercise may lead to the generation of NO from nitrite and XO to cause relaxation of constricted hypoxic vessels followed by a reperfusion with the associated oxygen radical generation also mediated by XO.

A possible hypothesis, taking into account the above information is that xanthine oxidase, as an ancient enzyme, was redox active and could utilise a range of substrates for the turnover of purines or NADH reducing equivalents with the subsequent fixation of nitrogen as nitrite in a oxygen free atmosphere. As oxygen became more abundant, the generation of reactive oxygen species began to occur. If the organisms were utilising the nitrite and NO as signalling molecules generated by xanthine oxidase in some manner, then the appearance of superoxide and therefore peroxynitrite would starve the organism of the required NO signal. Co-expression of the SOD enzyme would then allow the generated NO to cover a wider range of oxygen concentrations and allow functioning of the reactive nitrogen molecule.

In the circulation this can be used as a hypoxia escape mechanism for relaxation of hypoxic vessels when other oxygen-dependent enzymes such as NOS are starved of their substrate. The generation of NO may also include a signalling role in terms of oxygen-sensing mechanisms and the turnover of NAD+ and NADH ratios which are perturbed due to the lack of the terminal electron acceptor oxygen during times of hypoxia.

The dual role of oxygen and nitrite utilisation may also serve as an antibacterial agent in milk allowing natural control of the gut flora in the neonate at a time when other anti-bacterial mechanisms such as stomach acid production are not yet initiated.

The studies in this thesis have highlighted a level of mutifunctionality of xanthine oxidase that has been previously overlooked. Knowledge of this allows the consideration of many new physiological roles for the enzyme and the possibility of novel therapeutic intervention where the enzyme is beneficial but deficient or inappropriately expressed and pathogenic. In this respect, the studies of this thesis have formed the basis for two international patents:

1. International Patent No. PCT/GB99/02845 - Ingestible compositions comprising anti-bacterial agents.
2. International Patent No. PCT/GB99/02844 – Treatment of Lesions.

The higher profile of physiological importance given to xanthine oxidase by publications arising from these studies warrants an increase in research effort in specific areas. In this respect this work is being followed up and expanded upon within the laboratories at the University of Bath where these studies were made.

Appendix I

Krebs-Hensleit solution (KHS)

To prepare 5L of KHS

Chemical	Mass (g/5L)
NaCl	34.5
$NaHCO_3$	10.5
Glucose	10.45

Stock solution	Final concentration (mM)
KCl	4.7
$MgSO_4$	1.2
KH_2PO_4	1.2
$CaCl_2$	1.2

Made up in 5L distilled water. Once dissolved the solution was filtered through a 0.22μm filter (Sartorius).

Microscopy

Cells were visualised in culture on an inverted microscope Nikon Diaphot TMD® with phase contrast.

All photographs were taken using cells or tissue mounted on to polished glass slides or Thermanox® coated cover slips. Photographs were taken under white light using a Zeiss photomicroscope IIe® with filters for correction of the light emitted from the tungsten lamp.

Tissue fixation

Tissue fixation used the following procedure

I. Rat mesentery was stored in formal saline 40% volume formaldehyde in 0.9% NaCl (made up in ddH_2O, BDH, UK) for seven days.

II. Each tissue sample was enclosed within a plastic cassette and subjected to dehydration in increasing concentration of ethanol, 65, 75, 95% and absolute ethanol 3x with a residence time of 1 hour at each concentration.

III. This was followed by washes in xylene (BDH, UK) 3x each with a residence time of 1 hour.

IV. The tissues were then flooded with molten wax at 56°C over night before embedding into wax and allowing to cool to room temperature.

V. Wax blocks were kept at room temperature until use when sections of 5mm were cut using a sledge microtome.

VI. Sections were adhered to polished glass slides following the incubation of the slides in poly-L-lysine (SIGMA, UK) (0.1% MW>35,000 in Ultra pure water) until air dried.

VII. Sections were attached to slides by baking at 50°C overnight.

VIII. Dewaxing was performed by incubating the slides in xylene 2x 5 minutes followed by incubating 2x 5 minutes in industrial methylated spirit (IMS, BDH, UK)

Tissue staining

Haematoxylin / eosin (H+E) staining of formalin fixed paraffin wax embedded tissue

I. Dewaxed tissue sections were incubated in Harris haematoxylin for 45 minutes followed by washing in copious amounts of running tap waste.

II. Sections were counter stained in eosin for 30 seconds followed by acid alcohol wash 1x 5 minutes

III. Sections were dehydrated by incubation in IMS 2x 5 minutes and xylene 2x 5 minutes after which DPX was added for coverslip mounting

Antibody labelling of tissue

Tissue were fixed and dewaxed as described in tissue fixation above

I. Primary antibody (rabbit anti-bovine XO) was loaded onto dewaxed sections at a range of concentrations 1:50 – 1:1000 in PBS/Tween 20/Marvel (MPT) and incubated overnight at 4°C in a humidified atmosphere

II. The sections were washed in PBS/Tween 20 (PT) 2x 5 minutes before loading of the secondary swine anti-rabbit biotin conjugated antibody, 1:200 dilution (Dako, Denmark) for 2 hours

III. Sections were washed 2x PT

IV. Avidin biotin complex ABC (Dako, Denmark) was mixed in PT and allowed to stand for 30 minutes before being applied to sections for a further 30 minutes

V. Sections were washed 2x PT

VI. Diamino benzidine (DAB) was used as the chromagen from Fast DAB tablets (SIGMA, UK) by adding to the sections

VII. The reaction was followed until a brown colour was seen, followed by termination of the reaction with the addition of copious amounts of Ultra pure water

VIII. Sections were mounted under coverslips in Aquamount and stored at room temperature until visualisation

Peroxynitrite generation: chemical method (From Crow* et al *(1995))

The following stock solutions were generated

I. 0.6M $NaNO_2$, 0.7M H_2O_2, 0.6M HCl, 1.5M NaOH (SIGMA, UK)

II. $NaNO_2$ was made up in Ultra pure H_2O and mixed rapidly in equal volume with H_2O_2 made up in 0.6M HCl

III. The resultant mixture was then immediately reacted with the NaOH to quench the reaction

IV. To remove excess H_2O_2 the mixture was incubated with MnO_2 for 5 minutes before removing the MnO_2 using a 0.22μm filter.

V. The concentration of ONOO- was measured spectrophotometrically at 303nm in 0.3M NaOH and the mixture aliquotted into 5ml and frozen at –70°C.

VI. One aliquot was allowed to stand at room temperature for 3 days before use and was designated decomposed peroxynitrite (dONOO-)

Appendix II

Protein gel

8% SDS gel

Sodium-dodecyl-sulphate gels were prepared in the following manner for a 10ml mini-prep

I. Mix Ultra pure H_2O 5.384ml, 2ml acrylamide stock (acrylamide 40% w/v, bis-acrylamide 2.105% w/v, Anachem, UK), 2.51ml Tris pH8.8 (Tris base, SIGMA, UK), 100µl SDS (10% stock, SIGMA, UK)

II. Add 10µl TEMED (N,N,N',N'-tetramethyethylene diamine, Promega, UK) and 150µl ammonium persulphate (AMPS, 10% w/v in Ultra pure H_2O made fresh daily, SIGMA, UK) and add to gel apparatus immediately.

III. Add a layer of butan-1-ol saturated water until polymerisation has occurred

5% SDS Stacking gel

Remove butan-1-ol and make up the following mixture for a 3.3ml mini-prep

I. Mix Ultra pure H_2O 2.464ml, 0.416ml acrylamide stock (acrylamide 40% w/v, bis-acrylamide 2.105% w/v, Anachem, UK), 0.42ml Tris buffer pH6.8 (Tris HCl, SIGMA), 33.3µl SDS (10% stock, SIGMA, UK)

II. Add 17µl TEMED and 100µl ammonium persulphate (AMPS, 10%w/v in Ultra pure H_2O made fresh daily, SIGMA, UK) and add to gel apparatus immediately using a comb to generate the wells

Loading Buffer

For 10ml of 2x loading buffer the following amounts were used

I. 2ml SDS (20%w/v) in Ultra pure H_2O, 4ml 50% glycerol, 2ml 1M DTT (dithiothreitol), 1M Tris buffer pH 6.8 (Tris HCl) and 800ml (0.4% w/v stock) bromophenol blue.

Samples were mixed in a 1:1 ratio with bromophenol blue before being incubated at 100°C for 3 minutes for reducing gels.

Appendix II

Running Buffer

For 1L of running buffer the following amounts were used

3.06g Tris base (25mM final concentration) pH8.8, 14.4g glycine (190mM) and 1g SDS (0.001%) made up to 1l in Ultra pure H_20 and stored at room temperature.

Blotting Buffer

As for 1L running buffer with the following additions

200ml methanol (20% final) made up to 1l with Ultra pure H_2O

Washing buffer

1x PBS / 0.5% Tween 20 (final concentration)

Blocking Buffer

5% Non fat dried milk Marvel (Cadbury, UK) in 1x PBS / 0.5% Tween 20

Protein determination: Bradford's assay

The Bio-Rad Protein Assay is based on an observed shift in the absorbance maximum when Coomassie Brilliant Blue G-250 reacts with protein. Bradford first demonstrated the usefulness of this principle in protein assay. Over a broad range of protein concentrations, the dye-binding method gives an accurate, but not entirely linear response.

I. Using a standard of 1.4mgml^{-1} bovine serum albumin, a standard curve was generated by reacting protein with 200µl Bradford's reagent made up to 1ml in Ultra pure H_2O and measuring the coloured product at 595nm

II. Unknown protein concentrations were measured by adding a dilution of protein to 200µl Bradford's reagent and diluting to 1ml in ultra pure H_2O. The absorbance is read at 595nm and the result related to the known concentrations from the standard curve

Appendix II

Grams stain

Bacteria were assessed for their Gram staining to determine phenotype

Bacteria were grown overnight in nutrient broth

I. Crystal violet - 2g, Ammonium oxalate- 0.8g, 95% alcohol - 20mls, Distilled water - 80mls. Dissolve the dye in the alcohol, add the rest, stir for 3 hours and filter.

II. Iodine - 1g, potassium iodide- 2g, distilled water - 300ml. Dissolve iodine and potassium iodide in a small quantity of the water and then add the remainder.

III. A 10µl aliquot was added on to a polished glass slide and spread to generate a smear

IV. The smear was then dried by passing quickly through a yellow Bunsen flame to fix the bacteria

V. Cells were Stained with crystal violet - 1 minute. Washed off with tap water.

VI. Treated with Iodine solution - 2 minutes. Washed in tap water.

VII. Differentiate in acetone 1-2 seconds. Washed in tap water and checked using a microscope. The background should not be purple.

VIII. Counterstained with 1% neutral red for 3-5 minutes. (Filter stain onto slide). Washed in water.

Appendix III

Human Umbilical Vein Endothelial Cell media (HM)

To 500ml M199 media (GIBCO, UK) add

I. 100ml heat inactivated (56°C for 30 minutes) Foetal calf serum (FCS) (final concentration 20%) (GlobePharm, UK)

II. 5000IU Heparin (Monoparin, CP Pharmaceuticals, UK) (50IUml^{-1}) containing Heparin Sodium (Mucous) BP, water, HCl and NaOH for injection

III. 15mg Endothelial cell growth supplement (ECGS, SIGMA, UK) (30μgml^{-1})

IV. Penicillin / Streptomycin (Pen / Strep) 10,000IUml^{-1} / 10,000μgml^{-1} (GIBCO, UK) 100IU ml^{-1} and 100μgml^{-1} respectively

Synovial Microvascular Endothelial Cell media (SM)

As for HM above with the following additions

To 500ml M199 media (GIBCO, UK)

I. 75ml heat inactivated human serum (SIGMA, UK) (final concentration 15%)

II. 10ngml^{-1} Epidermal Growth Factor (EGF) (SIGMA)

Reduced serum SMEC media (rSMEC)

As for HM with the following changes and additions

I. 5ml heat inactivated (56°C for 30 minutes) Foetal calf serum (FCS) (final concentration 1%) (GlobePharm, UK)

Synovial Fibroblast media (SF)

To 500ml Dulbeccos modified eagles media (DMEM) (GIBCO, UK)

I. 50ml FCS heat inactivated (56°C for 30 minutes) (final concentration 10%) (GlobePharm, UK)

II. Penicillin / Streptomycin (Pen / Strep) 10,000IUml^{-1} / 10,000μgml^{-1} (GIBCO, UK) 100IU ml^{-1} and 100μgml^{-1} respectively

Homogenisation Wash (HW)

I. Pepstatin A ($1\mu gml^{-1}$)

II. Antipain ($1\mu gml^{-1}$)

III. Leupeptin ($1\mu gml^{-1}$)

IV. Dulbeccos phosphate buffered saline (PBS) (Oxid, UK)

Homogenisation Buffer (HB)

A for HW with the following additions

I. 50mM KPO_4 pH 7.3

II. 1mM EDTA

III. 1mM PMSF

IV. PBS was changed for Ultra Pure H_2O

Cell count and viability assay

Trypan blue is regarded as a vital dye as it is impermeable to cells with an intact plasma membranes while non viable cells take up the dye and appear blue in colour.

I. 100µl aliquots of call solution were mixed with equal volumes of 0.4% Trypan blue solution (SIGMA, UK) and allowed to stand for 5 minutes at room temperature.

II. A 10µl aliquot of this solution was added to an improved Neubauer haemocytometer by capillary action. Cells were viewed by low power transmitted light microscopy and cells within the central $0.1mm^3$ section of the haemocytometer were counted.

III. Total cell counts were calculated by counting all the cells, blue and clear, in the central area of the two counting chambers and dividing by two and then multiplying by $1x10^4$. This figure represents the original cell number before dilution and expressed as cells per ml.

IV. Viable counts were calculated by repeating the above procedure by counting only the unstained cells.

V. The percentage viable count was calculated by dividing the clear cell count by the total cell count and multiplying by 100.

References

Abbot, S., Kaul, A, Stevens, CR, and Blake, DR. 1992. Isolation and culture of synovial microvascular endothelial cells. Characterization and assessment of adhesion molecule expression. *Arthritis Rheum* 35: 401-6.

Abrams, J. 1980. Nitroglycerin and long-acting nitrates. *N Engl J Med* 302: 1234-7.

Abu-Soud, H., and Stuehr, DJ. 1993. Nitric oxide synthases reveal a role for calmodulin in controlling electron transfer. *Proc Natl Acad Sci U S A* 90: 10769-72.

Abu-Soud, H., Wang, J, Rousseau, DL, Fukuto, JM, Ignarro, LJ, and Stuehr, DJ. 1995. Neuronal nitric oxide synthase self-inactivates by forming a ferrous-nitrosyl complex during aerobic catalysis. *J Biol Chem* 270: 22997-3006.

Abu-Soud, H., Rousseau, DL, and Stuehr, DJ. 1996. Nitric oxide binding to the heme of neuronal nitric-oxide synthase links its activity to changes in oxygen tension. *J. Biol. Chem.* 271: 32515-8.

Adachi, T., Fukushima, T, Usami, Y, and Hirano, K. 1993. Binding of human xanthine oxidase to sulphated glycosaminoglycans on the endothelial-cell surface. *Biochem J* 289: 523-7.

Akaike, T., Sato, K, Ijiri, S, Miyamoto, Y, Kohno, M, Ando, M, and Maeda, H. 1992. Bactericidal activity of alkyl peroxyl radicals generated by heme-iron-catalyzed decomposition of organic peroxides. *Arch Biochem Biophys* 294: 55-63.

Alberts, B., Bray, D, Lewis, J, Raff, M, Roberts, K, and Watson, JD. 1989. *Molecular biology of the cell.* Garland Publishing Inc, New York and London.

Albina, J., Mills, CD, Barbul, A, Thirkill, CE, Henry, WL Jr, Mastrofrancesco, B, and Caldwell, MD. 1988. Arginine metabolism in wounds. *Am J Physiol* 254: E459-67.

Alhama, J., Ruiz-Laguna, J, Rodriguez-Ariza, A, Toribio, F, Lopez-Barea, J, and Pueyo, C. 1998. Formation of 8-oxoguanine in cellular DNA of *Escherichia coli* strains defective in different antioxidant defenses. *Mutagenesis* 13: 589-94.

Alikulov, Z., L'vov, NP, and Kretovich, VL. 1980. Nitrate and nitrite reductase activity of milk xanthine oxidase. *Biokhimiia* 45: 1714-8.

Andrews, C. 1998. Continental shift may have accelerated evolution. Pages 33. Aug 1 *New York Times*, New York.

Arnal, J., Munzel, T, Venema, RC, James, NL, Bai, CL, Mitch, WE, and Harrison, DG. 1995. Interactions between L-arginine and L-glutamine change endothelial NO production. An effect independent of NO synthase substrate availability. *J Clin Invest* 95: 2565-72.

Averill, B., and Vincent, JB. 1993. Electronic absorption spectroscopy of nonheme iron proteins. *Methods Enzymol* 226: 33-51.

Azadzoi, K., Vlachiotis, J, Pontari, M, and Siroky, MB. 1995. Hemodynamics of penile erection: III. Measurement of deep intracavernosal and subtunical blood flow and oxygen tension. *J Urol* 153: 521-6.

Bach. 1911. *Biochem Z* 33: 282.

Ball, E. 1939. *J Biol Chem* 128: 51-67.

Barber, M., and Kay, CJ. 1996. Superoxide production during reduction of molecular oxygen by assimilatory nitrate reductase. *Arch Biochem Biophys* 326: 227-32.

Bauer, M., Beckman, JS, Bridges, RJ, Fuller, CM, and Matalon, S. 1992. Peroxynitrite inhibits sodium uptake in rat colonic membrane vesicles. *Biochim Biophys Acta* 1104: 87-94.

Bautista, A., and Spitzer, JJ. 1994. Inhibition of nitric oxide formation in vivo enhances superoxide release by the perfused liver. *Am J Physiol* 266: G783-8.

Baylis, C, and Vallance, P. 1998. Measurement of nitrite and nitrate levels in plasma and urine--what does this measure tell us about the activity of the endogenous nitric oxide system? *Curr Opin Nephrol Hypertens* 7: 59-62.

Beaudeux, J., Cesarini, ML, Gardes-Albert, M, Maclouf, J, Merval, R, Esposito, B, Peynet, J, and Tedgui, A. 1997. Native and gamma radiolysis-oxidized lipoprotein(a) increase the adhesiveness of rabbit aortic endothelium. *Atherosclerosis* 132: 29-35.

Beaudry, M., Dufour, R, and Marcoux, S. 1995. Relation between infant feeding and infections during the first six months of life. *J Pediatr* 126: 191-7.

Beckman, J., Beckman, TW, Chen, J, Marshall, PA, and Freeman, BA. 1990. Apparent hydroxyl radical production by peroxynitrite: implications for endothelial injury from nitric oxide and superoxide. *Proc Natl Acad Sci U S A* 87: 1620-4.

Beckman, J., Ischiropoulos, H, Zhu L, van der Woerd, M, Smith, C, Chen, J, Harrison, J, Martin, JC, and Tsai, M. 1992. Kinetics of superoxide dismutase- and

iron-catalyzed nitration of phenolics by peroxynitrite. *Arch Biochem Biophys* 298: 438-45.

Beckman, J., and Koppenol, WH. 1996. Nitric oxide, superoxide, and peroxynitrite: the good, the bad, and ugly. *Am J Physiol* 271: C1424-37.

Benboubetra, M., Gleeson, A, Harris, CP, Khan, J, Arrar, L, Brennand, D, Reid, J, Reckless, JD, and Harrison R. 1997. Circulating anti-(xanthine oxidoreductase) antibodies in healthy human adults. *Eur J Clin Invest* 27: 611-9.

Benchimol, M., Almeida, JC, and de Souza W. 1996. Further studies on the organization of the hydrogenosome in *Tritrichomonas foetus*. *Tissue Cell* 28: 287-299.

Ben-Hamida, A., Man, WK, McNeil, N, and Spencer J. 1998. Histamine, xanthine oxidase generated oxygen-derived free radicals and Helicobacter pylori in gastroduodenal inflammation and ulceration. *Inflamm Res* 47: 193-9.

Benjamin, N., O'Driscoll, F, Dougall, H, Duncan, C, Smith, L, Golden, M, and McKenzie, H. 1994. Stomach NO synthesis. *Nature* 368: 502.

Bennett, B., McDonald, BJ, and St James, MJ. 1992a. Hepatic cytochrome P-450-mediated activation of rat aortic guanylyl cyclase by glyceryl trinitrate. *J Pharmacol Exp Ther* 261: 716-23.

Bennett, B., McDonald, BJ, Nigam, R, Long, PG, and Simon, WC. 1992b. Inhibition of nitrovasodilator- and acetylcholine-induced relaxation and cyclic GMP accumulation by the cytochrome P-450 substrate, 7-ethoxyresorufin. *Can J Physiol Pharmacol* 70: 1297-303.

Bennett, B., McDonald, BJ, Nigam, R, and Simon, WC. 1994. Biotransformation of organic nitrates and vascular smooth muscle cell function. *Trends Pharmacol Sci* 15: 245-9.

Berner, R., and Canfield, DE. 1989. A new model for atmospheric oxygen over Phanerozoic time. *American Journal of Science* 289: 333-361.

Biagini, G., Finlay, BJ, and Lloyd, D. 1997. Evolution of the hydrogenosome. *FEMS Microbiol Lett* 155: 133-140.

Blake, D., Stevens, CR, Sahinoglu, T, Ellis, G, Gaffney, K, Edmonds, S, Benboubetra, M, Harrison, R, Jawed, S, Kanczler, J, Millar, TM, Winyard, PG, and Zhang, Z. 1997. Xanthine oxidase: four roles for the enzyme in rheumatoid pathology. *Biochem Soc Trans* 25: 812-6.

Blake, P., Ramos, S, MacDonald, KL, Rassi, V, Gomes, TA, Ivey, C, Bean, NH, and Trabulsi, LR. 1993. Pathogen-specific risk factors and protective factors for acute diarrhoeal disease in urban Brazilian infants. *J Infect Dis* 167: 627-32.

Bogaert, M., and De Schaepdryver, AF. 1968. Tolerance towards glyceryl trinitrate (trinitrin) in dogs. *Arch Int Pharmacodyn Ther* 171: 221-4.

Boger, R., Bode-Boger, SM, Thiele, W, Junker, W, Alexander, K, and Frolich, JC. 1997. Biochemical evidence for impaired nitric oxide synthesis in patients with peripheral arterial occlusive disease. *Circulation* 95: 2068-74.

Bowdy, B., Marple, SL, Pauly, TH, Coonrod, JD, and Gillespie, MN. 1990. Oxygen radical-dependent bacterial killing and pulmonary hypertension in piglets infected with group B streptococci. *Am Rev Respir Dis* 141: 648-53.

Bower, J., Congeni, BL, Cleary, TG, Stone, RT, Wanger, A, Murray, BE, Mathewson, JJ, and Pickering, LK. 1989. *Escherischia coli* O114: nonmotile as a pathogen in an outbreak of severe diarrhea associated with a day care center. *J Infect Dis* 160: 243-7.

Boyum, A. 1968. Isolation of leucocytes from human blood. A two-phase system for removal of red cells with methylcellulose as erythrocyte-aggregating agent. *Scand J Clin Lab Invest Suppl* 97: 9-29.

Bray, R., Pettersson, R, and Ehrenberg, A. 1961. The chemistry of xanthine oxidase. Anaerobic reduction of xanthine oxidase studied by electron spin resonance and magnetic susceptibility. *Biochem J* 81: 178.

Bray, R., and Meriwether, LS. 1996. Electron spin resonance of xanthine oxidase substituted with molybdenum-95. *Nature* 212: 467-9.

Bredt, D., Hwang, PM, Glatt, CE, Lowenstein, C, Reed, RR, and Snyder, SH. 1991. Cloned and expressed nitric oxide synthase structurally resembles cytochrome P-450 reductase. *Nature* 351: 714-8.

Bredt, D., and Snyder, SH. 1994. Nitric oxide: a physiologic messenger molecule. *Annu Rev Biochem* 63: 175-95.

Bruchhaus, I., Richter, S, and Tannich, E. 1997. Characterization of two *E. histolytica* proteins that inactivate reactive oxygen species. *Arch Med Res* 28 Spec: 91-92.

Brul, S., and Stumm, CK. 1994. Symbionts and organelles in anaerobic protozoa and fungi. *Trends In Ecology and Evolution* 9: 319-324.

Brunelli, L., Crow, JP, and Beckman, JS. 1995. The comparative toxicity of nitric oxide and peroxynitrite to *Escherichia coli*. *Arch Biochem Biophys* 316: 327-34.

Buescher, E., and McIlheran, SM. 1993. Polymorphonuclear leukocytes and human colostrum: effects of in vivo and in vitro exposure. *J Pediatr Gastroenterol Nutr* 17: 424-33.

Bunn, H., and Poyton, RO. 1996. Oxygen sensing and molecular adaptation to hypoxia. *Physiol Rev* 76: 839-85.

Burney, S., Tamir, S, Gal, A, and Tannenbaum, SR. 1997. A mechanistic analysis of nitric oxide-induced cellular toxicity. *Nitric Oxide* 1: 130-44.

Burney, S., Caulfield, JL, Niles, JC, Wishnok, JS, and Tannenbaum, SR. 1999. The chemistry of DNA damage from nitric oxide and peroxynitrite. *Mutat Res* 424: 37-49.

Busolo, F., Francescon, L, Aragona, F, and Pagano, F. 1995. Solid-phase binding of clinical isolates of *Escherichia coli* expressing different piliation phenotypes. Effect of glycosaminoglycans. *Urol Res* 22: 399-402.

Busse, R., and Mulsch, A. 1990. Induction of nitric oxide synthase by cytokines in vascular smooth muscle cells. *FEBS Lett* 275: 87-90.

Butler, A., Flitney, FW, and Williams, DL. 1995. NO, nitrosonium ions, nitroxide ions, nitrosothiols and iron-nitrosyls in biology: a chemist's perspective. *Trends Pharmacol Sci* 16: 18-22.

Byun, J., Henderson, JP, Mueller, DM, and Heinecke, JW. 1999. 8-Nitro-2'-deoxyguanosine, a specific marker of oxidation by reactive nitrogen species, is generated by the myeloperoxidase-hydrogen peroxide-nitrite system of activated human phagocytes. *Biochemistry* 38: 2590-600.

Camara, L., Carbonare, SB, Scaletsky, IC, da Silva, ML, and Carneiro-Sampaio, MM. 1995. Inhibition of enteropathogenic *Escherichia coli* (EPEC) adherence to HeLa cells by human colostrum. Detection of specific sIgA related to EPEC outer-membrane proteins. *Adv Exp Med Biol* 371: 673-6.

Carpenter, J. 1966. New measurements of oxygen solubility in pure and natural water. *Limnol and Oceanog* 11: 267-77.

Carr, G., Page, MD, and Ferguson, SJ. 1989. The energy-conserving nitric-oxide-reductase system in *Paracoccus denitrificans*. Distinction from the nitrite reductase that catalyses synthesis of nitric oxide and evidence from trapping

experiments for nitric oxide as a free intermediate during denitrification. *Eur J Biochem* 179: 683-92.

Carr, G., and Ferguson, SJ. 1990. Nitric oxide formed by nitrite reductase of *Paracoccus denitrificans* is sufficiently stable to inhibit cytochrome oxidase activity and is reduced by its reductase under aerobic conditions. *Biochim Biophys Acta* 1017: 57-62.

Carreras, M., Pargament, GA, Catz, SD, Poderoso, JJ, and Boveris, A. 1994. Kinetics of nitric oxide and hydrogen peroxide production and formation of peroxynitrite during the respiratory burst of human neutrophils. *FEBS Lett* 341: 65-8.

Chung, S., Chong, S, Seth, P, Jung, CY, and Fung, HL. 1992. Conversion of nitroglycerin to nitric oxide in microsomes of the bovine coronary artery smooth muscle is not primarily mediated by glutathione-S-transferases. *J Pharmacol Exp Ther* 260: 652-9.

Chung-Welch, N., Patton, WF, Yen-Patton, GP, Hechtman, HB, and Shepro, D. 1989. Phenotypic comparison between mesothelial and microvascular endothelial cell lineages using conventional endothelial cell markers, cytoskeletal protein markers and in vitro assays of angiogenic potential. *Differentiation* 42: 44-53.

Cole, J. 1996. Nitrate reduction to ammonia by enteric bacteria: redundancy, or a strategy for survival during oxygen starvation? *FEMS Microbiol Lett* 136: 1-11.

Collins, P., Macey, MG, Cahill, MR, and Newland, AC. 1993. von Willebrand factor release and P-selectin expression is stimulated by thrombin and trypsin but not IL-1 in cultured human endothelial cells. *Thromb Haemost* 70: 346-50.

Corran, H., Dewan, JG, Gordon, AH and Green, DE. 1939. *Biochem. J.* 33: 1694-1708.

Cossins, A., and Prosser, CL. 1978. Evolutionary adaptation of membranes to temperature. *Proc Natl Acad Sci U S A* 75: 2040-3.

Craven, P., and DeRubertis, FR. 1978. Restoration of the responsiveness of purified guanylate cyclase to nitrosoguanidine, nitric oxide, and related activators by heme and hemeproteins. Evidence for involvement of the paramagnetic nitrosyl-heme complex in enzyme activation. *J Biol Chem* 253: 8433-43.

Cravioto, A., Tello, A, Villafan, H, Ruiz, J, del Vedovo, S, and Neeser, JR. 1991. Inhibition of localized adhesion of enteropathogenic *Escherichia coli* to HEp-2 cells by immunoglobulin and oligosaccharide fractions of human colostrum and breast milk. *J Infect Dis* 163: 1247-55.

Crawford, M., and Goldberg, DE. 1998. Regulation of the *Salmonella typhimurium* flavohemoglobin gene. A new pathway for bacterial gene expression in response to nitric oxide. *J Biol Chem* 273: 34028-32.

Crow, J., Beckman, JS, and McCord, JM. 1995. Sensitivity of the essential zinc-thiolate moiety of yeast alcohol dehydrogenase to hypochlorite and peroxynitrite. *Biochemistry* 34: 3544-52.

Crow, J. 1997. Dichlorodihydrofluorescein and dihydrorhodamine 123 are sensitive indicators of peroxynitrite in vitro: implications for intracellular measurement of reactive nitrogen and oxygen species. *Nitric Oxide* 1: 145-57.

Cunliffe, N., Kilgore, PE, Bresee, JS, Steele, AD, Luo, N, Hart, CA, and Glass, RI. 1998. Epidemiology of rotavirus diarrhoea in Africa: a review toassess the need for rotavirus immunization. *Bull World Health Organ* 76: 525-37.

Danson, M. 1988. Archaebacteria: the comparitive enzymology of their central metabolic pathways. *Advanced Microbial Physiology* 29: 165-231.

Darzynkiewicz, Z., and Crissman, HA. 1990. Flow cytometry. Pages 1-5 in Z. Darzynkiewicz, and Crissman, HA, ed. *Methods in cell biology: Flow cytometry.* Academic Press Inc, San Diego.

DeChatelet, L., Mulikin, D, and McCall, CE. 1975. The generation of superoxide anion by various types of phagocyte. *J Infect Dis* 131: 443-6.

DeJong, J., van der Meer, P, Nieukoop, AS, Huizer, T, Stroeve, RJ, and Bos, E. 1990. Xanthine oxidoreductase activity in perfused hearts of various species, including humans. *Circ Res* 67: 770-3.

Denicola, A., Souza, JM, and Radi, R. 1998. Diffusion of peroxynitrite across erythrocyte membranes. *Proc Natl Acad Sci U S A* 95: 3566-71.

DeRubertis, F., Craven, PA, and Pratt, DW. 1978. Electron spin resonance study of the role of nitrosyl-heme in the activation of guanylate cyclase by nitrosoguanidine and related agonists. *Biochem Biophys Res Commun* 83: 158-67.

Deutsch, A., Greshake, A, Personen, LJ and Pihlaja, P. 1998. Unaltered cosmic spherules in a 1.4-Gyr-old sandstone from Finland. *Nature* 395: 146-148.

Dhople, A. 1996. In vitro susceptibility of *Mycobacterium leprae* to oxygen-mediated damage. *Microbios* 85: 35-44.

Diamond, J., and Holmes, TG. 1975. Effects of potassium chloride and smooth muscle relaxants on tension and cyclic nucleotide levels in rat myometrium. *Can J Physiol Pharmacol* 53: 1099-107.

Diamond, J., and Blisard, KS. 1976. Effects of stimulant and relaxant drugs on tension and cyclic nucleotide levels in canine femoral artery. *Mol Pharmacol* 12: 668-92.

Diaz, J., and De Souza, W. 1997. Purification and biochemical characterization of the hydrogenosomes of the flagellate protozoan *Tritrichomonas foetus*. *Eur J Cell Biol* 74: 85-91.

Dillon, W., Hampl, V, Shultz, PJ, Rubins, JB, and Archer, SL. 1996. Origins of breath nitric oxide in humans. *Chest* 110: 930-8.

Dixon, M. 1926. XCIII. Studies on xanthine oxidase. VII. The specificity of the system. *Biochem J* 20: 703-18.

Dixon, M. and Thurlow., S. 1924. *Biochem J.* 18: 971-975.

Djuretic, T. 1997. Food poisoning: the increase is genuine. *Practitioner* 241: 752-6.

Donnenberg, M., and Kaper, JB. 1992. Enteropathogenic *Escherichia coli*. *Infect Immun* 60: 3956-61.

Donnenberg, M., Kaper, JB, and Finlay, BB. 1997. Interactions between enteropathogenic *Escherichia coli* and host epithelial cells. *Trends Microbiol* 5: 109-14.

Douglas, P., Moorhead, G, Hong, Y, Morrice, N, and MacKintosh, C. 1998. Purification of a nitrate reductase kinase from *Spinacea oleracea* leaves, and its identification as a calmodulin-domain protein kinase. *Planta* 206: 435-42.

Drapier, J., and Hibbs, JB Jr. 1986. Murine cytotoxic activated macrophages inhibit aconitase in tumor cells.
Inhibition involves the iron-sulfur prosthetic group and is reversible. *J Clin Invest* 78: 790-7.

Drapier, J. 1997. Interplay between NO and [Fe-S] clusters: relevance to biological systems. *Methods* 11: 319-29.

Drath, D., and Karnovsky, ML. 1975. Superoxide production by phagocytic leukocytes. *J Exp Med* 114: 257-62.

Dubourdieu, M., and DeMoss, JA. 1992. The narJ gene product is required for biogenesis of respiratory nitrate reductase in *Escherichia coli*. *J Bacteriol* 174: 867-72.

Dudley, R. 1998. Atmospheric oxygen, giant paleozoic insects and the evolution of ariel locomotor performance. *Journal of Experimental Biology* 201: 1043-1050.

Duensing, T., and Putten, JP. 1998. Vitronectin binds to the gonococcal adhesin OpaA through a glycosaminoglycan molecular bridge. *Biochem J* 334: 133-9.

Duensing, T., Wing, JS, and van Putten, JP. 1999. Sulfated polysaccharide-directed recruitment of mammalian host proteins: a novel strategy in microbial pathogenesis. *Infect Immun* 67: 4463-8.

Duncan, C., Dougall, H, Johnston, P, Green, S, Brogan, R, Leifert, C, Smith, L, Golden, M, and Benjamin, N. 1995. Chemical generation of nitric oxide in the mouth from the enterosalivary circulation of dietary nitrate. *Nat Med* 1: 546-51.

Dunn, J., Hochachka, PW, Davison, W, and Guppy, M. 1983. Metabolic adjustments to diving and recovery in the African lungfish. *Am J Physiol* 245: R651-7.

Dweik, R., Laskowski, D, Abu-Soud, HM, Kaneko, F, Hutte, R, Stuehr, DJ and Erzurum, SC. 1998. Nitric oxide synthesis in the lung. Regulation by oxygen through a kinetic mechanism. *J. Clin. Invest.* 101: 660-6.

Dykhuizen, R., Frazer, R, Duncan, C, Smith, CC, Golden, M, Benjamin, N, and Leifert, C. 1996. Antimicrobial effect of acidified nitrite on gut pathogens: importance of dietary nitrate in host defense. *Antimicrob Agents Chemother* 40: 1422-5.

Edwards, JO, and Plumb, RC. 1994. The chemistry of peroxonitrites. *Prog. Inorg. Chem.* 41: 599-635.

Elsayed, N., Nakashima, JM, and Postlethwait, EM. 1993. Measurement of uric acid as a marker of oxygen tension in the lung. *Arch Biochem Biophys* 302: 228-32.

Emeis, J., van den Eijnden-Schrauwen, Y, van den Hoogen, CM, de Priester, W, Westmuckett, A, and Lupu, F. 1997. An endothelial storage granule for tissue-type plasminogen activator. *J Cell Biol* 139: 245-56.

Enghild, J., Thogersen, IB, Oury, TD, Valnickova, Z, Hojrup, P, and Crapo, JD. 1999. The heparin-binding domain of extracellular superoxide dismutase is proteolytically processed intracellularly during biosynthesis. *J Biol Chem* 274: 14818-22.

Faulkner, K., and Fridovich, I. 1993. Luminol and lucigenin as detectors for O_2.-. *Free Radic Biol Med* 15: 447-51.

Fee, J. 1991. Regulation of sod genes in *Escherichia coli*: relevance to superoxide dismutase function. *Mol Microbiol* 5: 2599-610.

Feelisch, M., and Noack, E. 1987. Nitric oxide (NO) formation from nitrovasodilators occurs independently of hemoglobin or non-heme iron. *Eur J Pharmacol* 142: 465-9.

Feelisch, M., te Poel, M, Zamora, R, Deussen, A, and Moncada, S. 1994. Understanding the controversy over the identity of EDRF. *Nature* 368: 62-5.

Feelisch, M., Brands, F, and Kelm, M. 1995. Human endothelial cells bioactivate organic nitrates to nitric oxide: implications for the reinforcement of endothelial defense mechanisms. *Eur J Clin Invest* 25: 737-45.

Fenchel, T. 1996. Eukaryotic life: anaerobic physiology. Pages 185-203 in D. Roberts, Sharp, P, Alderson, G and Collins, M, ed. *Evolution of microbial life*. Cambridge University Press, Cambridge.

Foley, E., Lee, SW, and Hartley, NJ. 1946. The effect of penicillin on *Staphylococci* and *Streptococci* commonly associated with bovine mastitis. *J Food Technology* 8: 129-33.

Frankel, G., Phillips, AD, Rosenshine, I, Dougan, G, Kaper, JB, and Knutton, S. 1998. Enteropathogenic and enterohaemorrhagic *Escherichia coli*: more subversive elements. *Mol Microbiol* 30: 911-21.

Frevert, U., Sinnis, P, Cerami, C, Shreffler, W, Takacs, B, and Nussenzweig, V. 1993. Malaria circumsporozoite protein binds to heparan sulfate proteoglycans associated with the surface membrane of hepatocytes. *J Exp Med* 177: 1287-98.

Fridovich, I., and Handler, P. 1961. Detection of free radicals generated during enzymic oxidations by the initiation of sulphite oxidation. *J. Biol. Chem.* 236: 1836-1840.

Fridovich, I., and Handler, P. 1962. Xanthine oxidase: V. Differential inhibition of the reduction of various electron acceptors. *J Biol Chem* 237: 916-21.

Fujii, H., Ichimori, K, Hoshiai, K, and Nakazawa, H. 1997. Nitric oxide inactivates NADPH oxidase in pig neutrophils by inhibiting its assembling process. *J Biol Chem* 272: 32773-8.

Fukushima, T., Adachi, T, and Hirano, K. 1995. The heparin-binding site of human xanthine oxidase. *Biol Pharm Bull* 18: 156-8.

Furchgott, R., and Zawadzki, JV. 1980. The obligatory role of endothelial cells in the relaxation of arterial smooth muscle by acetylcholine. *Nature* 288: 373-6.

Furchgott, R. 1988. Studies on relaxation of rabbit aorta by sodium nitrite: The basis for the proposal that the acid-activatable inhibitory factor from retractor penis is inorganic nitrite and the endothelium-derived relaxing factor is nitric oxide. Pages 401-14 in P. Vanhoutte, ed. *Vasodilation: Vascular smooth muscle, peptides, autonomic nerves,and endothelium.* Raven Press, New York.

Gal, A., and Wogan, GN. 1996. Mutagenesis associated with nitric oxide production in transgenic SJL mice. *Proc Natl Acad Sci U S A* 93: 15102-7.

Gallin, J., Goldstein IM and Snyderman R. 1988. *Inflammation, Basic principles and clinical correlates.* Raven Press, New York.

Gardlik, S., Barber, MJ, and Rajagopalan, KV. 1987. A molybdopterin-free form of xanthine oxidase. *Arch Biochem Biophys* 259: 363-71.

Gardner, P., Costantino, G, Szabo, C, and Salzman, AL. 1997. Nitric oxide sensitivity of the aconitases. *J Biol Chem* 272: 25071-6.

Gardner, T., Stewart, JR, Casale, AS, Downey, JM, and Chambers, DE. 1983. Reduction of myocardial ischemic injury with oxygen-derived free radical scavengers. *Surgery* 94: 423-7.

Gaston, B., Drazen, JM, Loscalzo, J, and Stamler, JS. 1994. The biology of nitrogen oxides in the airways. *Am J Respir Crit Care Med* 149: 538-51.

Gest, H. 1980. The evolution of biological energy-transducing systems. *FEMS Microbiological Letters* 7: 73-77.

Ghio, S., de Servi, S, Perotti, R, Eleuteri, E, Montemartini, C, and Specchia, G. 1992. Different susceptibility to the development of nitroglycerin tolerance in the arterial and venous circulation in humans. Effects of N-acetylcysteine administration. *Circulation* 86: 798-802.

Gimbrone, M. J., Cotran, RS, and Folkman, J. 1974. Human vascular endothelial cells in culture. Growth and DNA synthesis. *J Cell Biol* 60: 673-84.

Glover, J. 1975. Chemiluminescence in gas analysis and Flame-emission spectrometry. *Analyst* 100: 449-64.

Godden, J., Turley, S, Teller, DC, Adman, ET, Liu, MY, Payne, WJ, and LeGall, J. 1991. The 2.3 angstrom X-ray structure of nitrite reductase from *Achromobacter cycloclastes*. *Science* 253: 438-42.

Gold, H., and Moellering, RC Jr. 1996. Antimicrobial-drug resistance. *N Engl J Med* 335: 1445-53.

Goldman, A., Thorpe, LW, Goldblum, RM, and Hanson, LA. 1986. Anti-inflammatory properties of human milk. *Acta Paediatr Scand* 75: 689-95.

Gonzalez, C., Almaraz, L, Obeso, A, and Rigual, R. 1992. Oxygen and acid chemoreception in the carotid body chemoreceptors. *Trends Neurosci* 15: 146-53.

Gort, A., and Imlay, JA. 1998. Balance between endogenous superoxide stress and antioxidant defenses. *J Bacteriol* 180: 1402-10.

Graham, J., Dudley, R, Aguilar, N and Gans, C. 1995. Implications of the late Palaeozoic oxygen pulse for physiology and evolution. *Nature* 375: 117-120.

Granger, D., Sennett, M, McElearney, P, and Taylor, AE. 1980. Effect of local arterial hypotension on cat intestinal capillary permeability. *Gastroenterology* 79: 474-80.

Granger, D., Rutili, G, and McCord, JM. 1981. Superoxide radicals in feline intestinal ischemia. *Gastroenterology* 81: 22-9.

Granger, D., and Kubes, P. 1996. Nitric oxide as antiinflammatory agent. *Methods Enzymol* 269: 434-42.

Granger, D., Anstey, NM, Miller, WC, and Weinberg, JB. 1999. Measuring nitric oxide production in human clinical studies. *Methods Enzymol* 301: 49-61.

Green, E., and Carritt, DE. 1967. New tables for oxygen saturation of seawater. *J Marine Res* 25: 140-47.

Green, L., Wagner, DA, Glogowski, J, Skipper, PL, Wishnok, JS, and Tannenbaum, SR. 1982. Analysis of nitrate, nitrite, and [15N]nitrate in biological fluids. *Anal Biochem* 126: 131-8.

Griffith, T., Edwards, DH, Lewis, MJ, Newby, AC, and Henderson, AH. 1984. The nature of endothelium-derived vascular relaxant factor. *Nature* 308: 645-7.

Grisham, M., Granger, DN, and Lefer, DJ. 1998. Modulation of leukocyte-endothelial interactions by reactive metabolites of oxygen and nitrogen: relevance to ischemic heart disease. *Free Radic Biol Med* 25: 404-33.

Grisham, M., Jourd'Heuil, D, and Wink, DA. 1999. Nitric oxide. I. Physiological chemistry of nitric oxide and its metabolites: implications in inflammation. *Am J Physiol* 276: G315-21.

Gruetter, C., Barry, BK, McNamara, DB, Gruetter, DY, Kadowitz, PJ, and Ignarro, L. 1979. Relaxation of bovine coronary artery and activation of coronary arterial guanylate cyclase by nitric oxide, nitroprusside and a carcinogenic nitrosoamine. *J Cyclic Nucleotide Res* 5: 211-24.

Gruetter, C., Barry, BK, McNamara, DB, Kadowitz, PJ, and Ignarro, LJ. 1980. Coronary arterial relaxation and guanylate cyclase activation by cigarette smoke, N'-nitrosonornicotine and nitric oxide. *J Pharmacol Exp Ther* 214: 9-15.

Gruetter, C., Gruetter, DY, Lyon, JE, Kadowitz, PJ, and Ignarro, LJ. 1981a. Relationship between cyclic guanosine 3':5'-monophosphate formation and relaxation of coronary arterial smooth muscle by glyceryl trinitrate, nitroprusside, nitrite and nitric oxide: effects of methylene blue and methemoglobin. *J Pharmacol Exp Ther* 219: 181-6.

Gruetter, C., Kadowitz, PJ, and Ignarro, LJ. 1981b. Methylene blue inhibits coronary arterial relaxation and guanylate cyclase activation by nitroglycerin, sodium nitrite, and amyl nitrite. *Can J Physiol Pharmacol* 59: 150-6.

Grulee, E., Sanford,HN, and Schwarz, H. 1934. Breast and artificial fed infants. *J Am Med Assoc* 103: 735-39.

Grum, C., Ragsdale, RA, Ketai, LH, and Shlafer, M. 1986. Absence of xanthine oxidase or xanthine dehydrogenase in the rabbit myocardium. *Biochem Biophys Res Commun* 141: 1104-8.

Gryglewski, R., Palmer, RM, and Moncada, S. 1986. Superoxide anion is involved in the breakdown of endothelium-derived vascular relaxing factor. *Nature* 320: 454-6.

Hackenthal, E., and Hackenthal, R. 1966. Competitive inhibitors of nitrate reduction by xanthine oxidase. *Naturwissenschaften* 53: 81.

Haenen, G., Paquay, JB, Korthouwer, RE, and Bast, A. 1997. Peroxynitrite scavenging by flavonoids. *Biochem Biophys Res Commun* 236: 591-3.

Halfpenny, E., and Robinson, PL. 1952. The nitration and hydroxylation of aromatic compounds by pernitrous acid. *J. Chem. Soc.* : 939-46.

Halfpenny, E., and Robinson, PI. 1952. Pernitrous acid. The reaction between hydrogen peroxide and nitrous acid and the properties of an intermediate product. *J. Chem. Soc.* : 928-38.

Hampton, M., Kettle, AJ, and Winterbourn, CC. 1998. Inside the neutrophil phagosome: oxidants, myeloperoxidase, and bacterial killing. *Blood* 92: 3007-17.

Hamzaoui, N., and Pringault, E. 1998. Interaction of microorganisms, epithelium, and lymphoid cells of the mucosa-associated lymphoid tissue. *Ann N Y Acad Sci* 859: 65-74.

Hancock, J., and Jones, OT. 1987. The inhibition by diphenyleneiodonium and its analogues of superoxide generation by macrophages. *Biochem J* 242: 103-7.

Harrison, J., and Svec, TA. 1998. The beginning of the end of the antibiotic era? Part I. The problem: abuse of the "miracle drugs". *Quintessence Int* 29: 151-62.

Hart, C., and Cunliffe, NA. 1997. Viral gastroenteritis. *Curr Opin Infect Dis* 10: 408-13.

Hassoun, P., Yu, FS, Cote, CG, Zulueta, JJ, Sawhney, R, Skinner, KA, Skinner, HB, Parks, DA,, and J. and Lanzillo. 1998. Upregulation of xanthine oxidase by lipopolysaccharide, interleukin-1, and hypoxia. Role in acute lung injury. *Am J Respir Crit Care Med* 158: 299-305.

Hattori, R., Hamilton, KK, McEver, RP, and Sims, PJ. 1989. Complement proteins C5b-9 induce secretion of high molecular weight multimers of endothelial von Willebrand factor and translocation of granule membrane protein GMP-140 to the cell surface. *J Biol Chem* 264: 9053-60.

Hausladen, A., Gow, AJ, and Stamler, JS. 1998. Nitrosative stress: metabolic pathway involving the flavohemoglobin. *Proc Natl Acad Sci U S A* 95: 14100-5.

Hawkes, T., and Bray, RC. 1984. Quantitative transfer of the molybdenum cofactor from xanthine oxidase and from sulphite oxidase to the deficient enzyme of the nit-1 mutant of Neurospora crassa to yield active nitrate reductase. *Biochem J* 219: 481-93.

Hawkey, P. 1998. The origins and molecular basis of antibiotic resistance. *BMJ* 317: 657-60.

Heinzel, B., John, M, Klatt, P, Bohme, E, and Mayer, B. 1992. Ca2+/calmodulin-dependent formation of hydrogen peroxide by brain nitric oxide synthase. *Biochem J* 281: 627-30.

Henry, Y., Ducrocq, C, Drapier, JC, Servent, D, Pellat, C, and Guissani, A. 1991. Nitric oxide, a biological effector. Electron paramagnetic resonance detection of nitrosyl-iron-protein complexes in whole cells. *Eur Biophys J* 20: 1-15.

Henry, Y., Lepoivre, M, Drapier, JC, Ducrocq, C, Boucher, JL, and Guissani, A. 1993. EPR characterization of molecular targets for NO in mammalian cells and organelles. *FASEB J* 7: 1124-34.

Heppel, L., and Hilmoe, RJ. 1950. *J Biol Chem* 183: 129.

Hille, R. 1996. The mononuclear molybdenum enzymes. *Chem Rev* 96: 2757-816.

Ho, F., Wong, RL, and Lawton, JW. 1979. Human colostral and breast milk cells. A light and electron microscopic study. *Acta Paediatr Scand* 68: 389-96.

Hochachka, P., Gunga, HC, and Kirsch, K. 1998. Our ancestral physiological phenotype: an adaptation for hypoxia tolerance and for endurance performance? *Proc Natl Acad Sci U S A* 95: 1915-20.

Hoidal, J., Xu, P, Huecksteadt, T, Sanders, KA, and Pfeffer, K. 1997. Transcriptional regulation of human xanthine dehydrogenase/xanthine oxidase. *Biochem Soc Trans* 25: 796-9.

Holland, H. 1994. Early proterozoic atmospheric change. Pages 237-244 in S. Bengtson, ed. *Early Life on Earth.* Columbia University Press, New York.

Horecker, B., and Heppel, LA. 1949. The reduction of cytochrome c by xanthine oxidase. *J.Biol. Chem* 178: 683-690.

Hotz, H., Uzzell, T, and Berger, L. 1997. Linkage groups of protein-coding genes in western palearctic water frogs reveal extensive evolutionary conservation. *Genetics* 147: 255-70.

Houston, M., Estevez, A, Chumley, P, Aslan, M, Marklund, S, Parks, DA, and Freeman, BA. 1999. Binding of xanthine oxidase to vascular endothelium. Kinetic characterization and oxidative impairment of nitric oxide-dependent signaling. *J Biol Chem* 274: 4985-94.

Hsia, C. 1998. Respiratory function of hemoglobin. *N Engl J Med* 338: 239-47.

Huber, R., Hof, P, Duarte, RO, Moura, JJ, Moura, I, Liu, MY, LeGall, J, Hille, R, Archer, M, and Romao, MJ. 1996. A structure-based catalytic mechanism for the xanthine oxidase family of molybdenum enzymes. *Proc Natl Acad Sci U S A* 93: 8846-51.

Hughes, M., and Nicklin, HG. 1968. The chemistry of pernitrites. Part I. Kinetics of decomposition of pernitrous acid. *J. Chem. Soc.* A: 450-52.

Hughes, M., and Nicklin, HG. 1970. A possible role for the species peroxonitrite in nitrification. *Biochim Biophys Acta* 222: 660-1.

Huie, R., and Padmaja, S. 1993. The reaction of NO with superoxide. *Free Radic Res Commun* 18: 195-9.

Humphries, D., Lee, SL, Fanburg, BL, and Silbert, JE. 1986. Effects of hypoxia and hyperoxia on proteoglycan production by bovine pulmonary artery endothelial cells. *J Cell Physiol* 126: 249-53.

Ichida, K., Amaya, Y, Noda, K, Minoshima, S, Hosoya, T, Sakai, O, Shimizu, N, and Nishino, T. 1993. Cloning of the cDNA encoding human xanthine dehydrogenase (oxidase): structural analysis of the protein and chromosomal location of the gene. *Gene* 133: 279-84.

Ichikawa, M., Nishino, T, Nishino, T, and Ichikawa, A. 1992. Subcellular localization of xanthine oxidase in rat hepatocytes: high-resolution immunoelectron microscopic study combined with biochemical analysis. *J Histochem Cytochem* 40: 1097-103.

Ichimori, K., Fukahori, M, Nakazawa, H, Okamoto, K, and Nishino, T. 1999. Inhibition of xanthine oxidase and xanthine dehydrogenase by nitric oxide. Nitric oxide converts reduced xanthine-oxidizing enzymes into the desulfo-type inactive form. *J Biol Chem* 274: 7763-8.

Ignarro, L., and Gruetter, CA. 1980. Requirement of thiols for activation of coronary arterial guanylate cyclase by glyceryl trinitrate and sodium nitrite: possible involvement of S-nitrosothiols. *Biochim Biophys Acta* 631: 221-31.

Ignarro, L., Byrns, RE, and Wood, KS. 1988. Biochemical and pharmacological properties of endothelium-derived relaxing factor and its similarity to nitric oxide radicals. Pages 427-36 in P. Vanhoutte, ed. *Vasodilation: Vascular*

smooth muscle, peptides, autonomic nerves, and endothelium. Raven Press, New York.

Ischiropoulos, H., Zhu, L, and Beckman, JS. 1992. Peroxynitrite formation from macrophage-derived nitric oxide. *Arch Biochem Biophys* 298: 446-51.

Iverson, D., DeChatelet, LR, Spitznagel, JK, and Wang, PJ. 1977. Comparison of NADH and NADPH oxidase activities in granules isolated from human polymorphonuclear leukocytes with a fluorometric assay. *J Clin Invest* 59: 282-90.

Iyengar, R., Stuehr, DJ, and Marletta, MA. 1987. Macrophage synthesis of nitrite, nitrate, and N-nitrosamines: precursors and role of the respiratory burst. *Proc Natl Acad Sci U S A* 84: 6369-73.

Jackson, T., Ellard, FM, Ghazaleh, RA, Brookes, SM, Blakemore, WE, Corteyn, AH, Stuart, DI, Newman, JW, and King, AM. 1996. Efficient infection of cells in culture by type O foot-and-mouth disease virus requires binding to cell surface heparan sulfate. *J Virol* 70: 5282-7.

Jaffe, E., Nachman, RL, Becker, CG, and Minick, CR. 1973. Culture of human endothelial cells derived from umbilical veins. Identification by morphologic and immunologic criteria. *J Clin Invest* 52: 2745-56.

James, B., and Keevil, CW. 1999. Influence of oxygen availability on physiology, verocytotoxin expression and adherence of Escherichia coli O157. *J Appl Microbiol* 86: 117-24

Johnson, J., Indermaur, LW, and Rajagopalan, KV. 1991. Molybdenum cofactor biosynthesis in *Escherichia coli.* Requirement of the chlB gene product for the formation of molybdopterin guanine dinucleotide. *J Biol Chem* 266: 12140-5.

Johnston, A. 1998. Use of antimicrobial drugs in veterinary practice. *BMJ* 317: 665-7.

Jones, R., Lamont, A, and Garland, PB. 1980. The mechanism of proton translocation driven by the respiratory nitrate reductase complex of *Escherichia coli. Biochem J* 190: 79-94.

Kameda, H., Morita, I, Handa, M, Kaburaki, J, Yoshida, T, Mimori, T, Murota, S, and Ikeda, Y. 1997. Re-expression of functional P-selectin molecules on the endothelial cell surface by repeated stimulation with thrombin. *Br J Haematol* 97: 348-55.

Kanner, J., Harel, S, and Granit, R. 1991. Nitric oxide as an antioxidant. *Arch Biochem Biophys* 289: 130-6.

Kantrow, S., Huang, YC, Whorton, AR, Grayck, EN, Knight, JM, Millington, DS and Piantadosi, CA. 1997. Hypoxia inhibits nitric oxide synthesis in isolated rabbit lung. *Am. J. Physiol.* 272: L1167-73.

Karlinsky, J., Rounds, S, and Farber, HW. 1992. Effects of hypoxia on heparan sulfate in bovine aortic and pulmonary artery endothelial cells. *Circ Res* 71: 782-9.

Kay, C., Solomonson, LP, and Barber, MJ. 1990. Oxidation-reduction potentials of flavin and Mo-pterin centers in assimilatory nitrate reductase: variation with pH. *Biochemistry* 29: 10823-8.

Keen, J., Habig, WH, and Jakoby, WB. 1976. Mechanism for the several activities of the glutathione S-transferases. *J Biol Chem* 251: 6183-8.

Kelm, M., Dahmann, R, Wink, D, and Feelisch, M. 1997. The nitric oxide/superoxide assay. Insights into the biological chemistry of the NO/O-2. interaction. *J Biol Chem* 272: 9922-32.

Kelm, M., Feelisch, M, Spahr, R, Piper, HM, Noack, E, and Schrader, J. 1998. Quantitative and kinetic characterization of nitric oxide and EDRF released from cultured endothelial cells. *Biochem Biophys Res Commun* 154: 236-44.

Kenkare, S., and Benet, LZ. 1993. Effect of ethacrynic acid, a glutathione-S-transferase inhibitor, on nitroglycerin-mediated cGMP elevation and vasorelaxation of rabbit aortic strips. *Biochem Pharmacol* 46: 279-84.

Kennedy, L., Moore, K Jr, Caulfield, JL, Tannenbaum, SR, and Dedon, PC. 1997. Quantitation of 8-oxoguanine and strand breaks produced by four oxidizing agents. *Chem Res Toxicol* 10: 386-92.

Kharitonov, V., Sundquist, AR, and Sharma, VS. 1994. Kinetics of nitric oxide autoxidation in aqueous solution. *J Biol Chem* 269: 5881-3.

Kim, N., Vardi, Y, Padma-Nathan, H, Daley, J, Goldstein, I, and Saenz de Tejada, I. 1993. Oxygen tension regulates the nitric oxide pathway. Physiological role in penile erection. *J Clin Invest* 91: 437-42.

Kimura, H., Mittal, CK, and Murad, F. 1975. Activation of guanylate cyclase from rat liver and other tissues by sodium azide. *J Biol Chem* 250: 8016-22.

Kissner, R., Nauser, T, Bugnon, P, Lye, PG, and Koppenol, WH. 1997. Formation and properties of peroxynitrite as studied by laser flash photolysis, high-

pressure stopped-flow technique, and pulse radiolysis. *Chem Res Toxicol* 10: 1285-92.

Kjellen, L., and Lindahl, U. 1991. Proteoglycans: structures and interactions. *Annu Rev Biochem* 60: 443-75.

Klausen, T., Poulsen, TD, Fogh-Andersen, N, Richalet, JP, Nielsen, OJ, and Olsen, NV. 1996. Diurnal variations of serum erythropoietin at sea level and altitude. *Eur J Appl Physiol* 72: 297-302.

Klocking, H., and Markwardt, F. 1994. Pharmacological stimulation of t-PA release. *Pharmazie* 49: 227-30.

Koike, K., Moore, FA, Moore, EE, Read, RA, Carl, VS, and Banerjee, A. 1993. Gut ischemia mediates lung injury by a xanthine oxidase-dependent neutrophil mechanism. *J Surg Res* 54: 469-73.

Kooistra, T., Schrauwen, Y, Arts, J, and Emeis, JJ. 1994. Regulation of endothelial cell t-PA synthesis and release. *Int J Hematol* 59: 233-55.

Kooy, N., Royall, JA, Ischiropoulos, H, and Beckman, JS. 1994. Peroxynitrite-mediated oxidation of dihydrorhodamine 123. *Free Radic Biol Med* 16: 149-56.

Koppenol, W., Moreno, JJ, Pryor, WA, Ischiropoulos, H, Beckman, JS. 1992. Peroxynitrite, a cloaked oxidant formed by nitric oxide and superoxide. *Chem Res Toxicol* 5: 834-42.

Koshland, D. J. 1992. The molecule of the year. *Science* 258: 1861.

Krenitsky, T. 1978. Aldehyde oxidase and xanthine oxidase--functional and evolutionary relationships. *Biochem Pharmacol* 27: 2763-4.

Kurose, I., Argenbright, LW, Wolf, R, Lianxi, L, and Granger, DN. 1997. Ischemia/reperfusion-induced microvascular dysfunction: role of oxidants and lipid mediators. *Am J Physiol* 272: H2976-82.

Lam, J., Chesebro, JH, and Fuster, V. 1988. Platelets, vasoconstriction, and nitroglycerin during arterial wall injury. A new antithrombotic role for an old drug. *Circulation* 78: 712-6.

Lancaster, J. J. 1994. Simulation of the diffusion and reaction of endogenously produced nitric oxide. *Proc Natl Acad Sci U S A* 91: 8137-41.

Landers, E., Gonzalez-Hevia, MA, and Mendoza, MC. 1998. Molecular epidemiology of *Salmonella* serotype *enteritidis*. Relationships between food, water and pathogenic strains. *Int J Food Microbiol* 43: 81-90.

Lapenna, D., Mezzetti, A, de Gioia, S, Ciofani, G, Marzio, L, Di Ilio, C, and Cuccurullo, F. 1992. Heparin: does it act as an antioxidant in vivo? *Biochem Pharmacol* 44: 188-91.

Laurent, M., Lepoivre, M, and Tenu, JP. 1996. Kinetic modelling of the nitric oxide gradient generated in vitro by adherent cells expressing inducible nitric oxide synthase. *Biochem J* 314: 109-13.

Law, D., and Chart, H. 1998. Enteroaggregative *Escherichia coli. J Appl Microbiol* 84: 685-97.

Lenski, R. 1997. The cost of antibiotic resistance--from the perspective of a bacterium. *Ciba Found Symp* 207: 131-51.

Levene, C., Kapoor, R, and Heale, G. 1982. The effect of hypoxia on the synthesis of collagen and glycosaminoglycans by cultured pig aortic endothelium. *Atherosclerosis* 44: 327-37.

Levin, B., Lipsitch, M, Perrot, V, Schrag, S, Antia, R, Simonsen, L, Walker, NM, and Stewart, FM. 1997. The population genetics of antibiotic resistance. *Clin Infect Dis* 24: S9-16.

Levine, M., Bergquist, EJ, Nalin, DR, Waterman, DH, Hornick, RB, Young, CR, and Sotman, S. 1978. *Escherichia coli* strains that cause diarrhoea but do not produce heat-labile or heat-stable enterotoxins and are non-invasive. *Lancet* 1: 1119-22.

Levine, M., and Edelman, R. 1984. Enteropathogenic *Escherichia coli* of classic serotypes associated with infant diarrhoea: epidemiology and pathogenesis. *Epidemiol Rev* 6: 31-51.

Levy, S. 1994. Balancing the drug resistance equation. *Trends Microbiol* 2: 341-43.

Lewis, R., and Deen, WM. 1994. Kinetics of the reaction of nitric oxide with oxygen in aqueous solutions. *Chem Res Toxicol* 7: 568-74.

Lewis, R., Tannenbaum, SR, and Deen, WM. 1995. Kinetics of N-nitrosation in oxygenated nitric oxide solutions at physiological pH: role of nitrous anhydride and effects of phosphate and chloride. *J Am Chem Soc* 117: 3933-39.

Leyva, F., Anker, S, Swan, JW, Godsland, IF, Wingrove, CS, Chua, TP, Stevenson, JC, and Coats, AJ. 1997. Serum uric acid as an index of impaired oxidative metabolism in chronic heart failure. *Eur Heart J* 18: 858-65.

Lindahl, T., and Andersson, A. 1972. Rate of chain breakage at apurinic sites in double-stranded deoxyribonucleic acid. *Biochemistry* 11: 3618-23.

Linder, N., Rapola, J, and Raivio, KO. 1999. Cellular expression of xanthine oxidoreductase protein in normal human tissues. *Lab Invest* 79: 967-74.

Liochev, S., and Fridovich, I. 1997. Lucigenin luminescence as a measure of intracellular superoxide dismutase activity in Escherichia coli. *Proc Natl Acad Sci U S A* 94: 2891-6.

Liu, Z., Brien, JF, Marks, GS, McLaughlin, BE, and Nakatsu, K. 1993. Lack of evidence for the involvement of cytochrome P-450 or other hemoproteins in metabolic activation of glyceryl trinitrate in rabbit aorta. *J Pharmacol Exp Ther* 264: 1432-9.

Loscalzo, J. 1992. Antiplatelet and antithrombotic effects of organic nitrates. *Am J Cardiol* 70: 18B-22B.

Lundberg, B., Wolf, RE Jr, Dinauer, MC, Xu, Y, and Fang, FC. 1999. Glucose 6-phosphate dehydrogenase is required for *Salmonella typhimurium* virulence and resistance to reactive oxygen and nitrogen intermediates. *Infect Immun* 67: 436-8.

Lundberg, J., Weitzberg, E, Lundberg, JM, and Alving, K. 1994. Intragastric nitric oxide production in humans: measurements in expelled air. *Gut* 35: 1543-6.

Lundberg, J., Carlsson, S, Engstrand, L, Morcos, E, Wiklund, NP, and Weitzberg, E. 1997. Urinary nitrite: more than a marker of infection. *Urology* 50: 189-91.

Lupu, C., Lupu, F, Dennehy, U, Kakkar, VV, and Scully, MF. 1995. Thrombin induces the redistribution and acute release of tissue factor pathway inhibitor from specific granules within human endothelial cells in culture. *Arterioscler Thromb Vasc Biol* 15: 2055-62.

Lyons, C., Orloff, GJ, and Cunningham, JM. 1992. Molecular cloning and functional expression of an inducible nitric oxide synthase from a murine macrophage cell line. *J Biol Chem* 267: 6370-4.

Macfadyen, A., Reiter, C, Zhuang, Y, and Beckman, JS. 1999. A novel superoxide dismutase-based trap for peroxynitrite used to detect entry of peroxynitrite into erythrocyte ghosts. *Chem Res Toxicol* 12: 223-9.

MAFF. 1998. Antibiotic use in agriculture. *Food Safety Information Bulletin* 98.

Margulis, L. 1970. *Origin of eukaryotic cells.* Yale University Press, New Haven.

Marletta, M., Yoon, PS, Iyengar, R, Leaf, CD, and Wishnok, JS. 1988. Macrophage oxidation of L-arginine to nitrite and nitrate: nitric oxide is an intermediate. *Biochemistry* 27: 8706-11.

Marletta, M. 1994. Nitric oxide synthase: aspects concerning structure and catalysis. *Cell* 78: 927-30.

Martinez, G., Dodd, DA, and Samartgedes, JA. 1981. Milk feeding patterns in the United States during the first 12 months of life. *Pediatrics* 68: 863-8.

Marzinzig, M., Nussler, AK, Stadler, J, Marzinzig, E, Barthlen, W, Nussler, NC, Beger, HG, Morris, SM Jr, and Bruckner, UB. 1997. Improved methods to measure end products of nitric oxide in biological fluids: nitrite, nitrate, and S-nitrosothiols. *Nitric Oxide* 1: 177-89.

Mason, S. 1989. The development of concepts of chiral discrimination. *Chirality* 1: 183-91.

Massey, V., and Harris, CM. 1997. Milk xanthine oxidoreductase: the first one hundred years. *Biochem Soc Trans* 25: 750-755.

Mathews, W., Caperna, J, Toerner, JG, Barber, RE, and Morgenstern, H. 1998. Neutropenia is a risk factor for gram-negative bacillus bacteremia in human immunodeficiency virus-infected patients: results of a nested case-control study. *Am J Epidemiol* 148: 1175-83.

May, J. 1988. Microbial contaminants and anti-microbial properties of human milk. *Microbiol Sciences* 5: 42-46.

May, J. 1994. Anti-microbial factors and microbial contaminants in human milk. *J Ped Child Health* 30: 470-75.

Mayer, B., John, M, Heinzel, B, Werner, ER, Wachter, H, Schultz, G, and Bohme, E. 1991. Brain nitric oxide synthase is a biopterin- and flavin-containing multi-functional oxido-reductase. *FEBS Lett* 228: 187-91.

McCord, J., and Fridovich, I. 1969a. Superoxide dismutase, an enzymic function for erythrocuporin (hemocuporin). *J. Biol. Chem.* 244: 6049-55.

McCord, J., and Fridovich, I. 1969b. The utility of superoxide dismutase in studying free radical reactions. *J. Biol. Chem.* 244: 656-69.

McCord, J. 1985. Oxygen-derived free radicals in postischaemic tissue injury. *N Engl J Med* 312: 159-63.

McCormick, M., Buettner, GR, and Britigan, BE. 1998. Endogenous superoxide dismutase levels regulate iron-dependent hydroxyl radical formation in *Escherichia coli* exposed to hydrogen peroxide. *J Bacteriol* 108: 622-5.

McDonald, B., and Bennett, BM. 1993. Biotransformation of glyceryl trinitrate by rat aortic cytochrome P450. *Biochem Pharmacol* 45: 268-70.

McKnight, G., Smith, LM, Drummond, RS, Duncan, CW, Golden, M, and Benjamin, N. 1997. Chemical synthesis of nitric oxide in the stomach from dietary nitrate in humans. *Gut* 40: 211-4.

McNiff, J., and Gil, J. 1983. Secretion of Weibel-Palade bodies observed in extra-alveolar vessels of rabbit lung. *J Appl Physiol* 54: 1284-6.

Meerson, F., Kagan, VE, Kozlov, YuP, Belkina, LM, and Arkhipenko, YuV. 1982. The role of lipid peroxidation in pathogenesis of ischemic damage and the antioxidant protection of the heart. *Basic Res Cardiol* 77: 465-85.

Melillo, G., Musso, T, Sica, A, Taylor, LS, Cox, GW, and Varesio, L. 1995. A hypoxia-responsive element mediates a novel pathway of activation of the inducible nitric oxide synthase promoter. *J Exp Med* 182: 1683-93.

Menon, N., Wolf, A, Zehetgruber, M, and Bing, RJ. 1989. An improved chemiluminescence assay suggests non nitric oxide-mediated action of lysophosphatidylcholine and acetylcholine. *Proc Soc Exp Biol Med* 191: 316-9.

Meyer, J. 1981. Comparison of carbon monoxide, nitric oxide, and nitrite as inhibitors of the nitrogenase from *Clostridium pasteurianum. Arch Biochem Biophys* 210: 246-56.

Miesel, R., and Zuber, M. 1993. Elevated levels of xanthine oxidase in serum of patients with inflammatory and autoimmune rheumatic diseases. *Inflammation* 17: 551-61.

Mietens, C., Keinhorst, H, Hilpert, H, Gerber, H, Amster, H, and Pahud, JJ. 1979. Treatment of infantile E. coli gastroenteritis with specific bovine anti-*E. coli* milk immunoglobulins. *Eur J Pediatr* 132: 239-52.

Miller, R., and Britigan, BE. 1997. Role of oxidants in microbial pathophysiology. *Clin Microbiol Rev* 10: 1-18.

Moellering, R. J. 1995. Past, present, and future of antimicrobial agents. *Am J Med* 99: 11S-18S.

Moncada, S., Radomski, MW, and Palmer, RM. 1988. Endothelium-derived relaxing factor. Identification as nitric oxide and role in the control of vascular tone and platelet function. *Biochem Pharmacol* 37: 2495-501.

Moncada, S., Palmer, RMJ, and Higgs, EA. 1989. Biosynthesis of nitric oxide from l-arginine. *Biochem Pharmacol* 38: 1709-15.

Monge, C., and Leon-Velarde, F. 1991. Physiological adaptation to high altitude: oxygen transport in mammals and birds. *Physiol Rev* 71: 1135-72.

Morel, F., Doussiere, J, and Vignais, PV. 1991. The superoxide-generating oxidase of phagocytic cells. Physiological, molecular and pathological aspects. *Eur J Biochem* 201: 523-46.

Morgan, E., Stewart, CP and Hopkins, FG. 1922. *Proc. R. Soc. London* 94: 109-131.

Morre, D., and Brightman, AO. 1991. NADH oxidase of plasma membranes. *J Bioenerg Biomembr* 23: 469-89.

Muranjan, M., Wang, Q, Li, YL, Hamilton, E, Otieno-Omondi, FP, Wang, J, Van Praagh, A, J. Grootenhuis, and Black, SJ. 1997. The trypanocidal Cape buffalo serum protein is xanthine oxidase. *Infect Immun* 65: 3806-14.

Murray, B. 1994. Can antibiotic resistance be controlled? *N Engl J Med* 330: 1229-30.

Murray, C., and Lopez, AD. 1997. Mortality by cause for eight regions of the world: Global Burden of Disease Study. *Lancet* 349: 1269-76.

Murrel, W. 1879. Nitroglycerin as a remedy for angina pectoris. *Lancet* 1: 80-113.

Nakane, M., Schmidt, HH, Pollock, JS, Forstermann, U, and Murad, F. 1993. Cloned human brain nitric oxide synthase is highly expressed in skeletal muscle. *FEBS Lett* 316: 175-80.

Nataro, J., and Kaper, JB. 1998. Diarrheagenic *Escherichia coli. Clin Microbiol Rev* 11: 142-201.

Needleman, P., Blehm, DJ, and Rotskoff, KS. 1969. Relationship between glutathione-dependent dentration and the vasodilator effectiveness of organic nitrates. *J Pharmacol Exp Ther* 165: 286-8.

Needleman, P., Blehm, DJ, Harkey, AB, Johnson, EM Jr, and Lang, S. 1971. The metabolic pathway in the degradation of glyceryl trinitrate. *J Pharmacol Exp Ther* 179: 347-53.

Needleman, P., and Hunter, FE. 1965. The transformation of glyceryl trinitrate and other nitrates by glutathione-organic nitrate reductase. *Mol Pharmacol* 1: 77-86.

Nelin, L., Thomas, CJ, and Dawson, CA. 1996. Effect of hypoxia on nitric oxide production in neonatal pig lung. *Am J Physiol* 271: H8-14.

Newburg, D. 1999. Human milk glycoconjugates that inhibit pathogens. *Curr Med Chem* 6: 117-27.

Nielsen, V., Tan, S, Baird, MS, Samuelson, PN, McCammon, AT, and Parks, DA. 1997. Xanthine oxidase mediates myocardial injury after hepatoenteric ischemia-reperfusion. *Crit Care Med* 25: 1044-50.

Nigam, R., Whiting, T, and Bennett, BM. 1993. Effect of inhibitors of glutathione S-transferase on glyceryl trinitrate activity in isolated rat aorta. *Can J Physiol Pharmacol* 71: 179-84.

Nishino, T. 1994. The conversion of xanthine dehydrogenase to xanthine oxidase and the role of the enzyme in reperfusion injury. *J Biochem (Tokyo)* 116: 1-6.

Nocek, J., Braund, DG, and Warner, RG. 1984. Influence of neonatal colostrum administration, immunoglobulin, and continued feeding of colostrum on calf gain, health, and serum protein. *J Dairy Sci* 67: 319-33.

Nunoshiba, T., deRojas-Walker, T, Wishnok, JS, Tannenbaum, SR, and Demple, B. 1993. Activation by nitric oxide of an oxidative-stress response that defends *Escherichia coli* against activated macrophages. *Proc Natl Acad Sci U S A* 90: 9993-7.

Nunoshiba, T., DeRojas-Walker, T, Tannenbaum, SR, and Demple, B. 1995. Roles of nitric oxide in inducible resistance of *Escherichia coli* to activated murine macrophages. *Infect Immun* 63: 794-8.

Nunoshiba, T. 1996. Two-stage gene regulation of the superoxide stress response soxRS system in *Escherichia coli*. *Crit Rev Eukaryot Gene Expr* 6: 377-89.

Ogawa, S., Gerlach, H, Esposito, C, Pasagian-Macaulay, A, Brett, J, and Stern, D. 1990. Hypoxia modulates the barrier and coagulant function of cultured bovine endothelium. Increased monolayer permeability and induction of procoagulant properties. *J Clin Invest* 85: 1090-8.

Oli, M., Petschow, BW, and Buddington, RK. 1998. Evaluation of fructooligosaccharide supplementation of oral electrolyte solutions for treatment of diarrhea: recovery of the intestinal bacteria. *Dig Dis Sci* 43: 138-47.

Ortega-Barria, E., and Pereira, ME. 1991. A novel *T. cruzi* heparin-binding protein promotes fibroblast adhesion and penetration of engineered bacteria and trypanosomes into mammalian cells. *Cell* 67: 411-21.

Oury, T., Crapo, JD, Valnickova, Z, and Enghild, JJ. 1996. Human extracellular superoxide dismutase is a tetramer composed of two disulphide-linked dimers: a simplified, high-yield purification of extracellular superoxide dismutase. *Biochem J* 317: 51-7.

Oyekan, A., McGiff, JC, and Quilley, J. 1991. Cytochrome P-450-dependent vasodilation of rat kidney by arachidonic acid. *Am J Physiol* 261: H714-9.

Pabst, M., Hedegaard, HB, and Johnston, RB Jr. 1982. Cultured human monocytes require exposure to bacterial products to maintain an optimal oxygen radical response. *J Immunol* 128: 123-8.

Padmaja, S., and Huie, RE. 1993. The reaction of nitric oxide with organic peroxyl radicals. *Biochem Biophys Res Commun* 195: 539-44.

Page, S., Powell, D, Benboubetra, M, Stevens, CR, Blake, DR, Selase, F, Wolstenholme, AJ,, and R. and Harrison. 1998. Xanthine oxidoreductase in human mammary epithelial cells: activation in response to inflammatory cytokines. *Biochim Biophys Acta* 1381: 191-202.

Palmer, G., Bray, RC, and Beinert, H. 1964. Direct studies on the electron transfer sequence in xanthine oxidase by electron paramagnetic resonance spectroscopy. Techniques and description of spectra. *J Biol Chem* 239: 2667.

Palmer, R., Ferrige, AG, and Moncada, S. 1987. Nitric oxide release accounts for the biological activity of endothelium-derived relaxing factor. *Nature* 327: 524-6.

Palmer, R., Rees, DD, Ashton, DS, and Moncada, S. 1988. L-arginine is the physiological precursor for the formation of nitric oxide in endothelium-dependent relaxation. *Biochem Biophys Res Commun* 153: 1251-6.

Palmer, R., Ashton, DS, and Moncada, S. 1988. Vascular endothelial cells synthesize nitric oxide from L-arginine. *Nature* 333: 664-6.

Palmer, R., and Moncada, S. 1989. A novel citrulline-forming enzyme implicated in the formation of nitric oxide by vascular endothelial cells. *Biochem Biophys Res Commun* 158: 348-52.

Panasyuk, A., Frati, E, Ribault, D, and Mitrovic, D. 1994. Effect of reactive oxygen species on the biosynthesis and structure of newly synthesized proteoglycans. *Free Radic Biol Med* 16: 157-67.

Parks, D., and Granger, DN. 1986. Xanthine oxidase: biochemistry, distribution and physiology. *Acta Physiol Scand Suppl* 548: 87-99.

Pateman, J., Cove,DJ, Rever, BM, and Roberts, DB. 1964. *Nature* 201: 58.

Patti, J., Allen, BL, McGavin, MJ, and Hook, M. 1994. MSCRAMM-mediated adherence of microorganisms to host tissues. *Annu Rev Microbiol* 48: 585-617.

Payne, W. 1973. Reduction of nitrogenous oxides by microorganisms. *Bacteriol Rev* 37: 409-52.

Peacock, A. 1998. ABC of oxygen: oxygen at high altitude. *BMJ* 317: 1063-6.

Perie, J., Riviere-Alric, I, Blonski, C, Gefflaut, T, Lauth de Viguerie, N, Trinquier, M, Willson, M, Opperdoes, FR and Callens M. 1993. Inhibition of the glycolytic enzymes in the trypanosome: an approach in the development of new leads in the therapy of parasitic diseases. *Pharmacol Ther* 60: 347-365.

Persichini, T., Colasanti, M, Fraziano, M, Colizzi, V, Ascenzi, P, and Lauro, GM. 1999. Nitric oxide inhibits HIV-1 replication in human astrocytoma cells. *Biochem Biophys Res Commun* 254: 200-2.

Pfeiffer, S., Gorren, ACF, Schmidt, K, Werner, ER, Hansert, B, Bohle, DS, and Mayer, B. 1997. Metabolic fate of peroxynitrite in aqueous solution. Reaction with nitric oxide and pH-dependent decomposition to nitrite and oxygen in a 2:1 stoichiometry. *J Biol Chem* 272: 3465-70.

Pick, E., Bromberg, Y, Shpungin, S, and Gadba, R. 1987. Activation of the superoxide forming NADPH oxidase in a cell-free system by sodium dodecyl sulfate. Characterization of the membrane-associated component. *J Biol Chem* 262: 16476-83.

Pickering, L., Cleary, TG, and Caprioli, RM. 1983. Inhibition of human polymorphonuclear leukocyte function by components of human colostrum and mature milk. *Infect Immun* 40: 8-15.

Pinsky, D., Naka, Y, Liao, H, Oz, MC, Wagner, DD, Mayadas, TN, Johnson, RC, Hynes, RO, Heath, M, Lawson, CA, andStern, DM. 1996. Hypoxia-induced exocytosis of endothelial cell Weibel-Palade bodies. A mechanism for rapid neutrophil recruitment after cardiac preservation. *J Clin Invest* 97: 493-500.

Pirie, N. 1985. Fact and assumption in studies on the origins of life. *Orig Life* 15: 207-12.

Pou, S., Pou, WS, Bredt, DS, Snyder, SH, and Rosen, GM. 1992. Generation of superoxide by purified brain nitric oxide synthase. *J Biol Chem* 267: 24173-6.

Pou, S., Nguyen, SY, Gladwell, T, and Rosen, GM. 1995. Does peroxynitrite generate hydroxyl radical? *Biochim Biophys Acta* 1244: 62-8.

Pou, S., Keaton, L, Surichamorn, W, and Rosen, GM. 1999. Mechanism of superoxide generation by neuronal nitric-oxide synthase. *J Biol Chem* 274: 9573-80.

Prentice, A., Watkinson, M, Prentice, AM, Cole, TJ, and Whitehead, RG. 1984. Breast-milk antimicrobial factors of rural Gambian mothers. II. Influence of season and prevalence of infection. *Acta Paediatr Scand* 73: 803-9.

Prentice, A., Ewing, G, Roberts, SB, Lucas, A, MacCarthy, A, Jarjou, LM, and Whitehead, RG. 1987. The nutritional role of breast-milk IgA and lactoferrin. *Acta Paediatr Scand* 76: 592-8.

Prinz, R., Schwermann, J, Buddecke, E, and von Figura, K. Endocytosis of sulphated proteoglycans by cultured skin fibroblasts. *Biochem J* 176: 671-6.

Pryor, W., Jin, X, and Squadrito, GL. 1994. One- and two-electron oxidations of methionine by peroxynitrite. *Proc Natl Acad Sci U S A* 91: 11173-7.

Pryor, W., and Squadrito, GL. 1995. The chemistry of peroxynitrite: a product from the reaction of nitric oxide with superoxide. *Am. J. Physiol.* 268: L699-L722.

Pryor, W., Cueto, R, Jin, X, Koppenol, WH, Ngu-Schwemlein, M, Squadrito, GL, Uppu, PL, and, and R. Uppu. 1995. A practical method for preparing peroxynitrite solutions of low ionic strength and free of hydrogen peroxide. *Free Radic Biol Med* 18: 75-83.

Radi, R., Beckman, JS, Bush, KM, and Freeman, BA. 1991. Peroxynitrite oxidation of sulfhydryls. The cytotoxic potential of superoxide and nitric oxide. *J Biol Chem* 266: 4244-50.

Radi, R., Cosgrove, TP, Beckman, JS, and Freeman, BA. 1993. Peroxynitrite-induced luminol chemiluminescence. *Biochem J* 290: 51-7.

Radi, R., Rubbo, H, Bush, K, and Freeman, BA. 1997. Xanthine oxidase binding to glycosaminoglycans: kinetics and superoxide dismutase interactions of immobilized xanthine oxidase-heparin complexes. *Arch Biochem Biophys* 339: 125-35.

Radomski, M., Palmer, RM, and Moncada, S. 1987. The role of nitric oxide and cGMP in platelet adhesion to vascular endothelium. *Biochem Biophys Res Commun* 148: 1482-9.

Raupach, B., Mecsas, J, Heczko, U, Falkow, S, and Finlay, BB. 1999. Bacterial epithelial cell cross talk. *Curr Top Microbiol Immunol* 236: 137-61.

Reed, J., Ho, HH and Jolly, WL. 1974. Chemical synthesis with a quenched flow reactor. Hydroxytrihydroborate and peroxynitrite. *J. Am. Chem. Soc.* 96: 1248-49.

Rees, D., Palmer, RM, Hodson, HF, and Moncada, S. 1989. A specific inhibitor of nitric oxide formation from L-arginine attenuates endothelium-dependent relaxation. *Br J Pharmacol* 96: 418-24.

Reinke, L., Nakamura, M, Logan, L, Christensen, HD, and Carney, JM. 1987. In vivo and in vitro 1-methylxanthine metabolism in the rat. Evidence that the dehydrogenase form of xanthine oxidase predominates in intact perfused liver. *Drug Metab Dispos* 15: 295-9.

Rengasamy, A., and Johns, RA. 1996. Determination of Km for oxygen of nitric oxide synthase isoforms. *J Pharmacol Exp Ther* 276: 30-3.

Richert, D., and Westerfeld, WW. 1951. A bioassay procedure for the dietary factor related to xanthine oxidase. *J Biol Chem* 192: 49-56.

Richert, D., and Westerfeld WW. 1953. Isolation and identification of the xanthine oxidase factor as molybdenum. *J Biol Chem* 203: 915-23.

Richert, D., and Westerfeld, WW. 1954. The relationship of iron to xanthine oxidase. *J Biol Chem* 209: 179.

Robins-Browne, R. 1987. Traditional enteropathogenic *Escherichia coli* of infantile diarrhea. *Rev Infect Dis* 9: 28-53.

Rogers, K. 1951. The spread of infantile gastroenteritis in a cubicled ward. *J Hyg* 49: 140-51.

Rootwelt, T., Almaas, R, Oyasaeter, S, Moen, A, and Saugstad, OD. 1995. Release of xanthine oxidase to the systemic circulation during resuscitation from severe hypoxemia in newborn pigs. *Acta Paediatr* 84: 507-11.

Rothbaum, R., McAdams, AJ, Giannella, R, and Partin, JC. 1982. A clinicopathologic study of enterocyte-adherent *Escherichia coli*: a cause of protracted diarrhea in infants. *Gastroenterology* 83: 441-54.

Rouquette, M., Page, S, Bryant, R, Benboubetra, M, Stevens, CR, Blake, DR, Whish, WD, Harrison, R, and Tosh, D. 1998. Xanthine oxidoreductase is asymmetrically localised on the outer surface of human endothelial and epithelial cells in culture. *FEBS Lett* 426: 397-401.

Routledge, M., Wink, DA, Keefer, LK, and Dipple, A. 1993. Mutations induced by saturated aqueous nitric oxide in the pSP189 supF gene in human Ad293 and E. coli MBM7070 cells. *Carcinogenesis* 14: 1251-4.

Rubbo, H., Radi, R, Trujillo, M, Telleri, R, Kalyanaraman, B, Barnes, S, Kirk, M, and Freeman, BA. 1994. Nitric oxide regulation of superoxide and peroxynitrite-dependent lipid peroxidation. Formation of novel nitrogen-containing oxidized lipid derivatives. *J Biol Chem* 269: 26066-75.

Ruiz-Palacios, G., Calva, JJ, Pickering, LK, Lopez-Vidal, Y, Volkow, P, Pezzarossi, H, and West, MS. 1990. Protection of breast-fed infants against *Campylobacter* diarrhoea by antibodies in human milk. *J Pediatr* 116: 707-13.

Rusin, P., Orosz-Coughlin, P, and Gerba, C. 1998. Reduction of faecal coliform, coliform and heterotrophic plate count bacteria in the household kitchen and bathroom by disinfection with hypochlorite cleaners. *J Appl Microbiol* 85: 819-28.

Russell, C. 1965. The effect of nitric oxide on the growth of *Escherichia coli* M. *Experientia* 21: 625.

Salceda, S., and Caro, J. 1997. Hypoxia-inducible factor 1alpha (HIF-1alpha) protein is rapidly degraded by the ubiquitin-proteasome system under normoxic conditions. Its stabilization by hypoxia depends on redox-induced changes. *J Biol Chem* 272: 22642-7.

Sanchez, L., Calvo, M, and Brock, JH. 1992. Biological role of lactoferrin. *Arch Dis Child* 67: 657-61.

Sanders, S., Eisenthal, R, and Harrison, R. 1997. NADH oxidase activity of human xanthine oxidoreductase--generation of superoxide anion. *Eur J Biochem* 245: 541-8.

Saran, M., Beck-Speier, I, Fellerhoff, B, and Bauer, G. 1999. Phagocytic killing of microorganisms by radical processes: consequences of the reaction of hydroxyl radicals with chloride yielding chlorine atoms. *Free Radic Biol Med* 26: 482-90.

Sarnesto, A., Linder, N, and Raivio, KO. 1996. Organ distribution and molecular forms of human xanthine dehydrogenase/xanthine oxidase protein. *Lab Invest* 74: 48-56.

Saura, M., Zaragoza, C, McMillan, A, Quick, RA, Hohenadl, C, Lowenstein, JM, and Lowenstein, CJ. 1999. An antiviral mechanism of nitric oxide: inhibition of a viral protease. *Immunity* 10: 21-8.

Scazzocchio, C., and Holl, FB. 1972. Nitrate repression of xanthine dehydrogenase II in *Aspergillus nidulans*. *Biochem J* 127: 17P.

Schaper, W. 1991. Molecular mechanisms in "stunned" myocardium. *Cardiovasc Drugs Ther* 5: 925-32.

Schardinger, F. 1902. *Z. Unters. Nahr. Genussm.* 5: 1113-1121.

Schoene, R. 1997. Control of breathing at high altitude. *Respiration* 64: 407-15.

Schrag, S., Perrot, V, and Levin, BR. 1997. Adaptation to the fitness costs of antibiotic resistance in *Escherichia coli*. *Proc R Soc Lond B Biol Sci* 264: 1287-91.

Schulz, R., Nava, E, and Moncada, S. 1992. Induction and potential biological relevance of a $Ca^{(2+)}$-independent nitric oxide synthase in the myocardium. *Br J Pharmacol* 105: 575-80.

Schwartz, C., Krall, J, Norton, L, McKay, K, Kay, D, and Lynch, RE. 1983. Catalase and superoxide dismutase in *Escherichia coli*. *J Biol Chem* 258: 6277-81.

Semenza, G., and Wang, GL. 1992. A nuclear factor induced by hypoxia via de novo protein synthesis binds to the human erythropoietin gene enhancer at a site required for transcriptional activation. *Mol Cell Biol* 12: 5447-54.

Sergeev, N., Ananiadi, LI, L'vov, NP, and Kretovich, WL. 1985. The nitrate reductase activity of milk xanthine oxidase. *J Appl Biochem* 7: 86-92.

Servent, D., Delaforge, M, Ducrocq, C, Mansuy, D, and Lenfant, M. 1989. Nitric oxide formation during microsomal hepatic denitration of glyceryl trinitrate: involvement of cytochrome P-450. *Biochem Biophys Res Commun* 163: 1210-6.

Sessa, W., Harrison, JK, Barber, CM, Zeng, D, Durieux, ME, D'Angelo, DD, Lynch, KR, and Peach, MJ. 1992. Molecular cloning and expression of a cDNA encoding endothelial cell nitric oxide synthase. *J Biol Chem* 267: 15274-6.

Sessa, W., Barber, CM, and Lynch, KR. 1993. Mutation of N-myristoylation site converts endothelial cell nitric oxide synthase from a membrane to a cytosolic protein. *Circ Res* 72: 921-4.

Shaw, R., Johnson, AR, Schulz, WW, Zahlten, RN, and Combes, B. 1984. Sinusoidal endothelial cells from normal guinea pig liver: isolation, culture and characterization. *Hepatology* 4: 591-602.

Shields, G., Stille, P, Brasier, MD and Atudorei, NV. 1997. Stratified oceans and oxygenation of the late Precambrian environment: a postglacial geochemical record from the Neoproterozoic of W Mongolia. *TERRA NOVA* 9: 218-222.

Simon, W., Anderson, DJ, and Bennett, BM. 1996. Inhibition of the pharmacological actions of glyceryl trinitrate after the electroporetic delivery of a glutathione S-transferase inhibitor. *J Pharmacol Exp Ther* 279: 1535-40.

Skulachev, V. 1998. Possible role of reactive oxygen species in antiviral defense. *Biochemistry* 63: 1438-40.

Smith, S., Rajagopalan, KV, and Handler, P. 1967. Purification and properties of xanthine dehydroganase from *Micrococcus lactilyticus*. *J Biol Chem* 242: 4108-17.

Spagnuolo, C., Rinelli, P, Coletta, M, Chiancone, E, and Ascoli, F. 1987. Oxidation reaction of human oxyhemoglobin with nitrite: a reexamination. *Biochim Biophys Acta* 911: 59-65.

Spiegelhalder, B., Eisenbrand, G, and Preussmann, R. 1976. Influence of dietary nitrate on nitrite content of human saliva: possible relevance to in vivo formation of N-nitroso compounds. *Food Cosmet Toxicol* 14: 545-8.

Sporn, L., Marder, VJ, and Wagner, DD. 1986. Inducible secretion of large, biologically potent von Willebrand factor multimers. *Cell* 46: 185-90.

Spratt, B. 1996. Antibiotic resistance: counting the cost. *Curr Biol* 6: 1219-21.

Srinivas, V., Zhu, X, Salceda, S, Nakamura, R, and Caro, J. 1998. Hypoxia-inducible factor 1 (HIF-1) is a non-heme iron protein. Implications for oxygen sensing. *J Biol Chem* 273: 18019-22.

Stamler, J., Vaughan, DE, and Loscalzo, J. 1989. Synergistic disaggregation of platelets by tissue-type plasminogen activator, prostaglandin E1, and nitroglycerin. *Circ Res* 65: 796-804.

Stamler, J., Jaraki, O, Osborne, J, Simon, DI, Keaney, J, Vita, J, Singel, D, Valeri, CR, and Loscalzo, J. 1992. Nitric oxide circulates in mammalian plasma primarily as an S-nitroso adduct of serum albumin. *Proc Natl Acad Sci U S A* 89: 7674-7.

Steiner, L., Kroncke, K, Fehsel, K, and Kolb-Bachofen, V. 1997. Endothelial cells as cytotoxic effector cells: cytokine-activated rat islet endothelial cells lyse syngeneic islet cells via nitric oxide. *Diabetologia* 40: 150-5.

Stephens, C., and Shapiro, L. 1997. Bacterial protein secretion--a target for new antibiotics? *Chem Biol* 4: 637-41.

Stevens, C., Williams, RB, Farrell, AJ, and Blake, DR. 1991. Hypoxia and inflammatory synovitis: observations and speculation. *Ann Rheum Dis* 50: 124-32.

Stevens, C., Benboubetra, M, Harrison, R, Sahinoglu, T, Smith, EC, and Blake, DR. 1991. Localisation of xanthine oxidase to synovial endothelium. *Ann Rheum Dis* 50: 760-2.

Stevenson, S. 1947. The adequacy of artificial feeding in infancy. *J Pediatr* 31: 616-30.

Struelens, M. 1998. The epidemiology of antimicrobial resistance in hospital acquired infections: problems and possible solutions. *BMJ* 317: 652-4.

Szabo, C., Zingarelli, B, O'Connor, M, and Salzman, AL. 1996. DNA strand breakage, activation of poly (ADP-ribose) synthetase, and cellular energy depletion are involved in the cytotoxicity of macrophages and smooth muscle cells exposed to peroxynitrite. *Proc Natl Acad Sci U S A* 93: 1753-8.

Szabo, C., and Ohshima, H. 1997. DNA damage induced by peroxynitrite: subsequent biological effects. *Nitric Oxide* 1: 373-85.

Tamir, S., Burney, S, and Tannenbaum, SR. 1996. DNA damage by nitric oxide. *Chem Res Toxicol* 9: 821-7.

Tan, S., Radi, R, Gaudier, F, Evans, RA, Rivera, A, Kirk, KA, and Parks, DA. 1993. Physiologic levels of uric acid inhibit xanthine oxidase in human plasma. *Pediatr Res* 34: 303-7.

Tan, S., Yokoyama, Y, Dickens, E, Cash, TG, Freeman, BA, and Parks, DA. 1993. Xanthine oxidase activity in the circulation of rats following hemorrhagic shock. *Free Radic Biol Med* 15: 407-14.

Tan, S., Gelman, S, Wheat, JK, and Parks, DA. 1995. Circulating xanthine oxidase in human ischemia reperfusion. *South Med J* 88: 479-82.

Tannenbaum, S., Weisman, M, and Fett, D. 1976. The effect of nitrate intake on nitrite formation in human saliva. *Food Cosmet Toxicol* 14: 549-52.

Tauxe, R. 1998. Foodborne illnesses. Strategies for surveillance and prevention. *Lancet* 352: SIV10.

Terada, L., Rubinstein, JD, Lesnefsky, EJ, Horwitz, LD, Leff, JA, and Repine, JE. 1991. Existence and participation of xanthine oxidase in reperfusion injury of ischemic rabbit myocardium. *Am J Physiol* 260: H805-10.

Terada, L., Dormish, JJ, Shanley, PF, Leff, JA, Anderson, BO, and Repine, JE. 1992. Circulating xanthine oxidase mediates lung neutrophil sequestration after intestinal ischemia-reperfusion. *Am J Physiol* 263: L394-401.

Terada, L., Piermattei, D, Shibao, GN, McManaman, JL, and Wright, RM. 1997. Hypoxia regulates xanthine dehydrogenase activity at pre- and posttranslational levels. *Arch Biochem Biophys* 348: 163-8.

Terao, M., Kurosaki, M, Zanotta, S, and Garattini, E. 1997. The xanthine oxidoreductase gene: structure and regulation. *Biochem Soc Trans* 25: 791-6.

Thomas, G., McCrossan, M, and Selkirk, ME. 1997. Cytostatic and cytotoxic effects of activated macrophages and nitric oxide donors on Brugia malayi. *Infect Immun* 65: 2732-9.

Torres, J., Cooper, CE, and Wilson, MT. 1998. A common mechanism for the interaction of nitric oxide with the oxidized
binuclear centre and oxygen intermediates of cytochrome c oxidase. *J Biol Chem* 273: 8756-66.

Totter, J., De Dugros, EC and Riviero, C. 1960. The use of chemiluminescent compounds as possible indicators of radical production during xanthine oxidase action. *J. Biol. Chem.* 235: 1839-1842.

Trujillo, M., Alvarez, MN, Peluffo, G, Freeman, BA, and Radi, R. 1998. Xanthine oxidase-mediated decomposition of S-nitrosothiols. *J Biol Chem* 273: 7828-34.

Tsunawaki, S., and Nathan, CF. 1984. Enzymatic basis of macrophage activation. Kinetic analysis of superoxide production in lysates of resident and activated mouse peritoneal macrophages and granulocytes. *J Biol Chem* 259: 4305-12.

Turnidge, J. 1998. What can be done about resistance to antibiotics? *BMJ* 317: 645-7.

Ultsch, G. 1974. Gas exchange and metabolism in the *Sirenidae* (Amphibia: Caudata)--I. Oxygen consumption of submerged sirenids as a function of body size and respiratory surface area. *Comp Biochem Physiol A* 47: 485-98.

Umezawa, K., Akaike, T, Fujii, S, Suga, M, Setoguchi, K, Ozawa, A, and Maeda, H. 1997. Induction of nitric oxide synthesis and xanthine oxidase and their roles in the antimicrobial mechanism against *Salmonella typhimurium* infection in mice. *Infect Immun* 65: 2932-40.

Uppu, R., Squadrito, GL, Cueto, R, and Pryor, WA. 1996. Selecting the most appropriate synthesis of peroxynitrite. *Methods Enzymol* 269: 285-96.

Utgaard, J., Jahnsen, FL, Bakka, A, Brandtzaeg, P, and Haraldsen, G. 1998. Rapid secretion of prestored interleukin 8 from Weibel-Palade bodies of microvascular endothelial cells. *J Exp Med* 188: 1751-6.

Vatner, S., Higgins, CB, Milland, RW, and Franklin, D. 1972. Direct and reflex effects of nitroglycerin on coronary and left ventricular dynamics in conscious dogs. *J Clin Invest* 51: 2872-82.

Venema, R., Sayegh, HS, Kent, JD, and Harrison, DG. 1996. Identification, characterization, and comparison of the calmodulin-binding domains of the endothelial and inducible nitric oxide synthases. *J Biol Chem* 271: 6435-40.

Ventom, A., Deistung, J, and Bray, RC. 1988. The isolation of demolybdo xanthine oxidase from bovine milk. *Biochem J* 255: 949-56.

Wang, G., and Semenza, GL. 1993. General involvement of hypoxia-inducible factor 1 in transcriptional response to hypoxia. *Proc Natl Acad Sci U S A* 90: 4304-8.

Wasserman, K., Beaver, WL, and Whipp, BJ. 1990. Gas exchange theory and the lactic acidosis (anaerobic) threshold. *Circulation* 81: 14-30.

Weber, M., Lenhoff, HM and Kaplan, NO,. 1956. The reduction of inorganic iron and cytochrome c by flavin enzymes. *J. Biol. Chem.* 220: 93-104.

Weibel, ER, and Palade, GE. 1964. New cytoplasmic components in arterial endothelia. *J Cell Biol* 23: 101-112.

Weinbroum, A., Nielsen, VG, Tan, S, Gelman, S, Matalon, S, Skinner, KA, Bradley, E Jr, and Parks, DA. 1995. Liver ischemia-reperfusion increases pulmonary permeability in rat: role of circulating xanthine oxidase. *Am J Physiol* 268: G988-96.

Weiner, C., Lizasoain, I, Baylis, SA, Knowles, RG, Charles, IG, and Moncada, S. 1994. Induction of calcium-dependent nitric oxide synthases by sex hormones. *Proc Natl Acad Sci U S A* 91: 5212-6.

Weir, E., Wyatt, CN, Reeve, HL, Huang, J, Archer, SL, and Peers, C. 1994. Diphenyleneiodonium inhibits both potassium and calcium currents in isolated pulmonary artery smooth muscle cells. *J Appl Physiol* 76: 2611-5.

Weitzeberg, E., and Lundberg, JON. 1998. Nonenzymatic nitric oxide production in humans. *Nitric Oxide* 2: 1-7.

Weller, R., Pattullo, S, Smith, L, Golden, M, Ormerod, A, and Benjamin, N. 1996. Nitric oxide is generated on the skin surface by reduction of sweat nitrate. *J Invest Dermatol* 107: 327-31.

Welsh, J., and May, JT. 1979. Anti-infective properties of breast milk. *J Pediatrics* 94: 1-9.

Wharton, D., and Weintraub, ST. 1980. Identification of nitric oxide and nitrous oxide as products of nitrite reduction by *Pseudomonas* cytochrome oxidase (nitrate reductase). *Biochem Biophys Res Commun* 97: 236-42.

White, C., Darley-Usmar, V, Berrington, WR, McAdams, M, Gore, JZ, Thompson, JA, Parks,, and T. DA, MM, and Freeman, BA. 1996. Circulating plasma xanthine oxidase contributes to vascular dysfunction in hypercholesterolemic rabbits. *Proc Natl Acad Sci U S A* 93: 8745-9.

Whorton, A., Simonds, DB and Piantadosi, CA. 1997. Regulation of nitric oxide synthesis by oxygen in vascular endothelial cells. *Am. J. Physiol.* 272: L1161-6.

Wiemer, E., Michels, PA and Opperdoes, FR. 1995. The inhibition of pyruvate transport across the plasma membrane of the bloodstream form of *Trypanosoma brucei* and its metabolic implications. *Biochem J* 312: 479-484.

Wink, D., Hanbauer, I, Laval, F, Cook, JA, Krishna, MC, and Mitchell, JB. 1994. Nitric oxide protects against the cytotoxic effects of reactive oxygen species. *Ann N Y Acad Sci* 738: 265-78.

Wink, D., and Mitchell, JB. 1998. Chemical biology of nitric oxide: Insights into regulatory, cytotoxic, and cytoprotective mechanisms of nitric oxide. *Free Radic Biol Med* 25: 434-56.

Woodford, N. 1998. Glycopeptide-resistant enterococci: a decade of experience. *J Med Microbiol* 47: 849-62.

Wu, S., and Peng, RQ. 1992. Studies on an outbreak of neonatal diarrhea caused by EPEC 0127:H6 with plasmid analysis restriction analysis and outer membrane protein determination. *Acta Paediatr* 81: 217-21.

Xia, Y., Dawson, VL, Dawson, TM, Snyder, SH, and Zweier, JL. 1996. Nitric oxide synthase generates superoxide and nitric oxide in arginine-depleted cells leading to peroxynitrite-mediated cellular injury. *Proc Natl Acad Sci U S A* 93: 6770-4.

Xia, Y., and Zweier, JL. 1997. Superoxide and peroxynitrite generation from inducible nitric oxide synthase in macrophages. *Proc. Natl. Acad. Sci. USA.* 94: 6954-8.

Xu, P., Zhu, XL, Hueckstead, TP, Brothman, AR, and Hoidal, JR. 1994. Assignment of human xanthine dehydrogenase gene to chromosome 2p22. *Genomics* 23: 289-91.

Ye, R., Averill, BA, and Tiedje, JM. 1994. Denitrification: production and consumption of nitric oxide. *Appl Environ Microbiol* 60: 1053-8.

Yokoyama, Y., Beckman, JS, Beckman, TK, Wheat, JK, Cash, TG, Freeman, BA, and Parks, DA. 1990. Circulating xanthine oxidase: potential mediator of ischemic injury. *Am J Physiol* 258: G564-70.

Zhang, Z., Blake, DR, Stevens, CR, Kanczler, JM, Winyard, PG, Symons, MC, Benboubetra, and M, Harrison, R. 1998. A reappraisal of xanthine dehydrogenase and oxidase in hypoxic reperfusion injury: the role of NADH as an electron donor. *Free Radic Res* 28: 151-64.

Zimmerman, B., Parks, DA, Grisham, MB, and Granger, DN. 1988. Allopurinol does not enhance antioxidant properties of extracellular fluid. *Am J Physiol* 255: H202-6.

Zweier, J., Wang, P, Samouilov, A, and Kuppusamy, P. 1995. Enzyme-independent formation of nitric oxide in biological tissues. *Nat Med* 1: 804-9.